# Characterization of the impacts of polycyclic aromatic hydrocarbons on the fish gut microbiome

A Thesis Submitted to the College of
Graduate and Postdoctoral Studies
In Partial Fulfillment of the Requirements
For the Degree of Doctor of Philosophy
In the Toxicology Graduate Program
University of Saskatchewan
Saskatoon, Saskatchewan, Canada
By
Abigail DeBofsky

## Permission to use

In presenting this thesis in partial fulfillment of the requirements for a postgraduate degree from the University of Saskatchewan, I agree that the Libraries of the University may make it freely available for inspection. I further agree that permission for copying of this thesis in any manner, in whole or in part, for scholarly purpose may be granted by the professor or professors who supervised this thesis work or, in their absence, by the Head of the Department or the Dean of the College in which this thesis work was done. It is understood that any copying or publication or use of this thesis or parts thereof for financial gain shall not be allowed without my written permission. It is also understood that due recognition shall be given to me and to the University of Saskatchewan in any scholarly use which may be made of any material in this thesis. Requests for permission to copy or to make other use of material in this thesis in whole or parts should be addressed to:

Chair of the Toxicology Graduate Program
Toxicology Centre
University of Saskatchewan
44 Campus Drive
Saskatoon, Saskatchewan S7N 5B3 Canada

OR

Dean College of Graduate and Postdoctoral Studies
University of Saskatchewan
116 Thorvaldson Building, 110 Science Place
Saskatoon, Saskatchewan S7N 5C9 Canada

# Abstract

The microbiome has been described as an additional host "organ" with well-established beneficial roles. In addition to aiding in digestion of food and uptake of nutrients, microbiota in guts of vertebrates are responsible for regulating several beneficial functions, including stimulating immune responses and maintaining homeostasis. However, effects of exposures to chemicals on both structure and function of the gut microbiome of fishes are understudied. The overall purpose of research reported in this thesis was to characterize the effects of polycyclic aromatic hydrocarbons (PAHs) on the gut microbiomes of freshwater fishes, using both laboratory- and field-based assessments. PAHs have a number of well-characterized deleterious impacts in fish and are known modulators of the aryl hydrocarbon receptor, a receptor that has a bidirectional relationship with the microbiome. As such, this chemical class was selected to investigate targeted effects on the microbiome. The objectives of this thesis were to: (1) Determine if aqueous exposures to BaP modulate the gut microbiome in fathead minnows (*Pimephales promelas*) and to discern whether these community shifts were sex-dependent; (2) Assess whether a dietary exposure to BaP also affects genomic and active microbiomes in juvenile fathead minnows; and (3) Evaluate the gut microbiomes in native fishes following exposure to an oil spill of heavy crude on the North Saskatchewan River. To accomplish this, adult male and female fathead minnows were aqueously exposed to a short-term environmentally-relevant low concentrations of benzo[*a*]pyrene (BaP) and composition of the gut microbiome were assessed with 16S rRNA metagenetics. Following this, juvenile fathead minnows were exposed *via* the diet to environmentally-relevant higher concentrations of BaP for two weeks, and composition of both the genomic and active gut microbiome were assessed with DNA- and RNA-based 16S rRNA metagenetics, respectively. Lastly, fishes from the North Saskatchewan River were collected a year after an oil spill, and differences in the microbiome based on fish species and measured PAH muscle concentrations were assessed with 16S rRNA metagenetics.

Studies presented in this thesis revealed a clear influence of PAHs on the microbiome, even with relatively small exposures, while exposures to higher concentrations of PAHs resulted in microbial communities of the gut that were distinctly altered, with lost community structure as determined by co-occurrence networks. Notably, microbiomes in guts of male and female fish were affected differently by exposure to BaP, suggesting sex specific responses to

the chemical. Moreover, certain bacterial taxa were correlated with exposure to BaP, many of which were associated with hydrocarbon degradation and disease. Predicted functional analyses revealed several pathways that were correlated with BaP exposure, including increases in aromatic degradation pathways. Many of the conclusions were similar when analyzing the genomic and active microbiomes, but the active and DNA-normalized (the RNA/DNA ratio of bacterial abundances) active microbiomes provided greater resolution of the effects of BaP exposure. Finally, with the field study, it was determined that among goldeye (*Hiodon alosoides*), walleye (*Sander vitreus*), northern pike (*Esox lucius*), and shorthead redhorse (*Moxostoma macrolepidotum*), host species drive the assemblages of gut microbiomes. Additionally, several taxa associated with hydrocarbon degradation, inflammation, and disease were correlated with PAH concentrations in muscle tissue across the field-collected fishes, and walleye community composition was correlated with concentrations of PAHs in muscle tissue. Across all studies, PAH exposure can be a driver of bacterial community composition, and *Desulfovibrionaceae, Shewanellaceae* and *Chitinophagaceae* were positively correlated with PAH exposure in both laboratory-exposed fathead minnows and wild-caught fishes. Overall, this thesis provides novel data and new understanding into the effects of PAHs on the gut microbiomes of freshwater fish that can ultimately be used to better understand the connection between a toxicant and an adverse outcome *via* the microbiome.

# Acknowledgements

It is impossible to fully encapsulate and express the amount of gratitude I have for those who have helped me along this journey. First, I am thankful for the Dean's scholarship and Global Waters Futures for funding. To John, thank you for all your support during these past four years and for encouraging and believing in me. Thank you for all the time you have given to educate me in science and life, for providing opportunities for me to travel and learn, and for those fun moments watching Michigan football (even though we mostly lost). To Yuwei, who taught me pretty much everything that I needed to know during my PhD and entertained my all too often basic questions, thank you. You have been a great friend and mentor, and I solidly admit that I would not be here without you. Thank you also for encouraging me to try foods I never thought I would enjoy, and some that I definitely did not enjoy.

Thank you to my committee members, Markus H., Paul, Natacha, Lynn, and Janet, who always listened to me and were available to provide advice, whether about research or life. Thank you for being such great role models. Thank you to Champika for being so nurturing and taking the time to teach me new techniques in the lab, and to Tim and Markus B. for all your help along the way. Of course, I need to thank the Giesy lab members, both old and new. Dave, Garrett, Hattan, Anne, Phil, Alana, Bunmi, Jenna C., Jon, Su, and Gong, thank you all for surrounding me with encouragement and friendship. Niteesh and Anna, thank you for being such awesome undergraduates. To Jenna Z., my friend and fellow forager, who brought me home from the hospital not once, but twice, with broken bones, thank you again. And the rest of the Tox Centre faculty, students, and staff, thank you for being such great friends and scientists and pushing me to always be the best version of myself. Thank you to the Saskatchewan Health Authority for putting this clumsy American back together three times.

To Mom, Dad, and Dana, thank you for supporting me and never telling me that I was wasting my time. Thank you for teaching me the value of education and encouraging me to pursue my dreams. Mom, sorry you had to get *C. diff* to get me interested in the microbiome. Dad, sorry I am as clumsy as you. And of course, a thank you to the dogs I had the pleasure of hanging out with during this period: Charlie and my special boy Benson. You kept me company and always brought a smile to my face.

Finally, to Jeff. Thank you for supporting me, for loving me, and for never doubting me. It was hard to be apart so much during this journey, but knowing you cared made it easier. Now on to the next adventure!

## Table of Contents

**Permission to use** ..... i

**Abstract** ..... ii

**Acknowledgements** ..... iv

**List of Tables** ..... ix

**List of Figures** ..... xi

**List of Abbreviations** ..... xviii

**Note to Readers** ..... xxi

**CHAPTER 1: GENERAL INTRODUCTION** ..... 1

**1.1 Preface** ..... 1

**1.2 Gut microbial colonization** ..... 1

**1.3 Gut microbial services within the host** ..... 3

**1.4 The relationship between the microbiome and toxicants** ..... 4

**1.5 Polycyclic aromatic hydrocarbons and fitness of fishes** ..... 10

**1.6 Connection between the gut microbiome and PAHs** ..... 14

**1.7 Conclusions** ..... 15

**1.8 Objectives** ..... 15

**CHAPTER 2: Differential responses of gut microbiota of male and female fathead minnow (*Pimephales promelas*) to a short-term environmentally-relevant, aqueous exposure to benzo[*a*]pyrene** ..... 18

**2.1 Preface** ..... 18

**2.2 Abstract** ..... 19

**2.3 Introduction** ..... 20

**2.4 Materials and Methods** ..... 22

2.4.1 Fish husbandry, aqueous exposure, and sampling ..... 22

2.4.2 Quantification of BaP in exposure media ..... 22

2.4.3 16S rRNA metagenetics ..... 23

2.4.4 Quantitative Reverse-Transcription Real-Time ..... 24

2.4.5 Bioinformatics ..... 24

2.4.6 Statistics ..... 25

**2.5 Results** ..... 26

2.5.1 Concentrations of BaP in water ..... 26

2.5.2 Composition and sex differences of gut microbiota of fathead minnows ..... 27

2.5.3 Sex-specific responses of fathead minnows to BaP ..... 31

2.5.4 Host gene expression analyses ..... 33

**2.6 Discussion** ..... 35

**2.7 Conclusions** ..... 38

**2.8 Acknowledgements** ..... 38

**CHAPTER 3: Responses of juvenile fathead minnow (*Pimephales promelas*) gut microbiome to a chronic dietary exposure of benzo[*a*]pyrene ..... 39**

**3.1 Preface ..... 39**

**3.2 Abstract ..... 40**

**3.3 Introduction ..... 41**

**3.4 Materials and Methods ..... 43**

3.4.1 Fish husbandry, dietary exposure, and sampling ..... 43
3.4.2 Quantification of BaP in food ..... 44
3.4.3 Relative quantification of metabolites of BaP in bile ..... 44
3.4.4 16S rRNA metabarcoding and bioinformatics ..... 44
3.4.5 Statistics ..... 45

**3.5 Results ..... 46**

3.5.1 Concentrations of BaP in food and bile metabolites ..... 46
3.5.2 Gut microbiome of juvenile fathead minnows ..... 49
3.5.3 Dietary exposure of BaP altered the compositions of gut microbiomes in fathead minnows ..... 51
3.5.4 Dietary exposure of BaP altered predicted functional bacterial pathways of the gut microbiome in fathead minnows ..... 53
3.5.5 Effects on structure of the gut microbiome in fathead minnows exposed to BaP ..... 53

**3.6 Discussion ..... 58**

**3.7 Conclusions ..... 61**

**3.8 Acknowledgments ..... 62**

**CHAPTER 4: RNA metabarcoding unearths the response of rare gut microbiome of fathead minnows exposed to benzo[a]pyrene ..... 63**

**4.1 Preface ..... 63**

**4.2 Abstract ..... 64**

**4.3 Introduction ..... 65**

**4.2 Materials and Methods ..... 66**

4.4.2 Quantification of BaP in food and BaP metabolites in bile ..... 67
4.4.3 Metabarcoding and bioinformatics ..... 67
4.4.4 Statistics ..... 68

**4.5 Results ..... 69**

4.5.1 Concentrations of BaP in food and bile metabolites ..... 69
4.5.2 Active gut microbiome of juvenile fathead minnows ..... 69
4.5.3 Changes in compositions of active gut microbiome were correlated with dietary exposure of BaP ..... 76
4.5.4 Dietary exposure of BaP altered structure of active gut microbiome ..... 78
4.5.5 Concentrations of BaP metabolites correlated with predicted metabolic pathways of the active gut microbiome ..... 82
4.5.6 DNA-normalized active gut microbiome ..... 82

**4.6 Discussion ..... 85**

**4.7 Acknowledgements ..... 89**

**CHAPTER 5: Effects of the Husky oil spill on gut microbiota of native fishes in the North Saskatchewan River, Canada ..... 91**

**5.1 Preface ..... 91**

**5.2 Abstract** ..... **92**
**5.3 Introduction** ..... **93**
**5.4 Methods** ..... **95**
5.4.1 Sample collection ..... 95
5.4.2 Quantification of PBPAHs in bile and PAHs in muscle tissue ..... 97
5.4.3 16S rRNA metagenetics and bioinformatics ..... 98
5.4.4 Statistics ..... 99
**5.5 Results** ..... **100**
5.5.1 Gut microbiomes of native fishes from the North Saskatchewan River ..... 100
5.5.2 Concentrations of PAHs and PBPAHs in fishes in the North Saskatchewan River ..... 105
5.5.3 Effects of the oil spill on individual fish species ..... 107
**5.6 Discussion** ..... **109**
**5.7 Conclusions** ..... **113**
**5.8 Acknowledgments** ..... **114**
**CHAPTER 6: General Discussion** ..... **115**
**6.1 History and project rationale** ..... **115**
**6.2 Summary – The effects of PAHs on the microbiome in laboratory-raised fathead minnows as well as wild fishes in the North Saskatchewan River** ..... **117**
6.2.1 Characterization of the microbiomes of fathead minnows, goldeye, northern pike, shorthead redhorse, and walleye ..... 117
6.2.2 The sex-specific microbiomes of fathead minnows ..... 118
6.2.3 The active microbiome of fathead minnows ..... 118
6.2.4 PAHs alter the community structure of microbiomes ..... 119
6.2.5 Several taxa from the microbiome are correlated with PAH exposure ..... 121
**6.3 Future directions for this research** ..... **124**
**6.4 Final thoughts** ..... **125**
**References** ..... **127**
**Appendices** ..... **164**
**Appendix A** ..... **164**
**Appendix B** ..... **168**
**Appendix C** ..... **185**
**Appendix D** ..... **194**

# List of Tables

Table 2.1. Shannon diversity index, number of observed amplicon sequence variants (ASVs), Chao1, and Faith Phylogenetic Distance (PD) are presented for male and female fish at the different exposure levels (mean ± standard error, sample size n = 7-10 for females, 4-8 for males). (p. 29)

Table 3.1. Mean values and standard error for Shannon Diversity Index and observed number of amplicon sequence variants (ASVs) for each exposure group. Asterisks denote statistical differences from the control groups. (p. 57)

Table 4.1. Shannon Index values and number of observed amplicon sequence variants (ASVs) for each exposure group from the active gut microbiome. Mean and standard error values are presented. Dunnett's test: * $p < 0.1$, ** $p < 0.05$. (p. 75)

Table 4.2. Number of nodes and edges from the neighborhood selection networks, as determined with SPIEC-EASI, of the active gut microbiome, as discovered by RNA metabarcoding. (p. 81)

Table 6.1. Positively and negatively correlated families with BaP or PAHs, for laboratory-based and field-based studies, respectively, from each chapter. The source of the fish is given, along with any details about the fish, including sex, nucleotides isolated, and study species. Because Chapter 2 did not contain any measured concentrations of PAHs within the fish, the two taxa associated with exposure were calculated with Kruskal-Wallis tests rather than Spearman correlation. (p. 131)

Table A.1. Primer sequences and references. (p. 173)

Table A.2. Metrics indicating input sequences after demultiplexing as well as the number of filtered, denoised, merged, remaining after removal of chimeras, and bacteria only for all samples sequenced in this study. (p. 1734

Table B.1. Limit of quantification (LOQ) and limit of detection (LOD) of OH-BaP, BaP-Gluc, and BaP-$SO_4$. (p. 179)

Table B.2. The number of sequenced, filtered, denoised, merged, non-chimeric, and bacteria only reads for each sample. (p. 180)

Table B.3. Concentrations of benzo[*a*]pyrene (BaP) in food and metabolites of BaP in bile. Reported as mean ± standard errors (S.E.). (p. 185)

Table C.1. The number of counts of sequenced, filtered, denoised, merged, non-chimeric, and bacteria only reads for each sample. (p. 193)

Table C.2. Concentration of food and BaP metabolites along with respective standard errors for the different exposure groups. (p. 197)

Table C.3. Number of nodes and edges from the neighborhood selection networks, as determined with SPIEC-EASI, of the genomic gut microbiome, as discovered by DNA metabarcoding. (p. 201)

Table D.1. Sampling locations with corresponding latitudes and longitudes as well as indication of whether the sites were up or downstream from the oil spill. Mossy River Delta was a far-field reference site. (p. 202)

Table D.2. Number of input, filtered, denoised, merged, non-chimeric, and bacteria-only reads for each sample. (p. 202)

Table D.3. Shared bacterial genera from the gut microbiomes of shorthead redhorse, walleye, northern pike, and goldeye. (p. 206)

# List of Figures

Figure 1.1. Mechanisms by which toxicants and gut microbiota might interact: (A). Direct metabolization by gut microbiota followed by partitioning across the intestinal wall. (B). Oxidation and conjugation of toxicants in the liver for excretion to the bile, where the toxicant can enter the intestine for microbial metabolizing. Microbiota can deconjugate and reduce toxicants for easier reabsorption back to the liver, where these toxicant might return to their original form or generate toxic metabolites. (C). Composition of the gut microbiome might change from exposure to toxicants. (D). Metabolic activity of the gut microbiome might change from exposure to toxicants, which can alter toxic potencies of chemicals via biotransformation by bacteria. From Claus et al., 2016. (p. 6)

Figure 1.2. Following an exposure, susceptibility biomarkers of the exposure can be measured at several time points prior to clinical disease. Flow chart is adapted from Goldstein et al. (1987), to include the significance of the microbiome, indicating that the chemical first encounters the microbiome within an organism. From Dietert and Silbergeld, 2015. (p. 7)

Figure 1.3. Proposed framework for integration of the microbiome into an Adverse Outcome Pathway, where exposure to a chemical may precede a molecular initiating event (MIE) and result in microbial changes that ultimately impair host health. From Adamovsky et al., 2018. (p. 9)

Figure 1.4. Chemical structure of benzo[a]pyrene. (p. 12)

Figure 1.5. The aryl hydrocarbon receptor (AHR) pathway. PAHs first bind to the AHR; this complex is translocated to the nucleus, forms a heterodimer with AHR-nuclear translocator (ARNT), and binds to the xenobiotic-response element (XRE), inducing transcription of a number of genes, including cytochrome p450 1a (CYP1A) . From Callero and Loaiza-Pérez, 2011. (p. 12)

Figure 2.1. Relative proportions of 19 most abundant bacterial families. The first bar shows relative proportions of these taxa for all fish within the study. The second two bars show female

and male fish, respectively. The final bars show proportions of taxa for females and males, exposed to each concentration of BaP, respectively. (p. 28)

Figure 2.2. (A.) Relative abundances (%) of bacterial families that were significantly different between male and female fish ($p < 0.05$). Females are shown in red and males are shown in blue. (B.) Ordination of bacterial communities based on sex (PCoA with Bray-Curtis dissimilarity matrix). Females are shown with red circles and males are shown with blue triangles. (p. 30)

Figure 2.3. (A). Relative abundances (%) of bacterial families that were significantly different in exposure groups relative to the solvent control ($p < 0.05$) in female fish. (B).Ordination of bacterial communities based on exposure (PCoA with Bray-Curtis dissimilarity matrix) in female fish. (C). Relative abundances (%) of bacterial families that were significantly different in exposure groups relative to the solvent control ($p < 0.05$) in male fish. (D). Ordination of bacterial communities based on exposure (PCoA with Bray-Curtis dissimilarity matrix) in male fish. In the relative abundance plots, solvent control is shown in red, low in green, medium in blue, and high in purple. In each PCoA, the solvent control group is shown in red circles, the low group in green triangles, the medium group in blue squares, and the highest group in purple crosses. (p. 32)

Figure 2.4. Relative fold change in expressions of androgen receptor (*ar*), BCL2 Associated X, Apoptosis Regulator (*bax*), Cytochrome P450, family 1, subfamily A, polypeptide 1 (*cyp1a1*), estrogen receptor alpha (*esr1*), and vitellogenin (*vtg*) in female fish after four days of exposure to BaP ($n = 4$-5). Solvent control fish are shown in light grey while the highest exposure group are shown in dark grey. No significant differences between the groups were observed ($p > 0.05$). (p. 34)

Figure 3.1. Concentrations of BaP metabolites (OH-BaP, BaP-Gluc, BaP-$SO_4$, and the sum of all metabolites) (ng $g^{-1}$) from bile (± S.E.) on a $\log_{10}$-scale for each exposure group. Letters denote statistical significance within metabolite groups. (p. 48)

Figure 3.2. Relative abundances of the more abundant bacterial (A) phyla, (B) class, and (C) families in guts of juvenile fathead minnows, both pooled and based on exposures. (p. 50)

Figure 3.3. (A) Correlation plot of families that are significantly correlated (Spearman correlation, $p < 0.05$) with log-transformed BaP-$SO_4$ bile concentrations as well as with each other. (B) MetaCyc pathways that are significantly correlated ($p < 0.05$) with log-transformed BaP-$SO_4$ bile metabolite concentrations. Various pathways are shown relative to their correlation coefficients (ρ). (C) Constrained Analysis of Principal Coordinates (CAP) of the different exposure groups constrained by the vectors of the measured metabolite concentrations, using unweighted Unifrac distances. Log-transformed OH-BaP and BaP-$SO_4$ metabolites are the significant environmental variables constraining the ordination ($F = 3.00$ and 2.64, $p = 0.003$ and 0.005, for lgOH-BaP and lgBaP-$SO_4$, respectively). (p. 52)

Figure 3.4. Association networks of taxa at the class level relative to exposure groups for the (A) control, (B) 1, (C) 10, (D) 100, and (E) 1,000 μg $g^{-1}$ exposure groups. Associations were generated by SparCC with 100 bootstraps to assign p-values. The associations were filtered to include only correlations with a correlation $\rho > 0.7$ and a 'two-tailed' p-value < 0.01. Only correlations with $\rho > 0.50$ and $p < 0.05$ (two-tailed) were included. Networks with genus labels are presented in Appendix B, Fig. B.2. (p. 55)

Figure 4.1 Compositions of active gut microbiomes of fathead minnows exposed to benzo[*a*]pyrene at the (A). phylum, (B). class, and (C). family level. Less abundant taxa (averaged portion < 0.1%) were grouped together as others. (p. 71)

Figure 4.2. (A). Number of observed amplicon sequence variants (ASVs) of active and genomic gut microbiome. (B). Venn diagram of number of genera in DNA- or RNA-based extractions or the overlap between the two. Data from the genomic microbiome is from Chapter 3. (p. 73)

Figure 4.3. Families of bacteria from the gut microbiome that were (A). positively and (B). negatively correlated with lgBaP-$SO_4$ with the genomic, active, and DNA-normalized active microbiomes. Bacterial families that correlated with the genomic microbiome from Chapter 3.

(C). Relative abundance of the taxa that were significantly different in the exposure groups relative to the control, based on Dunnett's tests. (D). Constrained Analysis of Principal Coordinates (CAP) of the different exposure groups constrained by the vectors of the measured metabolite concentrations, using Bray-Curtis dissimilarities. Both lgOH-BaP and lgBaP-$SO_4$ metabolites were the significant environmental variables constraining the ordination ($p = 0.001$ and $p = 0.04$, respectively). (p. 77)

Figure 4.4. Neighborhood selection networks of active gut microbiome, as determined with SPIEC-EASI, after exposure to (A). Control, (B). 1, (C). 10, (D). 100, (E). 1000 μg g-1 BaP. Shape of node: bacterial phylum; color of node: bacterial class; size of node: abundance. (p. 79)

Figure 4.5. Heatmap of the MetaCyc pathways that are significantly correlated with lgBaP-$SO_4$ at each of the exposure concentrations. The correlation value of each pathway with lgBaP-$SO_4$ is shown on the left. Colors denote a scaled relative abundance for visualization, from the pheatmap package in R, of the MetaCyc pathways, with red indicating more abundant, and blue indicating less abundant. (p. 80)

Figure 4.6. Bootstrap averages of Metric MDS plot for (A). the DNA-normalized active microbiome, (B). the active microbiome, and (C). the genomic microbiome (from Chapter 3). ASVs were agglomerated to the genus level. Av: averaged resemblance. (p. 83)

Figure 4.7. (A). Heatmap of the abundance of DNA-normalized active gut microbiome in each exposure group. (B). Percent relative abundance of genera across all samples. (D). Percent abundance of genera in the genomic, from Chapter 3, and (D). active microbiomes. (E). Percent relative abundance of genera in the control (F). 1, (G). 10, (H). 100, and (I) 1000 μg $g^{-1}$ groups. In total, 8 genera were abundant (>1%), shown in blue, 13 genera were less abundant (0.1%-1%), shown in pink, and the remaining 30 genera were rare (<0.1%), shown in purple. (p. 84)

Figure 5.1. (A). Sampling sites along the North Saskatchewan River in Saskatchewan, Canada. Green points indicate the two upstream sites, Highway 17 and Highway 3. The purple point is the Point of Entry. The two red points are two downstream sites, Highway 21 and Paynton Ferry.

The blue point is the far-field reference site, Mossy River Delta. (B). Number of fish (N) of each species collected at each sampling site. (p. 104)

Figure 5.2. (A). Ten most numerous phyla found in the guts of goldeye, northern pike, shorthead redhorse, and walleye. (B). Venn diagram of number of overlapping genera in goldeye, northern pike, walleye, and shorthead redhorse, shown in gold, green, blue, and red, respectively. The number of shared genera among fish species are shown above the relative percent of those genera found across all species. (C). Shannon diversity index (D). Evenness, and (E). Number of observed ASVs of goldeye, northern pike, short head redhorse, and walleye. Letters denote statistical significance ($p < 0.05$). (p. 110)

Figure 5.3. (A). PCoA of log-transformed Bray-Curtis dissimilarities for goldeye, northern pike, shorthead redhorse, and walleye. Colors indicate different species. (B). Heat map of the indicator genera and relative abundance in each species of fish. Legend denotes scaled relative abundances of the various taxa, with blues indicating lesser abundances, and reds denoting greater abundance. (p. 112)

Figure 5.4. Mean (A). sum PBPAH concentrations (ng/g) from bile and (B). sum PAH concentrations (ng/g) from muscle tissue from fish collected upstream and downstream of the oil spill, in addition to the far-field reference site, in each of the species collected. Error bars are standard error of the mean. Letters denote statistical differences ($p < 0.05$). (p. 114)

Figure 5.5. Cumulative Abundance Profile (CAP) of genera found in the microbiome of (A). shorthead redhorse and (B). walleye at each sampling site. No factors were significant for shorthead redhorse. For walleye, condition factor (CF) was a significant factor constraining the ordination ($p = 0.04$), while concentration of PAHs in muscle of fishes was less significant ($p = 0.08$). (C). Families that significantly correlated ($p < 0.05$) with concentrations of PAHs in goldeye, shorthead redhorse, and walleye. (p. 116)

Figure A.1. Rarefaction curve of Shannon diversity for all samples in this study. (p. 172)
Figure B.1. Rarefaction curve of Shannon Diversity values across sequencing depths. (p. 186)

Figure B.2. Condition factor of fish exposed to BaP within each exposure group. Exposure did not significantly affect the condition factors of these fish. (p. 187)

Figure B.3. Association networks generated through SparCC assembled at the level of genera for fathead minnows exposed to (A) Control, (B) 1, (C) 10, (D) 100, and (E) 1000 μg g-1 BaP. (p. 188)

Figure B.4. Number of nodes generated through SparCC relative to $log_{10}$-transformed nominal concentrations of BaP ($p < 0.05$, $R^2 = 0.88$). (p. 192)

Figure C.1. Rarefaction curve of Shannon Diversity values across sequencing depths. (p. 197)

Figure C.2. PCoA of log-transformed Bray-Curtis dissimilarities of DNA- and RNA-based 16S rRNA metagenetics, shown in red and blue, respectively. (p. 198)

Figure C.3. (A). Genomic (from Chapter 3), (B). Active and (C). DNA-normalized families from the microbiome that are significantly correlated with log-transformed BaP-$SO_4$, along with the correlation values. (p. 199)

Figure C.4. Neighborhood selection networks of the genomic gut microbiome, as determined with SPIEC-EASI, from exposure to (A). Control, (B). 1, (C). 10, (D). 100, (E). 1000 μg $g^{-1}$ BaP. Shape of node: bacterial phylum; color of node: bacterial class; size of node: abundance. (p. 200)

Figure D.1. Rarefaction curve for estimated Shannon diversity of each sample. (p. 206)

Figure D.2. Fifteen most abundant (A). orders and (B). families found in the guts of goldeye, northern pike, shorthead redhorse, and walleye. (p. 207)

Figure D.3. Number of observed ASVs relative to sum PAH concentration (ng/g) along with 95% confidence intervals, shaded in grey, for (A). goldeye, (B). shorthead redhorse, and (C). walleye. (p. 208)

Figure D.4. Shannon diversity index relative to sum PAH concentration (ng/g), along with 95% confidence intervals, shaded in grey, for (A). goldeye, (B). shorthead redhorse, and (C). walleye. (p. 209)

# List of Abbreviations

16S ribosomal RNA (16S rRNA)

18S ribosomal RNA (18S rRNA)

2,3,7,8-tetrachlorodibenzo-*p*-dioxin (TCDD)

Aitchison's centered log-ratio (CLR)

Amplicon sequence variant (ASV)

Analysis of variance (ANOVA)

Androgen receptor (AR)

ANOVA-Like Differential Expression tool (ALDEx2)

Aromatase (CYP19A)

Aryl hydrocarbon receptor (AHR)

Aryl hydrocarbon receptor-nuclear translocator (ARNT)

Base pair (bp)

BCL2 Associated X (BAX)

Benzo[*a*]pyrene (BaP)

Body mass (bm)

Calcium carbonate ($CaCO_3$)

Carbon dioxide ($CO_2$)

Centimeter (cm)

Complimentary DNA (cDNA)

Condition factor (K)

Constrained Analysis of Principal Coordinates (CAP)

Cubed meters (m3)

cytochrome P450 1A (CYP1A)

Degrees Celsius (ºC)

Deoxyribonucleic acid (DNA)

Deuterated BaP (BaP d-12)

Dimethyl sulfoxide (DMSO)

Double stranded DNA (dsDNA)

Dry mass (dm)

Elongation factor (EF1)

Estrogen receptor 1 (ESR1)

Phylogenetic distance (PD)

Fathead minnow (FHM)

Gas chromatography-mass spectrometry (GC-MS)

Hour (hr)

Hydrogen ($H_2$)

Kruskal Wallis (KW)

Kyoto Encyclopedia of Genes and Genomes (KEGG)

Limit of detection (LOD)

Limit of quantification (LOQ)

Liter (L)

$Log_{10}$-transformed BaP-Gluc (lgBaP-Gluc)

$Log_{10}$-transformed BaP-$SO_4$ (lgBaP-$SO_4$)

$Log_{10}$-transformed OH-BaP (lgOH-BaP)

Microgram per mililitre (µg/mL)

Microliter (µL)

Mililiter (mL)

Milimeter (mm)

Milimol per liter (mmol/L)

Milligram per liter (mg/L)

Minute (min)

Mixed function oxidase (MFO)

Mono-hydroxylated benzo[a]pyrene (OH-BaP)

Multidimensional scaling (MDS)

Sodium sulfate ($Na_2SO_4$)

OH-BaP-O-glucuronide (BaP-Gluc)

Persistent organic pollutant (POP)

Polycyclic aromatic hydrocarbon (PAH)

Polymerase chain reaction (PCR)

Principal coordinate analysis (PCoA)

Quantitative real-time polymerase chain reaction (qPCR)

Ribonucleic acid (RNA)

Sample size (N)

Solid-phase extraction (SPE)

Sparce Correlations for Compositional data (SparCC)

Sparse inverse covariance estimation for ecological association inference (SPIEC-EASI)

Statistical Analysis of Metagenomic Profile (STAMP)

Sulfate-BaP (BaP-$SO_4$)

Sulfuric acid ($H_2SO_4$)

Uridine diphosphate (UDP)

Vitellogenin (*vtg*)

# Note to Readers

This thesis is organized and formatted to follow the University of Saskatchewan College of Graduate and Postdoctoral Studies guidelines for a manuscript-style thesis. Chapter 1 is a general introduction and literature review, including the project goal and objectives, and Chapter 6 is a synthesis chapter, containing a general discussion and conclusions that tie the chapters together. Chapters 2, 3, 4 and 5 of this thesis are organized as manuscripts for publication in peer-reviewed scientific journals. Chapter 2 has been published in Chemosphere, Chapter 3 will be submitted to Environmental Science and Technology, Chapter 4 will be submitted to Environmental Toxicology and Chemistry, and Chapter 5 has been submitted to Aquatic Toxicology. Due to this manuscript-style format, there is some repetition in the introductions and materials and methods sections of the thesis. All tables, figures, supporting information, and references cited in the research chapters of this thesis have been reformatted to the thesis style. References cited in each chapter are combined and listed in the References section of this thesis. Supporting information associated with research chapters are presented in the Appendix section at the end of this thesis.

# CHAPTER 1: GENERAL INTRODUCTION

## 1.1 Preface

Chapter 1 is a general introduction and literature review regarding the topics of colonization and services of the gut microbiome, general effects of xenobiotics on the gut microbiome, the effects of polycyclic aromatic hydrocarbons (PAHs) in fish, and the connection between PAHs and the microbiome. As the scope of my research is focused on Teleostei, or an infraclass of ray finned fishes, this literature review will follow suit, drawing from the wealth of literature in mammal microbiomes to supplement knowledge gaps in the fish microbiome. Chapter 1 also includes the overall goals and objectives of this work and within each study.

## 1.2 Gut microbial colonization

Often referred to as the "forgotten organ," the gut microbiome is a critical part of development and fitness across the animal kingdom (O'Hara and Shanahan, 2006). The gut microbiome is an assemblage of commensal, mutualistic, and pathogenic bacteria that reside in a host and are associated with health and disease (Lederberg and McCray, 2001). Microbes inhabit the skin and gastrointestinal (GI) across metazoa, the urogenital and respiratory tracts in mammals, and gills of fishes; the GI tract contains the largest abundance and diversity of microbes (Llewellyn et al., 2014; Sekirov et al., 2010). In viviparous animals, it is believed that colonization by microbes begins at birth, as offspring pass through the birth canal (Penders et al., 2006), although recent evidence suggests that colonization begins *in utero* (Perez-Muñoz et al., 2017). In oviparous organisms, such as fish, colonization is believed to begin at hatching with the first environmental interaction (Llewellyn et al., 2014; Yan et al., 2016).

Early in development, the bacterial community is prone to be influenced by diet and environmental factors, but rapid changes in the microbial community quickly disappear, and the gut microbiome becomes more stable with age (Sekirov et al., 2010). In fish, a clear separation exists among gut microbiomes of the larval, juvenile, and adult stages, and microbial diversity tends to decrease as fish age and the digestive system develops (Yan et al., 2016). Because of their less-developed digestive system, young fish rely on the gut microbiome to assist with digestion of food. Thus, gut microbial communities of younger fishes are more diverse (Yan et al., 2016). As larvae, fish, regardless of species, tend to share a common microbiome, whereas separation among species becomes more distinguished as fish mature (Yan et al., 2016).

Animals that do not undergo initial colonization by bacteria are affected by several deleterious abnormalities, particularly related to the immune system. The gut microbiome is critical in development of the intestinal mucosal and systemic immune system. Gnotobiotic mice fail to properly develop spleens and lymph nodes; these mice also have variations in amounts of cytokines as well as fewer types of immunoglobulin A (IgA)-producing plasma cells and secreted immunoglobulins (Macpherson and Harris, 2004; Sekirov et al., 2010). Germ-free zebrafish begin showing signs of epidermal degradation by 9 days-post-fertilization (dpf) and fail to survive past 20 dpf. When a microbial community is added at three or six dpf, zebrafish survive to adulthood (Rawls et al., 2004). Germ-free zebrafish are unable to resist viral infections (Garcia-Moreno et al., 2012), do not have proper neutrophil migration following an injury (Kanther et al., 2014), have reduced expression of innate immune genes, and lack proper turnover of gut epithelium (Rawls et al., 2004). These individuals have impaired tissue repair after injury and fail to properly express innate immune genes, all functions that might return upon proper gut microbial colonization (Kelly and Salinas, 2017). Without properly functioning microbiomes, organisms are unlikely to survive (Rawls et al., 2004), thrive (Garcia-Moreno et al., 2012), or reproduce (Williams et al., 2020).

The bacterial composition of the microbiome varies among individuals, but the predominant genera, known as the enterotype, within individuals in hypothesized to be associated with either health or disease (Cryan and Dinan, 2012). Compositions of microbiomes also have genetic components and can be influenced by species of the host or even genetic mutations within individuals (Givens et al., 2015; Sekirov et al., 2010). Among fishes, *Proteobacteria* tend to comprise about a third of the total bacteria in the gut, and inhabit the gut with other abundant bacterial families such as *Shewanellaceae*, *Aeromonadaceae*, *Pseudomonadaceae*, *Fusobacteria*, *Clostridium*, and *Bacteroidetes* (Gómez and Balcázar, 2008; Narrowe et al., 2015; Pérez et al., 2010). In general, the guts of fishes contain $10^7$-$10^8$ bacteria per gram of gut tissue (Gómez and Balcázar, 2008; Pérez et al., 2010).

Compositions of microbial communities in guts of adult herbivorous, omnivorous, and carnivorous fishes are distinct from one another, with carnivorous fishes having the least diversity of microbes in the gut (Sullam et al., 2012). Abundance of *Proteobacteria* are often greater in fishes of higher trophic levels, whereas abundance of *Firmicutes* are prominent in fishes of lower trophic levels (Yan et al., 2016). Additionally, *Bacteroidetes* are relatively abundant in herbivorous fishes, but almost absent in omnivorous and carnivorous fishes (Yan et al., 2016). Differences in the gut microbiome among the different feeding strategies are potentially due to differing enzymatic requirements to digest animal tissue as opposed to plant matter (Liu et al., 2016).

## 1.3 Gut microbial services within the host

Gut microbiota are primarily associated with three functions: nutrition, innate immunity, and regeneration of epithelial cells (Kelly and Salinas, 2017). This includes a myriad of beneficial processes, including motility of the gut, distribution of lipids, and absorption of nutrients, all of which are critical for maintaining overall health and preventing disease (Bercik et al., 2012; Cryan and Dinan, 2012). Furthermore, the gut microbiome has been associated with preventing colonization of pathogenic bacteria and stimulating immune responses (Gaulke et al., 2016). Organisms rely on the diverse composition of the microbiome in their guts to provide these essential services (Kelly and Salinas, 2017), and rarer taxa might be as crucial as abundant taxa for proper functioning of organisms. These taxa provide “seed stock” that are not always required to be present in large numbers, but are available to respond to changing

conditions (Caporaso et al., 2012; Rolig et al., 2015).

The interface between gut bacteria and a fish host is the mucosal layer within the intestine, which contains a variety of enzymes, piscidins, and defensins that are protective and antimicrobial (Montalto et al., 2009; Pérez et al., 2010). Epithelial cells under the mucus layer act as a physical barrier that separates the intestinal lumen from the rest of the body, aid in food digestion, process information received from both the immune system and gut microbiota, and sense various components of the bacteria to distinguish pathogenic from commensal bacteria (Cario, 2005; Groschwitz and Hogan, 2009). Underneath epithelial cells, the gut-associated lymphoid tissue (GALT) is a major component of the immune system that protects the body from pathogens (Forchielli and Walker, 2005); proper development of the GALT is mediated through commensal bacteria (Cebra et al., 1998; Pérez et al., 2010).

In mammals, dysbiosis, or microbial imbalance, in the gut is associated with a number of deleterious effects, including inflammatory bowel disease, metabolic syndrome and even obesity (Carding et al., 2015; He et al., 2020). In teleosts, where information is more scarce, dysbiosis is linked to a greater prevalence of stress and disease (Llewellyn et al., 2014). Studies linking the gut microbiome and behavior have mostly been conducted in mammals (Cryan et al., 2019). Co-morbidity of disorders affecting the brain-gut axis is attributed to alterations of the gut microbiome; associated psychiatric disorders that overlap with gastrointestinal syndromes include anxiety, irritable bowel syndrome (IBS), and eating disorders (Cryan and Dinan, 2012; Lu et al., 2015). Additionally, disruption of the microbiome due to a singular stressor such as chronic stress differentially affects juveniles and adults. For example, dysbiosis in the juvenile microbiome is associated with decreased brain development, whereas dysbiosis of the adult microbiome is associated with increased presence of inflammatory cytokines (Cryan and Dinan, 2012; Galley et al., 2014). Stressful conditions, such as transport of live fish, have been shown to activate the immune system and alter the skin (Tacchi et al., 2015) and gut (Ringø et al., 2016) microbiomes.

## 1.4 The relationship between the microbiome and toxicants

Surrounding environmental conditions in a fish's habitat influence the microbiomes of fishes. Communities of microbes in the gut are first colonized from the environment in which they hatch and are then shaped by the environment in which they feed, live, and reproduce.

Perturbations in the environment can lead to the opportunity for pathogenic bacteria to dominate (Yan et al., 2016) or for improper gut colonization through development (Rawls et al., 2004).

The interplay of environmental contaminants with the gut microbiome has recently gained traction in the field of environmental toxicology (Adamovsky et al., 2018). The interaction between toxicants and the microbiome often begins with ingestion, or through contact with skin or gills (Schlenk et al., 2008). These toxicants can be transferred to blood and absorbed through the intestine, excreted into bile, and/or metabolized by gut microbiota (Figure 1.1; Claus et al., 2016). In addition to traditional absorption that is central to toxicology and pharmacology, when a chemical encounters the microbiome, whether in the gut, at the gill, or on the skin, the bacteria can change the properties of the chemical, ultimately altering the dose or even composition of the chemical being absorbed and then distributed, metabolized, and excreted (Van de Wiele et al., 2005). Interactions between toxicants and the microbiome can change the amount of toxicant to which an organism is exposed at an organismal-, tissue-, or even cellular-level, creating potential adverse outcomes at concentrations that are less than expected (Figure 1.2; Silbergeld, 2017). When the molecular mass of a toxicant is less than 325 kDa and is non-polar, the molecule can be transported in blood to the liver for phase II enzymatic conjugation with sulfate, glutathione or glucuronic acid, to eventually be excreted in urine (Boelsterli, 2007). For toxicants with greater molecular masses, epithelial cells in the intestine produce phase I and phase II enzymes to metabolize those toxicants (Buesen et al., 2003) and are responsible for resorption of toxicants to the intestine during enterohepatic circulation (Buesen et al., 2002). Gut microbiota can also deconjugate and reduce toxicants for reabsorption into the liver (Boelsterli, 2007; Claus et al., 2016).

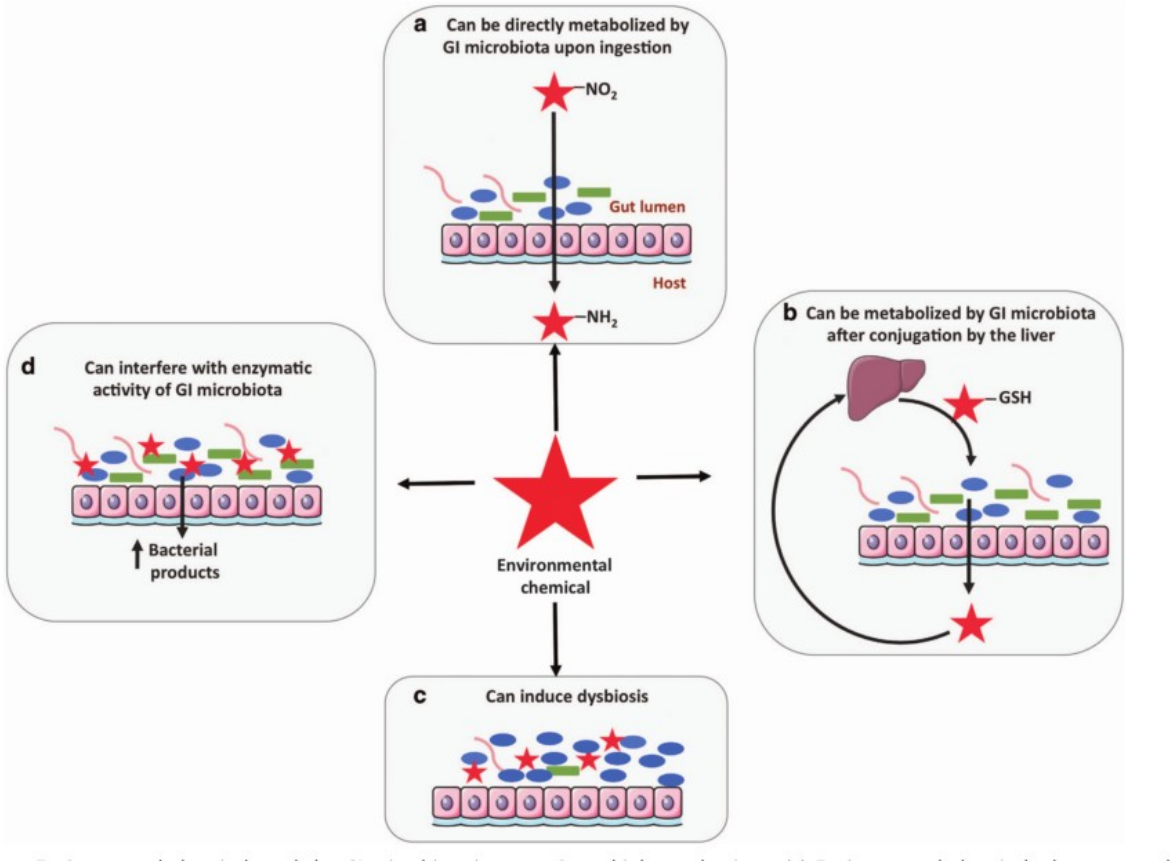


Figure 1.1. Mechanisms by which toxicants and gut microbiota interact: (A). Direct metabolization by gut microbiota followed by partitioning across the intestinal wall. (B). Oxidation and conjugation of toxicants in the liver for excretion to the bile, where the toxicant can enter the intestine for microbial metabolizing. Microbiota can deconjugate and reduce toxicants for easier reabsorption back to the liver, where these toxicant might return to their original form or generate toxic metabolites. (C). Composition of the gut microbiome might change from exposure to toxicants. (D). Metabolic activity of the gut microbiome might change from exposure to toxicants, which can alter toxic potencies of chemicals *via* biotransformation by bacteria. From Claus et al. 2016.

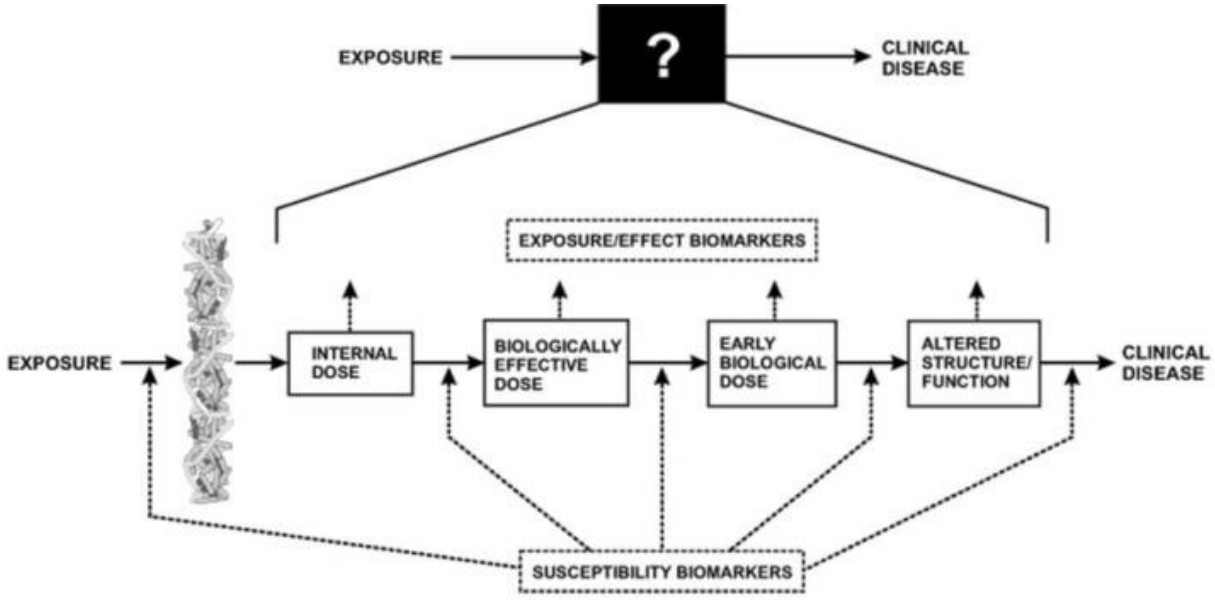


Figure 1.2. Following an exposure, susceptibility biomarkers of the exposure can be measured at several time points prior to clinical disease. Flow chart is adapted from Goldstein et al. (1987), to include the significance of the microbiome, indicating that the chemical first encounters the microbiome within an organism. From Dietert and Silbergeld 2015.

Three conceptual tiers by which gut microbiota can alter properties of xenobiotics exist: specific enzymes, specific taxa, and the overall community (Klünemann et al., 2014). Bacterial enzymes are inherently promiscuous and can often metabolize a large number of compounds. These enzymes are secreted by particular species that make up a community full of bacteria that not only differentially metabolize compounds, but metabolize the compounds of other bacteria within the community (Klünemann et al., 2014). Attempts have been made to model the microbial transformation of xenobiotics in a similar fashion as with liver biotransformation or bioremediation, but because of the complexity, this has been met with limited success (Haiser and Turnbaugh, 2013; Klünemann et al., 2014). Furthermore, certain taxa are capable of utilizing contaminants as growth substrates as they metabolize these compounds, allowing proliferation of those species when confronted with contaminants or the metabolites generated by other taxa (Cavalca et al., 2007; Ho et al., 2000). Finally, the composition of the overall community determines which taxa are present and how the taxa interact with one another as well as with a xenobiotic (Viñas et al., 2005).

Because the microbiome is an important factor in organismal health and can be modulated by toxicants, the microbiome can be incorporated into the Adverse Outcome Pathway (AOP) framework. AOPs are defined as a sequence of events from a molecular initiating event (MIE) through a cascade of molecular and cellular key events, modulated by key event relationships, within a host and lead to an apical, usually adverse, outcome at a given level of biological organization (Fig. 1.3; Ankley et al., 2010). Incorporation of the microbiome into toxicology framework necessitates a deep understanding of the ecological theories that underlay the complex microbial interactions and their relationship with the host (Greyson-Gaito et al., 2020). This concept of the integrating the microbiome into the AOP framework has been thoroughly discussed in Adamovsky et al. (2018).

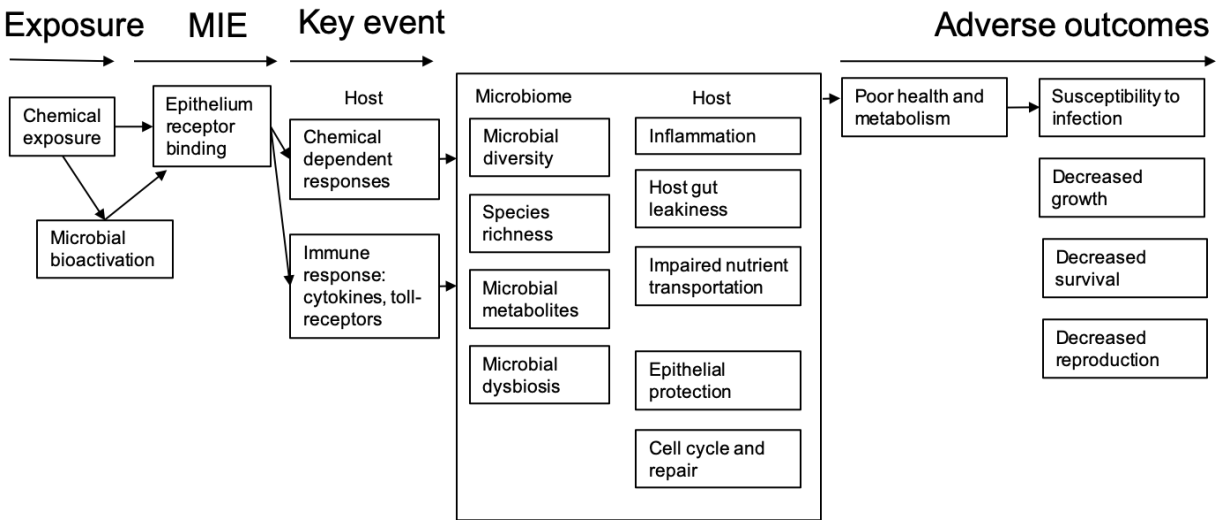


Figure 1.3. Proposed framework for integration of the microbiome into an Adverse Outcome Pathway, where exposure to a chemical may precede a molecular initiating event (MIE) and result in microbial changes that ultimately impair host health. From Adamovsky et al. 2018.

Several chemicals are associated with rapid, severe shifts in microbial communities of guts of fishes. During laboratory studies, triclosan, an antimicrobial agent used in consumer products, has been observed to cause alterations in microbial communities in guts of both zebrafish and fathead minnows (Gaulke et al., 2016; Narrowe et al., 2015). Results of those studies also indicate that changes in microbial communities are due to persistence of bacteria that are resistant to triclosan and a decrease in the bacterial communities that are sensitive to triclosan (Gaulke et al., 2016; Narrowe et al., 2015). It is also likely that bacteria in the gut have the ability to transform triclosan similar to bacteria found in the environment. This process could potentially lead to an unexpected exposure of the organism to degradation products of triclosan, which can also be toxic and bioaccumulate in fish (Narrowe et al., 2015).

Exposure of male zebrafish to imazalil, a fungicide used to control fungus growth on produce, is associated with several changes in the gut microbiome (Jin et al., 2017). Significant increase in bacterial diversity in the gut microbiomes were observed along with shifts in the abundance of several bacterial taxa (Jin et al., 2017). Results of this study suggest that the disruption of microbiota due to exposure to imazalil may be directly or indirectly affecting hepatic metabolism and associated disorders of energy metabolism (Jin et al., 2017).

Following perturbation of microbiota of the gut, relative proportions of bacteria within these communities can return to basal conditions once the stressor is removed (Narrowe et al., 2015). This provides a positive outlook for areas of moderate environmental contamination upon commencement of environmental remediation. However, timing is critical, and even a short-term disturbance in the gut microbiome might impair proper development in juvenile fishes or allow for opportunistic infections (Rawls et al., 2004; Yan et al., 2016). Bacterial dysbiosis in the gut can ultimately have direct consequences for the host and alter the impact of the contaminant on the organism (Levy et al., 2017; Thaiss et al., 2016).

## 1.5 Polycyclic aromatic hydrocarbons and fitness of fishes

Polycyclic aromatic hydrocarbons (PAHs) are defined as a chemical group with the fusion of two or more aromatic rings in linear, cluster, or angular formation and result from the biotransformation of aromatic amino acids or lignin compounds (biogenic), combustion

(pyrogenic), or petroleum or petroleum-derived sources (petrogenic) (Seo et al., 2009). Anthropogenic sources of PAHs in the environment are often derived from fossil fuel oils and found in industrial areas such as refineries and also in urban centers where automobile exhaust and tire wear debris are abundant (Srogi, 2007). PAHs bind to particles in the environment, leading to accumulation in soils and sediments (Baek et al., 1991), and PAHs enter the bodies of aquatic organisms when ingested or through aqueous exposure (Wang and Wang, 2006).

Heavy crude oil is a dense, viscous oil that is a complex mixture of saturates, resins, aromatics, and asphaltenes (Yang et al., 2020). Heavy crude oil can sink and become deposited in sediments, ultimately accumulating in and interacting with biota (Fitzpatrick et al., 2015). The ecotoxicological effects of oil spills in fish have been well-characterized in marine ecosystems (i.e. Barron, 2012; Beyer et al., 2016; Danion et al., 2011). Fish are exposed to crude oil *via* ingestion of prey or sediment, ventilation of water over gills, or through dermal absorption (Douben, 2003; Nichols et al., 1996). Exposure to high concentrations of PAHs, such as naphthalene, benzo[*a*]pyrene (BaP), and pyrene that would be found in crude oil, can result in a number of harmful sublethal effects in fish, including DNA damage, cardiotoxicity, immunosuppression, reduced reproductive capacity, and hepatic neoplasms (Brown-Peterson et al., 2017; Hicken et al., 2011; Tuvikene, 1995).

BaP, a constituent of heavy crude oil, is a high molecular weight, 5-ring PAH (Fig. 1.4) and is abundant in industrial and urban areas (Irwin, 1997). Heavier PAHs, such as BaP, have a higher potential to cause chronic impairment and are more carcinogenic (Irwin, 1997). Metabolic activation is required for BaP to become mutagenic (Stansbury et al., 1994; Fig. 1.5); BaP must first bind to the aryl hydrocarbon receptor (AHR), then becomes translocated to the nucleus, forming a heterodimer with AHR-nuclear translocator (ARNT) (Shimizu et al., 2000). This complex binds to the xenobiotic-response element (XRE) upstream on many genes, including the cytochrome p450 1a (CYP1A) gene to induce its expression. CYP1A then acts upon BaP to generate reactive metabolites (Shimizu et al., 2000).

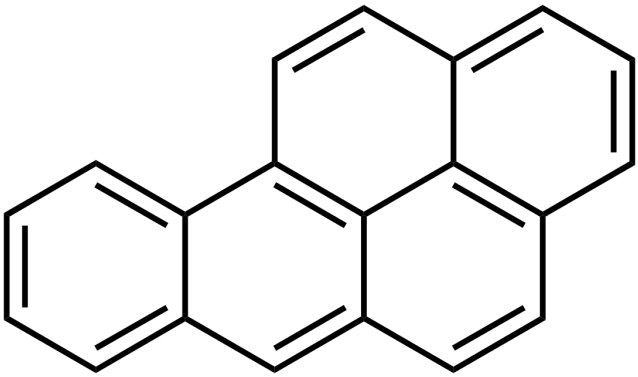

Figure 1.4. Chemical structure of benzo[*a*]pyrene.

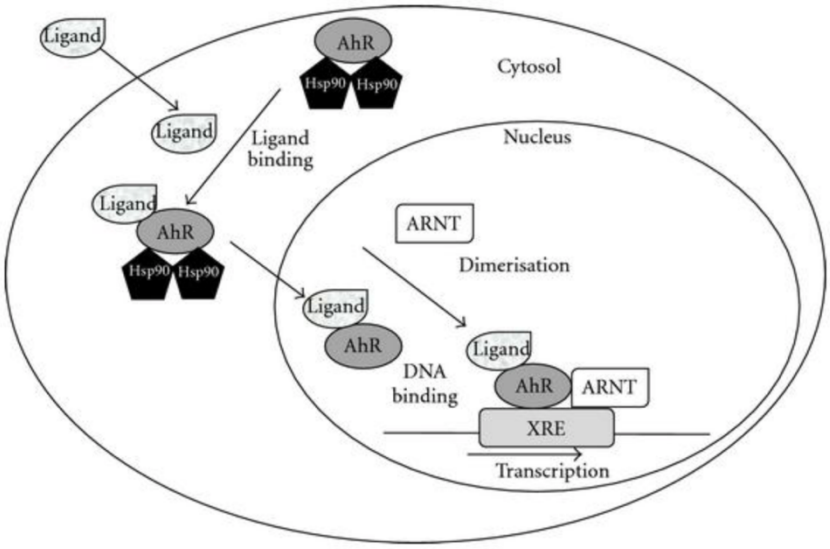


Figure 1.5. The aryl hydrocarbon receptor (AHR) pathway. PAHs first bind to the AHR; this complex is translocated to the nucleus, forms a heterodimer with AHR-nuclear translocator (ARNT), and binds to the xenobiotic-response element (XRE), inducing transcription of a

number of genes, including cytochrome p450 1a (CYP1A) . From Callero and Loaiza-Pérez 2011.

Phase I enzymes that convert BaP to hydrophilic intermediates include the cytochrome P450 mixed function oxidases (MFOs), epoxide hydrolases, and epoxide reductases, and Phase II conjugating enzymes include glutathione transferases, sulfotransferases, and uridine diphosphate (UDP)-glucuronyl transferases (Miller and Ramos, 2001). Cytochrome P450s generate epoxides that can covalently bind to proteins and nucleic acids, causing cellular impairment (Stansbury et al., 1994). When BaP binds to DNA, it can result in a base pair transversion, which can ultimately lead to a point mutation; if this inactivates a tumor suppressor gene or causes overexpression in a proto-oncogene, cancer may occur (Boelsterli, 2007). BaP can cause adverse outcomes such as lesions and tumors, in part due to the formation of reactive metabolites that can form adducts and cause damage to DNA, RNA, or proteins (Beyer et al., 2010; Tuvikene, 1995). BaP can also suppress the immune system (Carlson et al., 2004a), cause developmental defects (Corrales et al., 2014), and impair reproductive capacity (Booc et al., 2014).

Because PAHs are rapidly transformed to metabolites that can bind to tissues or can be excreted, body burdens of PAHs tend to be very low. Therefore, Products of Biotransformation of PAHs (PBPAHs) are often measured in the bile rather than traditional whole body or muscle measurements (Beyer et al., 2010; Ohiozebau et al., 2016). The liver is the primary site of phase I and phase II biotransformation of PAHs; PAHs undergo biotransformation and are stored in the bile in the liver. Following this, these products reenter the digestive system and undergo enterohepatic circulation (Beyer et al., 2010). Enterohepatic circulation is mainly considered a product of changes in pH from the bile to the intestine, causing PAH products to become hydrolyzed, and thus more hydrophobic, to facilitate re-entry into the portal vein and back to the liver (Beyer et al., 2010).

## 1.6 Connection between the gut microbiome and PAHs

Although deleterious effects of PAH to fish have been well defined (i.e. Carlson et al., 2004; Costa et al., 2011; Nacci et al., 2002; Phalen et al., 2014), effects of this class of compounds on the microbiome have seldom been studied, particularly in fish. Recently it has been recognized that the AHR is a regulator of host-microbiota communications (Zhang et al., 2017), and that this relationship is bidirectional (Korecka et al., 2016). Therefore, it is conceivable that PAHs can directly act upon the AHR and modulate bacterial communities in guts of fishes.

Studies have begun investigating connections between PAHs and gut microbial communities. Much of our understanding results from studies of fish in areas with highly contaminated sediment or soil. In sediments, environmental contamination and perturbation can reduce bacterial diversity and species complexity (Torsvik et al., 1996; Xie et al., 2016). In water and soil, biodegradation by bacteria is well-documented, with community compositions shifted towards taxa capable of degrading and utilizing PAHs as a growth substrate (Hazen et al., 2010). Through the process of oxidation-reduction reactions, bacteria can also transform PAHs into more polar, potentially less toxic byproducts (Blaga, 2013); several taxa in the classes *Alphaproteobacteria, Betaproteobacteria,* and *Deltaproteobacteria* have been identified as hydrocarbon degraders (Seo et al., 2009; Xie et al., 2016). To a lesser extent, some work has linked exposure of mammals to PAHs with shifts in microbial communities. In a simulated human gut system, bacteria were observed to metabolize BaP to several metabolites (Van de Wiele et al., 2005), including into estrogenic hydroxy-PAHs, potentially modulating the risk involved with exposure (Van de Wiele et al., 2005). Human skin bacterial isolates can similarly degrade BaP (Sowada et al., 2018). Exposure of mice (*Mus musculus*) to BaP resulted in shifts in bacterial community composition in the gut and enrichment of certain taxa associated with PAH degradation.

Examples of other studies investigating effects of PAHs on gut microbiomes in fish include an exposure of southern flounder (*Paralichthys lethostigma*) to oil from the Deepwater Horizon oil spill in the Gulf of Mexico (Bayha et al., 2017). This exposure resulted in taxonomically distinct microbial communities in the gut and the gills of exposed fish, predicted Kyoto Encyclopedia of Genes and Genomes (KEGG) pathways associated with organic molecule degradation, and a larger proportion of the oil-degrading bacteria

*Oceanospirillales, Thalassolituus* and *Alcanivorax* were observed (Bayha et al., 2017). Furthermore, aqueous exposure of Japanese sea cucumbers (*Apostichopus japonicus*) to BaP resulted in a shift in gut microbiota, where exposed sea cucumbers had fewer bacteria associated with beneficial functions within the host and growth of alkane-degrading bacteria (Zhao et al., 2019).

## 1.7 Conclusions

Sufficient evidence exists to support the notion that exposure to PAHs can result in changes in the microbiome that may ultimately impact host fitness, but very little data is available how the microbiome may change in response to that exposure. While it has been well agreed upon that consideration of the microbiome is essential for understanding the implications of a contaminant on an organism, data are lacking, particularly in environmentally-relevant species. PAHs are ubiquitous and found throughout the world; their well-defined toxicities allow for investigation into more complex questions. These contaminants are routinely released in our industrialized society, therefore the findings of this study will continue to be relevant. As discussed above, some studies have observed changes in the gut microbiome in response to PAH exposures, but no information is available on the effects of PAH exposure on the gut microbiome by different routes, ages, or exposures settings (i.e. laboratory-raised versus wild). The research presented in this thesis attempts to bridge these knowledge gaps and build foundation for future studies.

## 1.8 Objectives

The research carried out in this Ph.D. sought to use BaP and an opportunistic heavy crude oil spill to determine if bacterial shifts occur from exposure to aqueous and/or dietary routes of BaP in fathead minnows (*Pimephales promelas*), and whether any findings were consistent in field-collected fish from a site of heavy crude contamination. The overall goal of this research was to establish an association between exposure to PAHs and gut microbial dysbiosis.

**Objective 1**: Ascertain whether or not a four-day aqueous exposure to environmentally-

relevant concentrations of BaP modulated the gut microbiome of adult fathead minnows, and if any community shifts observed were sex dependent (Chapter 2). Specific objectives were to:

1) Characterize the gut microbiome in adult fathead minnows *via* the abundances of bacterial taxa
2) Evaluate whether there are differences in alpha- or beta-diversities or in the abundances of specific bacteria in the gut microbiome between males and females
3) Use alpha- and beta-diversities, as well as differential abundances of specific bacteria and predicted bacterial functions, to determine if there are changes in the gut microbiome in exposed fish, relative to unexposed controls
4) Determine if BaP alters the hepatic gene expression of *cyp1a*

**Objective 2:** Determine if a dietary exposure to BaP can modulate the gut microbiome in juvenile fathead minnows following a two-week dietary exposure to BaP (Chapter 3). Specific objectives were to:

1) Characterize the gut microbiome in juvenile fathead minnows *via* the abundances of bacterial taxa
2) Determine whether or not measured bile metabolite concentrations are correlated with dietary exposure to BaP
3) Ascertain the effects of BaP on the microbiome, using network analysis, alpha- and beta-diversities, as well as differential abundances of specific bacteria and predicted bacterial functions, in guts of individuals exposed to BaP, relative to that of unexposed controls
4) Assess whether or not alpha- and beta-diversities as well as abundances of specific bacteria and predicted bacterial functions are significantly correlated with measured BaP metabolite body burden

**Objective 3:** Establish if RNA-based 16S rRNA analyses are consistent with DNA-based methods or provide additional insight into the effects of a dietary exposure of BaP on the juvenile fathead minnow microbiome (Chapter 4). Specific objectives were to

1) Characterize the active gut microbiome in juvenile fathead minnows *via* the abundances of bacterial taxa

2) Ascertain the effects of BaP on the active microbiome, using network analysis, alpha- and beta-diversities, as well as differential abundances of specific bacteria and predicted bacterial functions, in guts of individuals exposed to BaP, relative to that of unexposed controls
3) Assess whether or not alpha- and beta-diversities as well as abundances of specific bacteria and predicted bacterial functions are significantly correlated with measured BaP metabolite body burden
4) Determine whether or not the genomic and active gut microbiomes share similar response patterns in individuals exposed to BaP

**Objective 4:** Investigate the overall gut microbial diversity as well as the effects of exposure to heavy crude oil on native, wild fishes in the North Saskatchewan River (Chapter 5). Specific objectives were to:

1) Characterize the gut microbiomes of walleye (*Sander vitreus*), northern pike (*Esox lucius*), goldeye (*Hiodon alosoides*), and shorthead redhorse (*Moxostoma macrolepidotum*) *via* the abundances of bacterial taxa and through alpha- and beta-diversity analyses
2) Assess whether or not concentrations of products of biotransformation of PAHs in bile and PAHs in muscle are associated with areas downstream of the oil spill
3) Determine the effects of the oil spill on the gut microbiomes of those native fishes using alpha- and beta-diversities as well as differential abundances of specific bacteria and correlating those metrics to measured PAH concentrations in fish bile and muscle tissue

# CHAPTER 2: Differential responses of gut microbiota of male and female fathead minnow (*Pimephales promelas*) to a short-term environmentally-relevant, aqueous exposure to benzo[*a*]pyrene

## 2.1 Preface

This chapter focuses on the effects of benzo[*a*]pyrene (BaP) on the gut microbiomes of male and female fathead minnows (*Pimephales promelas*) after a four-day, aqueous exposure, using environmentally-relevant low concentrations. Using 16S rRNA metagenetics, it was determined that exposure to BaP can alter the microbial composition of the gut microbiome, but only in female fish. Furthermore, gene expression levels of mRNA for *cyp1a1*, a biomarker of exposure to BaP, were not affected, signifying that the microbiome may have a greater sensitivity to BaP than the host. This work highlights that in addition to effects on well-studied molecular endpoints, relative compositions of the microbiota in guts of fish can quickly respond to exposure to chemicals, and that effects of toxicants on the microbiome can be sex-specific.

The content of Chapter 2 was reprinted (adapted) from Chemosphere (DOI: 10.1016/j.chemosphere.2020.126461). Abigail DeBofsky, Yuwei Xie, Chelsea Grimard, Alper James Alcaraz, Markus Brinkmann, Markus Hecker, John P. Giesy. "Differential responses of gut microbiota of male and female fathead minnow (*Pimephales promelas*) to a short-term environmentally-relevant, aqueous exposure to benzo[*a*]pyrene" Aug;252:126461.


Author contributions:

- Abigail DeBofsky: All bench work (except for qPCR) (100%), bioinformatics (90%), statistical analysis (90%), and completion of manuscript (100%)
- Dr. Yuwei Xie: Assistance with statistical analysis (10%), bioinformatics (10%), and revisions of the manuscript (80%)

- Chelsea Grimard: Design and setup of exposure (80%)
- Alper James Alcaraz: Performed the qPCR (100%)
- Dr. Markus Brinkmann: Assistance with design and setup of experiment and qPCR (20%) and edited the manuscript (5%)
- Drs. Markus Hecker and John P. Giesy: Provided scientific input and guidance, edited the manuscript (15%), and provided funding for the research

## 2.2 Abstract

In addition to aiding in digestion of food and uptake of nutrients, microbiota in guts of vertebrates are responsible for regulating several beneficial functions, including development of an organism and maintaining homeostasis. However, little is known about effects of exposures to chemicals on structure and function of gut microbiota of fishes. To assess effects of exposure to polycyclic aromatic hydrocarbons (PAHs) on gut microbiota, male and female fathead minnows (*Pimephales promelas*) were exposed to environmentally-relevant concentrations of the legacy model PAH benzo[*a*]pyrene (BaP) in water. Measured concentrations of BaP ranged from $2.3x10^{-3}$ to 1.3 μg $L^{-1}$. The community of microbiota in the gut were assessed by use of 16S rRNA metagenetics. Exposure to environmentally-relevant aqueous concentrations of BaP did not alter expression levels of mRNA for *cyp1a1*, a biomarker of exposure to BaP, but resulted in shifts in the relative compositions of gut microbiota in females rather than males. Results presented here illustrate that, in addition to effects on more well-studied molecular endpoints, relative compositions of the microbiota in the guts of fish can also quickly respond to exposure to chemicals, which can provide additional mechanisms for adverse effects on individuals.

## 2.3 Introduction

Microbiota in guts of animals are responsible for regulating a number of beneficial functions, from the development of animals (Phelps et al., 2017) to maintaining energy homeostasis (Butt et al., 2019). As in all organisms, bacteria line the intestinal tract of fish and, in addition to assisting with digestion of food and accumulation of nutrients (Dimitroglou et al., 2011), the microbiota modulate immune functions (Rolig et al., 2015), and provide structural and functional roles in regulating the intestinal barrier (Pérez et al., 2010). However, little is known about the effects of contaminant exposures on structure and function of microbial communities in guts of fishes. In mammals, dysbiosis, or deviations from a norm, of gut microbiota is associated with a number of deleterious effects, including inflammatory bowel disease, metabolic syndrome and even obesity (Carding et al., 2015; He et al., 2020). For commercially valuable fish species, as well as those used as ecotoxicological models, where information is more scarce, dysbiosis is linked to a greater prevalence of stress and disease (Llewellyn et al., 2014).

Alteration of the gut microbiome can be indicative of the health status of the host and potentially reflect the quality of the environment, since gut microbiota can be disturbed by several environmental chemical compounds (i.e. Adamovsky et al., 2018; Bayha et al., 2017; Lloyd et al., 2016). For example, Japanese sea cucumbers (*Apostichopus japonicus*) exposed to benzo[*a*]pyrene (BaP) exhibited a shift in gut microbiota; exposed sea cucumbers lost bacteria associated with beneficial functions within the host and instead saw increases in the proportion of alkane-degrading bacteria (Zhao et al., 2019). Enrichment of bacterial taxa associated with hydrocarbon degradation has also been observed in southern flounder (*Paralichthys lethostigma*) exposed to contaminated sediment from the Deepwater Horizon oil spill (Bayha et al., 2017), while African catfish (*Clarias gariepinus*) injected with BaP had reduced levels of *Pseudomonas aeruginosa* in the gut (Karami et al., 2012). In mice, it was found that BaP exposure did not alter alpha diversity indices, but rather altered overall community structure and relative abundance of certain taxa (Ribière et al., 2016). Also, *in vitro* in a simulated human gut system, bacteria can metabolize BaP to several metabolites (Van de Wiele et al., 2005). Finally, isolates of bacteria from skin of humans can degrade BaP (Sowada et al., 2018). Dysbiosis of communities of bacteria in the gut can ultimately have direct consequences for the

host and alter effects of BaP (Levy et al., 2017; Thaiss et al., 2016).

Cross-talk between the gut microbiome and chemicals is gaining attention as an added layer for deciphering the mechanisms of toxicity. Recently, it has been recognized that the aryl hydrocarbon receptor (AhR) is a regulator of host-microbiota communications (Zhang et al., 2017) and that this relationship is bidirectional (Korecka et al., 2016). Several persistent organic pollutants (POPs) are ligands of the AhR and stimulate a signal transduction pathway that results in pleiotropic effects, including up-regulation of expression of cytochrome P450 1A (CYP1A), which can, in turn, biotransform those POPs to reactive intermediates (Ortiz-Delgado et al., 2007).

Because of its abundance in the environment, mode of action, and relative well-studied background, BaP was chosen as a model compound. BaP is a ubiquitous, polycyclic aromatic hydrocarbon (PAH) that originates from pyrogenic sources, including incomplete combustion of fossil fuels and petrogenic processes such as oil spills (Srogi, 2007). BaP can cause adverse outcomes such as lesions, tumors, and developmental defects, in part due to the formation of reactive metabolites that can form adducts which cause damage to DNA, RNA, or proteins (Beyer et al., 2010; Tuvikene, 1995). BaP can also suppress the immune system (Carlson et al., 2004b) and impair reproductive capacity (Booc et al., 2014). Although the deleterious effects of BaP exposure in fish have been well-defined (i.e. Carlson et al., 2004; Costa et al., 2011; Nacci et al., 2002; Phalen et al., 2014), direct effects of BaP on structure and function of the microbiome are poorly studied, particularly in fishes. Therefore, it is conceivable that BaP can act directly upon the AhR and modulate bacterial communities in guts of fishes.

This study assessed the alteration of gut microbiome resulting from exposure of fathead minnows (*Pimephales promelas*) to environmentally-relevant aqueous concentrations of BaP. Specific objectives were to: 1) Characterize the gut microbiome in adult fathead minnows; 2) Determine whether differences existed in gut bacterial communities between males and females; 3) Characterize effects of BaP on the microbiome in guts of individuals exposed to BaP, relative to that of unexposed controls; 4) Compare shifts in the microbiome to a biomarker of exposure. To satisfy these objectives, the microbiota in guts of fathead minnows were characterized by use of 16S rRNA metagenetics, after aqueous exposure to environmentally-relevant concentrations of BaP for four days.

## 2.4 Materials and Methods

*2.4.1 Fish husbandry, aqueous exposure, and sampling*

Adult fathead minnows of approximately two years of age were obtained from an in-house stock population of the Aquatic Toxicology Research Facility at the University of Saskatchewan. Fish were acclimated at a density of two males and three females per 20-L, flow-through tank in aerated, ammonia-removed, dechlorinated facility water, sourced from the municipal Saskatoon water supply, held at 25 ± 1 °C. Conditions provided approximately three replacements of water per day with a 16h-light:8h-dark photoperiod. Fish were fed larvae of midges (*Chironomidae*), three times daily on a maintenance food ration (2% of their average wet body mass (bm) per day). Water quality conditions were monitored and were: pH 7.6 ± 0.1, dissolved oxygen 6.4 ± 0.2 mg $L^{-1}$, hardness 131.8 ± 6.8 mg $L^{-1}$ as $CaCO_3$.

After two-week acclimation, fish were exposed to a solvent control (0.02% DMSO), low, medium, or high concentrations of BaP for four days, with five replicate tanks per exposure (n = 25; 3 females and 2 males per tank). Nominal concentrations of control, low, medium and high doses were set at 0, 1.3, 4.0, and 12.0 µg BaP $L^{-1}$, which were in accordance with reported ranges of aqueous BaP concentrations (Adeniji et al., 2019; CCME, 2010).

At the end of the exposure, fish were euthanized *via* blunt force. Samples of whole gut, containing both tissues of the fish and microbes, were excised from two females and one male per tank (n = 15; 10 females and 5 males per treatment) using sterile techniques. Gut contents were gently removed and discarded, leaving only microbes adhered to the gut tissue in the sample. Samples were placed in sterile cryovials, and held on ice until transport to a -80 °C freezer. Livers (n = 25; 15 females and 10 males per treatment) were removed and immediately placed in sterile cryovials in liquid nitrogen prior to storage at -80 °C. Remaining fish (n = 10; 5 females and 5 males per treatment) were taken for chemical and molecular analyses for a separate project (Grimard et al., *in prep*). All fish were housed following the animal use protocol (Protocol #20130142) approved by the Animal Research Ethics Board at the University of Saskatchewan.

*2.4.2 Quantification of BaP in exposure media*

SGS AXYS Analytical Services Ltd. (Sidney, BC) determined real exposure concentrations by means of gas chromatography-mass spectrometry (GC-MS) following C18

solid-phase extraction (SPE) of 0.5- to 1-L water samples. The analysis followed the SGS AXYS method MLA-021 Rev. 12. BaP d-12 was used as the internal standard, the recovery of which ranged from 39 to 81%. Matrix spike samples exhibited recoveries of 101-102%, and lab blanks did not test positively for BaP.

*2.4.3 16S rRNA metagenetics*

Total DNA was extracted from guts using the DNeasy PowerSoil Kit (Qiagen Inc., Mississauga, ON). Concentrations were measured by use of a Qubit 4 Fluorometer and dsDNA HS assay kit (ThermoFisher Scientific, Waltham, MA). The V3-V4 hypervariable region of the 16S rRNA gene was amplified by use of dual-tagged primer set: forward primer (Bact-341: 5'-CCTACGGGNGGCWGCAG-3') (Klindworth et al., 2013) and reverse primer (Bact-806: 5'-GGACTACNVGGGTWTCTAAT-3') (Apprill et al., 2015; Fadrosh et al., 2014). The V3-V4 region was selected based on the sequencing platform, the length of hypervariable regions, and the performance of representing bacterial phyla (Graspeuntner et al., 2018; Lozupone et al., 2013; Osman et al., 2018; Yang et al., 2016). Samples were amplified by use of the Phusion Hot Start II High-Fidelity DNA Polymerase green kit (ThermoFisher Scientific) with a SimpliAmp thermal cycler (ThermoFisher Scientific) under the following conditions: Initial denaturation at 98 °C for 30 s, followed by 25 cycles of 98 °C for 30 s, 58 °C for 30 s, and 72 °C for 30 s, with a final extension at 72 °C for 10 min. PCR products were assessed for size and specificity using electrophoresis on a 1.2% w/v agarose gel and purified using the Qiagen QIAquick PCR Purification Kit (Qiagen Inc.). Negative controls were checked by electrophoresis on a 1.2% w/v agarose gel. All purified products were quantified with the Qubit dsDNA HS assay kit and concentrations were adjusted to 1 ng/µL with molecular-grade water. Purified products were pooled at equal concentrations for subsequent sequencing, and libraries were constructed using the NEBNext® DNA Library Prep Master Mix Set for Illumina® kit (New England BioLabs Inc., Whitby, ON). Libraries were quantified prior to sequencing using the NEBNext® Library Quant Kit for Illumina®. Phi-X (15%) was spiked in to increase complexity of the library and assess sequencing error. Sequencing was performed on an Illumina® MiSeq sequencer (Illumina, San Diego, CA) using a 2x300 base pair (bp) paired-end chemistry kit.

*2.4.4 Quantitative Reverse-Transcription Real-Time*

Liver tissues of individual fish were homogenized in QIAzol lysis reagent (Qiagen Inc.) in a TissueLyser II (Qiagen Inc.) by use of one 5-mm stainless-steel bead (Omni International, Kennesaw GA, USA). Total RNA was extracted in a QIAcube automatic extraction unit (Qiagen Inc.) by use of the RNeasy Plus Universal kit (Qiagen Inc.), following the manufacturer's protocol. The concentration and purity of extracted RNA were assessed by spectral content profiling using a QIAxpert instrument (Qiagen Inc.). RNA samples were stored at –80 °C until further analysis.

Quantitative Reverse-Transcription Real-Time PCR (qPCR) was used to quantify expression of select genes (*cyp1a1, ar, bax*, *esr1*, *vtg*) in liver of individual fish. These genes were selected based on their known dysregulation from exposure to BaP (Hoffmann and Oris, 2006). Primers were designed using Primer-BLAST (Ye et al., 2012) and based on results of previous studies (Appendix A, Table A.1), and purchased from Thermo-Fisher Scientific. Complementary DNA (cDNA) was synthesized from 2.5 µg total RNA by use of QuantiNova™ Reverse Transcription kit (Qiagen Inc.). Expressions of targeted genes were measured by use of a QuantStudio™ 6 Flex Real-Time PCR System (Applied Biosystems, Carlsbad CA, USA) and the QuantiNova™ SYBR Green PCR kit (Qiagen Inc.), following the manufacturers' protocol and including a melt curve to ensure specificity of primers. Reactions were done in duplicates of 10 µL reaction volumes. Relative expressions of target genes were normalized against expression of two housekeeping genes, *ef1* and 18S rRNA (Appendix A, Table A.1), according to methods described by Simon (2003).

*2.4.5 Bioinformatics*

Dual-tagged raw reads were checked for quality and demultiplexed using a custom pipeline with USEARCH v. 11 (Edgar, 2010) and QIIME1 v. 1.9.0 (Caporaso et al., 2010). Demultiplexed sequences were then imported to QIIME2 v. 2019.4 (Bolyen et al., 2019). To describe microbial communities, amplicon sequence variants (ASVs) were generated and chimeras were removed using the DADA2 algorithm (Callahan et al., 2016). To remove low quality base pairs at ends of reads, the forward read was truncated to 280 base pairs, while the reverse read was truncated to 230. Additionally, to remove the primer region from each

sequence, the first 35 bases were removed. Taxonomy was then assigned in QIIME2 by use of the feature classifier trained against the SILVA 132 reference database (Bokulich et al., 2018; Quast et al., 2013). ASVs that did not align to bacterial kingdoms were discarded as well as sequences that were found fewer than ten times (Bokulich et al., 2013). The majority of ASVs that did not align to bacterial kingdoms were classified as "unknown". On average, 40% of reads assigned to each sample survived through the cleaning process. A full list of reads per sample pre- and post-cleaning can be found in Appendix A, Table A.2. To reduce biases resulting from differences in sequencing depth, based on a rarefaction graph (Appendix A, Fig. A.1), the feature table was rarefied at the lowest sequencing depth (7,884 sequences per sample). Alpha diversities (Shannon diversity, observed ASVs, Chao1, and Faith phylogenetic distance (PD)), or diversity of prokaryotic communities within samples, and beta-diversities (Bray-Curtis dissimilarity, unweighted UniFrac, and weighted UniFrac (Lozupone and Knight, 2005)), or diversity of prokaryotic communities between samples, were calculated in QIIME2. Tax4Fun2 was used to predict functional profiles, which use UProC to match microbes with known protein families (Meinicke, 2015), then match those profiles to metabolic pathways by use of Kyoto Encyclopedia of Genes and Genomes (KEGG) orthologs (Kanehisa et al., 2015) based on 16S rRNA bacterial sequences (Wemheuer et al., 2018). Data can be accessed at https://dx.doi.org/10.20383/101.0196.

### *2.4.6 Statistics*

Statistical analyses were performed using R Statistical Language v. 3.6.1 (R Core Team, 2013). Because there were no differences in any measured parameters, each individual fish was considered a replicate. For all statistical tests, assumptions of normality and equal variance were tested by visual inspection using a Q-Q plot, a Shapiro-Wilk test, and a Levene's test (Borcard et al., 2011). If these conditions were met, a two-sided Student's t-test was used to compare sex effects, and analysis of variance (ANOVA) was used to assess exposure effects. If conditions were not met, Welch's t-test was used when comparing sex effects and the Kruskal-Wallis test was used when comparing exposures (Dalgaard, 2006). Shannon diversity values were cubed to obtain normality of data for the purpose of statistical analysis. Dunnett's tests were used to compare exposure groups to the solvent control using the DescTools package in R (Signorell, 2019). A nested ANOVA design was used to investigate

effects of exposure within sex for alpha diversity, but since sex appeared to drive the separation of alpha diversity ($p < 0.001$) whereas exposure did not ($p > 0.05$), the two sexes were analyzed separately to assess effects of BaP exposure on species composition and alpha diversity of gut microbiota. Unless otherwise noted, statistics were calculated using vegan statistical package (Oksanen et al., 2019) and visualized with gglot2 (Wickham, 2016).

Statistical Analysis of Metagenomic Profile (STAMP) bioinformatics software v. 2.1.3 was used to visualize significantly different bacterial taxa at the family level and KEGG pathways based on sex and exposure (Parks et al., 2014). Beta diversity was analyzed with the phyloseq package (McMurdie and Holmes, 2013), by use of the feature table and rooted tree generated in QIIME2. Principal coordinate analysis (PCoA) plots were generated with Bray-Curtis dissimilarities by use of an agglomerated feature table to combine taxa of the same genus and reduce complexity of ordination. To determine statistical differences in the Bray-Curtis dissimilarities between males and females, the Adonis2 test was performed using the vegan statistical package in R (Oksanen et al., 2019). First a nested Adonis design was used with exposure nested in sex, but because the results returned a significant interaction between the variables ($F = 5.74$, $p < 0.001$), the sexes were analyzed and plotted separately to assess exposure effects. The significant interaction implied that ordination of samples based on treatment was not the same between male and female fish. Gut microbial community differences based on exposure were calculated using the agglomerated taxa table using the pairwise.adonis2 function in R (Martinez Arbizu, 2019). To correct for multiple comparisons, a Benjamin-Hochberg False Discovery Rate adjustment was used.

For gene expression analyses, only females in the highest exposure group were selected for qPCR analyses. Had any changes in gene expression been observed, gene expression from other exposure groups would have been analyzed. Gene expression results from qPCR were tested for statistical significance using a one-way ANOVA. In all cases, results were considered significant at a significance level of $\alpha < 0.05$.

## 2.5 Results

### *2.5.1 Concentrations of BaP in water*

Measured concentrations of BaP in water were 0.83 ng $L^{-1}$ (solvent control), 32 ng $L^{-1}$ (low), 88 ng $L^{-1}$ (medium), and 1,338 ng $L^{-1}$ (high). These values were less than nominal

concentrations of 0, 1300, 4000, and 12000 ng BaP $L^{-1}$. The disparity likely resulted from BaP binding to the plastic materials in the exposure apparatus.

### *2.5.2 Composition and sex differences of gut microbiota of fathead minnows*

Metagenetics of 16S rRNA revealed the composition of gut microbiome of fathead minnows exposed to BaP under controlled laboratory conditions. A total of 9,346 ASVs were identified, but after contingency-based filtering, 2,715 non-singleton ASVs of 123 unique genera of bacteria among 58 samples (23 males, 35 females) remained. The dominant phyla in the gut of fathead minnows (% ± S.E.) were *Proteobacteria* (63% ± 3%), *Fusobacteria* (18% ± 2%), *Bacteroidetes* (8% ± 1%), *Firmicutes* (7% ± 2%), *Spirochaetes* (1.7% ± 0.04%), and *Planctomycetes* (1.4% ± 0.04%).

Female and male fathead minnows exhibited significantly different microflora in their guts. Microbiota in guts of females exhibited greater biodiversity than microbiomes of males (Shannon diversity: $t = 5.77$, $p < 0.001$; Chao1: $t = 6.45$, $p < 0.001$; Faith PD: $t = 7.44$, $p < 0.001$; observed ASVs: $t = 6.59$, $p < 0.001$); Table 2.1). Of the 19 most abundant families (Fig. 2.1), ten families exhibited significantly greater abundances in guts of female relative to males (Fig. 2.2A; Welch's t-test, corrected $p < 0.05$). *Vibrionaceae* was the only abundant family significantly more abundant in guts of male fish relative to females ($p < 0.001$). Community structure of microbiomes in guts of fish were significantly different between male and female fish (Adonis test: $F = 21.15$, $p < 0.001$). This separation was also supported by results of PCoA, with the first axis explaining 46.1% of the variation due to sex (Fig. 2.2B). In total, 232 pathways within predicted metagenomic functional profiles were significantly different between male and female fish. For instance, fatty acid biosynthesis (fatty acid metabolism and fatty acid degradation) was enriched in female fish (adjusted $p < 0.001$) and bacterial chemotaxis (bacterial invasion of epithelial cells) was enriched in males (adjusted $p < 0.001$).

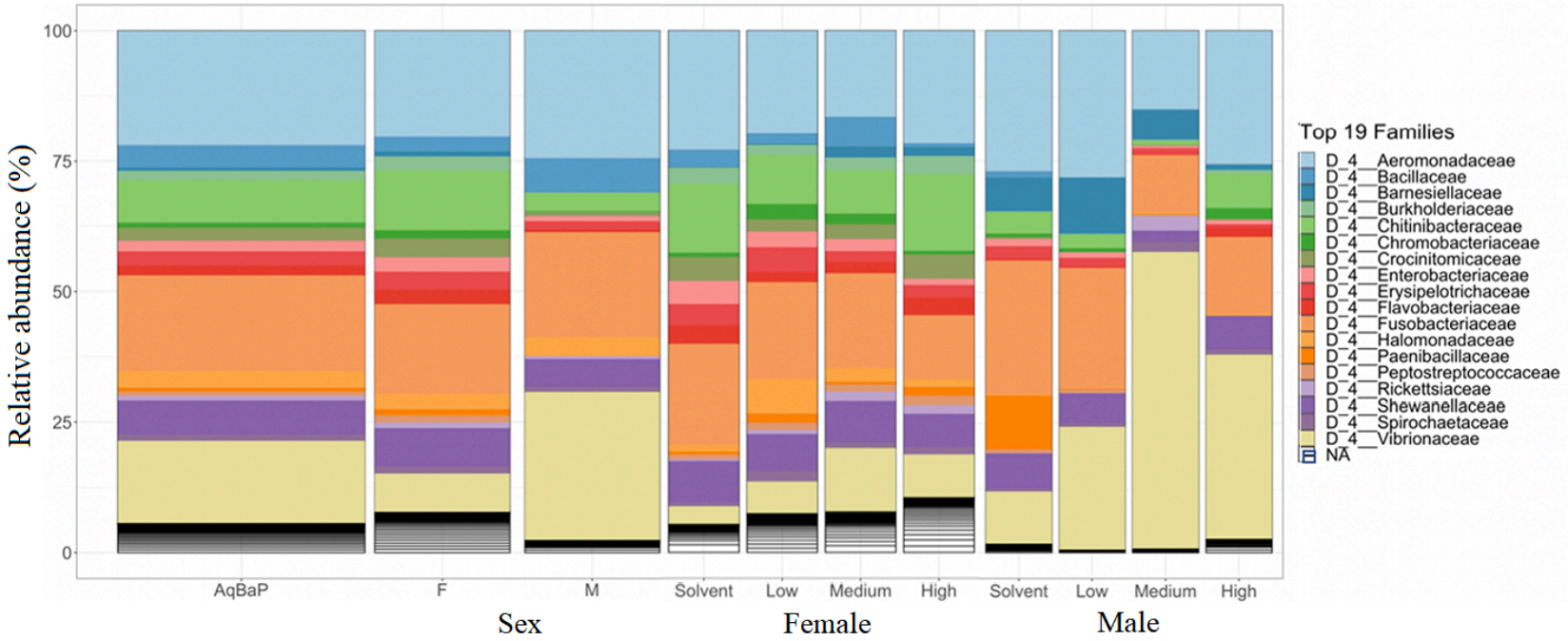


Figure 2.1. Relative proportions of 19 most abundant bacterial families. The first bar shows relative proportions of these taxa for all fish within the study. The second two bars show female and male fish, respectively. The final bars show proportions of taxa for females and males, exposed to each concentration of BaP, respectively.

Table 2.1. Shannon diversity index, number of observed amplicon sequence variants (ASVs), Chao1, and Faith Phylogenetic Distance (PD) are presented for male and female fish at the different exposure levels (mean ± standard error, sample size n = 7-10 for females, 4-8 for males).

| Sex | Male | | | | Female | | | |
|---|---|---|---|---|---|---|---|---|
| Treatment | Solvent | Low | Medium | High | Solvent | Low | Medium | High |
| Shannon | 3.16 ± 0.35 | 3.15 ± 0.21 | 2.36 ± 0.57 | 3.07 ± 0.61 | 4.18 ± 0.24 | 4.03 ± 0.32 | 4.20 ± 0.25 | 4.36 ± 0.28 |
| Observed ASVs | 44.38 ± 7.34 | 32.67 ± 3.37 | 29.20 ± 7.12 | 38.00 ± 7.38 | 60.67 ± 4.48 | 62.40 ± 6.48 | 71.86 ± 4.38 | 80.44 ± 8.45 |
| Chao1 | 45.01 ± 7.65 | 32.83 ± 3.42 | 29.20 ± 7.12 | 38.00 ± 7.38 | 60.70 ± 4.49 | 62.40 ± 6.48 | 72.26 ± 4.43 | 80.82 ± 8.55 |
| Faith PD | 6.48 ± 0.71 | 5.12 ± 0.42 | 5.39 ± 0.62 | 6.12 ± 0.67 | 8.45 ± 0.57 | 8.69 ± 0.62 | 9.78 ± 0.43 | 10.10 ± 0.69 |

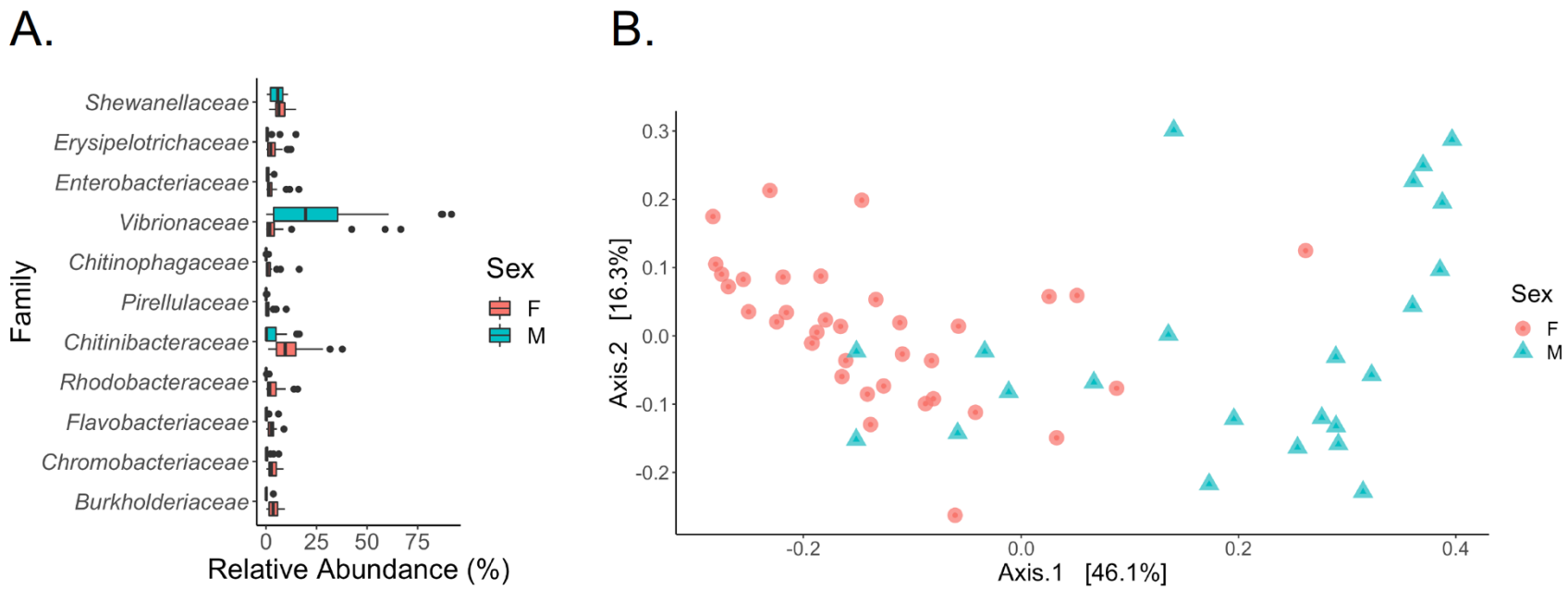


Figure 2.2. (A.) Relative abundances (%) of bacterial families that were significantly different between male and female fish ($p < 0.05$). Females are shown in red and males are shown in blue. (B.) Ordination of bacterial communities based on sex (PCoA with Bray-Curtis dissimilarity matrix). Females are shown with red circles and males are shown with blue triangles.

*2.5.3 Sex-specific responses of fathead minnows to BaP*

Exposure to BaP did not result in significant differences in alpha diversities (Chao1, number of ASVs, Shannon, Faith Phylogenetic Distance) in male or female fish ($p > 0.05$; Table 2.1). Based on results of a Dunnett's test, in female fish, only three bacterial families were present in greater relative abundance compared to that of the solvent control (Fig. 2.3A): *Isosphaeraceae* (absent in solvent control, but 0.53% of total reads in the highest exposure group, adjusted $p = 0.04$), *Rubritaleaceae* (4.1x more in the highest exposure group relative to the control, adjusted $p = 0.03$) and *Xanthobacteraceae* (absent in solvent control, but 0.05% of total reads in fish exposed to the greatest concentration of BaP; adjusted $p = 0.04$). In male fish (Fig. 2.3B), *Vibrionaceae* were enriched in the two highest exposure groups relative to that in the solvent control, but only statistically significant in the medium group relative to control (adjusted $p = 0.02$).

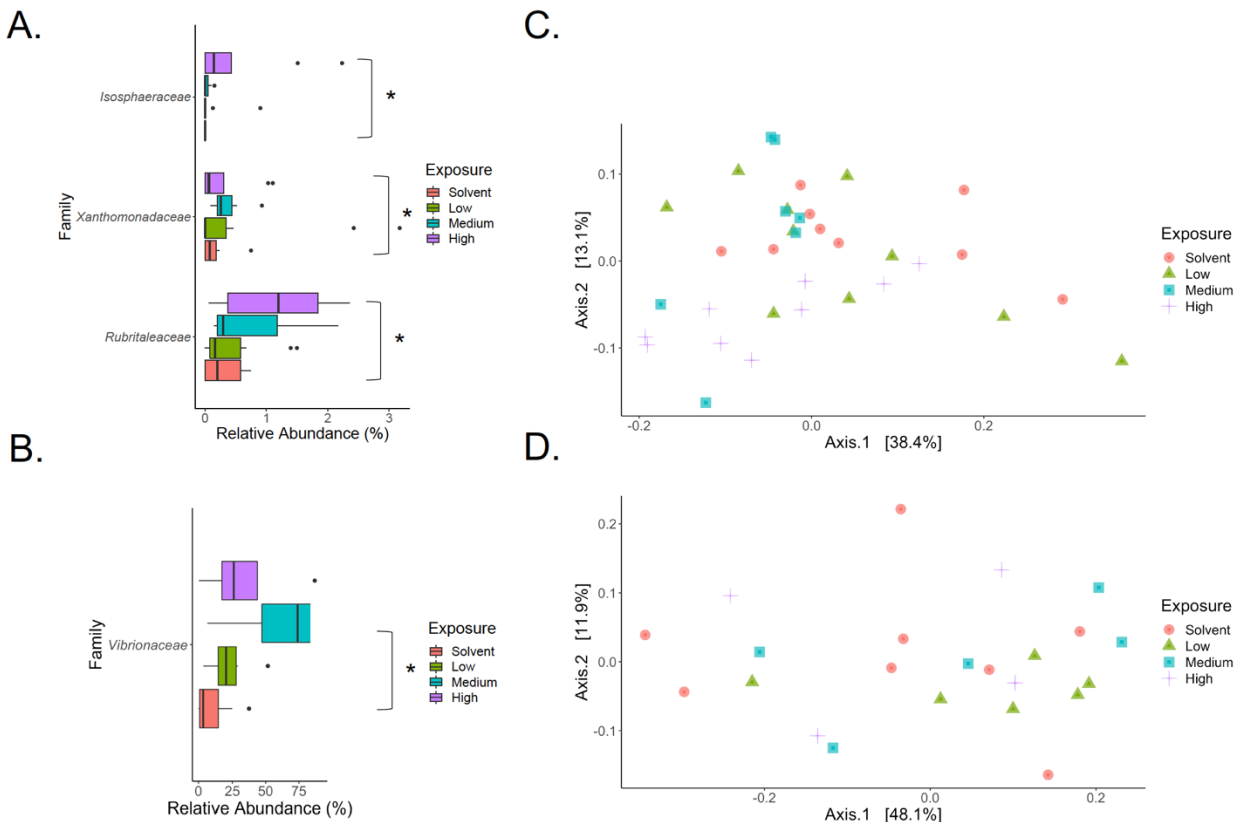


Figure 2.3. (A). Relative abundances (%) of bacterial families that were significantly different in exposure groups relative to the solvent control ($p < 0.05$) in female fish. (B). Ordination of bacterial communities based on exposure (PCoA with Bray-Curtis dissimilarity matrix) in female fish. (C). Relative abundances (%) of bacterial families that were significantly different in exposure groups relative to the solvent control ($p < 0.05$) in male fish. (D). Ordination of bacterial communities based on exposure (PCoA with Bray-Curtis dissimilarity matrix) in male fish. In the relative abundance plots, solvent control is shown in red, low in green, medium in blue, and high in purple. In each PCoA, the solvent control group is shown in red circles, the low group in green triangles, the medium group in blue squares, and the highest group in purple crosses.

Exposure to BaP significantly altered beta diversities in female gut microbiota, but not in males. The highest exposure group showed significant separation from the solvent group (Adonis test: $F = 2.32$, $p = 0.04$); the medium exposure group approached significance separation from the solvent group (Adonis test: $F = 1.97$, $p = 0.06$). Clustering in a PCoA showed these differences, with the solvent control group clustering separately from communities in guts of fish exposed to the highest and medium concentrations of BaP (Fig. 2.3C), with the first axis explaining 38.4% of the variation. There were no significant differences among exposure groups for the male fish ($p > 0.05$; Fig. 2.3D), although the first axis did explain 48.1% of the variation, suggesting another variable was contributing to this separation.

While not statistically significant ($p = 0.08$), the predicted polycyclic aromatic hydrocarbon degradation pathway did increase from the solvent group (0.008% ± 0.001%) to the highest exposure group (0.02% ± 0.004%) in female fish. KEGG pathway analysis predicted no pathways with differential enrichment among BaP exposure groups in male fish.

### *2.5.4 Host gene expression analyses*

Analysis of differential expression of genes revealed minimal effects of a short-term exposure on the relative gene expression of genes in female fathead minnows exposed to the highest concentration. Abundances of transcripts of all measured genes was reduced relative to the controls; however, none of these results were statistically significant (Fig. 2.4).

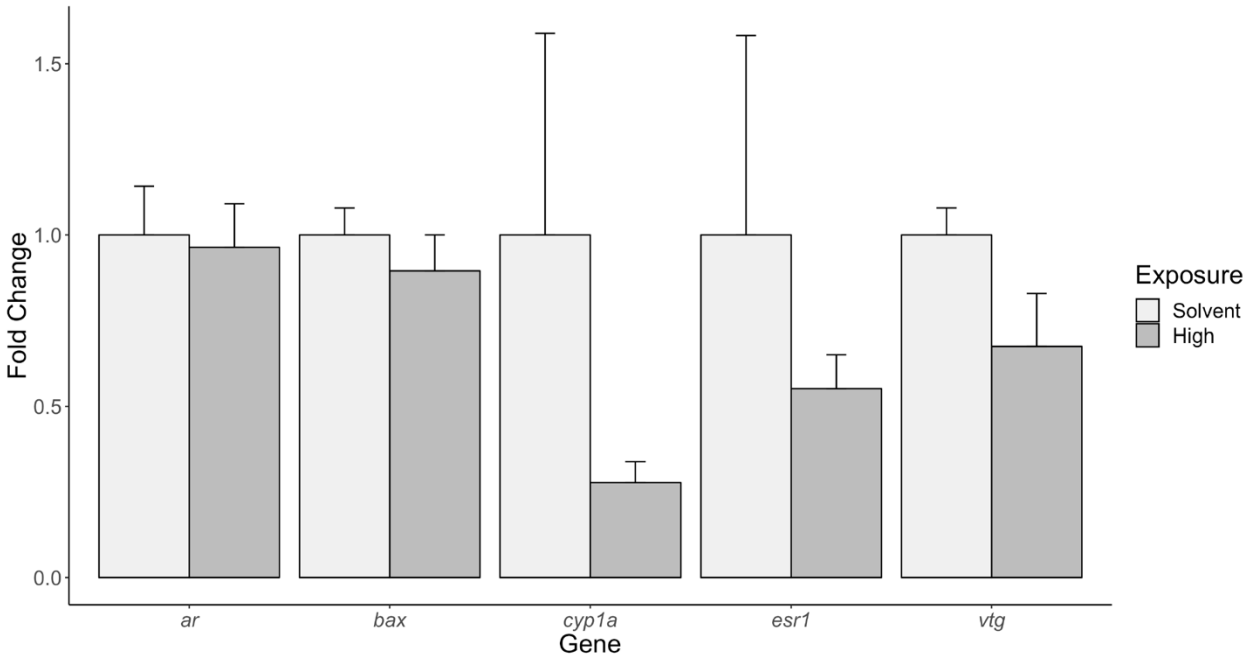


Figure 2.4. Relative fold change in expressions of androgen receptor (*ar*), BCL2 Associated X, Apoptosis Regulator (*bax*), Cytochrome P450, family 1, subfamily A, polypeptide 1 (*cyp1a1*), estrogen receptor alpha (*esr1*), and vitellogenin (*vtg*) in female fish after four days of exposure to BaP (n = 4-5). Solvent control fish are shown in light grey while the highest exposure group are shown in dark grey. No significant differences between the groups were observed ($p > 0.05$).

## 2.6 Discussion

Results of this study confirmed that the community composition of gut microbiota in fathead minnows is consistent with other freshwater fish. Dominance of *Proteobacteria* has been found in mummichog (*Fundulus heteroclitus*) (Givens et al., 2015), rainbow trout (*Oncorhynchus mykiss*) (Desai et al., 2012), and fathead minnow (Narrowe et al., 2015). *Fusobacteria*, *Bacteroidetes*, *Firmicutes*, *Spirochaetes*, and *Planctomycetes* are also commonly found phyla in guts of fishes (Colston and Jackson, 2016). Furthermore, at the family level, consistent with Narrowe et al. (2015), *Aeromonadaceae, Shewanellaceae, Flavobacteriaceae,* and *Fusobacteriaceae*, were dominant in guts of both male and female fathead minnows. In addition to these families, Roeselers et al. (2011) found *Vibrionaceae, Burkholderiaceae*, and *Enterobacteriaceae* as core members of the microbiome in guts of zebrafish, which is consistent with the results of this study.

Within the animal kingdom, microbial composition differs by sex, which was supported in this study. The composition of the bacterial community was significantly different between males and females. Significantly greater alpha diversity of microbiota in guts of females, relative to that of male fish as well as significant separation between communities of males and females based on beta diversity metrics, indicates that sex is associated with microbial composition. This finding in intestinal bacterial communities of fish is consistent with results of other studies that found significantly greater diversity of bacterial communities in guts of wild, female, largemouth bronze gudgeon (*Coreius guichenoti*) (Li et al., 2016), and sex-dependent responses to diet in three-spined stickleback (*Gasterosteus aculeatus*) and Eurasian perch (*Perca fluviatilis*). Differences in microbiomes of mice have been observed (Org et al., 2016; Yurkovetskiy et al., 2013), where microbiota in guts of female mice also have a greater alpha diversity value than do male mice. Furthermore, this pattern has also been observed in humans (Gao et al., 2018; Ying et al., 2015).

KEGG pathway analysis also predicted significant differences between microbiota in male and female fish. Fatty acid pathways were enriched in females relative to males; enrichment of fatty acid metabolism has been observed in the microbiota of female relative to male mice (Davis et al., 2017), which might be attributed to hormonal differences (Decsi and Kennedy, 2011). In male fish, enrichment of bacterial chemotaxis and bacterial invasion of epithelial cells may be reflective of the BaP exposure inducing susceptibility of pathogen attack, as discussed below (Carlson et al., 2004b). Differences in microbial communities between guts of males and females are believed to result from hormonal regulation, driven by androgen receptor activity (Markle et al., 2013), with the cyclic nature of estrogen cycles maintaining a greater microbial diversity (Yurkovetskiy et al., 2013). Furthermore, disparities in growth and behavior between males and females might also regulate this pattern (Bolnick et al., 2014; Jašarević et al., 2016a; Schnorr et al., 2014).

The gut microbiome was potentially more sensitive to a four-day environmentally-relevant BaP exposure than host gene expression (*cyp1a1* gene). In addition to differences between male and female fathead minnows, this study revealed that following exposure to a low concentration of aqueous BaP of duration as short as four days, the microbiome was significantly altered, even when gene expression did not reflect this change. It was expected that a four-day exposure to BaP would result in induction of *cyp1a1*, since the binding of BaP to the AhR induces expression of *cyp1a1* (Shimizu et al., 2000), but it is likely that the concentration of BaP in the water was too low to stimulate this change. Similar patterns of sensitivity were observed in earthworms (*Eisenia fetida*), where microbial groups were more sensitive to triclosan than enzyme activity within the organisms (Ma et al., 2017).

Sex-specific responses to contaminant exposure are well-documented in the field of ecotoxicology. For example, Vega-López et al., (2007) found that CYP1A mediated ethoxyresorufin *O*- deethylase activity and alcohol dehydrogenase activity in male, Chapultepec splitfin fish (*Girardinichthys viviparous*) was more up-regulated than females when exposed to polychlorinated biphenyls. Sex is also a significant factor in understanding toxicokinetics following xenobiotic exposure (Gochfeld, 2017). Specifically in regards to BaP, Booc et al. (2014) reported reproductive functions are more impaired in male fish than in female fish. Males are also more susceptible to the pathogen attack from bacteria, viruses, and parasites than females (Galligan and Fish, 2015; Thornton et al., 2018), and since BaP is an

immunosuppressant (Carlson et al., 2004b), it is conceivable that males would be more impacted by these effects.

In the context of this study, differences in responses of the microbial communities in guts of male and female fish to BaP might be linked to microbial degradation of BaP within guts of female fish and immune impairment in male fish. Although BaP did not result in significant changes in alpha diversity of the microbiota in guts of either sex, community composition was significantly different in the highest two exposure groups relative to the control in female fish. Female fish in the highest exposure group had increased levels of *Xanthobacteraceae*, a bacterial taxa associated with hydrocarbon degradation (Oren, 2014). Enrichment of the PAH degradation pathway in female fish along with bacterial taxa associated with PAH degradation support the hypothesis that bacteria are degrading BaP in female fish. To test this hypothesis that specific strains of bacteria present in the guts of these fish can degrade BaP, *Xanthobacteraceae* would need to be cultured and exposed to BaP, similar to the study by Sowada et al., (2018), where bacteria cultures from human skin were exposed to BaP. This would also allow for confirmation that PAH degrading pathways are enriched using transcriptomics rather than the predictive analysis of Tax4Fun2. However, the potential exists that *Xanthobacteraceae* does not interact with BaP in the same manner outside the body, as was the case with *P. aeruginosa* cultured from African catfish (Karami et al., 2012).

In this study, in guts of males exposed to the greatest concentration of BaP, the microbiome was enriched with *Vibrionaceae,* a bacterial family associated with disease in fish (Colwell and Grimes, 1984). Although not significantly correlated in this study, relative abundance of *Vibrio* can be negatively correlated with *Aeromonas* growth and result in an increase in neutrophil recruiting (Rolig et al., 2015). Neutrophils release cytokines that recruit immune cells and mediate a proinflammatory response to an infection; therefore neutrophils are imperative for host defense (Harvie and Huttenlocher, 2015; Rolig et al., 2015).

Results of this study highlight the need to incorporate the microbiome as well as ecological theory, particularly in regards to differences between males and females, into our understanding of the link between chemical exposure, the microbiome, and the host organism (Adamovsky et al., 2018; Jašarević et al., 2016b). A relatively well-characterized toxicant perturbs the microbiome at environmentally-relevant concentrations, which may result in

deleterious effects on the host, or it may provide protection (Dietert and Silbergeld, 2015). Either way, these rapid shifts in the microbiota may be useful as an early-warning sign of exposure. Limitations of this study include a small range of concentrations used to elucidate these effects, the use of a single time point in this study, and the use of Tax4Fun2. It should be noted that Tax4Fun2, while informative, is predictive and might not reflect actual functioning of the bacteria within the fish (Evariste et al., 2019), nor should it replace metabolomic studies.

## 2.7 Conclusions

This study revealed that short-term low-dose BaP exposure significantly altered the community structure of gut microbiota in female, but not male, fathead minnows. Taxonomic analyses revealed minimal effects of BaP exposure on male fish, but no changes were observed in predictive KEGG pathway analysis. In female fish, the exposure revealed the potential for hydrocarbon-degrading functionality and taxa. Gene expression did not reveal any impacts of BaP on internal processes within the fish. More work is needed to elucidate the mechanisms behind changing community composition and to better understand the relationships between BaP exposure, the bacteria, and the effect on the host.

## 2.8 Acknowledgements

Funding was provided by “Next generation solutions to ensure healthy water resources for future generations” funded by the Global Water Futures program, Canada First Research Excellence Fund (#419205) and the GenomeCanada EcoToxChip project. Dr. Brinkmann was also supported through the Global Water Futures program. Profs Giesy and Hecker were supported by the Canada Research Chairs Program of the Natural Sciences and Engineering Research Council of Canada (NSERC). Prof. Giesy was also supported by a distinguished professor in residence by the Environmental Science Department of Baylor University, Waco, Texas.

# CHAPTER 3: Responses of juvenile fathead minnow (*Pimephales promelas*) gut microbiome to a chronic dietary exposure of benzo[*a*]pyrene

## 3.1 Preface

This chapter focuses on the effects of benzo[*a*]pyrene (BaP) on the gut microbiomes of juvenile fathead minnows (*Pimephales promelas*) after a fourteen-day dietary exposure, using environmentally-relevant concentrations. Using 16S rRNA metagenetics, it was determined that exposure to BaP can alter the microbial composition and disrupt network complexity of the gut microbiome. Because BaP metabolites were measured in the bile from each fish, specific taxa that correlated with exposure could be determined. This work builds upon the research from Chapter 2; use of a higher concentration of BaP along with a longer exposure and larger sample size allowed for the use of more advanced tools for bioinformatics and analysis. Furthermore, a larger sample allowed for the analysis of correlations between measured BaP metabolite concentrations and alpha-diversity, beta-diversity, bacterial taxa, and predicted bacterial functions.

Author contributions:

- Abigail DeBofsky: All experimental design (90%), bench work (80%), bioinformatics (80%), and statistical analysis (90%), with the exception of running the GCMS and LCMS for food and bile detection of BaP/metabolites, as well as creation of the manuscript (90%)
- Dr. Yuwei Xie: Assistance with design of experiment (10%), bioinformatics (20%), statistical analysis (10%), and revisions of the manuscript (80%)
- Dr. Jonathan Challis: Assistance with running the LCMS (100%), interpreting the

chemical data (100%), writing the LCMS portion of the manuscript (5%), and revising the manuscript (5%)

- Niteesh Jain: Undergraduate assistant who helped with running the experiment and performing benchwork (20%)
- Dr. Markus Brinkmann: Developed the methods for analyzing the BaP metabolites in bile and edited the manuscript (5%)
- Dr. Paul D. Jones: Assistance with running the GCMS (100%), interpreting the chemical data (100%), writing the GCMS portion of the manuscript (5%), and and revising the manuscript (5%)
- Dr. John P. Giesy: Provided scientific input and guidance, edited the manuscript (5%), and provided funding for the research

## 3.2 Abstract

The microbiome has been described as an additional host "organ" with well-established beneficial roles. However, the effects of exposures to chemicals on both structure and function of the gut microbiome of fishes are understudied. To determine effects of benzo[*a*]pyrene (BaP), a model persistent organic pollutant, on structural shifts of gut microbiome in juvenile fathead minnows (*Pimephales promelas*), fish were exposed *ad libitum* in the diet to concentrations of 1, 10, 100, or 1,000 µg BaP $g^{-1}$ food, in addition to a vehicle control, for two weeks. To determine the link between exposure to BaP and changes in the microbial community, concentrations of metabolites of BaP were measured in fish bile and 16S rRNA metagenetics was used to evaluate the microbiome. Exposure to BaP only reduced alpha-diversity at the greatest exposure concentrations, but it did alter community composition, assessed as differential abundance of taxa, and reduced network complexity of the microbial community at lower exposure concentrations. Results presented here illustrate that environmentally-relevant concentrations of BaP *via* a dietary exposure can alter the diversity of the gut microbiome and community network connectivity.

## 3.3 Introduction

The gut microbiome is a crucial component of an animal host and is responsible for a number of important biological processes, including energy and nutrient cycling (Dimitroglou et al., 2011), regulation of intestinal barrier functions (Pérez et al., 2010), and modulation of the immune system (Rolig et al., 2015). Disturbance of structure of the gut microbiome is associated with several harmful effects, including inflammatory bowel disease, metabolic syndromes, stress, and disease (Carding et al., 2015; He et al., 2020; Llewellyn et al., 2014). Although considerable research efforts to understand links between xenobiotics and the gut microbiome have been conducted in mammals, the effects of toxicants on gut microbial community structure and function in fish are largely unknown.

Complex interactions between the host microbiome and xenobiotics can vary by route of exposure. In fish, due to partitioning and bioaccumulation, exposure to environmental toxicants can occur *via* multiple routes, and persistent organic pollutants (POPs) tend to accumulate in food chains (Schlenk et al., 2008; Wang and Wang, 2006). POPs can be taken up through the gut, skin, and gill (Schlenk et al., 2008) and can ultimately have deleterious effects on fish in freshwater ecosystems. The mucosal layers of the skin, gill, and gut all contain microbiomes that provide protective barriers for fish defense against pathogens (Salinas and Magadán, 2017) and act as an intermediary in the metabolism pathway of some toxicants (Adamovsky et al., 2018).

Benzo[*a*]pyrene (BaP) is a model polycyclic aromatic hydrocarbon (PAH) used to study the effects of toxicants on the gut microbiome; while much is known about the effects of BaP in fish, little is known about the effects on the gut microbiome. BaP originates from sources such as the incomplete combustion and oil spills (Srogi, 2007) and has well-characterized deleterious effects in fishes (Carlson et al., 2004b; Costa et al., 2011; Nacci et al., 2002; Phalen et al., 2014). BaP up-regulates the expression of a number of genes, including cytochrome P450 1A (CYP1A), which results in the biotransformation of BaP to reactive intermediates (Ortiz-Delgado et al., 2007). Adverse outcomes of exposure to BaP include the development of lesions and tumors, as well as suppression of immune function (Beyer et al., 2010; Carlson et al., 2002; Tuvikene, 1995). Conjugated products from phase II metabolism of BaP often end up in the bile of exposed fish (Nishimoto et al., 1992). In fish, routes of exposure to BaP are primarily through ingestion with food, incidental ingestion of

sediment, dermal contact, and *via* ventilation across the gills (McCarthy et al., 2003; Nichols et al., 1996; Snyder et al., 2015; Tuvikene, 1995). Route of exposure is a critical component of the distribution of BaP. For example, aqueous exposure of BaP in rainbow trout (*Oncorhynchus mykiss*) results in detectable BaP throughout the body, while dietary exposure mainly results in accumulation of BaP in the bile and intestine (Sandvik et al., 1998).

Although BaP tends to be a small component of total PAH concentrations at a contaminated site, health risks from total PAH concentrations are often assessed relative to BaP toxicity (Ohiozebau et al., 2017); therefore concentrations of BaP for this study were modeled off total PAH concentrations found in fish prey at contaminated sites. For instance, in Norway, concentrations in tissues of the common limpet (*Patella vulgate*), a marine mollusk, were observed to be as great as 15 µg PAHs $g^{-1}$ (Knutzen and Sortland, 1982) while 303 µg PAHs $g^{-1}$ has been measured in the tissue of mussels from the French coast (Claisse, 1989). In sediments, concentrations as high as 142 µg PAHs $g^{-1}$ in Puget Sound (Malins et al., 1987), and 7,283 µg PAHs $g^{-1}$ in weathered creosote-contaminated sediment in Eagle Harbor, Washington (Neff et al., 2005) have been reported. Thus, dietary exposures could be as great as these concentrations (Silva et al., 2008).

Effects of BaP on the structure and function of the gut microbiome of fishes are not well studied. Aqueous exposures of adult fathead minnows to small concentrations of BaP resulted in an enrichment of taxa associated with hydrocarbon degradation and community compositional shifts (DeBofsky et al., 2020), and aqueous exposure of Japanese sea cucumbers (*Apostichopus japonicus*) to BaP resulted in fewer bacteria associated with beneficial functions within the host accompanied by an increase in alkane-degrading bacteria (Zhao et al., 2019).

This study assessed alterations of the gut microbiome following dietary exposure of juvenile fathead minnows to BaP. A limited duration exposure *via* the diet can deliver BaP into the intestine more directly and at comparably greater concentrations than *via* aqueous routes. Specific objectives of this study were to: 1) Characterize the gut microbiome in juvenile fathead minnows; 2) Measure bile metabolites resulting from exposure to BaP; 3) Characterize effects of BaP on the microbiome in guts of fish exposed to BaP, relative to that of unexposed controls; 4) Compare shifts in the microbiome to measured concentrations of BaP metabolites in the bile. To satisfy these objectives, the gut microbiome of juvenile

fathead minnows were characterized using 16S rRNA metabarcoding after dietary exposure to BaP for two weeks.

## 3.4 Materials and Methods

### *3.4.1 Fish husbandry, dietary exposure, and sampling*

Juvenile fathead minnows of approximately 2-3 months of age were obtained from an in-house stock population of the Aquatic Toxicology Research Facility at the University of Saskatchewan. After a one-week acclimation, fish were randomly assigned to each group ($n$ = 10 fishes per tank; 3 tanks per group) and were exposed to a solvent control (0.02% methanol, the solvent carrier for BaP), or nominal concentrations of 1, 10, 100, or 1,000 μg BaP $g^{-1}$ in food (dry mass, dm) for two weeks. Food was prepared by adding a solution of BaP to the food and allowing the methanol to evaporate.

At the end of the exposure, fish were euthanized *via* blunt force. Whole-body mass and total length were measured prior to dissection. Samples of whole gut, containing both tissues of the fish and adherent microbes, were excised from all fish. Gallbladders were also removed for quantification of BaP metabolites. Samples were placed in sterile cryovials, and held in liquid nitrogen until storage in a -80 °C freezer. Experiments proceeded as that outlined in the animal use protocol (Protocol #20090108) approved by the Animal Research Ethics Board at the University of Saskatchewan. The detailed methods for fish husbandry are described in Appendix B, Text B.1.

### *3.4.2 Quantification of BaP in food*

To quantify BaP in food, internal calibration and isotope dilution were used to quantify BaP in samples using an eight-point calibration curve between 0.5 and 500 ng BaP $mL^{-1}$, each containing 100 ng $mL^{-1}$ with BaP-d12. Pressurized liquid extraction was conducted to extract the target compounds. A blank cell (no fish food) was also loaded and extracted to serve as an extraction blank. Quantification of BaP was done on a GC-QE-Orbitrap mass spectrometer system (Q Exactive GC, Thermo Scientific, Mississauga, ON) with a Thermo RSH autosampler and a TRACE 1310 GC with a heated split/splitless injector running in splitless mode. For detailed information about the extraction and instrumental analysis methods, please refer to the method section of Appendix B, Text B.2.

### *3.4.3 Relative quantification of metabolites of BaP in bile*

A semi-quantitative method was applied due to the lack of available standards for Gluc and $SO_4$ metabolites of BaP. Concentrations of mono-hydroxylated benzo[a]pyrene (OH-BaP) were quantified directly with the use of analytical standards and external calibration. Semi-quantification of OH-BaP-O-glucuronide (BaP-Gluc), and sulfate-BaP (BaP-$SO_4$) was conducted using a relative response factor approach (Tang et al., 2016). Detailed methods for quantification can be found in Appendix B, Text B.3. Instrument detection limits of OH-BaP were determined using the lowest calibration standard (0.3 ng $mL^{-1}$) estimated as 3x and 10x the signal-to-noise ratio for the limit of detection (LOD) and limit of quantification (LOQ), respectively. Detection limits for BaP-Gluc and BaP-$SO_4$ had to be estimated from OH-BaP using the reported response factors, as was done for the bile concentrations (Appendix B, Table B.1).

### *3.4.4 16S rRNA metabarcoding and bioinformatics*

Total DNA was isolated from intestines using the AllPrep DNA/RNA Mini Kit (Qiagen Inc., Mississauga, ON). Amplification of the V3 -V4 hypervariable region of the 16S rRNA gene, construction of the sequencing library, 2x300 base pair (bp) sequencing on

MiSeq platform (Illumina, San Diego, CA), and bioinformatics were performed as described in DeBofsky et al., (2020). Extraction and no-template PCR controls were carried through sequencing to assess any impacts of contamination on the workflow. On average, 69% of demultiplexed reads survived through the cleaning process. In total, 99% of the cleaned reads aligned to bacteria. A full table of number of reads per sample, including the controls, pre- and post-cleaning can be found in Appendix B, Table B.2. To avoid biases resulting from differences in sequencing depth, based on a rarefaction curve (Appendix B, Fig. B.1), the feature table was rarefied at a depth of 13,133 sequences per sample. Alpha-diversities (Shannon diversity and observed amplicon sequence variants (ASVs)), or diversity within samples, and beta-diversities (unweighted UniFrac (Lozupone and Knight, 2005)), or differences between samples, were calculated in QIIME2 (Bolyen et al., 2019). PICRUSt2 (Douglas et al., 2019) was used to predict functional abundances of MetaCyc pathways (Caspi et al., 2017) based on 16S rRNA gene sequences. Data can be accessed at https://dx.doi.org/10.20383/101.0247.

*3.4.5 Statistics*

Statistical analyses were performed using the R Statistical Language v. 3.6.1 (R Core Team, 2013). Unless otherwise noted, statistics were calculated using vegan v. 2.5-6 (Oksanen et al., 2019). The distribution of variables was checked and compared between groups following previous pipelines (DeBofsky et al., 2020). No significant differences in measurements were observed among tanks. Condition factor was calculated as (Equation 3.1).

$$Condition\ Factor\ (K) = \frac{Mass\ (g)}{Standard\ Length\ (mm)^3} \times 100 \quad (3.1)$$

To normalize data, concentrations of BaP metabolites were $\log_{10}$-transformed; to account for the presence of zeros in this data set, an arbitrary value of 0.0001 ($ng^{-1}$ g) was given to these zero values. In some cases, volumes of bile were too small to obtain a sufficient response, which resulted in an N/A for those samples. To retain as much microbiome data as possible, empty bile values were assigned an average value from their treatment group. Outlier values were removed based on the following criteria: fish showing sexual differentiation or

statistical outlier fish of larger masses and/or length in each treatment group. Differentially abundant bacterial taxa and MetaCyc pathways were calculated using an ANOVA-Like Differential Expression tool (ALDEx2) v. 1.18.0 (Fernandes et al., 2014). ALDEx2 transforms the data using Aitchison's centered log-ratio (CLR). Additional Spearman correlations were also computed using CLR-transformed abundances of taxa and MetaCyc pathways. Differences among community compositions based on unweighted Unifrac distances were assessed using adonis2 (Oksanen et al., 2019), and the pairwise.adonis2 function with Bonferroni p-value adjustment (Martinez Arbizu, 2019). A Constrained Analysis of Principal Coordinates (CAP) was conducted using the capscale function in vegan to ordinate the data and view the clusters of samples. Significant BaP metabolites contributing to the ordination were assessed using an ANOVA. Association networks of abundant ASVs within treatment groups were inferred using Sparce Correlations for Compositional data (SparCC) (Friedman and Alm, 2012) with 100 bootstraps to assign p-values. Networks were displayed and analyzed with Cytoscape v. 3.8.0 (Shannon et al., 2003).

## 3.5 Results

### *3.5.1 Concentrations of BaP in food and bile metabolites*

Measured concentrations of BaP in food were close to the nominal concentrations (within 20% relative difference, Appendix B, Table B.3). Concentrations of metabolites in bile confirmed exposure of fish to BaP. Concentrations of $\log_{10}$-transformed OH-BaP (lgOH-BaP) metabolites were significantly different from control (Fig. 3.1; Kruskal-Wallis (KW) chi-squared = 57.2, $p < 0.001$). Based on a Dunnett's test, the lgOH-BaP metabolites only had a significantly ($p < 0.001$) greater concentration in fish fed 1,000 µg BaP $g^{-1}$ in the diet, relative to the control. The $\log_{10}$- transformed BaP-Gluc (lgBaP-Gluc) metabolites were significantly different among exposures (KW chi-squared = 67.4, $p < 0.001$). Concentrations of lgBaP-Gluc metabolites were significantly greater in the 100 and 1,000 µg $g^{-1}$ exposure groups relative to the control ($p < 0.001$ in all cases). Concentrations of $\log_{10}$-transformed BaP-$SO_4$ (lgBaP-$SO_4$) metabolites were also significantly different among exposures (KW chi-squared = 66.2, $p < 0.001$). Concentrations were greater in the 100 and 1,000 µg BaP $g^{-1}$ groups relative to the control ($p < 0.001$), and concentrations in fish fed 10 µg BaP $g^{-1}$ were greater than those of the

control ($p = 0.08$). Concentrations of $\log_{10}$-transformed sum of BaP metabolites were likewise significantly different among exposures (KW chi-squared = 66.3, $p < 0.001$). Concentrations were greater in fish fed 100 or 1,000 µg BaP $g^{-1}$ in the diet, relative to the control ($p < 0.001$), and concentrations in fish fed 10 µg BaP $g^{-1}$ were greater than those in the control ($p = 0.08$). The condition factor of these fish was not significantly impacted by exposure to BaP (Appendix B, Fig. B.2).

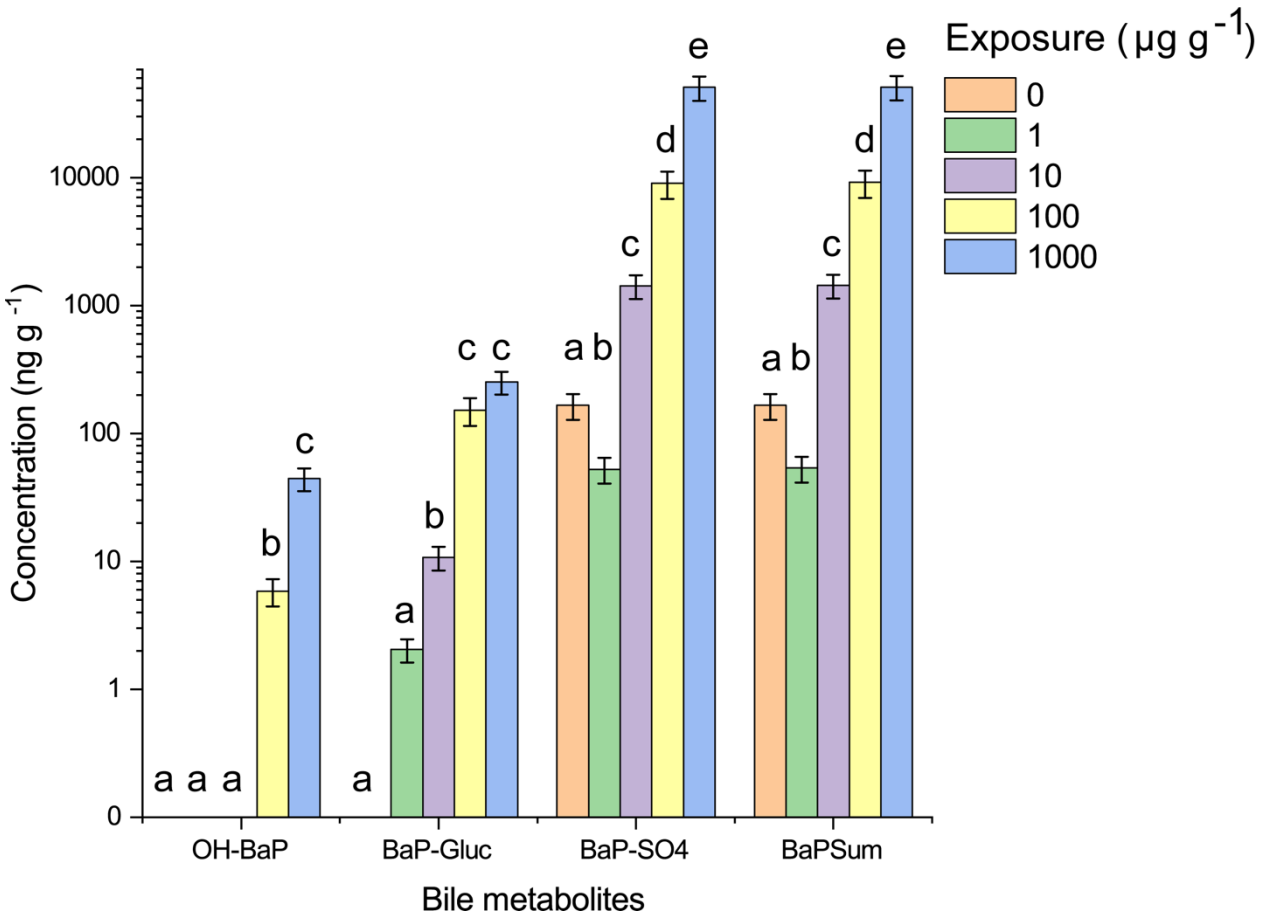


Figure 3.1. Concentrations of BaP metabolites (OH-BaP, BaP-Gluc, BaP-$SO_4$, and the sum of all metabolites) (ng $g^{-1}$) from bile (± S.E.) on a $log_{10}$-scale for each exposure group. Letters denote statistical significance within metabolite groups.

*3.5.2 Gut microbiome of juvenile fathead minnows*

Using metabarcoding of the V3-V4 hypervariable region of the 16S rRNA gene, the gut microbiome was characterized in juvenile fathead minnows. A total of 1,309 non-singleton ASVs of 64 unique genera of bacteria among 83 samples (control: $n$ = 17; 1 µg g-1: $n$ = 16; 10 µg g-1: $n$ = 16; 100 µg g -1: $n$ = 16; 1,000 µg g -1: $n$ = 18) remained after filtering. Filtering removed 67 total samples of the 150 total samples; 33 samples were removed due to low sequencing depth and 34 samples were removed due to sexual differentiation over the course of the exposure. The dominant phyla (± standard error) in guts of fathead minnows were *Fusobacteria* (65% ± 1%), *Proteobacteria* (26% ± 1%), and *Firmicutes* (2% ± 0.05%) (Fig. 3.2A). The dominant classes were *Fusobacteriia* (65% ± 0.3%), *Gammaproteobacteria* (25% ± 0.05%), and *Bacteroidia* (6% ± 0.008%) (Fig. 3.2B), while the dominant families were Fusobacteriaceae (65% ± 1%), Aeromonadaceae (19% ± 1%), Pseudomonadaceae (3% ± 0.3%), and *Flavobacteriaceae* (3% ± 0.3%) (Fig. 3.2C).

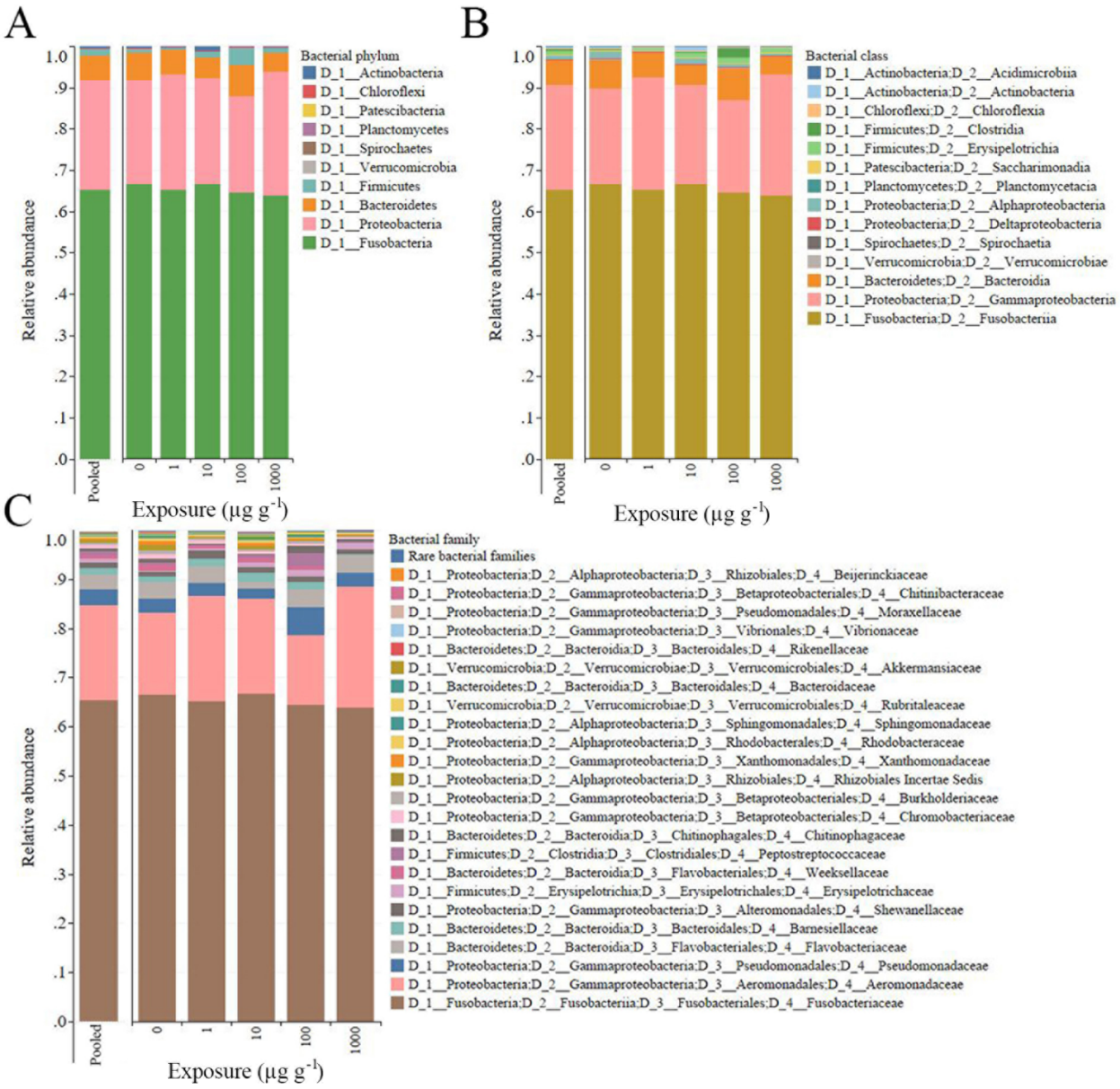


Figure 3.2. Relative abundances of the more abundant bacterial (A) phyla, (B) class, and (C) families in guts of juvenile fathead minnows, both pooled and based on exposures.

*3.5.3 Dietary exposure of BaP altered the compositions of gut microbiomes in fathead minnows*

Exposure to BaP altered families with lower abundances rather than the dominant bacterial families. Based on exposure groups, several CLR-transformed relative abundances of families were significantly different relative to the control group. *Barnesiellaceae* (KW chi-squared = 41.7, $p < 0.001$), *Rubritaleaceae* (KW chi-squared = 25.9, $p < 0.001$), *Bacteroidaceae* (KW chi-squared = 37.3, $p < 0.001$), *Xanthomonadaceae* (KW chi-squared = 15.0, $p = 0.004$), *Weeksellaceae* (KW chi-squared = 14.4, $p = 0.006$), *Chromobacteriaceae* (KW chi-squared = 11.7, $p = 0.02$) and *Rikenellaceae* (KW chi-squared = 37.3, $p < 0.001$) were all significantly different among exposure groups. *Barnesiellaceae* ($p = 0.03$), *Rubritaleaceae* ($p < 0.001$), *Xanthomonadaceae* ($p = 0.02$), *Weeksellaceae* ($p = 0.01$), and *Chromobacteriaceae* ($p = 0.007$) were all significantly lower in abundance in fish fed 1,000 µg BaP g -1 relative to the control group. Based on Spearman rank correlations, several CLR-transformed relative abundances of families were significantly correlated with concentrations of lgBaP-SO4 metabolites. Relative abundances of families that were significantly negatively correlated with lgBaP-SO4 included *Bacteroidaceae, Barnesiellaceae,* and *Chromobacteriaceae.* Significantly positively correlated families with lgBaP-SO4 include *Brevinemataceae*, *Caulobacteraceae*, *Microbacteriaceae, Erysipelotrichaceae*, *Chitinibacteraceae,* and *Moraxellacea* (Fig. 3.3A).

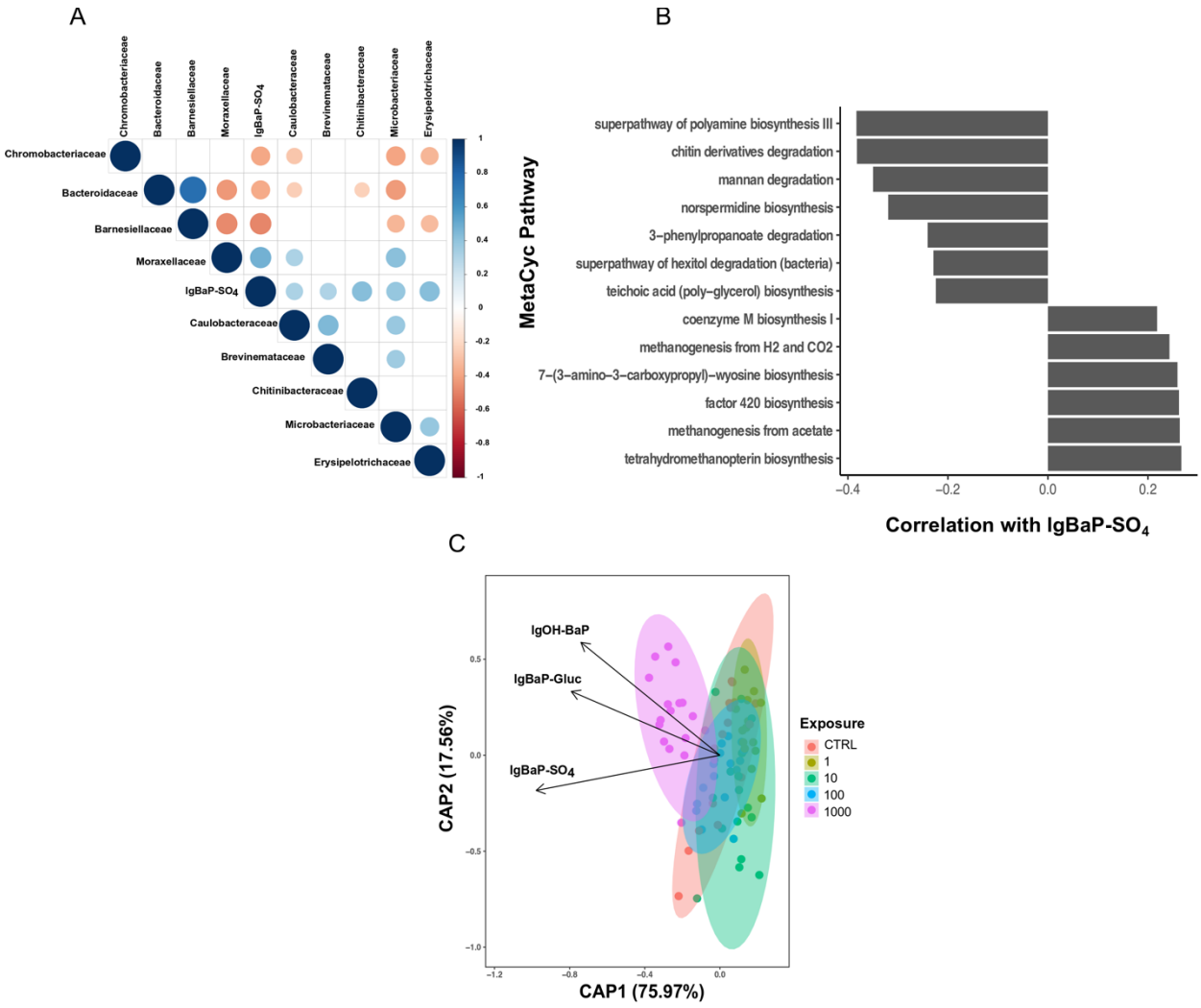


Figure 3.3. (A) Correlation plot of families that are significantly correlated (Spearman correlation, $p < 0.05$) with log-transformed BaP-SO4 bile concentrations as well as with each other. (B) MetaCyc pathways that are significantly correlated ($p < 0.05$) with log-transformed BaP-SO4 bile metabolite concentrations. Various pathways are shown relative to their correlation coefficients (ρ). (C) Constrained Analysis of Principal Coordinates (CAP) of the different exposure groups constrained by the vectors of the measured metabolite concentrations, using unweighted Unifrac distances. Log-transformed OH-BaP and BaP-SO4 metabolites are the significant environmental variables constraining the ordination ($F = 3.00$ and 2.64, $p = 0.003$ and 0.005, for lgOH-BaP and lgBaP-SO4, respectively).

*3.5.4 Dietary exposure of BaP altered predicted functional bacterial pathways of the gut microbiome in fathead minnows*

Functional responses of the gut microbiome to BaP were also assessed with PiCRUST2. In total, based on Spearman correlations, 13 MetaCyc pathways were significantly correlated with lgBaP-$SO_4$. Seven pathways [superpathway of polyamine biosynthesis III, chitin derivatives degradation, mannan degradation, norspermidine biosynthesis, 3-phenylpropanoate degradation, superpathway of hexitol degradation (bacteria), and teichoic acid (poly-glycerol) biosynthesis] were negatively correlated with lgBaP-$SO_4$. Six pathways [coenzyme M biosynthesis I, methanogenesis from H2 and CO2, 7-(3-amino-3-carboxypropyl)-wyosine biosynthesis, factor 420 biosynthesis, methanogenesis from acetate, and tetrahydromethanopterin biosynthesis] were positively correlated with concentrations of lgBaP-$SO_4$ (Fig. 3.3B).

*3.5.5 Effects on structure of the gut microbiome in fathead minnows exposed to BaP*

Community structure of the gut microbiomes were significantly different dependent upon exposure to BaP. The 1, 10, and 1,000 µg BaP $g^{-1}$ exposure groups all exhibited significantly distinctive community structures compared to that of the controls (Adonis test on unweighted Unifrac distances: 1 µg $g^{-1}$ vs. control $F = 2.6$, $p = 0.007$, 10 µg $g^{-1}$ vs. control $F = 2.5$, $p = 0.017$, 1,000 µg $g^{-1}$ vs. control $F = 5.1$, $p < 0.001$). It was expected that all groups would have significantly different community compositions relative to that of the controls, but the microbiomes of fish fed 100 µg BaP $g^{-1}$ did not follow this pattern. That group exhibited greater variation than did other groups, both in terms of metabolites and microbial composition, which may have contributed to its position as an exception.

Comparison of community structure and metabolite concentration *via* a CAP, using lgOH-BaP, lgBaP-gluc, and lgBaP-$SO_4$, was significant (ANOVA test: $F = 2.06$, $p = 0.002$) with lgOH-BaP and lgBaP-$SO_4$ being the significant environmental variables constraining the ordination (Fig. 3.3C: $F = 3.00$ and 2.64, $p = 0.003$ and 0.005, for lgOH-BaP and lgBaP-$SO_4$,

respectively). The BaP metabolites used in the CAP revealed that the exposure groupings ordinated in the logical direction of the metabolite vectors, visually indicating that the metabolites were defining the groupings (Fig. 3.3C). Exposure to BaP also altered the network of gut microbiomes in fathead minnows. Network analysis revealed a reduction in the complexity of community structures of gut microbiome in the exposure groups (Fig. 3.4). The number of nodes within networks were significantly negatively correlated with the $\log_{10}$-transformed nominal concentration of BaP (linear regression: $p < 0.05$, $R_2 = 0.88$; Appendix B, Fig. B.3).

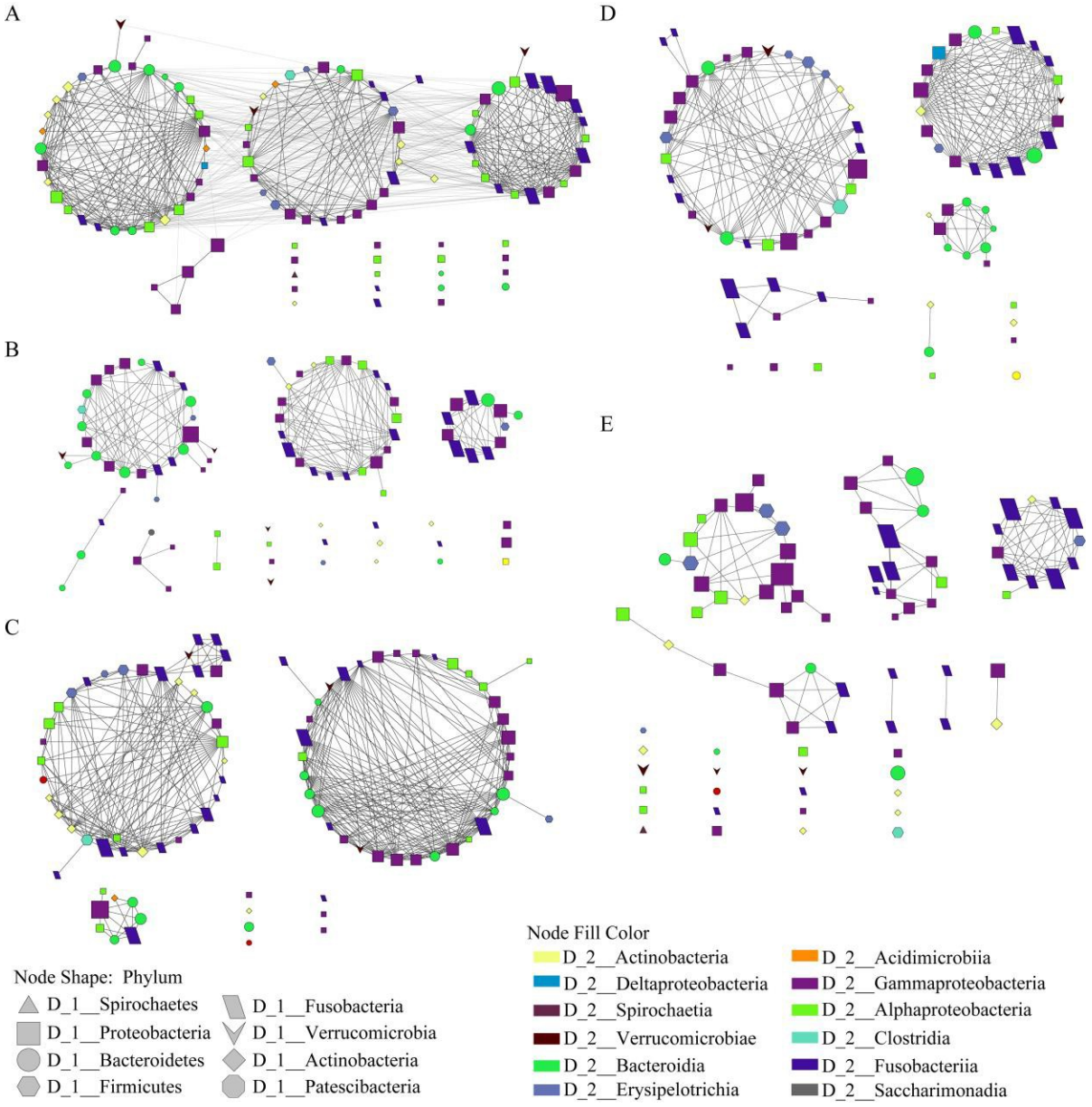


Figure 3.4**.** Association networks of taxa at the class level relative to exposure groups for the (A) control, (B) 1, (C) 10, (D) 100, and (E) 1,000 µg $g^{-1}$ exposure groups. Associations were generated by SparCC with 100 bootstraps to assign p-values. The associations were filtered to include only correlations with a correlation $\rho > 0.7$ and a 'two-tailed' *p*-value < 0.01. Only correlations with $\rho > 0.50$ and $p < 0.05$ (two-tailed) were included. Networks with genus labels are presented in Appendix B, Fig. B.2.

Alpha-diversity indices of gut microbiome were reduced in the fish exposed to greater concentrations of BaP. Shannon diversity, which accounts for both evenness and abundance of species present, was marginally different among exposures (KW chi-squared = 9.2, $p = 0.06$), but the Shannon diversity value for the 1,000 µg BaP $g^{-1}$ exposure group was significantly less than that of the controls (Dunnett's test, $p = 0.03$; Table 1). Overall, there was an inverse correlation ($p = 0.06$) between Shannon diversity and concentrations of lgBaP-$SO_4$. The number of observed ASVs was also significantly inversely proportional to exposure concentrations (ANOVA, F = 8.93, $p < 0.001$), with the communities in fish fed 1,000 µg BaP $g^{-1}$ having significantly fewer ASVs than the control group (Dunnett's test, $p < 0.001$; Table 3.1). While there was an overall inverse trend between the number of ASVs as a function of lgBaP-$SO_4$, the correlation was less significant ($p = 0.1$).

Table 3.1. Mean values and standard error for Shannon Diversity Index and observed number of amplicon sequence variants (ASVs) for each exposure group. Asterisks denote statistical differences from the control groups.

| | **Exposure (µg $g^{-1}$)** | **Mean ± S.E** |
|---|---|---|
| **Shannon** | Control | 4.38 ± 0.13 |
| | 1 | 4.28 ± 0.08 |
| | 10 | 4.43 ± 0.06 |
| | 100 | 4.28 ± 0.18 |
| | 1000 | 4.02 ± 0.12 * |
| **ASVs** | Control | 91.45 ± 4.75 |
| | 1 | 82.64 ± 4.39 |
| | 10 | 96.5 ± 4.36 |
| | 100 | 86.64 ± 4.4 |
| | 1000 | 62.67 ± 3.11* |

## 3.6 Discussion

The dominant bacterial phyla of the gut microbiome in juvenile fathead minnows are consistent with those of other freshwater fishes, which indicates a conserved microbiome among fishes. Dominance of *Fusobacteria* and *Proteobacteria* has been observed not only in other studies utilizing fathead minnows (DeBofsky et al., 2020; Narrowe et al., 2015), but also in other species, such as zebrafish (*Danio rerio*) (Roeselers et al., 2011) and common carp (*Cyprinus carpio*) (Li et al., 2013). Minor differences occurred between the dominant taxa reported in this study and those reported previously for the fathead minnow (DeBofsky et al., 2020). In this study, *Fusobacteria* was dominant (65%), whereas we previously reported the dominance of *Proteobacteria* (63%). This disparity could have resulted from maturation of these fish, since age and sexual maturation are driving factors in bacterial community composition (Org et al., 2016; Stephens et al., 2015; Wong et al., 2015). Although we previously reported that sex was a major factor that shaped the microbiome, the fish in this study had not yet reached a stage of sexual differentiation, making the distinction between male and female fishes impossible.

Concentrations of BaP metabolites measured in this study were also consistent with those found in contaminated sites around the world. Concentrations of biliary metabolites, expressed as BaP equivalents, have been found at concentrations as great as 193 ng $ml^{-1}$ in *Alepocephalus rostratus*, a deep-sea fish, in the Mediterranean Sea (Escartín and Porte, 1999). Sum concentrations of PAH metabolites in bile of lake whitefish (*Coregonus clupeaformis*) in the Athabasca River at Fort McKay in the oil sands region of Canada were as great as 8,100 ng $ml^{-1}$ (Ohiozebau et al., 2016). In this study, mean concentrations of sum BaP metabolites expressed as ng $ml^{-1}$ in bile of fish exposed to 1,000 ug BaP $g^{-1}$ was 517 ng $ml^{-1}$. Therefore, concentrations of BaP fed to fathead minnows resulted in concentrations of metabolites in bile that are in the range of concentrations observed in fishes at moderately contaminated sites. Measuring biliary metabolites reflects recent exposure to PAHs; incorporating concentrations of BaP metabolites into this study allows for comparison to environmental monitoring studies of PAHs, where this is a common practice (Ohiozebau et al., 2016).

The results of this study revealed that a dietary exposure to BaP at environmentally-relevant concentrations has significant, dose-dependent effects on the fathead minnow gut microbiome. BaP might be altering the gut microbiome directly or since BaP is a ligand of the aryl hydrocarbon receptor (AhR), via modulation of pathways associated with the AhR (Ortiz-Delgado et al., 2007). The AhR regulates host-microbiome communications (Zhang et al., 2017) in a bidirectional manner (Korecka et al., 2016). Exposure to BaP not only altered the composition of certain taxa and overall diversity, but also changed network connectivity of those taxa.

Due to exposure to BaP, there were taxa that were significantly enriched, signifying that certain taxa might be able to use BaP as a growth substrate. Altered conditions, both in the microbial community and within the host, might allow pathogenic taxa to proliferate (Fig. 3D). Overall, *Caulobacteraceae, Microbacteriaceae and Erysipelotrichaceae* were significantly positively correlated with the BaP-$SO_4$ metabolite. The family *Caulobacteraceae* has been observed in soils contaminated with crude and diesel oils (Bell et al., 2011; Yergeau et al., 2012) and is capable of degradation of aromatic compounds (Nierman et al., 2001). Enrichment of the family *Microbacteriaceae* has similarly been associated with contaminated soil sites (Bell et al., 2011; Jacques et al., 2007). Increased abundance of the family *Erysipelotrichaceae* was also observed in mice that were exposed via the diet to BaP (Ribière et al., 2016) and via drinking water to heavy metals (Breton et al., 2013). Studies in humans have related abundance of *Erysipelotrichaceae* with colorectal cancer (Chen et al., 2012), a particularly interesting finding since BaP is carcinogenic (Gelboin, 1980). Increases in abundances of bacteria in the family *Moraxellaceae,* which contains several opportunistic pathogens (Austin and Austin, 2016), is associated with increased stress in fish (Boutin et al., 2013). Furthermore, these same taxa are capable of degrading BaP when isolated from human skin (Sowada et al., 2014).

Analyses of individual taxa also revealed several taxa that were negatively correlated with the BaP-$SO_4$ metabolite that might be associated with direct deleterious effects on the

physiology of the host. The presence of the family *Bacteroidaceae* in the gut of a host is considered mutualistic, with both the bacteria and the host benefiting from the interaction (Bäckhed et al., 2005). *Bacteroidaceae* are in part responsible for the production of digestive enzymes and the digestion of polysaccharides (Bäckhed et al., 2005; Ikeda-Ohtsubo et al., 2018; Thomas et al., 2011) and is involved in regulation of the immune system (Hiippala et al., 2018). Mice exposed to 2,3,7,8-tetrachlorodibenzo-*p*-dioxin (TCDD), another AhR modulator, exhibited lesser abundances of several families of Bacteroidetes (Lefever et al., 2016). These results suggest that the reduction in *Bacteroidaceae,* and possibly *Barnesiellaceae*, another member of the order Bacteroidales, might be associated with deleterious effects caused by exposure to BaP, including impairment of immune function (Carlson et al., 2004a; Reynaud and Deschaux, 2006).

Several MetaCyc pathways were positively or negatively associated with concentrations of BaP-$SO_4$. One pathway, chitin derivatives degradation, which had a negative relationship with BaP-$SO_4$, is associated with *Bacteroidaceae* (Olsen et al., 1996). Inability to degrade chitin might result in lesser ability to obtain nutrients from food for proper health or defend against pathogens (Ringø et al., 2012). The same holds true for the reduction in the mannan degradation pathway, where reduced ability to degrade mannan might result in increased susceptibility to pathogens (Dimitroglou et al., 2009; Torrecillas et al., 2012), and reduction of teichoic acid (poly-glycerol) biosynthesis, which is involved in activating the innate immune response (Bron et al., 2012; Hoseinifar et al., 2015). Pathways that were positively correlated with lgBaP-$SO_4$ in bile included methanogenesis from $H_2$ and $CO_2$ and methanogenesis from acetate. Anaerobic degradation of hydrocarbons to methane and $CO_2$ requires $H_2$ and $CO_2$ utilizing bacteria as well as acetate-utilizing methanogenic bacteria (Chang et al., 2005; Zengler et al., 1999). It is therefore plausible that the exposure results in an enrichment of bacteria capable of degrading hydrocarbons. While these pathways are informative, it should be noted that they are predictive and not confirmed with functional transcriptomic analysis.

The reduction in network complexity was an unexpected result of exposure to BaP. Reduction in the number of nodes represents fewer taxa present in those samples, while a reduction in the number of edges reflects fewer connections among those nodes (Friedman and Alm, 2012). Although interactions between microbes have not been well-explored (Hunt and Ward, 2015), ecological network responses to anthropogenic perturbation are not new

(Elmqvist et al., 2003; Power et al., 1996; Vinebrooke et al., 2004). Loss of co-occurrence of taxa within a microbial community might result in altered interactions among taxa, which can change function of certain taxa or allow proliferation of others (Karimi et al., 2017). At greater concentrations of BaP in the diet, numbers of associations with other taxa decreased, meaning that the abundance of those taxa was independent of other taxa (Karimi et al., 2017). The greater the number of edges, the greater the complexity of the system (Tylianakis et al., 2009), and a large degree of connectedness can be considered a shared ecological niche within the community (Karimi et al., 2017). A reduction in network complexity has been observed in terrestrial systems with high concentrations of air pollution (Karimi et al., 2016) and at a chlor-alkali tailings dump (Zappelini et al., 2015). Losses of nodes, or taxa, and edges, or those connections, signifies the breakdown of the ecological niche. Therefore, loss of community structure in the microbiome could be an indicator of exposure to a toxicant (Derocles et al., 2018).

## 3.7 Conclusions

Overall, this study revealed that chronic exposure to BaP in the diet significantly altered the community structure of gut microbiome of fathead minnows. The measurement of concentrations of metabolites of BaP in bile was more closely related to effects on individual and community responses and more thoroughly explained diversity than did nominal exposure concentrations in the diet. Several taxa associated with health and hydrocarbon degradation were significantly correlated with measured metabolite concentrations. Community compositions shifted and network associations were drastically altered based on the exposures. These results

highlight the need for future work to determine mechanistic causes of community compositional differences and ultimately how gut microbial changes may interplay with host adverse outcomes.

## 3.8 Acknowledgments

Funding was provided by “Next generation solutions to ensure healthy water resources for future generations” funded by the Global Water Futures program, Canada First Research Excellence Fund ( #419205). Dr. Brinkmann was also supported through the Global Water Futures program. Dr. Challis was funded by the Banting Post-Doctoral Fellowship. Prof. Giesy was supported by the Canada Research Chairs Program of the Natural Sciences and Engineering Research Council of Canada (NSERC).

# CHAPTER 4: RNA metabarcoding unearths the response of rare gut microbiome of fathead minnows exposed to benzo[a]pyrene

## 4.1 Preface

Unlike the previous chapter, this chapter focuses on the effects of benzo[*a*]pyrene (BaP) on the *active* gut microbiomes of juvenile fathead minnows (*Pimephales promelas*) after the same fourteen-day dietary exposure, using environmentally-relevant concentrations. The active gut microbiome was characterized using 16S rRNA-based RNA metabarcoding, to determine its response to dietary exposure to BaP. Contrary to findings in Chapter 3 with the genomic microbiome, the active microbiome neighborhood networks were not reduced in response to BaP exposure, showing a degree of ecological resistance and resilience in the active bacteria. This work builds upon the research from Chapter 3; differences between the genomic and active microbiomes highlights the need to assess both DNA- and RNA-based 16S rRNA metagenetics to fully ascertain community-level variations in the microbiome in response to contaminant exposure.

Author contributions:

- Abigail DeBofsky: Experimental design (90%), bench work (100%), bioinformatics (80%), and statistical analysis (90%), with the exception of running the GCMS and LCMS for food and bile detection of BaP/metabolites, as well as creation of the manuscript (90%)
- Dr. Yuwei Xie: Assistance with design of experiment (10%), bioinformatics (20%),

statistical analysis (10%), and revisions of the manuscript (80%)

- Dr. Jonathan Challis: Assistance with running the LCMS (100%), interpreting the chemical data (100%), writing the LCMS portion of the manuscript (5%), and editing the manuscript (5%)
- Dr. Markus Brinkmann: Developed the methods for analyzing the BaP metabolites in bile and edited the manuscript (5%)
- Dr. Paul D. Jones: Assistance with running the GCMS (100%), interpreting the chemical data (100%), writing the GCMS portion of the manuscript (5%), and editing the manuscript (5%)
- Dr. John P. Giesy: Provided scientific input and guidance, edited the manuscript (5%), and provided funding for the research

## 4.2 Abstract

Activity of the gut microbiome is often overlooked in assessments of ecotoxicological effects of environmental contaminants. Effects of the polycyclic aromatic hydrocarbon, benzo[a]pyrene (BaP), a model persistent organic pollutant, on gut microbiomes of juvenile fathead minnows (*Pimephales promelas*) were investigated. Fish were exposed for two weeks, to concentrations of 0, 1, 10, 100, or 1,000 μg BaP $g^{-1}$ in the diet. The active gut microbiome was characterized using 16S rRNA-based RNA metabarcoding, to determine its response to dietary exposure to BaP. BaP only reduced alpha-diversity at the greatest exposure concentrations, but exposure to BaP did alter community composition and result in differential abundance of taxa associated with hydrocarbon degradation and fish health. Neighborhood selection networks were not reduced with greater concentrations of BaP, which suggests ecological resistance and/or resilience. The taxa represented by either DNA- or RNA-based 16S rRNA metagenetics were largely the same, but did not overlap entirely, providing complementary results of the overall impact of BaP on the microbiome of the gut. Analysis of the DNA-normalized microbiome revealed taxa that became active or dormant due to exposure to BaP. These differences highlight the need to assess both DNA- and RNA-based 16S rRNA to fully derive bacterial compositional changes resulting from exposure to contaminants.

## 4.3 Introduction

The gut microbiome is a crucial component of host health and is dynamic and varied across environmental conditions (Coyte and Rakoff-Nahoum, 2019; Ikeda-Ohtsubo et al., 2018). Facing environmental fluctuation, the biodiversity of the gut microbiome is vital to the stabilization of the internal ecosystem for proper functioning and host well-being (Van den Abbeele et al., 2013; Vinebrooke et al., 2004). Vertebrate gut microbiomes are typically dominated by a few abundant species and several rarer species (Antwis et al., 2019; Jousset et al., 2017; Rolig et al., 2015). Rare species can have overlooked roles such as modulating hormone metabolites (Antwis et al., 2019) or the immune system (Rolig et al., 2015), which can ultimately be linked to effects on fitness of host metazoans (Chen et al., 2016; Sfanos et al., 2018). Additionally, environmental contaminants are capable of shaping structures of gut microbiomes, which can result in disturbed homeostasis (Adamovsky et al., 2018; Claus et al., 2016). However, effects of environmental contaminants on rare gut microbiomes are still largely unknown.

Although DNA and RNA metabarcoding provide powerful tools for characterizing rare flora (i.e. Chen et al., 2016; Jousset et al., 2017; Revetta et al., 2011; Rolig et al., 2015), RNA metabarcoding has advantages for better detection of rare species under environmental variability. In most microbiome studies, the distinction between active and total bacteria has been overlooked, often focusing solely on the genomic characterization of the gut microbiome. Since it presents the entire microbiome, including the dormant flora, DNA metabarcoding can be described as the genomic capability of the microbiome, while RNA metabarcoding serves as a proxy for transcriptomic activity of the microbial community (De Vrieze et al., 2016). Since bacteria in the microbiome of the gut can be abundant or rare, DNA can provide insights into more abundant taxa with little activity, while RNA can give information on less abundance taxa with greater activity (Revetta et al., 2011).

Benzo[a]pyrene (BaP) is an optimal toxicant to stimulate and study rarer flora. BaP has a clear effect on the microbiome in aquatic animals, as deciphered through DNA metabarcoding, but never RNA metabarcoding. Aqueous exposures of small concentrations of BaP to adult fathead minnows (*Pimephales promelas*) resulted in shifts in compositions of microbiomes of the gut, as well as enrichment of taxa associated with degradation of hydrocarbons (DeBofsky et al., 2020). Aqueous exposure of Japanese sea cucumbers

(*Apostichopus japonicus*) to BaP resulted in an increase of bacteria associated with beneficial functions within the host and growth of alkane-degrading taxa (Zhao et al., 2019). Furthermore, exposing juvenile fathead minnows to BaP not only elicits community compositional shifts, but also results in the degradation of association networks of bacteria (Chapter 3). RNA metabarcoding can elucidate the response of rarer taxa to a known modulator of the microbiome that may be crucial to the overall host homeostatic response in the face of a toxicant.

In order to investigate the response of the active microbiome, this study utilized dietary exposure of juvenile fathead minnows (*Pimephales promelas*) to BaP. Specific objectives were to: 1) Describe the active gut microbiome in juvenile fathead minnows; 2) Characterize the responses of the active gut microbiome to exposure of BaP; and 3) Compare responses of abundant and rare gut microbiome to exposure of BaP. To satisfy these objectives, the microbiome in guts of fathead minnows were characterized using 16S rRNA-based RNA metabarcoding after dietary exposure to BaP for two weeks.

## 4.2 Materials and Methods

### *4.4.1 Fish husbandry, dietary exposure, and sampling*

Fish husbandry procedures from this exposure have been fully described previously in Chapter 3. Briefly, juvenile fathead minnows were acclimated at ten juvenile fish per 5-gallon tank at a temperature of 25 ± 1 °C with a 16h-light:8h-dark photoperiod. Fish were fed EWOS® Micro Crumble trout chow (Cargill Inc., Wayzata, MN), two times daily on a maintenance food ration (2% of mean, wet body mass per day). After a one-week acclimation, fish were randomly assigned to each group (n = 10 fish per tank; 3 tanks per treatment), and exposed to a solvent control (0.02% methanol), or nominal concentrations of 1, 10, 100 or 1,000 µg $g^{-1}$ dry mass (dm) of BaP in food for two weeks. Nominal concentrations were based on environmentally-relevant concentrations of PAHs found at highly contaminated sites (Claisse, 1989; Knutzen and Sortland, 1982). At the end of the two-week exposure, the whole intestinal tract was excised from each fish to collect the microbiome, and gallbladders were removed for quantification of BaP metabolites. Samples were held in liquid nitrogen until transport to a -80 °C freezer. All fish procedures followed the animal use protocol

(#20090108) approved by the Animal Research Ethics Board at the University of Saskatchewan.

### *4.4.2 Quantification of BaP in food and BaP metabolites in bile*

Detailed procedures of quantification of BaP in food and BaP metabolites in bile are available in Chapter 3. Briefly, to quantify BaP in food, stock solutions of BaP and deuterium labelled BaP-d12 were made at 1,000 µg $mL^{-1}$ in acetone. Internal calibration based on isotope dilution was used to quantify BaP in samples using an eight-point calibration curve between 0.5 and 500 ng $mL^{-1}$, each spiked at 100 ng $mL^{-1}$ with BaP-d12. Triplicate 0.05 g aliquots of prepared food were spiked with BaP-d12 at a target concentration of 100 ng $mL^{-1}$ in the final 1 mL extract. Each sample was extracted using an accelerated solvent extraction cell. Bile samples were first weighed then diluted 1:10 in acetonitrile before analysis. In order to maintain concentrations within the linear dynamic range of the calibration curve, extracts were either blown-down by nitrogen evaporation or diluted and subsampled. Concentrations of mono-hydroxyalated benzo[a]pyrene (OH-BaP) were quantified directly by use of analytical standards and external calibration. Semi-quantification of OH-BaP-O-glucuronide (BaP-Gluc) and sulfate- BaP (BaP-$SO_4$) was accomplished by use of a relative response factor approach. Analysis was done by GC-QE-Orbitrap mass spectrometer system (Q Exactive, Thermo Scientific). Detailed results of the BaP in food and BaP metabolites in bile have been presented previously (Chapter 3).

### *4.4.3 Metabarcoding and bioinformatics*

The active gut microbiome was characterized by RNA metabarcoding targeting the 16S rRNA gene. Total RNA was co-isolated with DNA from intestines using the AllPrep DNA/RNA Mini Kit (Qiagen Inc., Mississauga, ON). Genomic DNA was removed by on-column digestion with DNAse I. Complementary DNA (cDNA) was synthesized with the SuperScript™ IV Reverse Transcriptase kit (ThermoFisher Scientific, Waltham, MA), following the manufacturer's instructions. PCR amplification of the V3-V4 region of the 16S rRNA gene, construction of the sequencing libraries, 2x300 base pair dual index sequencing on the MiSeq platform (Illumina, San Diego, CA), and bioinformatics were performed as

previously described (DeBofsky et al., 2020). Reads of DNA and RNA metabarcoding were pooled and analyzed together in the same bioinformatics pipeline to compare the two metabarcoding techniques. On average, 69% of demultiplexed reads survived through the cleaning process, and 99% of the cleaned reads aligned to bacteria. A table of number of reads per sample, including extraction and PCR controls, pre- and post-cleaning are summarized in Appendix C, Table C.1. The feature table was rarefied at 13,133 sequences per sample to avoid biases introduced by different sequencing depths (Appendix C, Figure C.1). Alpha- (Shannon diversity and number of observed amplicon sequence variants (ASVs)) and beta-diversities (Bray-Curtis dissimilarities) were calculated in QIIME2 (Bolyen et al., 2019). PICRUSt2 (Douglas et al., 2019) was used to predict functional abundances of MetaCyc pathways (Caspi et al., 2017) based on 16S rRNA gene sequences (Czech et al., 2020). Data can be accessed at: https://dx.doi.org/10.20383/101.0247. Thirty-four samples were removed due to low sequencing depth, and 32 samples were removed due to sexual differentiation, as determined by gonadal inspection upon dissection, over the course of the exposure.

*4.4.4 Statistics*

Statistical analyses were performed using R Statistical Language v. 3.6.1 (R Core Team, 2013). Because there were no differences among replicate tanks, each individual fish was considered a replicate within the exposure groups. Assumptions of normality and equal variance were assessed, then depending on whether the assumptions of parametric statistics were met or not, either an analysis of variance (ANOVA) followed by a Tukey Post-Hoc test or a Kruskal-Wallis (KW) test followed by a Dunnett's test to compare exposure groups to the solvent control was used. Unless otherwise noted, statistics were completed using the 'vegan' package (Oksanen et al., 2019). Concentrations of metabolites of BaP were $\log_{10}$-transformed prior to statistical analysis. To avoid taking logs of zero, an arbitrary value of 0.0001 ng $g^{-1}$ was assigned to zero values. To retain as much microbiome data as possible, samples where the gall bladder was empty were assigned as the average value from their exposure group. The ratio of RNA to DNA was assessed independently to assess relative activity of bacterial genus. The DNA normalized active microbiome was calculated (Equation 4.1).

$$\lambda_{f,i} = \frac{R_{f,i}}{\sum_f^n R_{f,i}} \div \left[\frac{D_{f,i}}{\sum_f^n D_{f,i}} + \frac{1}{2} \times \frac{t}{\sum_f^n D_{f,i}}\right] \quad (4.1)$$

$R_{f,i}$ and $D_{f,i}$ are the counts of feature *f* in sample *i*, for the RNA metabarcoding and DNA metabarcoding respectively. The variable *t* is the detection limit, here set to 1 read, and *n* is the sample size after filtering.

Differentially abundant bacterial taxa and MetaCyc pathways were calculated using the ANOVA-Like Differential Expression tool (ALDEx2) (Fernandes et al., 2013). Spearman correlations between taxa or MetaCyc pathways and log-transformed BaP-$SO_4$ (lgBaP-$SO_4$) were also computed by use of Aitchison's centered log-ratio (CLR)-transformed data. To determine differences among community composition based on nucleotide and exposure conditions, Bray- Curtis dissimilarities for log-transformed ASV values at the level of genera for each exposure group were assessed using 'adonis2' (Oksanen et al., 2019), and the pairwise.adonis2 function with Bonferroni p-value adjustment (Martinez Arbizu, 2019). A Constrained Analysis of Principal Coordinates (CAP) was conducted to ordinate the data and view the clusters of samples as constrained by the log-transformed BaP metabolite data. Significant BaP metabolites contributing to the ordination were assessed using an ANOVA of the terms. To visualize community differences, bootstrapped Bray-Curtis dissimilarity averages of the genus tables for each exposure group were plotted using metric MDS (PRIMER-e v.7). Neighborhood selection network (Meinshausen and Bühlmann, 2006) was constructed by the SPIEC-EASI package (Kurtz et al., 2015).

## 4.5 Results

### *4.5.1 Concentrations of BaP in food and bile metabolites*

Concentrations of BaP in the food and in bile metabolites are detailed in Chapter 3 (Appendix C, Table C.2). Concentrations in the food were near the nominal concentrations set at 0, 1, 10, 100 and 1,000 µg $g^{-1}$, and concentrations in the bile followed a dose-dependent pattern. Because concentrations of BaP-$SO_4$ were predominant in the bile, it was used for downstream correlation analysis.

### *4.5.2 Active gut microbiome of juvenile fathead minnows*

The active gut microbiome was diverse but dominated by limited numbers of key taxa. In total, 1,575 non-singleton active ASVs of 75 bacterial genera among 84 samples (*n* = control:

19, 1 µg $g^{-1}$: 15, 10 µg $g^{-1}$: 20, 100 µg $g^{-1}$: 15, 1,000 µg $g^{-1}$: 15) were recovered using RNA metabarcoding. The active gut microbiomes were dominated by *Proteobacteria* (48% ± 1%), *Fusobacteria* (43.5% ± 1%), and *Bacteroidetes* (4% ± 0.4%) at the phylum level (Fig. 4.1A). The dominant classes were *Gammaproteobacteria* (46% ± 1%), *Fusobacteriia* (43% ± 1%), and *Bacteroidia* (4% ± 0.4%) (Fig. 4.1B). The dominant families were *Fusobacteriaceae* (43% ± 1%), *Aeromonadaceae* (26% ± 1%), and *Pseudomonadaceae* (13% ± 1%) (Fig. 4.1C).

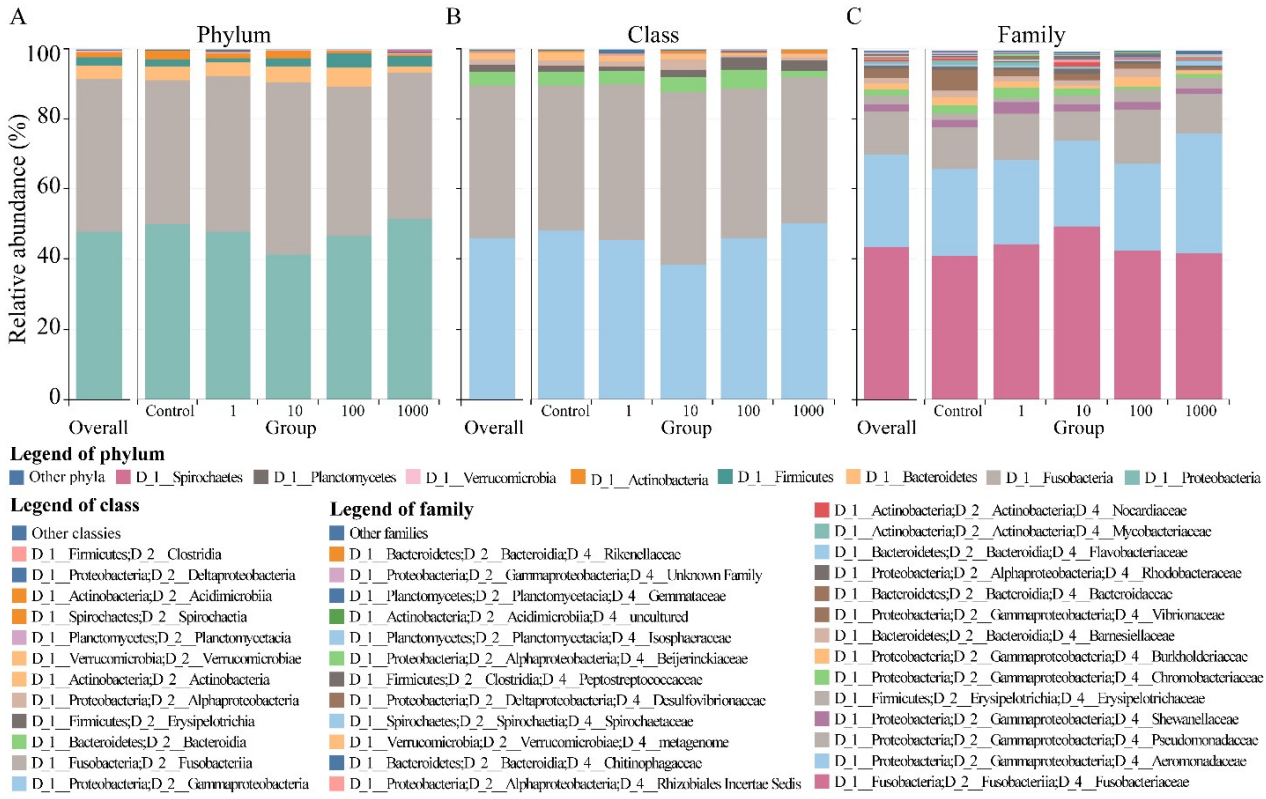


Figure 4.1. Compositions of active gut microbiomes of fathead minnows exposed to benzo[*a*]pyrene at the (A). phylum, (B). class, and (C). family level. Less abundant taxa (averaged portion < 0.1%) were grouped together as others.

The profile of the active gut microbiome was significantly different from that of the genomic gut microbiome (adonis, $F = 5.5$, $p < 0.001$; Appendix C, Fig. C.2). More ASVs were revealed by RNA metabarcoding than DNA metabarcoding (Fig. 4.2A; Welch's t test: $t = -4.6$, $p < 0.001$). Fifty-eight genera were detected by both DNA and RNA metabarcoding, while six were unique to DNA metabarcoding and 17 were unique to RNA metabarcoding (Fig. 4.2B). Details about the genomic microbiome from this exposure can be found in Chapter 3.

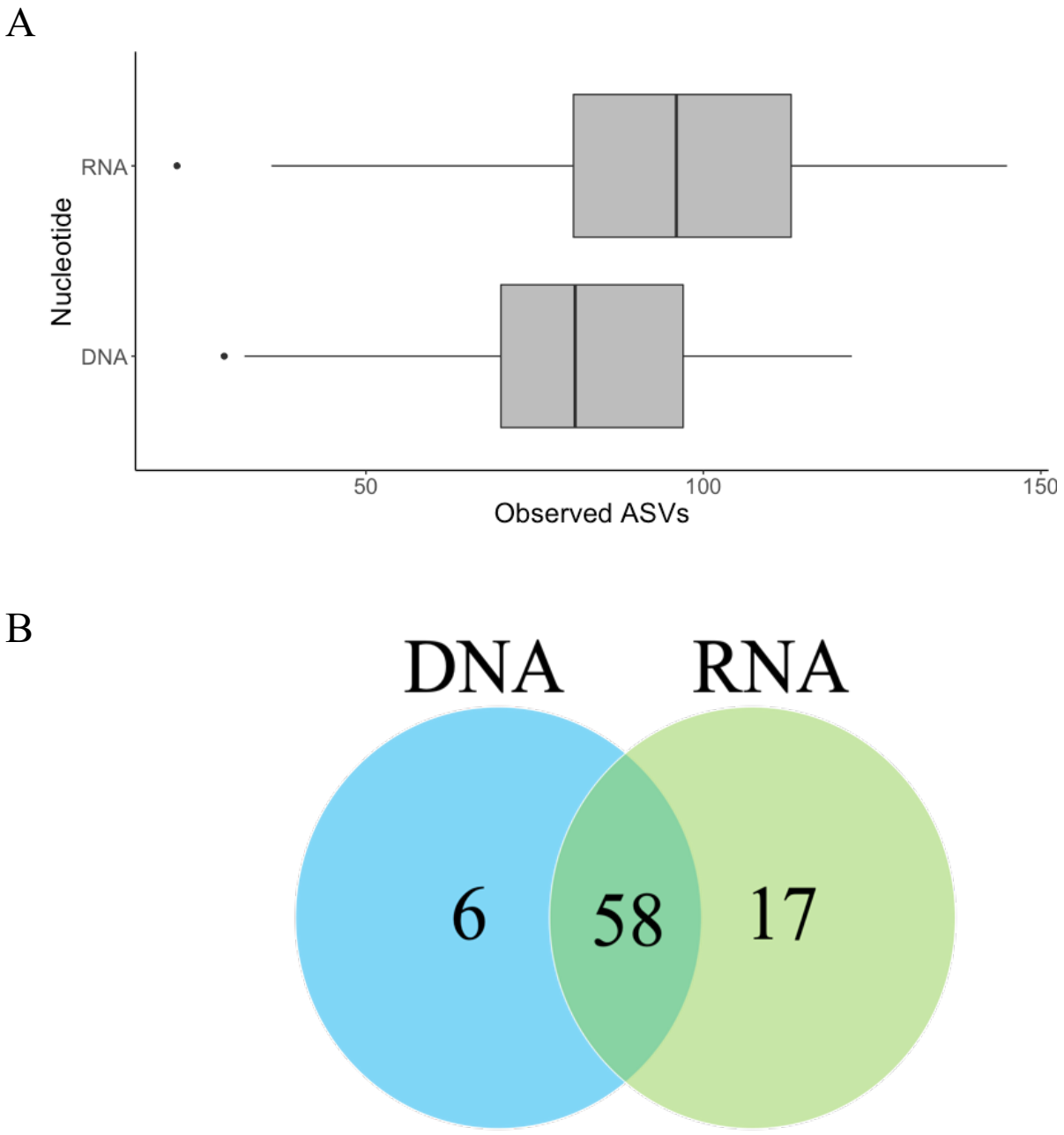


Figure 4.2. (A). Number of observed amplicon sequence variants (ASVs) of active and genomic gut microbiome. (B). Venn diagram of number of genera in DNA- or RNA-based extractions or the overlap between the two. Data from the genomic microbiome is from Chapter 3.

*4.5.1 Dietary exposure of BaP reduced the alpha-diversity of active gut microbiome*

Biodiversity of the active gut microbiome declined due to dietary exposure to BaP. Dietary exposure to BaP reduced Shannon diversity of the active gut microbiome (Table 4.1, KW = 12.9, p = 0.01), and the reduction approached significance in the highest exposure group relative to the control group (Dunnett's Test, $p = 0.09$). The number of observed active ASVs approached a significant reduction based on exposure to BaP (ANOVA test, F = 2.2, $p = 0.08$), and the greatest exposure concentration had significantly fewer ASVs than the control group (Table 4.1: Dunnett's Test, p = 0.04).

Table 4.1. Shannon Index values and number of observed amplicon sequence variants (ASVs) for each exposure group from the active gut microbiome. Mean and standard error values are presented. Dunnett's test: * $p < 0.1$, ** $p < 0.05$.

| Exposure | Shannon index | Observed ASVs |
|---|---|---|
| Control | 4.55 ± 0.12 | 104.35 ± 5.12 |
| 1 μg $g^{-1}$ | 4.54 ± 0.09 | 103.53 ± 5.19 |
| 10 μg $g^{-1}$ | 4.5 ± 0.08 | 99.3 ± 4.5 |
| 100 μg $g^{-1}$ | 4.44 ± 0.17 | 94.12 ± 6.06 |
| 1,000 μg $g^{-1}$ | 4.17 ± 0.11* | 84.56 ± 6.07** |

*4.5.3 Changes in compositions of active gut microbiome were correlated with dietary exposure of BaP*

Dietary exposure to BaP altered the composition of active gut microbiomes (Fig. 4.1 & 4.3). Based on exposure groups, several active families (CLR-transformed) were significantly different in abundance relative to the control group. *Barnesiellaceae* (KW chi-squared = 36.2, $p < 0.001$), *Bacteroidaceae* (KW chi-squared = 34.2, $p < 0.001$), *Chromobacteriaceae* (KW chi-squared = 22.5, $p < 0.001$), *Flavobacteriaceae* (KW chi-squared = 18.1, $p = 0.001$), and *Mycobacteriaceae* (KW chi-squared = 17.9, $p = 0.001$) were all significantly different from the control group. The abundances of *Barnesiellaceae* and *Bacteroidaceae* significantly decreased in the 1,000 µg $g^{-1}$ groups relative to the control group ($p < 0.001$, $p = 0.005$, respectively). Abundance of *Barnesiellaceae* was greater in the 100 µg g -1 group relative to the control group ($p = 0.02$), while abundance of *Chromobacteriaceae* was significantly reduced in the 100 µg g -1 group relative to the control group ($p = 0.004$). Abundance of *Flavobacteriaceae* was significantly increased in the 1,000 µg g -1 groups relative to the control group ($p < 0.001$). *Mycobacteriaceae* was significantly decreased in abundance in the 10 µg g -1 ($p = 0.005$) and 100 µg g -1 ($p = 0.002$) groups relative to control; the decrease in the 1,000 µg g -1 group was not significant.

Furthermore, several relative abundances of families (CLR-transformed) were significantly correlated with measured lgBaP-SO4 metabolites ($p < 0.05$; Fig. 4.3 & Appendix C, C.3). The active relative abundances of *Erysipelotrichaceae*, *Flavobacteriaceae, Pseudomonadaceae, Burkholderiaceae, Spirosomaceae, Isosphaeraceae*, *Weeksellaceae, Moraxellaceae, Chitinophagaceae,* and *Chitinibacteraceae* were all significantly positively correlated with lgBaP-SO4 (Fig. 4.3A), while that of *Bacteroidaceae, Chromobacteriaceae, Barnesiellaceae,* and *Rikenellaceae* were significantly negatively correlated with lgBaP-SO4 (Fig. 4.3B).

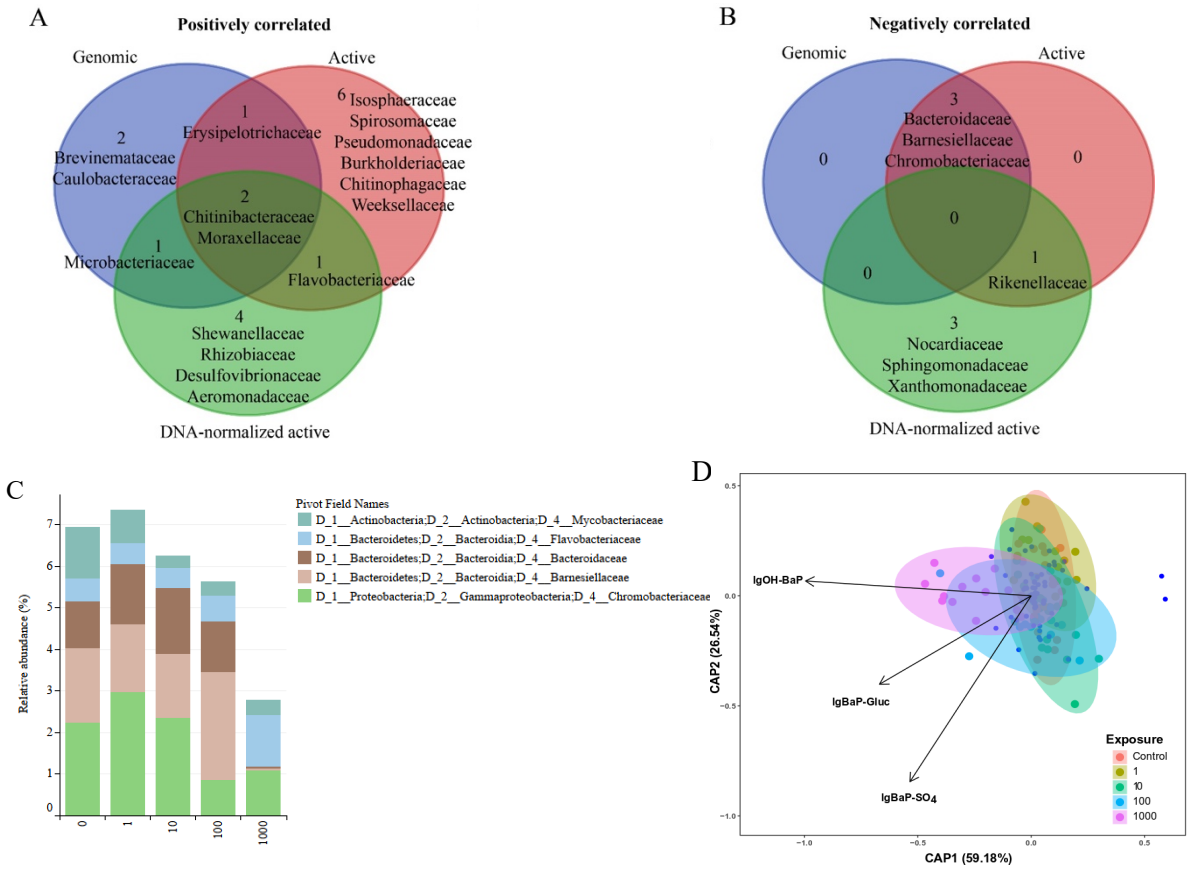


Figure 4.3. Families of bacteria from the gut microbiome that were (A). positively and (B). negatively correlated with lgBaP-$SO_4$ with the genomic, active, and DNA-normalized active microbiomes. Bacterial families that correlated with the genomic microbiome were previously discussed in Chapter 3. (C). Relative abundance of the taxa that were significantly different in the exposure groups relative to the control, based on Dunnett's tests. (D). Constrained Analysis of Principal Coordinates (CAP) of the different exposure groups constrained by the vectors of the measured metabolite concentrations, using Bray-Curtis dissimilarities. Both lgOH-BaP and lgBaP-$SO_4$ metabolites were the significant environmental variables constraining the ordination ($p = 0.001$ and $p = 0.04$, respectively).

*4.5.4 Dietary exposure of BaP altered structure of active gut microbiome*

There was a significant effect of dietary exposure of BaP on community structure agglomerated to genus level (adonis test, $F = 3.2$, $p = 0.001$; Fig. 4.3D & 4.5B). The structure of the active gut microbiome was significantly affected by exposure to BaP at the greatest exposure concentrations; while the control group community structure was not significantly different from the 1 or 10 µg $g^{-1}$ groups, it was significantly different from the 100 (Pairwise adonis test, $F = 2.4$, $p = 0.02$) and 1,000 µg $g^{-1}$ (Pairwise adonis test, $F = 4.9$, $p = 0.001$) groups. Metabolites of BaP, lgOH-BaP, lgBaP-Gluc, and lgBaP-$SO_4$, were significant environmental variables (ANOVA test, $F = 2.97$, $p = 0.001$) constraining the ordination of the CAP (Fig. 4.3D) (ANOVA test, $p = 0.001$ and $p = 0.04$, respectively). Exposure to BaP did not alter the neighborhood selection networks of active gut microbiomes (Fig. 4.4). While the number of nodes and edges decreased in the genomic microbiome (Appendix C, Fig. C.4 & Table C.3), the trend did not hold true in the active microbiome (Table 4.2). The active microbiome networks did not show any clear patterns across treatments.

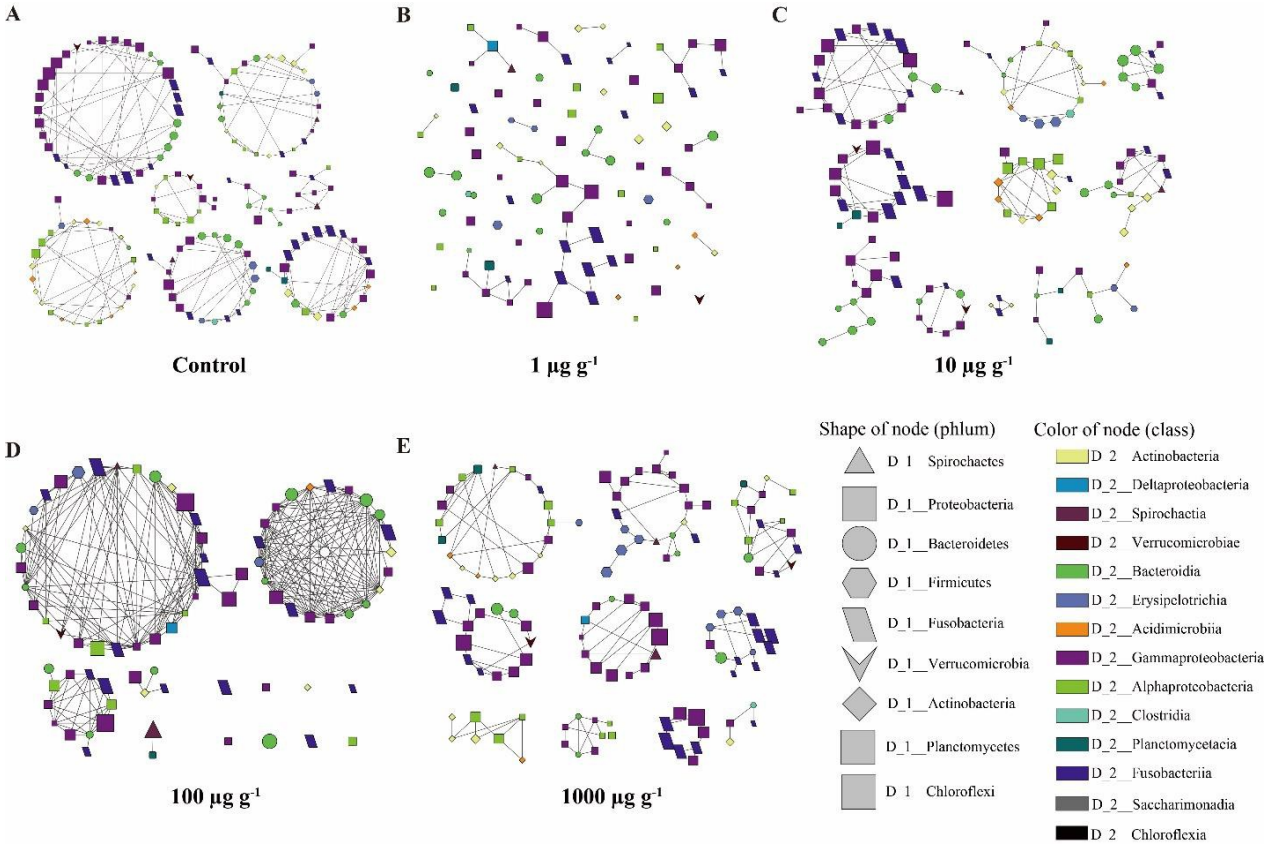


Figure 4.4. Neighborhood selection networks of active gut microbiome, as determined with SPIEC-EASI, after exposure to (A). Control, (B). 1, (C). 10, (D). 100, (E). 1000 µg g-1 BaP. Shape of node: bacterial phylum; color of node: bacterial class; size of node: abundance.

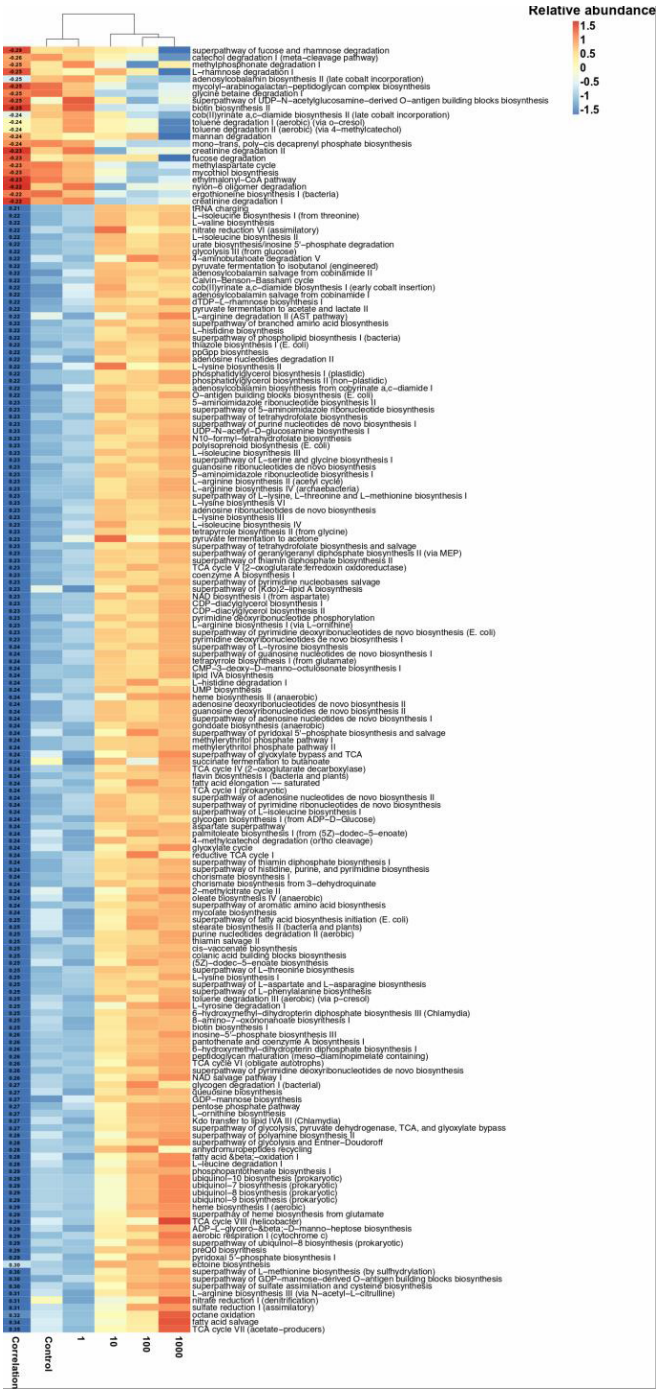


Figure 4.5. Heatmap of the MetaCyc pathways that are significantly correlated with lgBaP-$SO_4$ at each of the exposure concentrations. The correlation value of each pathway with lgBaP-$SO_4$ is shown on the left. Colors denote a scaled relative abundance for visualization, from the *pheatmap* package in R, of the MetaCyc pathways, with red indicating more abundant, and blue indicating less abundant.

Table 4.2. Number of nodes and edges from the neighborhood selection networks, as determined with SPIEC-EASI, of the active gut microbiome, as discovered by RNA metabarcoding.

| Exposure | Number of nodes | Number of nodes (non-alone) | Number of edges | cluster-edges |
|---|---|---|---|---|
| Control | 160 | 160 | 325 | 267 |
| 1 μg $g^{-1}$ | 94 | 54 | 41 | 40 |
| 10 μg $g^{-1}$ | 129 | 129 | 205 | 168 |
| 100 μg $g^{-1}$ | 78 | 68 | 332 | 263 |
| 1,000 μg $g^{-1}$ | 127 | 127 | 201 | 164 |

*4.5.5 Concentrations of BaP metabolites correlated with predicted metabolic pathways of the active gut microbiome*

One hundred seventy-nine MetaCyc pathways of active gut microbiomes were significantly correlated with lgBaP-$SO_4$ (Fig. 4.5). In total, 22 pathways were negatively correlated with BaP-$SO_4$, while 157 pathways were positively correlated with BaP-$SO_4$. Pathways showed a clear separation among the treatment groups, with the control and 1 µg $g^{-1}$ groups clustering with each other and separate from the 10, 100 and 1000 µg $g^{-1}$ groups. Several negatively correlated pathways were associated with degradations of sugars such as mannan and fucose. A number of positively correlated pathways with lgBaP-$SO_4$.were associated with the tricarboxylic acid cycle or biosynthesis of amino acids such as methionine, arginine, and tyrosine. Notably, both 4-methylcatechol degradation (ortho cleavage) and toluene degradation III (aerobic) (via p-cresol) were positively correlated with lgBaP-$SO_4$.

*4.5.6 DNA-normalized active gut microbiome*

The DNA-normalized active microbiome (Pseudo-F = 2.0, $p < 0.001$) resulted in more statistical significance in the structural differences among exposure groups than the genomic (Pseudo-F = 1.4, $p = 0.20$), as discussed further in Chapter 3, or active gut microbiome (Pseudo-F = 1.7, $p = 0.03$) (Fig. 4.6). DNA normalized activity allowed for analysis of the activity-dormancy dynamics of overlapping taxa; taxa with higher abundances of RNA are considered active while taxa with higher abundances of DNA are considered dormant. The DNA-normalized active microbiome gives insight into the rarer taxa that are often overlooked when only assessing DNA- or RNA-based microbiome analyses (Fig. 4.7). Several relative abundances of DNA-normalized active families (CLR-transformed) were significantly correlated with measured lgBaP-$SO_4$ metabolites (Fig. 4.3 & Appendix C, Fig. C.3). *Rikenellaceae, Sphingomonadaceae, Nocardiaceae*, and *Xanthomonadaceae* were all negatively correlated with lgBaP-$SO_4$, while *Desulfovibrionaceae, Microbacteriaceae, Flavobacteriaceae, Shewanellaceae*, *Aeromonadaceae, Rhizobiaceae, Chitinibacteraceae*, and *Moraxellaceae* were positively correlated with lgBaP-$SO_4$. Except for *Aeromonadaceae* and *Shewanellaceae*, which were abundant taxa (>1%), the rest of these taxa were less abundant (0.1%-1%) or rare (<0.1%).

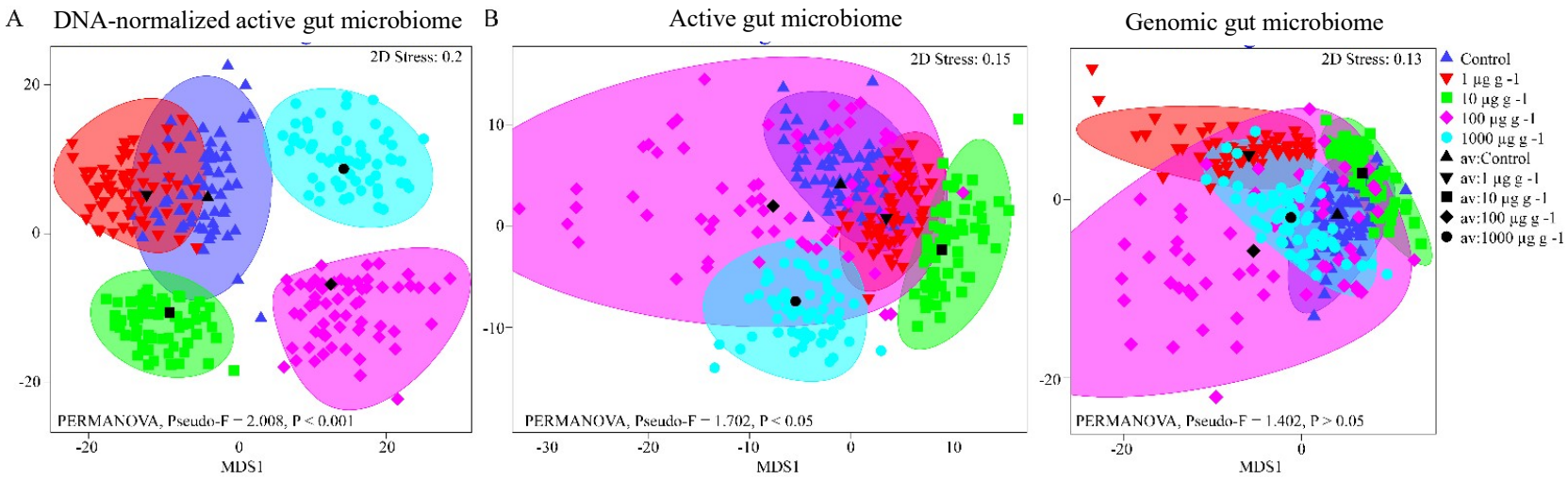


Figure 4.6. Bootstrap averages of Metric MDS plot for (A). the DNA-normalized active microbiome, (B). the active microbiome, and (C). the genomic microbiome (from Chapter 3). More ASVs were agglomerated to the genus level. Av: averaged resemblance.

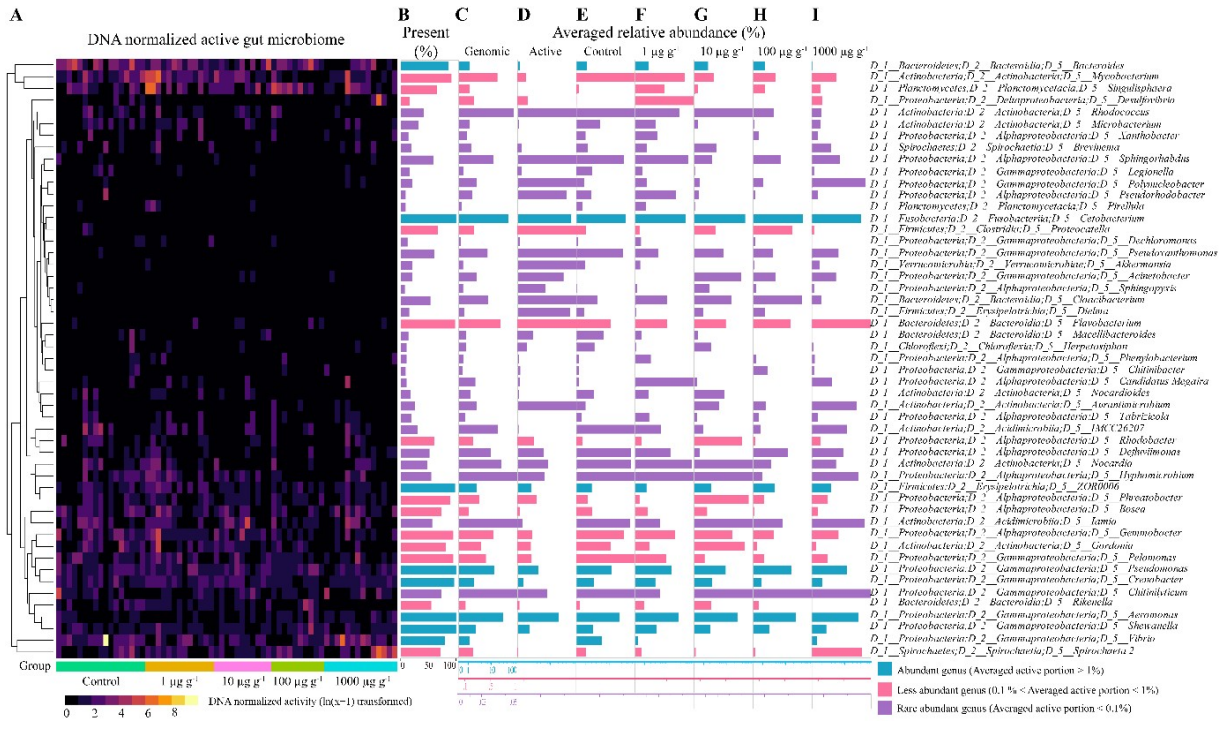


Figure 4.7. (A). Heatmap of the abundance of DNA-normalized active gut microbiome in each exposure group. (B). Percent relative abundance of genera across all samples. (D). Percent abundance of genera in the genomic, from Chapter 3, and (D). active microbiomes. (E). Percent relative abundance of genera in the control (F). 1, (G). 10, (H). 100, and (I) 1000 µg $g^{-1}$ groups. In total, 8 genera were abundant (>1%), shown in blue, 13 genera were less abundant (0.1%-1%), shown in pink, and the remaining 30 genera were rare (<0.1%), shown in purple.

## 4.6 Discussion

This study provided a unique opportunity to explore the active microbiome using RNA coded by the 16S rRNA gene and comparing those results to the DNA-normalized active microbiome. Since up to 80% of a microbial community can be dormant (Jones et al., 2010), the use of RNA and the RNA/DNA ratio provides meaningful insights into the impacts of BaP on the microbiome. Additionally, the use of RNA for microbiome analyses can give insight into the rare gut microbiome. Characterizing the function of the rare gut microbiome is challenging due to the enormous biodiversity of the microbiome. Traditional techniques to manipulate microbial biodiversity and study rare taxa include dilution and artificially defining the microbial community (Rolig et al., 2015; Yan et al., 2015). Dilution has been used in soil and sewage studies, where sterilized media is inoculated with suspensions of the study media to allow new community development to capture rarer species and understand ecological function (Hol et al., 2010; Yan et al., 2015). This technique, however, is not practical to study rarer species within a complex gut ecosystem. Artificially defining a microbiome can also be used to decipher the role of rare taxa on ecosystem functioning; this can be done by creating gnotobiotic organisms, but the overall complexity of a healthy host individual is lost in this situation (Rolig et al., 2015). With limited sequencing effort, RNA metabarcoding overcomes these limitations of unrealistic conditions and allows for analysis of rarer taxa in the gut microbiome (İnceoğlu et al., 2015).

The dominant microbiome is primarily shaped by its genomic capability. The abundant active gut microbiome in fathead minnows was consistent with the genomic gut microbiome from previous studies (DeBofsky et al., 2020; Gaulke et al., 2016; Narrowe et al., 2015). The small compositional differences between the active and genomic gut microbiome might be caused by uneven transcript activity, where certain taxa quickly respond to fluctuations in environmental factors or the health status of hosts (Revetta et al., 2011). Although it was previously determined that the microbiomes of male and female fish are dissimilar (Chapter 2), these fish were not sexually differentiated, and therefore sex-related effects could not be observed.

The effects of BaP on alpha- and beta-diversity, as well as structure, of the gut microbiome were consistent across the genomic and active microbiomes (Chapter 3). When comparing the genomic and active microbiomes, it was expected that the genomic microbiome

would have larger alpha-diversity values, since it would be representative of all bacteria, not just the active fraction (Inkinen et al., 2016). The discrepancy found in this study could result from some bacteria having high RNA to DNA ratios, where the detection of DNA was missed with 16S rRNA metagenetics, but RNA was still amplified due to its larger activity relative to other active taxa (Eichler et al., 2006). Cases where taxa in the genomic microbiome are more abundant may be due to a large population of inactive bacteria, while abundant taxa in the active microbiome may reveal populations with relatively small abundances that are exceedingly active (Revetta et al., 2011). This supports the notion that RNA is able to detect potentially important rarer, but active, taxa that would otherwise be missed with DNA analyses.

Exposure to BaP also resulted in the reduction in network connectivity and complexity for the genomic, but not the active microbiomes. A large degree of connectedness can illustrate an ecological niche (Karimi et al., 2017) and loss of network structure can indicate a loss of relationships among keystone taxa (Banerjee et al., 2018). Maintenance of the network structure of the active microbiome across treatments suggests resiliency and resistance of the microbial communities in response to the BaP exposure (Elmqvist et al., 2003). Additionally, the overall complexity of networks of the active microbiome was greater than that of the genomic microbiome. This suggests that the genomic microbiome contains a number of dormant taxa, whereas the active microbiome represents the taxa that are active and interacting with one another (Blazewicz et al., 2013).

Alteration of the gut microbiome by BaP might lead to adverse host outcomes (Claus et al., 2016). *Bacteroidaceae* and *Barnesiellaceae*, both negatively correlated with lgBaP-$SO_4$, are associated with host health and homeostasis. *Bacteroidaceae* are in part responsible for digestion (Bäckhed et al., 2005; Ikeda-Ohtsubo et al., 2018; Thomas et al., 2011) and immune regulation (Hiippala et al., 2018); therefore reduction in abundance of this family may be associated with decreased digestive function and immune capacity, a known deleterious effect of BaP exposure (Carlson et al., 2004a; Reynaud and Deschaux, 2006). Intestinal colonization with *Barnesiellaceae* is negatively correlated with bloodstream infections in humans (Montassier et al., 2016), signifying that loss of this taxa is also associated with reduced immune capacity. BaP is a known immunosuppressant (Carlson et al., 2004b) and carcinogen (Gelboin, 1980), so alterations in abundance of taxa associated with these processes is not unexpected.

The gut microbiome might stimulate BaP biodegradation (Claus et al., 2016). Greater abundance of *Erysipelotrichaceae* has been observed in mice exposed to BaP (Ribière et al., 2016) and is associated with colorectal cancer (Chen et al., 2012). Some species of *Moraxellaceae* from human skin isolates are capable of degrading BaP (Sowada et al., 2014) while others are recognized as opportunistic pathogens in fish (Austin and Austin, 2016). It is plausible that a longer-term exposure may have resulted in an infection or tumor growth in exposed fish. More work would need to be completed to determine if proliferation of this active bacteria is contributing to pathogenic load or degrading BaP.

Several taxa in the active microbiome were found to be correlated with lgBaP-$SO_4$ that were not correlated with the genomic microbiome. This means that the activity, rather than abundance, of these taxa is either enhanced or reduced due to exposure to BaP. *Rikenellaceae,* for example, was significantly negatively correlated with lgBaP-$SO_4$. Exposing mice to the fungicide imazalil resulted in a reduction in abundance of *Rikenellaceae* and was associated with colonic inflammation (Zeng et al., 2016), suggesting that the reduction in *Rikenellaceae* might be indicative of reduced health of fish in this study. Reduction in *Rikenellaceae* was also seen in an *in vitro* assay exposing fecal microbiomes to BaP (Defois et al., 2017). In addition, RNA metabarcoding showed a positive relationship between lgBaP-$SO_4$ and *Flavobacteriaceae* as well as *Pseudomonadaceae*, which are families that contain known opportunistic pathogens in fish (Austin and Austin, 2016; Loch and Faisal, 2015). There are also a number of bacterial species from *Flavobacteriaceae* and *Pseudomonadaceae* that are capable of degrading hydrocarbons (Balba et al., 1998; Šyvokiene and Mickeniene, 2011). *Burkholderiaceae*, another family positively correlated with lgBaP-$SO_4$ are also capable of degrading hydrocarbons and are found in higher abundances at contaminated sites (Laurie and Lloyd-Jones, 2000; Seo et al., 2009; S. Yang et al., 2016). In the study exposing mice to BaP, exposure resulted in increased abundance of *Alcaligenaceae*, which are also part of the *Burkholderiales* order (Ribière et al., 2016).

Finally, a positive correlation between *Isosphaeraceae* and fish exposed to BaP was also seen in DeBofsky et al., (2020), although the function of this taxa is uncertain. Use of PICRUSt2 to analyze the active microbiome identified a large number of pathways associated with lgBaP-$SO_4$ (Fig. 4.4). The significance of pathways identified with the active microbiome is unclear. Of note, both 4-methylcatechol degradation (ortho cleavage) and toluene degradation

III (aerobic) (via p-cresol) were positively correlated with lgBaP-$SO_4$. These are both part of the aromatic compound degradation pathways. Furthermore, creatinine degradation was negatively correlated with lgBaP-$SO_4$. Higher concentrations of creatinine are associated with PAH exposure in humans (Srogi, 2007). Overall, the pathways do not point to a clear function in terms of BaP degradation as was seen with the genomic microbiome (Chapter 3), but do suggest that fish health is compromised in response to BaP exposure. The pathways analysis also showed a clear separation of the treatments, grouping them to their nearest concentration neighbor. This indicates that the patterns of pathway dysregulation were dose-dependent and should be explored further with transcriptomic analyses.

Analysis of the DNA-normalized microbiome attempts to discern the active bacteria from overall community composition, giving a measure of activity relative to abundance. A large value for this ratio indicates a certain taxon is highly active relative to its abundance, whereas a small value for this ratio indicates that a taxon is largely dormant (Blazewicz et al., 2013). Bacteria that are more active produce a greater number of copies of the 16S rRNA transcript; with DNA as a proxy for abundance, the DNA-normalized activity of the bacteria is scaled to the population size and can be considered the growth rate (Campbell et al., 2011).

A relationship between the DNA-normalized microbiome and lgBaP-$SO_4$ suggests that the relative proportion of taxa that are active may be dependent upon the exposure to BaP. Using the DNA-normalized microbiome, *Desulfovibrionaceae, Microbacteriaceae, Flavobacteriaceae, Shewanellaceae*, *Aeromonadaceae, Rhizobiaceae* were all positively correlated with lgBaP-$SO_4$. DNA-normalization detected correlations between certain taxa (*Desulfovibrionaceae, Shewanellaceae*, *Aeromonadaceae, Rhizobiaceae,* and *Nocardiaceae*) and lgBaP-$SO_4$ that were not observed within the active or genomic microbiomes. *Desulfovibrionaceae* becomes more active with increasing exposure to BaP; an increase in abundance of *Desulfovibrionaceae* was also seen in mice after 2,3,7,8-tetrachlorodibenzo-*p*-dioxin (TCDD) exposure, and this bacterium is correlated with pro-inflammatory phenotypes (Lefever et al., 2016). Enrichment of the family *Microbacteriaceae* has also been associated with contaminated soil sites (Jacques et al., 2007). The families *Shewanellaceae* and *Aeromoadaceae* contain known pathogens (Austin and Austin, 2016), and *Shewanellaceae* is negatively correlated with neutrophil recruitment (Rolig et al., 2015). Increased activity of this taxa may be modulating the immune response along with the BaP exposure and would

potentially present as a pathogen had the study continued.

Interestingly, *Sphingomonadaceae* and *Nocardiaceae* were negatively correlated with lgBaP-$SO_4$; several members of these families are capable of degrading hydrocarbons (Juhasz and Naidu, 2000). Certain genera within *Nocardiaceae* are also pathogenic in fish (Austin and Austin, 2016). While other potential hydrocarbon-degraders and pathogens increased in abundance with increasing concentrations of lgBaP-$SO_4$, these taxa may have become dormant as concentrations increased. The dormancy implies that other taxa have a competitive advantage when exposed to BaP (Blazewicz et al., 2013). Several of these taxa correlated with lgBaP-SO4 metabolites are the least abundant, indicating that rarer taxa may serve a role in regulating the response to an exposure to BaP.

The results of this study show that exclusively analyzing the genomic or active microbiome study might miss some of the relationships between bacterial presence and a particular stressor. Not all taxa in the genomic microbiome may be active, but this pool of species represents a potential "seed bank" that can become active at any time, conferring advantage for rapid adaptation to change (Caporaso et al., 2012; İnceoğlu et al., 2015). The DNA-normalized microbiome may be a better indicator of the response to a stressor, but the issue of "phantom microbes" that are present in the active microbiome but not the genomic microbiome complicates solely relying on DNA-normalized analyses (Bowsher et al., 2019). The issue of how to handle these taxa has not been resolved, and therefore, the importance of these taxa is unknown (Bowsher et al., 2019).

Overall, this study revealed that chronic exposure to BaP significantly altered the community structure of gut microbiome in fathead minnows, and that while overall community shifts were relatively consistent, nuances differed based on which nucleic acids were isolated. Utilization of multiple techniques is necessary to best understand the impacts of a toxicant on microbial communities, and more work is needed to conclusively address the correlations between taxa abundance and putative function within the host.

## 4.7 Acknowledgements

Funding was provided by "Next generation solutions to ensure healthy water resources for future generations" funded by the Global Water Futures program, Canada First Research Excellence Fund (#419205). Dr. Brinkmann was also supported through the Global Water

Futures program. Dr. Challis was funded by the Banting Post-Doctoral Fellowship. Prof. Giesy was supported by the Canada Research Chairs Program of the Natural Sciences and Engineering Research Council of Canada (NSERC).

# CHAPTER 5: Effects of the Husky oil spill on gut microbiota of native fishes in the North Saskatchewan River, Canada

## 5.1 Preface

This chapter focuses on the effects of an oil spill on the North Saskatchewan River on the gut microbiomes of native, wild goldeye (*Hiodon alosoides*), walleye (*Sander vitreus*), northern pike (*Esox lucius*), and shorthead redhorse (*Moxostoma macrolepidotum*). This study showed that host species are a significant driver in shaping the gut microbiome and that increased concentrations of PAHs in fish muscle were correlated with a number of bacterial families across the different species as well as gut community composition in walleye. This work builds upon all previous chapters, where it was observed that exposure to BaP can result in altered bacterial community composition and proliferation or loss of certain taxa in fathead minnows. Results from the controlled laboratory exposure  are supported in this field study. This was one of the first studies to investigate the community composition of gut microbiota from wild fishes in response to chemical stressors.

*Author contributions:*

- Abigail DeBofsky: All microbiome experimental design (90%), bench work (100%), bioinformatics (90%), and statistical analysis (90%), with the exception of running the GCMS and LCMS for muscle and bile detection of PAHs and PBPAHs, as well as creation of the manuscript (100%)
- Dr. Yuwei Xie: Assistance with design of experiment (10%), bioinformatics (10%), statistical analysis (10%), and revisions of the manuscript (80%)
- Dr. Tim Jardine: Designed the field experiments (100%), assisted with field work (25%),

provided scientific input and guidance, edited the manuscript (5%), and provided some funding for the research

- Dr. Janet E. Hill: Provided assistance with learning bench work and interpreting the data, edited the manuscript (5%)
- Dr. Paul D. Jones: Assisted with running the GCMS and interpreting the chemical data (100%), edited the manuscript (5%)
- Dr. John P. Giesy: Provided scientific input and guidance, edited the manuscript (5%), and provided funding for the research

## 5.2 Abstract

In July 2016, a Husky Energy pipeline spilled 225,000 liters of diluted heavy crude oil, with a portion of the oil entering the North Saskatchewan River near Maidstone, SK, Canada. This event provided a unique opportunity to assess potential effects of a crude oil constituent (namely polycyclic aromatic hydrocarbons, PAHs) on a possible sensitive indicator of freshwater ecosystem health, the gut microbiota of native fishes. In summer 2017, goldeye (*Hiodon alosoides*), walleye (*Sander vitreus*), northern pike (*Esox lucius*), and shorthead redhorse (*Moxostoma macrolepidotum*) were collected at six locations upstream and downstream of the spill. Muscle and bile were collected from individual fish for quantification of PAHs and intestinal contents were collected for characterization of the microbial community of the gut. Gut microbiota were assessed by 16S rRNA metagenetics. Results suggested that host species is a significant determinant of gut microbiota, with significant differences among the species across sites. Concentrations of PAHs in dorsal muscle of fishes were significantly correlated with gut community compositions of walleye, but not of the other fishes. Concentrations of PAHs in dorsal muscle of fishes were also correlated with abundances of several families of bacteria among fishes. This study represents one of the first to investigate the response of the gut microbiome of wild fishes to chemical stressors.

## 5.3 Introduction

There has been increasing interest in the potential effects of heavy, crude oil from northeastern Alberta, Canada on ecologically and culturally important fishes (Bari et al., 2016). While oil spills in marine environments, such as Deepwater Horizon or Exxon Valdez, garner attention, the majority of spills occur in inland environments (Yoshioka and Carpenter, 2002) for which studies of freshwater ecosystems are sparse (Dew et al., 2015). Due to its density, heavy crude oil can rapidly sink and become deposited in sediments, where it can accumulate and interact with biota (Fitzpatrick et al., 2015). Sulfur-containing and heavier molecular weight polycyclic aromatic hydrocarbons (PAHs), can remain in freshwater ecosystems for years after a spill (Yang et al., 2020), where they can cause ongoing ecotoxicological effects on fishes (Milani et al., 2017).

Previous studies on effects of oil spills have focused on effects on marine fishes (Barron, 2012; Beyer et al., 2016; Danion et al., 2011). After an oil spill, fish are exposed *via* ingestion of prey or sediment, ventilation of water over gills, or through dermal absorption (Douben, 2003; Nichols et al., 1996). Exposure to greater concentrations of PAHs, such as naphthalene, benzo[*a*]pyrene, and pyrene that would be found in crude oil, can cause multiple sub-lethal effects on fish, including DNA damage, cardiotoxicity, immunosuppression, reduced reproductive capacity and neoplasms in the liver (Brown-Peterson et al., 2017; Hicken et al., 2011; Tuvikene, 1995). In laboratory studies, exposure to PAHs can also alter the composition of gut microbial communities in fishes (Bayha et al., 2017; DeBofsky et al., 2020). Few studies, however, have investigated links between actual spilled oil and gut microbiomes of fishes. To date, the only studies published have used saltwater species in laboratory settings (Bagi et al., 2018; Bayha et al., 2017; Brown-Peterson et al., 2017).

Gut microbiomes of wild fishes could become a key part of ecotoxicological assessments, since their activities in hosts are crucial for regulating a number of functions, including modulating immunity (Rolig et al., 2015) and regulating the intestinal barrier (Pérez et al., 2010). Perturbation of the gut microbiome is associated with various deleterious effects, such as immune dysfunction (Steinmeyer et al., 2015) and behavioral abnormalities (Lyte, 2013).

Because several environmental chemical compounds, including PAHs, can disturb the gut

microbiome, the gut microbiome can be an indicator of environmental stress (i.e. Adamovsky et al., 2018; Bayha et al., 2017; Lloyd et al., 2016). To fully incorporate the microbiome into ecotoxicological assessments, more information is needed on the diversity of microorganisms in guts across host species, as well as dysbiosis resulting from exposure to toxicants.

On July 21, 2016, approximately 225 $m^3$ of heavy, crude oil spilled from the Husky Energy 16 TAN pipeline approximately 75 km upstream of Paynton Ferry, Saskatchewan, Canada and 160 m inland from the bank of the North Saskatchewan River. Approximately 40% of the spilled oil entered the North Saskatchewan River, and by the end of September, Husky Energy Inc. estimated more than 80% of the total spilled crude had been recovered (Yang et al., 2020). The spilled material contained 88% heavy crude and 12% condensate, with 10% resins, 13% asphaltenes, 35% aromatics, and 42% saturates (Yang et al., 2020). With the oil spill came an opportunity to characterize the microbiome of native fishes as well as the effects of the crude oil on these microbiomes.

It was hypothesized that gut microbiomes of native, freshwater fishes could have altered community composition and proliferation of disease-causing and hydrocarbon-degrading bacteria in response to the crude oil spill. Specific objectives were to: 1) Characterize the gut microbial communities of walleye (*Sander vitreus*), northern pike (*Esox lucius*), goldeye (*Hiodon alosoides*) and shorthead redhorse (*Moxostoma macrolepidotum*); 2) Measure concentrations of transformation products of PAHs in bile and PAHs in muscle that might be indicative of exposure to the spilled oil; and 3) Assess effects of the oil spill on the gut microbiomes of those native fishes by correlating the microbial communities and abundance of specific taxa to measured PAH concentrations at upstream and downstream sites.

## 5.4 Methods

### *5.4.1 Sample collection*

Fishes were collected in August 2017 by use of gill nets (4.25 in. mesh and index nets with multiple mesh sizes) set overnight. Each morning, all target species fish were removed from nets and placed on ice for transportation to the field laboratory. For this study, species collected were walleye, goldeye, northern pike, and shorthead redhorse. Fish were collected at sites in Saskatchewan, Canada on the North Saskatchewan River upstream and downstream of the Husky oil spill (Fig. 5.1; Appendix D, Table D.1). Upstream sites included areas near Highway 17 (50 km upstream) and Highway 3 (20 km upstream). Downstream sites included the point of entry (<1 km below the spill), an area near Highway 21 (20 km downstream), and Paynton Ferry (75 km downstream). A far-field downstream reference site was also included in the Mossy River Delta near Cumberland House (>600 km downstream). The two upstream sites were combined, as were all downstream sites; the far-field reference site was analyzed separately.

A.

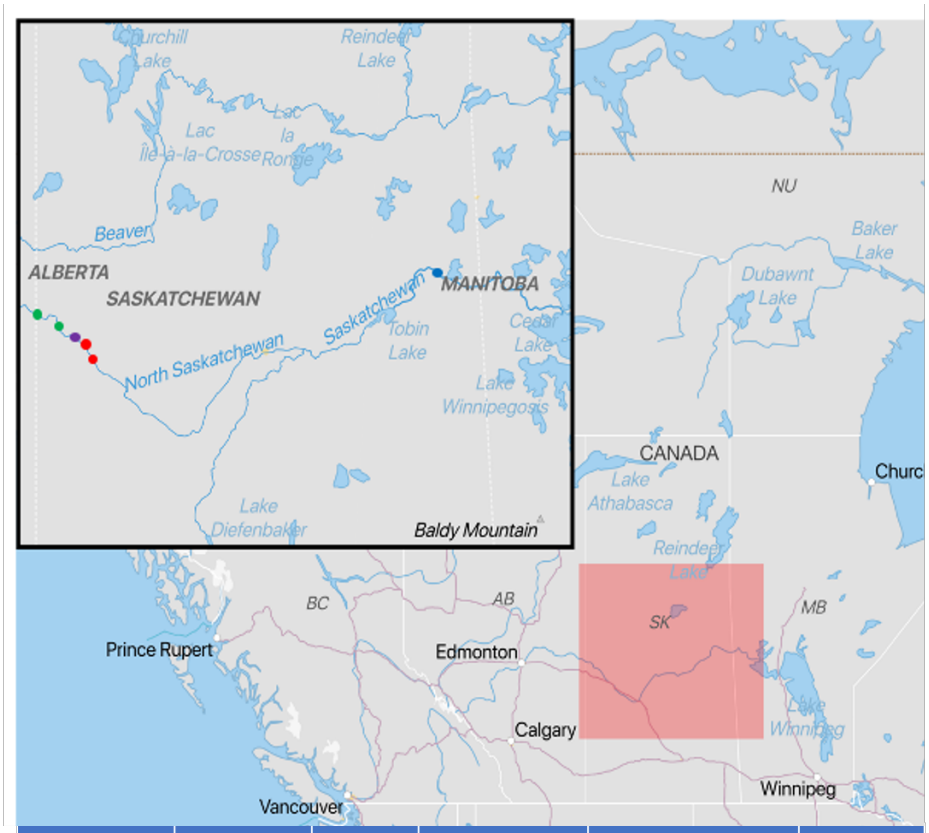


B.

| | | Goldeye | Northern pike | Shorthead redhorse | Walleye |
|---|---|---|---|---|---|
| | Location | N | N | N | N |
| Upstream | Highway 17 | 4 | - | 3 | 3 |
| | Highway 3 | 3 | - | 11 | 5 |
| Downstream | Point of Entry | 5 | - | 5 | 4 |
| | Highway 21 | 6 | 1 | - | 3 |
| | Paynton Ferry | 1 | 1 | 2 | 6 |
| Far-field | Mossy River Delta | - | 7 | 1 | 7 |
| Total | - | 19 | 9 | 22 | 28 |

Figure 5.1. (A). Sampling sites along the North Saskatchewan River in Saskatchewan, Canada. Green points indicate the two upstream sites, Highway 17 and Highway 3. The purple point is the Point of Entry. The two red points are two downstream sites, Highway 21 and Paynton Ferry. The blue point is the far-field reference site, Mossy River Delta. (B). Number of fish (N) of each species collected at each sampling site.

Once the fish were brought to the field laboratory, length and mass of each fish were measured and each fish was examined for external abnormalities, including lesions or evidence of infection. Evaluations were compatible with Canada's environmental effects monitoring procedures (Environment Canada, 2010). To avoid contamination of the intestines with any extraneous bacteria, prior to dissection, fish were wiped with 70% ethanol. An internal examination was then performed, followed by dissection of internal organs. For microbiome analyses, lower portions of intestines were removed by use of sterile procedures and contents were carefully emptied into a 15-mL, conical, centrifuge tube. Gut contents were placed on ice until long-term storage at -20 ºC. For characterization of products of biotransformation of PAHs (PBPAHs), gallbladders were then removed and immediately placed into liquid nitrogen until long-term storage at -80 ºC. Finally, for quantification of PAHs in dorsal muscle, a representative fillet was collected from the mid-body dorsal area and placed on ice until long- term storage at -20 ºC. All procedures involving fishes followed the animal use protocol (#20160046) approved by the Animal Research Ethics Board at the University of Saskatchewan.

### *5.4.2 Quantification of PBPAHs in bile and PAHs in muscle tissue*

Quantification of PBPAHs in bile from these fish was analyzed as described previously (Ohiozebau et al., 2016). Briefly, quantification was calibrated with a seven-point, external calibration curve of pure standards (AccuStandard, New Haven, CT) of anthracene (4000 ng/ml), chrysene (2000 ng/ml), benzo[*a*]pyrene (150 ng/ml), and naphthalene (6000 ng/ml). Calibration standards were measured concurrently with the samples. Samples containing 10 µL of bile were diluted with 1000 µl of 50 % methanol/$H_2O$ (v/v). To remove particulates, samples were centrifuged at 10,000 x g for 15 min., then added to a quartz cuvette for analysis by use of synchronous fluorescence spectroscopy (SFS) with a Lumina fluorescence spectrometer (Thermo Fisher Scientific, Waltham, MA). Fluorescence of samples and standards was detected

at 290/335 nm for two- and three-ring, 341/383 nm for four-ring and 380/430 nm for five-ring PBPAHs.

Quantification of PAHs in muscle tissue was accomplished by use of previously described methods (Ohiozebau et al., 2017). Briefly, fish muscle tissues were homogenized and dried with $Na_2SO_4$. A Soxhlet apparatus was used for extraction with approximately 15 g wet mass of tissue with 250 ml dichloromethane (DCM). Prior to extraction, deuterated PAHs were added as surrogate standards from which recoveries could be corrected. Extracts were then concentrated, cleaned, and eluted prior to identification and quantification of PAHs using an Agilent (Agilent, Palo Alto, CA) gas chromatograph (GC) and HP 5975 series mass selective detector.

### *5.4.3 16S rRNA metagenetics and bioinformatics*

Prior to extraction of DNA, gut contents of fishes were freeze-dried and thoroughly homogenized. DNA was extracted from a 0.2 g aliquot of gut contents by use of the DNeasy PowerSoil Kit (Qiagen Inc., Mississauga, ON). PCR amplification of the 16S rRNA V3-V4 region, construction of a sequencing library, sequencing using a 2x300 base pair paired-end kit on a MiSeq (Illumina, San Diego, CA), and bioinformatics were performed as described previously (Chapter 2).

On average, 88% of demultiplexed reads survived through the data cleaning process, and 95% of the cleaned reads could be aligned to bacteria, using the SILVA v. 132 reference database (Quast et al., 2013). A table of the number of reads per sample pre- and post-cleaning can be found Appendix D, Table D.2. To avoid biases introduced by different sequencing depths, the feature table was rarefied at 7,220 sequences per sample (Appendix D, Fig. D.1). Alpha- (Shannon diversity, evenness, and number of observed amplicon sequence variants (ASVs)) and beta-diversities (Bray-Curtis dissimilarity) were calculated by use of QIIME2 (Bolyen et al., 2019) and with the phyloseq package v. 1.30.0 (McMurdie and Holmes, 2013)

in R v. 3.6.1 (R Core Team, 2013). Data can be accessed at: https://dx.doi.org/10.20383/101.0255

*5.4.4 Statistics*

All statistics were performed in R. All bile metabolites were summed and reported as a PBPAH, and PAHs in muscle were summed and reported as a total concentration of PAH value. Concentrations among sites were compared by use of the Kruskal Wallis test, followed by Dunn's test of multiple comparisons due to assumptions of normality and equality of variance not being met. Condition factor was calculated (Equation 5.1).

$$Condition\ Factor\ (K) = \frac{Mass\ (g)}{Standard\ Length\ (mm)^3} \times 100 \quad (5.1)$$

Because this study represents a subset of all fishes collected for fish health assessment (Jardine et al., *in prep*), condition factor was only used to describe the ordination of the microbiome data. Alpha-diversities were analyzed by use of nested ANOVA, with sampling location nested within species. The number of observed ASVs were $\log_{10}$-transformed prior to analysis to achieve normality and homogeneity of variance. To ascertain any associations between alpha-diversity and concentrations of PBPAHs or PAHs, a linear regression was fitted to each of the alpha-diversity indices and the sum concentration of PBPAHs or PAHs.

Differentially abundant bacterial taxa were identified by use of an ANOVA-Like Differential Expression tool (ALDEx2) v 1.18.0 (Fernandes et al., 2014, 2013; Gloor et al., 2016), which transformed data by use of Aitchison's centered, log-ratio (CLR). A Kruskal Wallis test was then performed on CLR-transformed taxa, followed by a Dunn's test to ascertain differences among fishes. Furthermore, to determine which taxa could be considered to be indicators for each of the fishes, based on their abundance, the indicspecies v. 1.7.9 package (De Cáceres and Legendre, 2009) was used. To determine which taxa were

significantly correlated with concentrations of PAHs or PBPAHs, in muscle or bile, respectively, a Spearman regression with CLR-transformed taxa was calculated.

Differences in compositions of microbial communities of guts among species were analyzed by use of the phyloseq package (McMurdie and Holmes, 2013), with the feature table and rooted tree generated in QIIME2. Principal coordinate analysis (PCoA) plots were generated with log-transformed Bray-Curtis dissimilarities by use of an agglomerated feature table to combine taxa of the same genus to reduce complexity of ordination. Community differences, using Bray-Curtis dissimilarities, were first assessed by use of an ANOVA of the dispersion of dissimilarities by use of the *betadisper* function in vegan (Oksanen et al., 2019). Overall community differences were then calculated by use of adonis2 (Oksanen et al., 2019), and the pairwise.adonis2 function with a Bonferroni *p*-value adjustment (Martinez Arbizu, 2019). A Constrained Analysis of Principal Coordinates (CAP) was conducted using the capscale function in vegan to ordinate the condition factor and PAH data, and view the clusters of samples, relative to location. Significant factors contributing to the ordination were assessed using an ANOVA. Effects of PAHs on northern pike were not analyzed because only two samples were from a site other than the far-field reference site.

## 5.5 Results

### *5.5.1 Gut microbiomes of native fishes from the North Saskatchewan River*

Native, wild-caught fishes hosted distinct gut microbiomes. DNA metabarcoding revealed a total of 32,804 ASVs among 78 samples. However, after removing non-bacterial taxa and bacteria without further classification, as well as chloroplast and mitochondrial sequences, 16,333 ASVs in 40 phyla remained. Among all fishes, predominant phyla were *Firmicutes* and *Proteobacteria* (Fig. 5.2A). In the microbiome of walleye, the predominant phyla were (± standard error): *Firmicutes* (39% ± 6%), *Proteobacteria* (21% ± 5%), and *Tenericutes* (15% ± 5%) across 22 phyla. Predominant phyla in goldeye were *Firmicutes* (50%

± 8%), *Proteobacteria* (32% ± 7%), and *Fusobacteria* (6% ± 5%) across 28 phyla. In northern pike, predominant phyla were *Proteobacteria* (66% ± 9%), *Fusobacteria* (19% ± 7%), and *Firmicutes* (11% ± 4%) across 8 phyla. In shorthead redhorse, the predominant phyla were *Firmicutes* (56% ± 7%), *Proteobacteria* (18% ± 5%), and *Actinobacteria* (10% ± 4%) across 22 phyla. The most predominant orders and families are given (Appendix D, Fig. D.2).

In total, 23 genera were shared among the four fishes; this represents 3.5% of all genera observed among fishes (Fig. 5.2B; Appendix D, Table D.3). Among the four fishes, three genera were observed exclusively in northern pike, which represented 0.5% of all genera found across species. Overall, 199, 134, and 60 genera were found exclusively in goldeye, shorthead redhorse, and walleye, respectively, representing 30%, 20%, and 9% of the total genera observed among species. Northern pike had the least percent of genera observed at 6% of the total genera observed among the four fishes studied, followed by walleye (40%), shorthead redhorse (55%), and goldeye (62%).

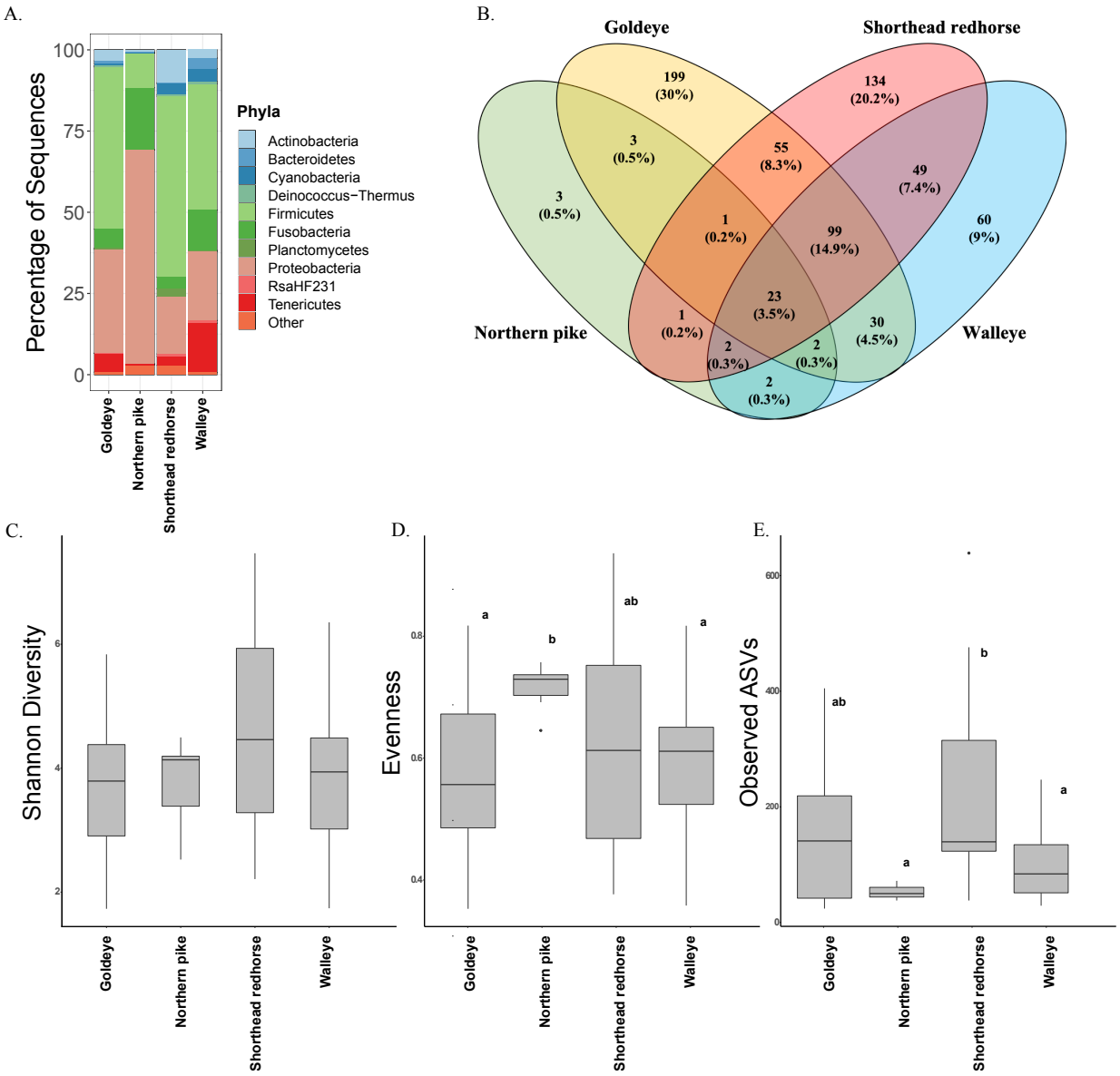


Figure 5.2. (A). Ten most numerous phyla found in the guts of goldeye, northern pike, shorthead redhorse, and walleye. (B). Venn diagram of number of overlapping genera in goldeye, northern pike, walleye, and shorthead redhorse, shown in gold, green, blue, and red, respectively. The number of shared genera among fish species are shown above the relative percent of those genera found across all species. (C). Shannon diversity index (D). Evenness, and (E). Number of observed ASVs of goldeye, northern pike, short head redhorse, and walleye. Letters denote statistical significance ($p < 0.05$).

Species diversity of the microbiome was dependent upon the identity of the host fish species, with alpha-diversity indices varying among fishes. While Shannon diversity did not differ among species (Fig. 5.2C), evenness and the number of observed ASVs did (Nested ANOVA: Evenness $F = 3.7$, $p = 0.02$; Observed ASVs $F = 6.2$, $p < 0.001$). Northern pike had significantly greater evenness values than goldeye ($p = 0.013$) and walleye ($p = 0.023$) (Fig. 5.2D). Shorthead redhorse had significantly more observed ASVs than northern pike ($p = 0.001$) and walleye ($p = 0.009$), as well as marginally more ASVs than goldeye ($p = 0.091$) (Fig. 5.2E).

Dispersions of beta-diversities were significantly different among fishes (ANOVA: $F = 11.5$, $p < 0.001$), with all fishes having dispersion patterns that were significantly different from each other ($p < 0.05$), except for walleye and shorthead redhorse, which had similar dispersion patterns (Fig. 5.3A). Northern pike had significantly less dispersion in their community compositions than did goldeye ($p < 0.001$), walleye ($p = 0.002$), and shorthead redhorse ($p = 0.001$). Goldeye had significantly greater dispersion than walleye ($p = 0.015$) and shorthead redhorse ($p = 0.055$). Beta-diversities were also significantly different among fish species (adonis: $F = 5.6$, $p = 0.001$; Fig. 5.3A). All pairwise comparisons were significantly different ($p < 0.05$). Indicator genera were identified for each of the different fish species; 16 were identified for goldeye, five for northern pike, 62 for shorthead redhorse, and one for walleye (Fig. 5.3B).

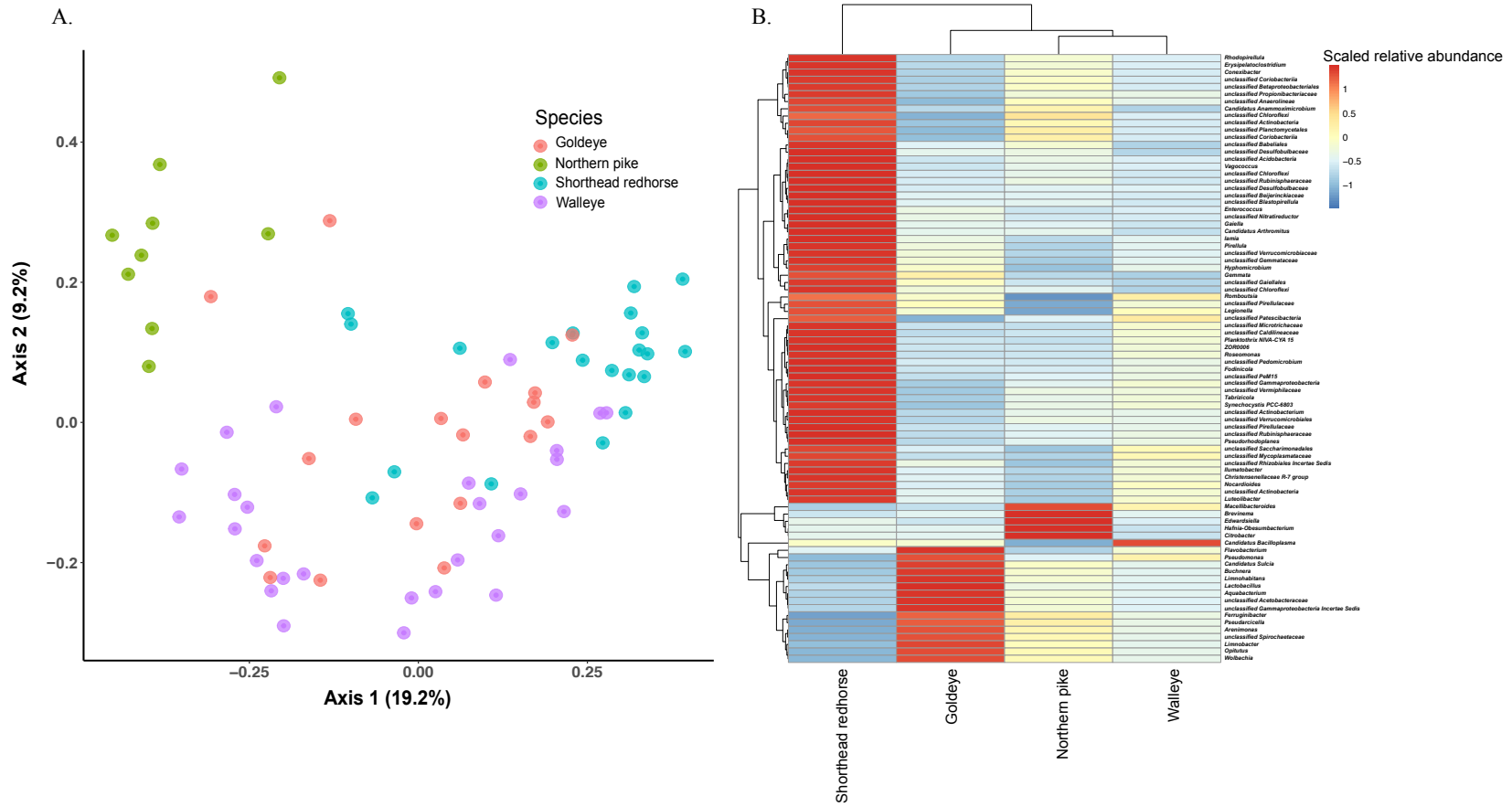


Figure 5.3. (A). PCoA of log-transformed Bray-Curtis dissimilarities for goldeye, northern pike, shorthead redhorse, and walleye. Colors indicate different species. (B). Heat map of the indicator genera and relative abundance in each species of fish. Legend denotes scaled relative abundances of the various taxa, with blues indicating lesser abundances, and reds denoting greater abundance.

### *5.5.2 Concentrations of PAHs and PBPAHs in fishes in the North Saskatchewan River*

Concentrations of PBPAHs (Fig. 5.4A) in native fishes did not differ greatly among sites, but PAHs (Fig. 5.4B) in native fishes were greater downstream of the Husky oil spill relative to upstream and far-field sites. The only significant differences among upstream, downstream, and the far-field site for PBPAHs (Fig. 5.4A) were for northern pike, which had significantly greater concentrations at the downstream site as compared to the far-field site ($F = 48.22$, $p = 0.020$). Fish collected from downstream sites had higher concentrations of PAHs in muscle tissue than both the upstream and the far-field sites (Fig. 5.2C). In walleye, sites were significantly different ($F = 5.6$, $p = 0.015$), with concentrations higher downstream compared to both the upstream sites ($p = 0.043$) and the far-field site ($p = 0.031$). Concentrations of PAHs in goldeye and shorthead redhorse were not significantly different, and northern pike did not have a large enough sample size to draw a conclusion.

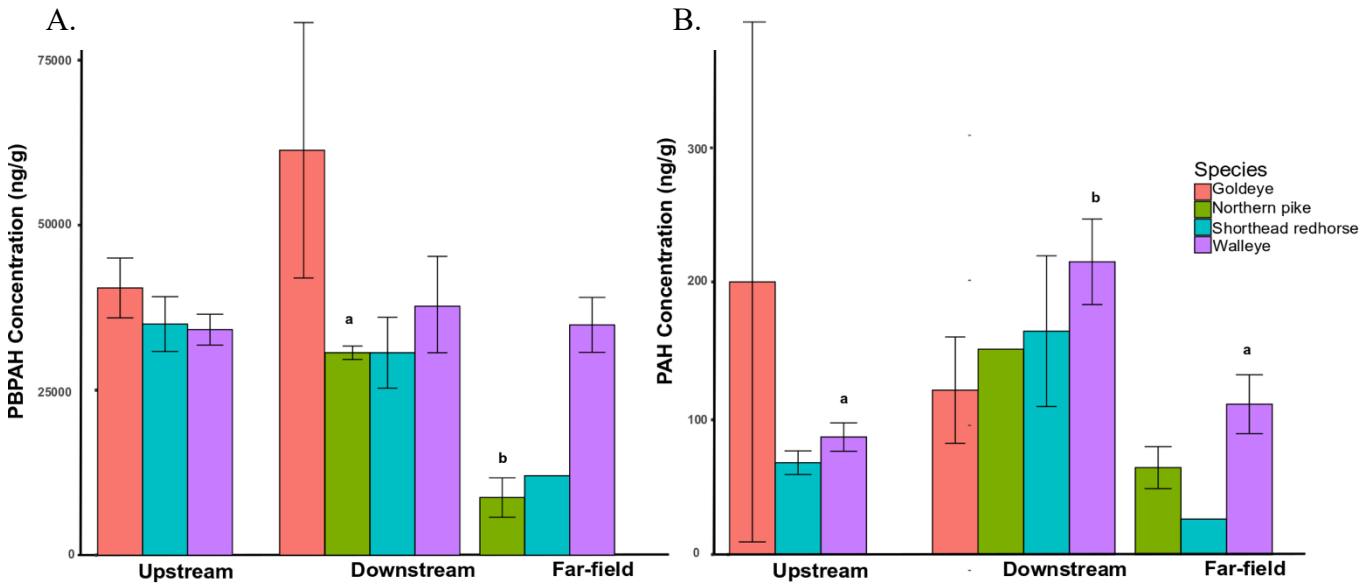


Figure 5.4. Mean (A). sum PBPAH concentrations (ng/g) from bile and (B). sum PAH concentrations (ng/g) from muscle tissue from fish collected upstream and downstream of the oil spill, in addition to the far-field reference site, in each of the species collected. Error bars are standard error of the mean. Letters denote statistical differences ($p < 0.05$).

*5.5.3 Effects of the oil spill on individual fish species*

Because of large variations of gut microbiomes between fishes, effects of exposure on each species of fish was analyzed independently. Greater concentrations of PAHs did not have a major effect on alpha-diversities of exposed fishes. While Shannon diversity (Appendix D, Fig. D.3) and numbers of observed ASVs (Appendix D, Fig. D.4) were generally inversely proportional to concentrations of PAHs in muscle of each species, the trends were not significant. Concentrations of PBPAHs in bile were not correlated with any index of alpha-diversity in any fishes.

Contributions to ordination of log-transformed Bray-Curtis dissimilarities were assessed with a CAP for each individual fish species, relative to location. No factors were significant for shorthead redhorse (Fig. 5.5A). The use of CAP ($F = 1.6$, $p = 0.026$) revealed that condition factor ($p = 0.037$), which can be interpreted as an indicator of fish health (Bolger and Connolly, 1989), and to a lesser extent, total concentrations of PAHs in muscle ($p = 0.080$), were significant factors in the ordination for walleye (Fig. 5.5B). Goldeye were not analyzed because the sample size was too small at each site.

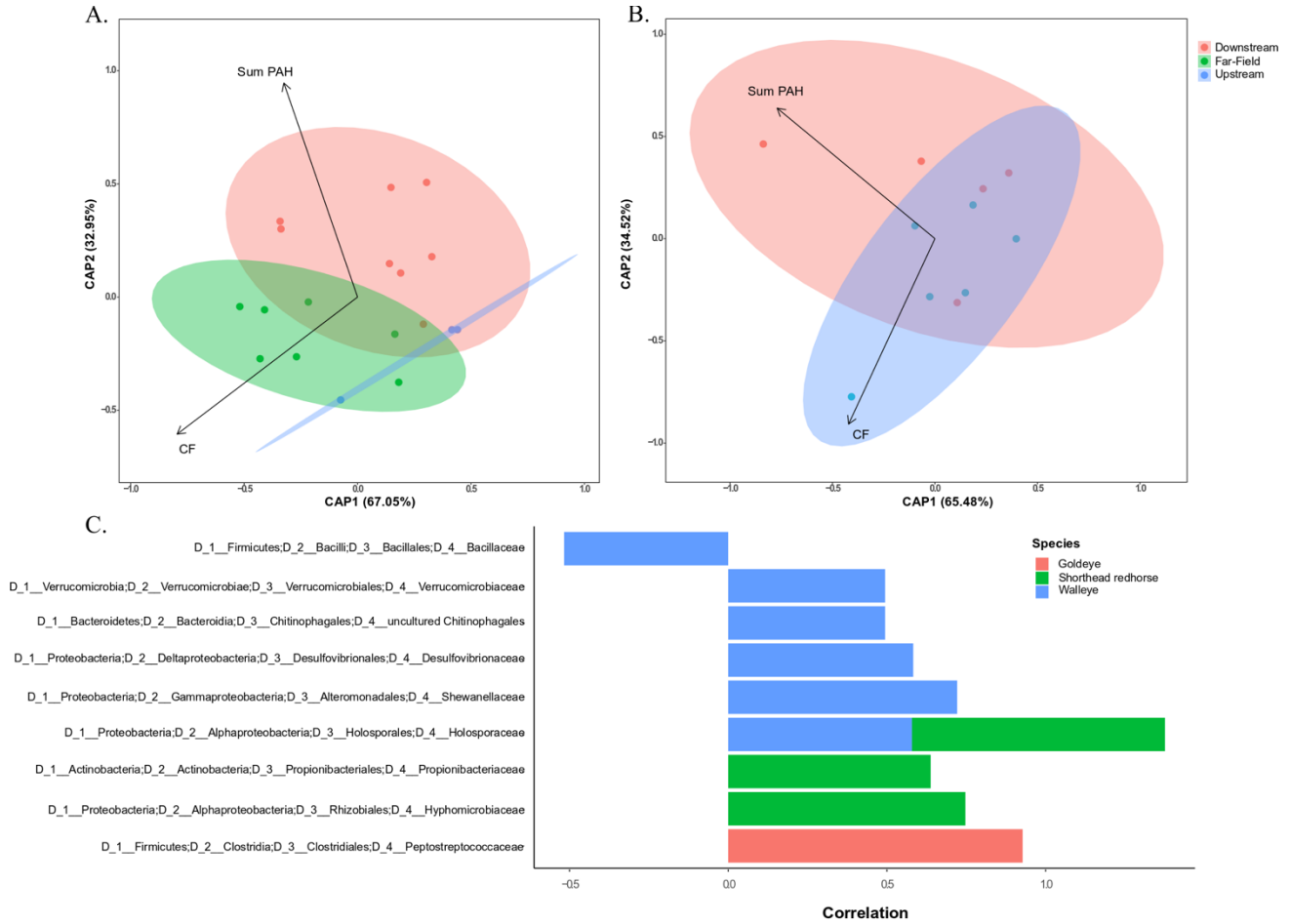


Figure 5.5. Cumulative Abundance Profile (CAP) of genera found in the microbiome of (A). shorthead redhorse and (B). walleye at each sampling site. No factors were significant for shorthead redhorse. For walleye, condition factor (CF) was a significant factor constraining the ordination ($p = 0.04$), while concentration of PAHs in muscle of fishes was less significant ($p = 0.08$). (C). Families that significantly correlated ($p < 0.05$) with concentrations of PAHs in goldeye, shorthead redhorse, and walleye.

Relative abundances of several families were correlated with greater concentrations of PAHs in muscle (Spearman correlation: $p < 0.05$; Fig. 5.5C). In shorthead redhorse, *Hyphomicrobiaceae, Propionibacteriaceae,* and *Holosporaceae* were all positively correlated with concentrations of PAHs. In walleye, *Bacillaceae* was negatively correlated with PAH concentrations, while *Verrucomicrobiaceae*, *Desulfovibrionaceae*, uncultured *Chitinophagales, Holosporaceae,* and *Shewanellaceae* were all positively correlated with concentrations of PAHs. Only *Peptostreptococcaceae* were positively correlated with concentrations of PAHs in goldeye. No statistically significant correlations were observed between relative abundances of families and PBPAH concentrations in any fish species.

## 5.6 Discussion

The oil spill on the North Saskatchewan River provided a unique opportunity to study the gut microbiomes of native, economically, and culturally important fishes in Saskatchewan, Canada, as well as potential effects the oil spill on the microbiome of those fishes. Measured concentrations of PAHs in muscle of fishes suggests continued exposure to some constituents of the spilled oil a year after the incident. Due to rapid metabolism of PAHs, concentrations of transformation products in bile are a better indicator of recent exposures (Ohiozebau et al., 2016), but PAHs can accumulate in muscle and represent an exposure from the past (Ohiozebau et al., 2017). Concentrations of PBPAHs were relatively similar across sites, potentially indicating a source of PAHs other than the oil spill. Additionally, the scattered pattern might be a factor of the passage of time between the oil spill and when these fish were collected (Yang et al. 2020).

Identity of the host species was the dominant driver in shaping relative proportions of bacteria in microbiomes of the gut. While most studies on the gut microbiome of fish investigate a single species of cultivated fish, this study provided a perspective on gut microbiomes of several fishes of various natural histories with different feeding patterns from a natural setting. Dominance of *Firmicutes* and *Proteobacteria* among the four fishes, as well as dominance of *Fusobacteria* in goldeye and northern pike is consistent with fish other species such as fathead minnows (*Pimephales promelas*) and grass carps (*Ctenopharyngodon idella*) (DeBofsky et al., 2020; Liu et al., 2016). Dominance of *Tenericutes* in walleye and

*Actinobacteria* in shorthead redhorse, while they are less commonly reported in literature, are still phyla found in microbiomes of fishes such as king mackerels (*Scomberomorus cavalla*) and red snappers (*Lutjanus campechanus*) (Arias et al., 2013; Givens et al., 2015; Sullam et al., 2012).

Observed variation in alpha-diversity, as well as bacterial distribution among species was expected given differences in life history and feeding preferences of the four fishes. Northern pike are specialist piscivores that occasionally eat insects and are often found with empty stomachs (Beaudoin et al., 1999). Walleye are carnivorous, with a more varied diet, consuming fish, insects, snails and crayfish (Scott and Crossman, 1979). Goldeye are also opportunistic carnivores with a diet that includes insects, mollusks, crustaceans, and small fishes (Donald and Kooyman, 1977). As bottom feeding omnivores, shorthead redhorse have the most varied diets, consuming primarily benthic invertebrates and bivalves, but also consuming sediment and detritus due to their strategy for feeding (Sule and Skelly, 1985).

As was hypothesized, alpha-diversities of microbial communities of guts varied among the four fishes (Tarnecki et al., 2017). It has been well-established that diversity in microbial communities of guts is greater in omnivorous than carnivorous organisms (Liu et al., 2016). Shorthead redhorse, with the most diverse diet, had the greatest number of observed ASVs, while northern pike, with the least diverse diet, had the least number of observed ASVs. Conversely, northern pike had greater evenness of microbial communities than did goldeye or walleye (Fig. 5.2D). Greater values of evenness, which measures distributions of species in an environment, indicate that species are more equally distributed (Ma, 2005). Clustering of indicator taxa also showed that northern pike and walleye shared a number of taxa, which is consistent with their similar diets, whereas goldeye and shorthead redhorse clustered separately, which suggested that diet is a strong factor in determining compositions of microbiomes (Fig. 5.3B). Clustering does not align with phylogenetic diversity of these fishes, since while walleye and northern pike are most closely related, goldeye is the most distantly related fish, not shorthead redhorse (http://phylot.biobyte.de/).

Dispersion of community compositions among fishes was related to diets of these fish (Fig. 5.3A). Northern pike showed the least dispersion, reflecting similarities in diets of all the analyzed fish. Beta-diversity analysis revealed that the microbial compositions among all fishes were significantly different. Considering these species all have different feeding patterns and

preferences; it was expected that microbiomes of their guts would also be significantly different from one another. Although it has been documented that sex has a major effect on the composition of the gut microbiome (Chapter 2), the majority of fishes collected in this study were females, and therefore sex could not be analyzed.

Effects of the oil spill on microbiomes of the exposed fishes were hypothesized. The ability for an oil spill to alter relative compositions of bacterial communities has been observed in sediments and soils when they were exposed to petroleum hydrocarbons. Enrichment of hydrocarbon-degrading bacteria have been found in areas contaminated with oil spills (Xie et al., 2018; Yang et al., 2016). Significantly different community compositions were observed along with more hydrocarbon-degrading bacteria in the guts of southern flounder (*Paralichthys lethostigma*) exposed to oil from the Deepwater Horizon spill (Bayha et al., 2017; Brown-Peterson et al., 2017), while similar effects were observed in Atlantic cod (*Gadus morhua*) (Bagi et al., 2018).

The lack of significant negative correlations between alpha-diversities of microbiota in guts of fishes and concentrations of PAHs is consistent with previously reported results, where Shannon diversity as well as the number of ASVs observed were only inversely correlated with very high concentrations of benzo[*a*]pyrene to which fathead minnows were exposed (Chapter 3). Had we collected fish immediately after the oil spill, this trend might have been more apparent. Furthermore, the lack of any pattern between PBPAHs and alpha-diversity was likely due to the similarity in concentrations of PBPAHs in fishes among locations.

Community compositions of gut microbiomes were correlated with concentrations of PAHs in muscle. In walleye, microbiomes from upstream, downstream, and far-field sites clustered separately, suggesting that PAH concentrations in the muscle contributed to the separation of the downstream sites while condition factor contributed to the separation of the far- field site (Fig. 5.5B). With shorthead redhorse, upstream and downstream sites did cluster separately (Fig. 5.5A), but the large degree of overlap between the two groups suggests that PAH concentration and condition factor are not strong factors driving community composition in this species of fish.

Walleye also had the greatest number of taxa correlated with concentrations of PAHs in muscle, with several families being positively correlated. One of these, *Desulfovibrionaceae* is associated with pro-inflammatory phenotypes (Lefever et al., 2016), and enrichment has been

seen in guts of fathead minnows exposed to BaP (Chapter 3) and in mice after exposure to 2,3,7,8-tetrachlorodibenzo-*p*-dioxin (TCDD) (Lefever et al., 2016). Another family, the *Shewanellaceae,* contains known pathogens (Austin and Austin, 2016) and has been found to be negatively correlated with neutrophil recruitment, meaning a potentially reduced immune response to a challenge (Rolig et al., 2015). Furthermore, both *Shewanellaceae* and *Chitinophagaceae*, a member of *Chitinophagales*, are enriched in the guts of fathead minnows exposed to BaP (Chapter 4), which suggested that these taxa might be indicators of exposure to PAHs. Several strains of *Bacillaceae* are used as probiotics in aquaculture for their ability to improve growth performance and reduce colonization of pathogenic bacteria (Sun et al., 2009); a negative correlation between this taxa and concentrations of PAHs suggests these fish do not have optimal fitness or ability to fight infection. The greater influence of PAHs on the microbiome in guts of walleye, might be due to the greater sample sizes of walleye among locations. The role of increased abundance of *Verrucomicrobiaceae* and *Holosporaceae* in fish containing greater concentrations of PAHs is unclear.

For shorthead redhorse, only three taxa exhibited significant, positive correlations with concentrations of PAHs in muscle. As in walleye, *Holosporaceae* were positively correlated with concentrations of PAHs in muscle, but the cause of this result is unclear. The family *Hyphomicrobiaceae* is associated with hydrocarbon degradation and has been found at oil-contaminated sites (Sun et al., 2019), which suggests that this bacteria might assist with degrading hydrocarbons within the gut (Claus et al., 2016) or it might merely proliferate at the sites of higher contamination. Members of the third family, *Propionibacteriaceae,* are capable of stimulating immune responses and synthesizing bacteriocins (Chaia et al., 1999), suggesting an indirect pathway between proliferation of this bacterium and exposure to PAHs, which are immunosuppressants (Bayha et al., 2017). In goldeye, only *Peptostreptococcaceae* was positively correlated with concentrations of PAHs. Enrichment of this taxa has also been observed in mice exposed to TCDD (Lefever et al., 2016) and has been associated with colorectal cancer in humans (Ahn et al., 2013).

While this study provided several novel insights into the diversity of microbiomes among native fishes and potential effects of an oil spill on the gut microbiomes of these fishes, several limitations warrant mentioning. First, the sample sizes were limited. The density of fish in the North Saskatchewan River is low, so it would have been problematic to collect greater

numbers of fish without potentially depleting local populations. Secondly, nets were set overnight because of the limited density of fish, and some fish died overnight, leaving gut microbiomes that were not completely fresh in the morning. In human cadaver studies, the gut microbiome remains intact for up to four days post-mortem (DeBruyn and Hauther, 2017), but it is currently unknown how long the microbiome would remain unchanged in fish in a northern river. Although the delay in collection may have caused some shift in the microbiomes, it likely did not have much effect, since the fish were collected within 12 hours of setting the nets. Finally, these samples were collected one year after the oil spill; while we did see some correlations between PAH concentrations and microbial communities, the effects likely would have been more dramatic had these fish been collected immediately after the spill (Yang et al. 2020).

## 5.7 Conclusions

Overall, the results of this study show that multiple factors can shape the gut microbiome. Despite living in the same environments, the life history traits of the different fish species shape the overall microbiome, with omnivores having greater diversity and lower evenness than carnivores and piscivores, and with community compositions being reliant upon host species. Future work to determine consistency of the gut microbiome across environmental conditions would be necessary to assess the relative importance of environmental variables. Likewise, it would be worthwhile to investigate the role of the different taxa that inhabit the guts of these different species as well as those that are shared among species.

The effect of the oil spill on the gut microbiome is less clear. While several taxa did correlate with concentrations of PAH in muscle tissue, it is difficult to ascertain a direct cause and effect. If PBPAHs had correlated with certain taxa, it could be assumed that PAHs were undergoing enterohepatic circulation and directly interacting with the microbiome (Schlenk et al., 2008), but any correlations between concentrations of PAHs in muscle and the microbiome would reflect a longer-term exposure. Interestingly, the taxa that did correlate with PAH concentrations had considerable overlap with taxa that were enriched or depleted in fathead minnows exposed to BaP (Chapters 2-4), signifying a shared microbial response among teleosts. This work highlights the need to incorporate field studies in microbiome

toxicology research.

## 5.8 Acknowledgments

We thank Michaela Carriere, Stephen Srayko, Aaron Bell, Kiara Calladine, Iain Phillips, Brett Tendler, Ehimai Ohiozebau, Will Fincham, Alex Vien, Tess Engel, and Anuja Thapa for their help in the field and in the lab. Thank you to Champika Fernando of the Hill Lab for all the additional help in the lab. Funding was provided by "Next generation solutions to ensure healthy water resources for future generations" funded by the Global Water Futures program, Canada First Research Excellence Fund (#419205) and Fisheries and Oceans Canada's National Contaminants Advisory Group. Prof. Giesy was supported by the Canada Research Chairs Program of the Natural Sciences and Engineering Research Council of Canada (NSERC).

# CHAPTER 6: General Discussion

## 6.1 History and project rationale

Advances in biotechnology have dramatically altered and augmented the field of toxicology and rapidly enhanced understanding of interactions between toxicants and organisms. Toxicology has adopted molecular-based techniques to quantify the 'omics and assess cellular to ecosystem responses to toxicants. This has led to adoption of the organizing concept of Adverse Outcome Pathways (AOPs), which connect exposure to a toxicant to organism- and population- level responses *via* molecular and cellular responses (Ankley et al., 2010). This conceptual framework anchors molecular-based technologies into the fundamentals of toxicology.

Furthermore, as technologies have progressed, microbiology has advanced from culture-based techniques to the new 'omics era. Taxonomic profiling can be conducted with amplicon sequencing, most commonly with the 16S rRNA gene. Metagenomics, or the use of random shotgun sequencing of DNA, attempts to sequence the entire genomic information of a community (Warnecke and Hugenholtz, 2007), while metatranscriptomics, metaproteomics, and metabolomics characterize mRNA, proteins, and metabolites, respectively, of the bacterial community (Ghanbari et al., 2015). However, even with the advent of these technologies, the environmental toxicology community has been slow to incorporate the microbiome into existing frameworks.

In the field of medicine, the microbiome as a construct that can affect health has been adopted more readily. For example, fecal microbiota transplants have been used to treat inflammatory bowel disease (Goyal et al., 2018) and *Clostridium difficile* (Kelly et al., 2015). More recently, attention has been placed on the concept of postbiotics, which are supplementations of bacterial constituents, including metabolites, to relieve inflammatory diseases (Maslowski et al., 2009). Furthermore, data on the microbiome is now being incorporated into drug pharmacokinetics for development of precision medicine (Clarke et al., 2019).

Changes in the microbiome have also been explored in the field of nutrition, and in particular in relation to obesity (Turnbaugh et al., 2006) and the potential for personalized diets (Zeevi et al., 2015). Agriculture and aquaculture, areas where disease and antimicrobial-resistance are rampant, have also been quick to adopt microbiome research (Yukgehnaish et al., 2020). Research on the microbiome, as well as into the use of probiotics, or live microorganisms that confer a health benefit (WHO, 2001), and prebiotics, which are essentially foods for beneficial bacteria (Scantlebury Manning and Gibson, 2004), has resulted in reduced risk of infection and improved growth performance (Sun et al., 2010; Yeoman and White, 2014).

Albeit slower to implement than medicine directed research, toxicology research in humans has also embraced the interplay between the microbiome and toxicants (Dietert and Silbergeld, 2015), with research on pharmaceuticals informing much of the current field (Koontz et al., 2019). It has been established that toxicants can be transformed to become more or less toxic by bacteria and their enzymes, and that the communities of bacteria themselves may be altered in response to exposure (Koontz et al., 2019). While there are many gaps in knowledge, research is progressing in this area. All of these areas of microbiome research highlight the delicate balance between harmful and beneficial bacteria present in every body, and the implications dysbiosis can have on host fitness (Scotti et al., 2017).

Over the past four years since I began my Ph.D. program, the environmental toxicology community has begun to acknowledge the role of the microbiome in aquatic toxicology, and particularly in fish health (Adamovsky et al., 2018). While studies in human and mammal microbiome health have progressed to the point of functional characterization and manipulation, much of the research in fish continues in the phase of characterization and description. The impetus of my research through my Ph.D. was to develop the knowledge-base of the microbiome in fishes native to Saskatchewan, in both a laboratory- and field-based setting and characterize effects of PAHs, and specifically BaP, on the microbiome. This

research was designed to contribute to the fundamental understanding of the microbiome in fishes to advance the concept of the microbiome becoming a component of AOPs in the future.

## 6.2 Summary – The effects of PAHs on the microbiome in laboratory-raised fathead minnows as well as wild fishes in the North Saskatchewan River

### *6.2.1 Characterization of the microbiomes of fathead minnows, goldeye, northern pike, shorthead redhorse, and walleye*

In this thesis, the microbiomes of fathead minnows (*Pimephales promelas*), goldeye (*Hiodon alosoides*), northern pike (*Esox lucius*), shorthead redhorse (*Moxostoma macrolepidotum*), and walleye (*Sander vitreus*) were characterized using 16S rRNA metagenetics. In Chapter 2, with adult fathead minnows, it was determined that the dominant phyla in fathead minnows were: *Proteobacteria*, *Fusobacteria,* and *Bacteroidetes*. However, in Chapter 3, with juvenile fathead minnows, the dominant phyla were: *Fusobacteria*, *Proteobacteria,* and *Firmicutes*. In Chapter 4, the active microbiome in juvenile fathead minnows was assessed, where the dominant phyla were again *Proteobacteria, Fusobacteria*, and *Bacteroidetes.* In Chapter 5, it was shown that goldeye and northern pike are also dominated by *Fusobacteria* and *Proteobacteria,* while *Firmicutes* and *Proteobacteria* dominated the walleye and shorthead redhorse microbiomes. Across all studies and fish species, only three genera were shared: *Cetobacterium, Aeromonas, and Pseudomonas*, suggesting these three taxa might be common across all fish. Overall, dominance of *Fusobacteria* and *Proteobacteria* is common throughout fishes, including in other studies utilizing fathead minnows (Narrowe et al., 2015) and zebrafish (*Danio rerio*) (Roeselers et al., 2011), while *Firmicutes* is also a dominant phyla across a number of carp species (Liu et al., 2016). While the search for a core microbiome amongst all fishes is ongoing, this work was in accordance with published research and shows that the fish microbiome is relatively consistent across fishes, with some impacts of fish age and species (Tarnecki et al., 2017).

### *6.2.2 The sex-specific microbiomes of fathead minnows*

In Chapter 2, it was established that sex is a major determinant of the diversity of the microbiome. Bacterial community compositions were significantly different between male and female fish, and alpha diversity indices were greater in female fish than in male fish. This finding is consistent with results of other studies, which found that females have significantly greater diversity of bacterial communities in largemouth bronze gudgeon (*Coreius guichenoti*) (Li et al., 2016), and that microbial responses to diet are sex-dependent in three-spined stickleback (*Gasterosteus aculeatus*) and Eurasian perch (*Perca fluviatilis*) (Bolnick et al., 2014). Moreover, gut microbiomes of female mice have greater alpha diversities than do gut microbiomes of male mice (Org et al., 2016; Yurkovetskiy et al., 2013), which is a pattern that has also been observed in humans (Gao et al., 2018; Ying et al., 2015). Because the scope of this research is toxicology, this finding further highlights the need to incorporate sex as a factor into scientific investigations beyond merely reproductive endpoints (Liang et al., 2017).

### *6.2.3 The active microbiome of fathead minnows*

Because DNA and RNA were co-isolated from the guts of juvenile fathead minnows in Chapters 3 and 4, respectively, the results of these two chapters provided insight into the genomic (DNA), active (RNA), and DNA-normalized (RNA:DNA ratio) microbiomes. Interestingly, the genomic and active gut microbiomes had significantly different community compositions. While 58 genera overlapped between the two microbiomes, six were unique to the genomic microbiome and 17 were unique to active microbiome; the active microbiome also had significantly more ASVs, which are used as a proxy for species, than the genomic microbiome. The DNA-normalized microbiome revealed unique insight into the effects of BaP, as will be discussed below. Use of DNA for metagenetics can provide insight into more abundant taxa with little activity, and the use of RNA for metagenetics can give information

on low abundance taxa with high activity (Revetta et al., 2011). The ratio of the two (RNA:DNA) quantifies the relative amount of potential activity, or the protein synthesis potential (Blazewicz et al., 2013). These two chapters highlight that the genomic microbiome is not the full picture, and that co-isolation of DNA and RNA from the microbiome can provide additional insight into the community composition and response to a toxicant. This was the first study to compare the genomic, active, and DNA-normalized microbiomes in fish.

### *6.2.4 PAHs alter the community structure of microbiomes*

Results of studies presented in this thesis reveal a distinct influence of PAHs on the microbiome, even at small concentrations of exposure. Chapters 2, 3, 4, and 5 showed that bacterial community structure was dependent upon BaP exposure groups, and that certain taxa were associated with exposure. In Chapter 2, adult fathead minnows were aqueously exposed to environmentally-relevant low concentrations of BaP for four days, and while gene expression data did not show any influence of the exposure on the fish, the female fish microbiome had already changed, with altered community structure at the two highest exposure concentrations. The microbiome in male fish, however, did not change over the duration of this experiment. This study highlighted sex-dependent effects of exposure to BaP on the microbiome. While sex-dependent effects of toxicants on the microbiome has been explored in mammals (Chi et al., 2016; Lozano et al., 2018), this relationship has not been explored in fish. Similar to the findings in Chapter 2, Chi et al., 2016 found that female mice exposed to arsenic had greater differences in their microbiomes than in male mice. Like with susceptibility to BaP (Booc et al., 2014), males are more susceptible to the effects of arsenic exposure, suggesting that the microbiome may be an important factor in sex-related sensitivities to toxicants (Chi et al., 2016).

PAHs also transformed bacterial community structure in fathead minnows in Chapters 3 and 4, and marginally impacted walleye in Chapter 5. Chapters 3 and 4 brought new insight into

the response of the microbiome to BaP with the analysis of the genomic, active, and DNA-normalized microbiomes. With higher concentrations of BaP and an experiment with a longer duration, it became easier to elucidate major effects of BaP on the gut microbiome, and to look for some of these same effects in wild fish exposed to crude oil in Chapter 5. In Chapters 3 and 4, community structure was again observed to be impacted by exposure to BaP, and correlation between measured BaP metabolites and community structure was significant. Because the major individual metabolites were measured, it could be determined that OH-BaP and BaP-$SO_4$, but not BaP-Gluc, were dominant drivers in ordinating the communities. The active microbiome showed better resolution of the community separation among exposure groups than the genomic microbiome, but the DNA-normalized microbiome had the greatest separation. Evaluation of the active and DNA-normalized microbiomes has been performed in a number of systems, including in oil production facilities (Salgar-Chaparro and Machuca, 2019), office drinking water systems (Inkinen et al., 2016), and in an African lake (İnceoğlu et al., 2015), but studies in fish are limited and do not focus on toxicological responses (Navarrete et al., 2012). Finally, in Chapter 5, PAH concentration in the muscle approached significance as a factor driving community structure in walleye, but not in shorthead redhorse or goldeye. Furthermore, Chapter 5 was potentially the first study assessing the effects of a toxicant on the microbiome of wild-caught fish in a contaminated site using 16S rRNA metagenetics.

Most interestingly, in Chapter 3, it was determined that exposure to BaP resulted in a complete loss of network connectivity among the microbes in the genomic microbiome. This concept has not been well-explored in the field of gut microbiome research, but ecological network responses to anthropogenic perturbation have been documented (Elmqvist et al., 2003; Power et al., 1996; Vinebrooke et al., 2004). High concentrations of air pollution (Karimi et al., 2016) and areas with pollution from chlor-alkali tailings (Zappelini et al., 2015) have observed a reduction in microbial network complexity, signifying the breakdown of the ecological niche.

Individual taxa or ratios of taxa are often used as indicators of disease or health

(Hiippala et al., 2018), which could be analogous to analysis of specific genes, but this method is not always reliable (Finucane et al., 2014). The loss of community structure in the genomic microbiome, however, could be used as a biomarker to indicate exposure to a toxicant, since it is less reliant on individual variations in the microbiome (Derocles et al., 2018; Dietert and Silbergeld, 2015). Surprisingly, this relationship did not hold in Chapter 4, with the active microbiome maintaining network structure in each exposure condition, signifying potential resistance and resilience in response to a toxicant (Elmqvist et al., 2003).

### *6.1.1 PAHs have limited effects on alpha-diversity of microbiomes*

Across Chapters 3, 4, and 5, alpha-diversity was reduced in fish exposed to PAHs, but the results were not consistently significant. Chapters 3 and 4 showed that the genomic and active microbiomes had significantly reduced Shannon diversity values and number of observed ASVs in the highest exposure groups. In Chapter 5, alpha-diversity did not correlate at all with concentrations of PBPAHs from bile, but although the results were not significant, values were reduced in fishes with higher concentrations of PAHs in muscle. With a larger sample size of fishes with higher concentrations of PAHs, this trend could be further clarified.

### *6.2.5 Several taxa from the microbiome are correlated with PAH exposure*

Across all chapters, several taxa were correlated with exposure to PAHs (Table 6.1). Many of the taxa that were positively correlated with exposure to PAHs, such as *Xanthobacteraceae, Caulobacteraceae, Hyphomicrobiaceae,* and *Burkholderiaceae* have known hydrocarbon degradation functions (Oren, 2014; Sun et al., 2019; S. Yang et al., 2016; Yergeau et al., 2012). Others, such as *Vibrionaceae, Erysipelotrichaceae*, *Desulfovibrionaceae, Shewanellaceae, Verrucomicrobiaceae, Propionibacteriaceae, Peptostreptococcaceae,* and *Aeromoadaceae* are associated with inflammation and disease (Ahn et al., 2013; Austin and Austin, 2016; Chaia et al., 1999; Chen et al., 2012; Colwell and Grimes, 1984; Cryan et al.,

2019; Lefever et al., 2016; Rolig et al., 2015). *Flavobacteriaceae, Moraxellaceae,* and *Pseudomonadaceae* contain taxa that are capable of degrading hydrocarbons as well as causing disease (Austin and Austin, 2016; Balba et al., 1998; Loch and Faisal, 2015; Sowada et al., 2018). Fewer families were negatively correlated with PAHs; these families were associated with digestion and immune regulation, such as *Bacteroidaceae* (Ikeda-Ohtsubo et al., 2018), *Barnesiellaceae* (Montassier et al., 2016), *Rikenellaceae* (Zeng et al., 2016), and *Bacillaceae* (Sun et al., 2009).

Remarkably, even across species and exposure conditions, three families were enriched in fishes exposed to greater concentrations of PAHs: *Desulfovibrionaceae, Shewanellaceae, and Chitinophagaceae* (although not identified down to family in walleye, it was identified to order). In fathead minnows, these families were only identified in the active and DNA-normalized microbiomes, highlighting that both DNA- and RNA-based 16S rRNA metagenetics are important. Were these studies seeking biomarkers of exposure in the microbiome, these three taxa would be strong candidates.

Table 6.1. Positively and negatively correlated families with BaP or PAHs, for laboratory-based and field-based studies, respectively, from each chapter. The source of the fish is given, along with any details about the fish, including sex, nucleotides isolated, and study species. Because Chapter 2 did not contain any measured concentrations of PAHs within the fish, the two taxa associated with exposure were calculated with Kruskal-Wallis tests rather than Spearman correlation.

| Chapter | Species | Details | Positively Correlated | Negatively Correlated |
|---|---|---|---|---|
| 2 | Adult FHM | Females | *Xanthobacteraceae* | |
| | | | *Isosphaeraceae* | |
| | | | *Rubritaleaceae* | |
| | | Males | *Vibrionaceae* | |
| 3 | Juvenile FHM | Genomic | *Brevinemataceae* | *Bacteroidaceae* |
| | | | *Caulobacteraceae* | *Barnesiellaceae* |
| | | | *Chitinibacteraceae* | *Chromobacteriaceae* |
| | | | *Erysipelotrichaceae* | |
| | | | *Microbacteriaceae* | |
| | | | *Moraxellaceae* | |
| 4 | | Active | *Burkholderiaceae* | *Bacteroidaceae* |
| | | | *Chitinibacteraceae* | *Barnesiellaceae* |
| | | | *Chitinophagaceae* | *Chromobacteriaceae* |
| | | | *Erysipelotrichaceae* | *Rikenellaceae* |
| | | | *Flavobacteriaceae* | |
| | | | *Isosphaeraceae* | |
| | | | *Moraxellaceae* | |
| | | | *Pseudomonadaceae* | |
| | | | *Spirosomaceae* | |
| | | | *Weeksellaceae* | |
| | | DNA-normalized active | *Aeromonadaceae* | *Nocardiaceae* |
| | | | *Chitinibacteraceae* | *Rikenellaceae* |
| | | | *Desulfovibrionaceae* | *Sphingomonadaceae* |
| | | | *Flavobacteriaceae* | *Xanthomonadaceae* |
| | | | *Microbacteriaceae* | |
| | | | *Moraxellaceae* | |
| | | | *Rhizobiaceae* | |
| | | | *Shewanellaceae* | |
| 5 | Wild-caught | Shorthead redhorse | *Holosporaceae* | |
| | | | *Hyphomicrobiaceae* | |
| | | | *Propionibacteriaceae* | |
| | | Walleye | *Desulfovibrionaceae* | *Bacillaceae* |
| | | | uncultured *Chitinophagale* | |
| | | | *Shewanellaceae* | |
| | | | *Holosporaceae* | |
| | | | *Verrucomicrobiaceae* | |
| | | Goldeye | *Peptostreptococcaceae* | |

## 6.3 Future directions for this research

The research presented in this thesis advance the fundamental understanding of the gut microbiome in fishes and the role PAHs have in affecting community structure and composition of the microbiome. While this research did not directly address the role of the microbiome in an AOP for PAHs, it did highlight that the microbiome could be an important step in assessing the adverse outcomes that could result from exposure to a PAH. For example, exposure to PAHs might directly impact the gut microbiome and result in altered community composition, as well as result in the established molecular initiating event of binding of the PAHs to the AHR. This produces a key event of induction of *cyp1a* and the generation of toxic metabolites within the organism. These toxic metabolites lead to immunomodulatory events (Bo et al., 2014) that can potentially interplay with an altered gut microbiome community composition (O'Hara and Shanahan, 2006). Alternatively, the microbiome that has been altered from direct exposure to PAHs could similarly modulate the immune response in the host. Ultimately, this could result in disease and decreased survival of the organism. In this study, a number of inflammatory and immune-related bacteria were correlated with exposure to PAHs, suggesting that this pathway warrants further research.

This research also highlights several other areas to further investigate the microbiome and its interplay with PAHs:

1) I have presented clear sex-specific effects of BaP on the microbiome, but this area warrants further investigation. The endocrine system is intimately involved with development of the microbiome, with microbiota producing and secreting hormones that respond to and regulate hormones produced by the host (Neuman et al., 2015). A lot of unknowns remain with how and why this happens, and how toxicants may interfere with and enhance this process. Sex-specific effects of toxicants are well-documented (Liang et al., 2017), but perhaps the differences in sensitivity may be influenced by the microbiome.

2) This research provided presumptive functions of certain taxa that responded to BaP exposure, as gleaned from the literature, as well as through predicted functions from Tax4Fun2 and PICRUSt2. These tools are informative, but do not replace the utility of metatranscriptomics, metaproteomics, and metabolomics (Evariste et al., 2019). To fully understand the role of microbes within the gut and their response to toxicants, higher-level analyses should be conducted. Microbiome studies are fundamentally rooted in ecology, and should be studied as such (Greyson-Gaito et al., 2020). Understanding how certain taxa may respond to toxicants is useful, but ultimately relationships among taxa and between the microbiome and the host should be explored further. This would be beneficial in tying these responses to apical outcomes in the host if the microbiome is to be adopted into the AOP framework.
3) The work presented here with field-collected fishes is only the beginning to understand firstly, the diversity and composition of microbiomes of wild fishes, and secondly, the impact environmental stressors may have on the microbiome of wild fishes. The breadth of knowledge on the microbiome of wild fishes is limited (Tarnecki et al., 2017), and the response of the fish gut microbiome to contaminants in the wild is relatively unknown. It has been suggested that wild-caught and laboratory-reared fishes do not necessarily share a microbiome (Tarnecki et al., 2017), and that sex-specific patterns in the microbiome are limited to laboratory-reared fishes (Bolnick et al., 2014), but there are so few studies in these areas that repetition across species and across toxicants is needed to further this area of research. As discussed above, there may be fingerprints of exposure in the microbiome that can be used as biomarkers of exposure, but without additional studies, this cannot be discovered.

## 6.4 Final thoughts

Throughout the duration of my Ph.D. program, the microbiome has continued its steady push to prominence in the discourse of health and toxicology. As discussed above, the gut

microbiome has legitimate function within the body of everything from worms (Ma et al., 2017) to humans (Scotti et al., 2017), but as popularity of the construct of the microbiome grows, the amount of questionable sources follows. As I am writing this dissertation, COVID-19 is attacking the world, and with it, page upon page of hastily written scientific journal articles are published on the correlation between the virus and the microbiome (scholar.google.com, Accessed: June 4, 2020). To advance this field from descriptive correlations to actually develop biomarkers or even predictive tools, a lot more solid research is needed, particularly in toxicology. The research from my Ph.D. program helped advance the basic understanding of a class of chemicals on a very limited, albeit scientifically and culturally important, number of fishes. As environmental regulations change and AOPs advance, it will be important to be mindful of the microbiome to truly protect ecosystems.

# References

Adamovsky, O., Buerger, A., Wormington, A.M., Ector, N., Griffitt, R.J., Bisesi, J.H., Martyniuk, C.J., 2018. The gut microbiome and aquatic toxicology: An emerging concept for environmental health. Environ. Toxicol. Chem. https://doi.org/10.1002/etc.4249

Adeniji, A.O., Okoh, O.O., Okoh, A.I., 2019. Levels of Polycyclic Aromatic Hydrocarbons in the Water and Sediment of Buffalo River Estuary, South Africa and Their Health Risk Assessment. Arch. Environ. Contam. Toxicol. 76, 657–669. https://doi.org/10.1007/s00244-019-00617-w

Ahn, J., Sinha, R., Pei, Z., Dominianni, C., Wu, J., Shi, J., Goedert, J.J., Hayes, R.B., Yang, L., 2013. Human Gut Microbiome and Risk for Colorectal Cancer. J Natl Cancer Inst 105, 1907–1911. https://doi.org/10.1093/jnci/djt300

Ankley, G.T., Bennett, R.S., Erickson, R.J., Hoff, D.J., Hornung, M.W., Johnson, R.D., Mount, D.R., Nichols, J.W., Russom, C.L., Schmieder, P.K., Serrrano, J.A., Tietge, J.E., Villeneuve, D.L., 2010. Adverse outcome pathways: A conceptual framework to support ecotoxicology research and risk assessment. Environ. Toxicol. Chem. 29, 730–741. https://doi.org/10.1002/etc.34

Antwis, R.E., Edwards, K.L., Unwin, B., Walker, S.L., Shultz, S., 2019. Rare gut microbiota associated with breeding success, hormone metabolites and ovarian cycle phase in the critically endangered eastern black rhino. Microbiome 7, 27. https://doi.org/10.1186/s40168-019-0639-0

Apprill, A., Mcnally, S., Parsons, R., Weber, L., 2015. Minor revision to V4 region SSU rRNA 806R gene primer greatly increases detection of SAR11 bacterioplankton. Aquat. Microb. Ecol. 75, 129–137. https://doi.org/10.3354/ame01753

Arias, C.R., Koenders, K., Larsen, A.M., 2013. Predominant Bacteria Associated with Red Snapper from the Northern Gulf of Mexico. J. Aquat. Anim. Health 25, 281–289.

https://doi.org/10.1080/08997659.2013.847872

Austin, B., Austin, D.A., 2016. Bacterial Fish Pathogens, Sixth. ed, Bacterial Fish Pathogens. Springer. https://doi.org/10.1007/978-1-4020-6069-4

Bäckhed, F., Ley, R.E., Sonnenburg, J.L., Peterson, D.A., Gordon, J.I., 2005. Host-bacterial mutualism in the human intestine. Science (80-. ). https://doi.org/10.1126/science.1104816

Baek, S.O., Field, R.A., Goldstone, M.E., Kirk, P.W., Lester, J.N., Perry, R., 1991. A review of atmospheric polycyclic aromatic hydrocarbons: Sources, fate and behavior. Water. Air. Soil Pollut. 60, 279–300. https://doi.org/10.1007/BF00282628

Bagi, A., Riiser, E.S., Molland, H.S., Star, B., Haverkamp, T.H.A.A., Sydnes, M.O., Pampanin, D.M., 2018. Gastrointestinal microbial community changes in Atlantic cod (Gadus morhua) exposed to crude oil. BMC Microbiol. 18, 25. https://doi.org/10.1186/s12866-018-1171-2

Balba, M.T., Al-Awadhi, N., Al-Daher, R., 1998. Bioremediation of oil-contaminated soil: microbiological methods for feasibility assessment and field evaluation. J. Microbiol. Methods 32, 155–164. https://doi.org/10.1016/S0167-7012(98)00020-7

Banerjee, S., Schlaeppi, K., A Heijden, M.G., 2018. Keystone taxa as drivers of microbiome structure and functioning. https://doi.org/10.1038/s41579-018-0024-1

Bari, M.A., Kindzierski, W.B., Spink, D., 2016. Twelve-year trends in ambient concentrations of volatile organic compounds in a community of the Alberta Oil Sands Region, Canada. Environ. Int. 91, 40–50. https://doi.org/10.1016/j.envint.2016.02.015

Barron, M.G., 2012. Ecological Impacts of the Deepwater Horizon Oil Spill: Implications for Immunotoxicity. Toxicol. Pathol. 40, 315–320. https://doi.org/10.1177/0192623311428474

Bayha, K.M., Ortell, N., Ryan, C.N., Griffitt, K.J., Krasnec, M., Sena, J., Ramaraj, T., Takeshita, R., Mayer, G.D., Schilkey, F., Griffitt, R.J., 2017. Crude oil impairs immune function and increases susceptibility to pathogenic bacteria in southern flounder. PLoS One 12, 1–21. https://doi.org/10.1371/journal.pone.0176559

Beaudoin, C.P., Tonn, W.M., Prepas, E.E., Wassenaar, L.I., 1999. Individual specialization and

trophic adaptability of northern pike (Esox lucius): An isotope and dietary analysis. Oecologia 120, 386–396. https://doi.org/10.1007/s004420050871

Bell, T.H., Yergeau, E., Martineau, C., Juck, D., Whyte, L.G., Greer, C.W., 2011. Identification of nitrogen-incorporating bacteria in petroleum-contaminated arctic soils by using [15N]DNA-based stable isotope probing and pyrosequencing. Appl. Environ. Microbiol. 77, 4163–4171. https://doi.org/10.1128/AEM.00172-11

Bercik, P., Collins, S.M., Verdu, E.F., 2012. Microbes and the gut-brain axis. Neurogastroenterol. Motil. 24, 405–413. https://doi.org/10.1111/j.1365-2982.2012.01906.x

Beyer, J., Jonsson, G., Porte, C., Krahn, M.M., Ariese, F., 2010. Analytical methods for determining metabolites of polycyclic aromatic hydrocarbon (PAH) pollutants in fish bile: A review. Environ. Toxicol. Pharmacol. 30, 224–244. https://doi.org/10.1016/j.etap.2010.08.004

Beyer, J., Trannum, H.C., Bakke, T., Hodson, P. V., Collier, T.K., 2016. Environmental effects of the Deepwater Horizon oil spill: A review. Mar. Pollut. Bull. 110, 28–51. https://doi.org/10.1016/j.marpolbul.2016.06.027

Blaga, A.C., 2013. The action of microorganisms from organic pollutants in water , air , soil. Curr. Top. concepts Res. priorities Environ. Chem.

Blazewicz, S.J., Barnard, R.L., Daly, R.A., Firestone, M.K., 2013. Evaluating rRNA as an indicator of microbial activity in environmental communities: Limitations and uses. ISME J. https://doi.org/10.1038/ismej.2013.102

Bo, J., Gopalakrishnan, S., Chen, F.-Y.Y., Wang, K.-J.J., 2014. Benzo[a]pyrene modulates the biotransformation, DNA damage and cortisol level of red sea bream challenged with lipopolysaccharide. Mar. Pollut. Bull. 85, 463–470. https://doi.org/10.1016/j.marpolbul.2014.05.023

Boelsterli, U.A., 2007. Mechanistic toxicology: the molecular basis of how chemicals disrupt biological targets. CRC Press.

Bokulich, N.A., Kaehler, B.D., Rideout, J.R., Dillon, M., Bolyen, E., Knight, R., Huttley, G.A., Gregory Caporaso, J., 2018. Optimizing taxonomic classification of marker-gene amplicon sequences with QIIME 2's q2-feature-classifier plugin. Microbiome 6. https://doi.org/10.1186/s40168-018-0470-z

Bokulich, N.A., Subramanian, S., Faith, J.J., Gevers, D., Gordon, J.I., Knight, R., Mills, D.A., Caporaso, J.G., 2013. Quality-filtering vastly improves diversity estimates from Illumina amplicon sequencing. Nat. Methods 10, 57–59. https://doi.org/10.1038/nmeth.2276

Bolger, T., Connolly, P.L., 1989. The selection of suitable indices for the measurement and analysis of fish condition. J. Fish Biol. 34, 171–182. https://doi.org/10.1111/j.1095-8649.1989.tb03300.x

Bolnick, D.I., Snowberg, L.K., Hirsch, P.E., Lauber, C.L., Org, E., Parks, B., Lusis, A.J., Knight, R., Caporaso, J.G., Svanbäck, R., 2014. Individual diet has sex-dependent effects on vertebrate gut microbiota. Nat. Commun. 5, 4500. https://doi.org/10.1038/ncomms5500

Bolyen, E., Rideout, J.R., Dillon, M.R., Bokulich, N.A., Abnet, C.C., Al-Ghalith, G.A., Alexander, H., Alm, E.J., Arumugam, M., Asnicar, F., Bai, Y., Bisanz, J.E., Bittinger, K., Brejnrod, A., Brislawn, C.J., Brown, C.T., Callahan, B.J., Caraballo-Rodríguez, A.M., Chase, J., Cope, E.K., Da Silva, R., Diener, C., Dorrestein, P.C., Douglas, G.M., Durall, D.M., Duvallet, C., Edwardson, C.F., Ernst, M., Estaki, M., Fouquier, J., Gauglitz, J.M., Gibbons, S.M., Gibson, D.L., Gonzalez, A., Gorlick, K., Guo, J., Hillmann, B., Holmes, S., Holste, H., Huttenhower, C., Huttley, G.A., Janssen, S., Jarmusch, A.K., Jiang, L., Kaehler, B.D., Kang, K. Bin, Keefe, C.R., Keim, P., Kelley, S.T., Knights, D., Koester, I., Kosciolek, T., Kreps, J., Langille, M.G.I., Lee, J., Ley, R., Liu, Y.X., Loftfield, E., Lozupone, C., Maher, M., Marotz, C., Martin, B.D., McDonald, D., McIver, L.J., Melnik, A. V., Metcalf, J.L., Morgan, S.C., Morton, J.T., Naimey, A.T., Navas-Molina, J.A., Nothias, L.F., Orchanian, S.B., Pearson, T., Peoples, S.L., Petras, D., Preuss, M.L., Pruesse, E., Rasmussen, L.B., Rivers, A., Robeson, M.S., Rosenthal, P., Segata, N., Shaffer, M., Shiffer,

A., Sinha, R., Song, S.J., Spear, J.R., Swafford, A.D., Thompson, L.R., Torres, P.J., Trinh, P., Tripathi, A., Turnbaugh, P.J., Ul-Hasan, S., van der Hooft, J.J.J., Vargas, F., Vázquez-Baeza, Y., Vogtmann, E., von Hippel, M., Walters, W., Wan, Y., Wang, M., Warren, J., Weber, K.C., Williamson, C.H.D., Willis, A.D., Xu, Z.Z., Zaneveld, J.R., Zhang, Y., Zhu, Q., Knight, R., Caporaso, J.G., Guerrini, C.J., Botkin, J.R., McGuire, A.L., 2019. Reproducible, interactive, scalable and extensible microbiome data science using QIIME 2. Nat. Biotechnol. 37, 850–852. https://doi.org/10.1038/s41587-019-0190-3

Booc, F., Thornton, C., Lister, A., Maclatchy, D., Willett, K.L., 2014. Benzo[a]pyrene Effects on Reproductive Endpoints in Fundulus heteroclitus. Toxicol. Sci. 140, 73–82. https://doi.org/10.1093/toxsci/kfu064

Borcard, D., Gillet, F., Legendre, P., 2011. Numerical Ecology with R. Springer New York, New York, NY. https://doi.org/10.1007/978-1-4419-7976-6_6

Boutin, S., Bernatchez, L., Audet, C., Derôme, N., 2013. Network Analysis Highlights Complex Interactions between Pathogen, Host and Commensal Microbiota. https://doi.org/10.1371/journal.pone.0084772

Bowsher, A.W., Kearns, P.J., Shade, A., 2019. 16S rRNA/rRNA Gene Ratios and Cell Activity Staining Reveal Consistent Patterns of Microbial Activity in Plant-Associated Soil. mSystems 4, 1–14. https://doi.org/10.1128/msystems.00003-19

Breton, J., Massart, S., Vandamme, P., De Brandt, E., Pot, B., Foligné, B., 2013. Ecotoxicology inside the gut: impact of heavy metals on the mouse microbiome. BMC Pharmacol. Toxicol. 14, 62. https://doi.org/10.1186/2050-6511-14-62

Bron, P.A., Van Baarlen, P., Kleerebezem, M., 2012. Emerging molecular insights into the interaction between probiotics and the host intestinal mucosa. Nat. Rev. Microbiol. https://doi.org/10.1038/nrmicro2690

Brown-Peterson, N.J., Krasnec, M.O., Lay, C.R., Morris, J.M., Griffitt, R.J., 2017. Responses of juvenile southern flounder exposed to Deepwater Horizon oil-contaminated sediments.

Environ. Toxicol. Chem. 36, 1067–1076. https://doi.org/10.1002/etc.3629

Buesen, R., Mock, M., Nau, H., Seidel, A., Jacob, J., Lampen, A., 2003. Human intestinal Caco-2 cells display active transport of benzo [a] pyrene metabolites 142, 201–221.

Buesen, R., Mock, M., Seidel, A., Jacob, J., Lampen, A., 2002. Interaction between Metabolism and Transport of Benzo[a]pyrene and Its Metabolites in Enterocytes Interaction between Metabolism and Transport of Benzo-[a]pyrene and Its Metabolites in Enterocytes. Toxicol. Appl. Pharmacol 183, 168–178. https://doi.org/10.1006/taap.2002.9484

Butt, R.L., Volkoff, H., Delgado, M.J., Wong, A.O.L., Kong, H., Pardesi, B., Volkoff, H., Butt, R.L., Volkoff, H., 2019. Gut Microbiota and Energy Homeostasis in Fish. Front. Endocrinol. (Lausanne). 10, 6–8. https://doi.org/10.3389/fendo.2019.00009

Callahan, B.J., McMurdie, P.J., Rosen, M.J., Han, A.W., Johnson, A.J.A., Holmes, S.P., 2016. DADA2: High-resolution sample inference from Illumina amplicon data. Nat. Methods 13, 581–583. https://doi.org/10.1038/nmeth.3869

Callero, M.A., Loaiza-Pérez, A.I., 2011. The Role of Aryl Hydrocarbon Receptor and Crosstalk with Estrogen Receptor in Response of Breast Cancer Cells to the Novel Antitumor Agents Benzothiazoles and Aminoflavone. Int. J. Breast Cancer 2011, 1–9. https://doi.org/10.4061/2011/923250

Campbell, B.J., Yu, L., Heidelberg, J.F., Kirchman, D.L., 2011. Activity of abundant and rare bacteria in a coastal ocean. Proc. Natl. Acad. Sci. U. S. A. 108, 12776–12781. https://doi.org/10.1073/pnas.1101405108

Caporaso, J.G., Kuczynski, J., Stombaugh, J., Bittinger, K., Bushman, F.D., Costello, E.K., Fierer, N., Pẽa, A.G., Goodrich, J.K., Gordon, J.I., Huttley, G.A., Kelley, S.T., Knights, D., Koenig, J.E., Ley, R.E., Lozupone, C.A., McDonald, D., Muegge, B.D., Pirrung, M., Reeder, J., Sevinsky, J.R., Turnbaugh, P.J., Walters, W.A., Widmann, J., Yatsunenko, T., Zaneveld, J., Knight, R., 2010. QIIME allows analysis of high-throughput community sequencing data. Nat. Methods. https://doi.org/10.1038/nmeth.f.303

Caporaso, J.G., Paszkiewicz, K., Field, D., Knight, R., Gilbert, J.A., 2012. The Western English Channel contains a persistent microbial seed bank. ISME J. 6, 1089–1093. https://doi.org/10.1038/ismej.2011.162

Carding, S., Verbeke, K., Vipond, D.T., Corfe, B.M., Owen, L.J., 2015. Dysbiosis of the gut microbiota in disease. Microb. Ecol. Health Dis. 26, 26191. https://doi.org/10.3402/mehd.v26.26191

Cario, E., 2005. Recent advances in basic science bacterial interactions with cells of the intestinal mucosa: toll- like receptors and nod2. Gut 54, 1182–1193. https://doi.org/10.1136/gut.2004.062794

Carlson, E.A., Li, Y., Zelikoff, J.. T., 2002. Exposure of Japanese medaka (Oryzias latipes) to benzo[a]pyrene suppresses immune function and host resistance against bacterial challenge, Aquatic Toxicology. Elsevier. https://doi.org/10.1016/S0166-445X(01)00223-5

Carlson, E.A., Li, Y., Zelikoff, J.T., 2004a. Benzo[a]pyrene-induced immunotoxicity in Japanese medaka (Oryzias latipes): Relationship between lymphoid CYP1A activity and humoral immune suppression. Toxicol. Appl. Pharmacol. 201, 40–52. https://doi.org/10.1016/j.taap.2004.04.018

Carlson, E.A., Li, Y., Zelikoff, J.T., 2004b. Suppressive effects of benzo[a]pyrene upon fish immune function: Evolutionarily conserved cellular mechanisms of immunotoxicity, in: Marine Environmental Research. pp. 731–734. https://doi.org/10.1016/j.marenvres.2004.03.023

Caspi, R., Billington, R., Fulcher, C.A., Keseler, I.M., Kothari, A., Krummenacker, M., Latendresse, M., Midford, P.E., Ong, Q., Ong, W.K., Paley, S., Subhraveti, P., Karp, P.D., 2017. The MetaCyc database of metabolic pathways and enzymes. Nucleic Acids Res. 46, 633–639. https://doi.org/10.1093/nar/gkx935

Cavalca, L., Guerrieri, N., Colombo, M., Pagani, S., Andreoni, V., 2007. Enzymatic and genetic profiles in environmental strains grown on polycyclic aromatic hydrocarbons. Antonie van

Leeuwenhoek, Int. J. Gen. Mol. Microbiol. 91, 315–325. https://doi.org/10.1007/s10482-006-9119-1

CCME (Canadian Council of Ministers of the Environment), 2010. Canadian Soil Quality Guidelines for Carcinogenic and Other Polycyclic Aromatic Hydrocarbons (Environmental and Human Health Effects), Scientific Criteria Document (revised).

Cebra, J.J., Periwal, S.B., Lee, G., Lee, F., Shroff, K.E., 1998. Lymphoid Tissue (GALT): The Roles of Enteric Bacteria and Viruses. Dev. Immunol. 6, 13–18.

Chaia, A.P., Zárate, G., Oliver, G., 1999. The probiotic properties of propionibacteria. Lait 79, 175–185. https://doi.org/10.1051/lait:1999114

Chang, W., Um, Y., Hoffman, B., Pulliam Holoman, T.R., Holoman, T.R.P., 2005. Molecular characterization of polycyclic aromatic hydrocarbon (PAH)-degrading methanogenic communities. Biotechnol. Prog. 21, 682–688. https://doi.org/10.1021/bp049579l

Chen, J., Wright, K., Davis, J.M., Jeraldo, P., Marietta, E. V, Murray, J., Nelson, H., Matteson, E.L., Taneja, V., 2016. An expansion of rare lineage intestinal microbes characterizes rheumatoid arthritis. https://doi.org/10.1186/s13073-016-0299-7

Chen, W., Liu, F., Ling, Z., Tong, X., Xiang, C., 2012. Human intestinal lumen and mucosa-associated microbiota in patients with colorectal cancer. PLoS One 7. https://doi.org/10.1371/journal.pone.0039743

Chi, L., Bian, X., Gao, B., Ru, H., Tu, P., Lu, K., 2016. Sex-Specific Effects of Arsenic Exposure on the Trajectory and Function of the Gut Microbiome. Chem. Res. Toxicol. 29, 949–951. https://doi.org/10.1021/acs.chemrestox.6b00066

Claisse, D., 1989. Chemical Contamination of French Coasts. Mar. Pollut. Bull. 20, 523–528.

Clarke, G., Sandhu, K. V, Griffin, B.T., Dinan, T.G., Cryan, J.F., Hyland, N.P., 2019. Gut reactions: Breaking down xenobiotic–microbiome interactions. Pharmacol. Rev. 71, 198–224. https://doi.org/10.1124/pr.118.015768

Claus, S.P., Guillou, H., Ellero-Simatos, S., 2016. The gut microbiota: a major player in the

toxicity of environmental pollutants? npj Biofilms Microbiomes 2, 16003. https://doi.org/10.1038/npjbiofilms.2016.3

Colston, T.J., Jackson, C.R., 2016. Microbiome evolution along divergent branches of the vertebrate tree of life: what is known and unknown. Mol. Ecol. 25, 3776–3800. https://doi.org/10.1111/mec.13730

Colwell, R.R., Grimes, D.J., 1984. Vibrio diseases of marine fish populations. Helgoländer Meeresuntersuchungen 37, 265–287. https://doi.org/10.1007/BF01989311

Corrales, J., Thornton, C., White, M., Willett, K.L., 2014. Multigenerational effects of benzo[a]pyrene exposure on survival and developmental deformities in zebrafish larvae. Aquat. Toxicol. 148, 16–26. https://doi.org/10.1016/j.aquatox.2013.12.028

Costa, J., Ferreira, M., Rey-Salgueiro, L., Reis-Henriques, M.A., 2011. Comparision of the waterborne and dietary routes of exposure on the effects of Benzo(a)pyrene on biotransformation pathways in Nile tilapia (Oreochromis niloticus). Chemosphere 84, 1452–1460. https://doi.org/10.1016/j.chemosphere.2011.04.046

Coyte, K.Z., Rakoff-Nahoum, S., 2019. Understanding Competition and Cooperation within the Mammalian Gut Microbiome. Curr. Biol. https://doi.org/10.1016/j.cub.2019.04.017

Cryan, J.F., Dinan, T.G., 2012. Mind-altering microorganisms: the impact of the gut microbiota on brain and behaviour. Nat. Rev. Neurosci. 13, 701–712. https://doi.org/10.1038/nrn3346

Cryan, J.F., O'Riordan, K.J., Cowan, C.S.M., Sandhu, K. V., Bastiaanssen, T.F.S., Boehme, M., Codagnone, M.G., Cussotto, S., Fulling, C., Golubeva, A. V., Guzzetta, K.E., Jaggar, M., Long-Smith, C.M., Lyte, J.M., Martin, J.A., Molinero-Perez, A., Moloney, G., Morelli, E., Morillas, E., O'Connor, R., Cruz-Pereira, J.S., Peterson, V.L., Rea, K., Ritz, N.L., Sherwin, E., Spichak, S., Teichman, E.M., van de Wouw, M., Ventura-Silva, A.P., Wallace-Fitzsimons, S.E., Hyland, N., Clarke, G., Dinan, T.G., 2019. The Microbiota-Gut-Brain Axis. Physiol. Rev. 99, 1877–2013. https://doi.org/10.1152/physrev.00018.2018

Czech, L., Barbera, P., Stamatakis, A., 2020. Genesis and Gappa: processing, analyzing and

visualizing phylogenetic (placement) data. Bioinformatics. https://doi.org/10.1093/bioinformatics/btaa070

Dalgaard, P., 2006. Introductory Statistics with R, in: Introductory Statistics with R. Springer. https://doi.org/10.1002/0471667196.ess7015.pub2

Danion, M., Deschamps, M.-H., Thomas-Guyon, H., Bado-Nilles, A., Le Floch, S., Quentel, C., Sire, J.-Y., 2011. Effect of an experimental oil spill on vertebral bone tissue quality in European sea bass (Dicentrarchus labrax L.). Ecotoxicol. Environ. Saf. 74, 1888–1895. https://doi.org/10.1016/J.ECOENV.2011.07.027

Davis, D.J., Hecht, P.M., Jasarevic, E., Beversdorf, D.Q., Will, M.J., Fritsche, K., Gillespie, C.H., 2017. Sex-specific effects of docosahexaenoic acid (DHA) on the microbiome and behavior of socially-isolated mice. Brain. Behav. Immun. 59, 38–48. https://doi.org/10.1016/j.bbi.2016.09.003

De Cáceres, M., Legendre, P., 2009. Associations between species and groups of sites: Indices and statistical inference. Ecology 90, 3566–3574. https://doi.org/10.1890/08-1823.1

De Vrieze, J., Regueiro, L., Props, R., Vilchez-Vargas, R., Jáuregui, R., Pieper, D.H., Lema, J.M., Carballa, M., Vilchez-Vargas, R., Jáuregui, R., Pieper, D.H., Lema, J.M., Carballa, M., Vilchez-Vargas, R., Jáuregui, R., Pieper, D.H., Lema, J.M., Carballa, M., 2016. Presence does not imply activity: DNA and RNA patterns differ in response to salt perturbation in anaerobic digestion. Biotechnol. Biofuels 9, 244. https://doi.org/10.1186/s13068-016-0652-5

DeBofsky, A., Xie, Y., Grimard, C., Alcaraz, J., Brinkmann, M., Hecker, M., Giesy, J.P., 2020. Differential responses of gut microbiota of male and female fathead minnow (Pimephales promelas) to a short-term environmentally-relevant, aqueous exposure to benzo[a]pyrene. https://doi.org/10.1016/j.chemosphere.2020.126461

DeBruyn, J.M., Hauther, K.A., 2017. Postmortem succession of gut microbial communities in deceased human subjects. PeerJ 5, e3437. https://doi.org/10.7717/peerj.3437

Decsi, T., Kennedy, K., 2011. Sex-specific differences in essential fatty acid metabolism. Am. J. Clin. Nutr. 94, 1914S-1919S. https://doi.org/10.3945/ajcn.110.000893

Defois, C., Ratel, J., Denis, S., Batut, B., Beugnot, R., Peyretaillade, E., Engel, E., Peyret, P., Poretsky, R.S., Nelson, W.C., Herbst, F.-A., Peyret, P., Defois, C., Ratel, J., Denis, S., Batut, B., Beugnot, R., Peyretaillade, E., Engel, E., 2017. Environmental pollutant Benzo[a]Pyrene impacts the volatile metabolome and transcriptome of the human gut microbiota. Front. Microbiol. 8, 1–12. https://doi.org/10.3389/fmicb.2017.01562

Derocles, S.A.P., Bohan, D.A., Dumbrell, A.J., Kitson, J.J., Massol, F., Pauvert, C., Plantegenest, M., Vacher, C., Evans, D.M., 2018. Biomonitoring for the 21st Century: Integrating Next-Generation Sequencing Into Ecological Network Analysis, in: Advances in Ecological Research. pp. 1–62. https://doi.org/10.1016/bs.aecr.2017.12.001

Desai, A.R., Links, M.G., Collins, S.A., Mansfield, G.S., Drew, M.D., Van Kessel, A.G., Hill, J.E., 2012. Effects of plant-based diets on the distal gut microbiome of rainbow trout (Oncorhynchus mykiss). Aquaculture 350–353, 134–142. https://doi.org/10.1016/j.aquaculture.2012.04.005

Dew, W.A., Hontela, A., Rood, S.B., Pyle, G.G., 2015. Biological effects and toxicity of diluted bitumen and its constituents in freshwater systems. J. Appl. Toxicol. https://doi.org/10.1002/jat.3196

Dietert, R.R., Silbergeld, E.K., 2015. Biomarkers for the 21st century: Listening to the microbiome. Toxicol. Sci. 144, 208–216. https://doi.org/10.1093/toxsci/kfv013

Dimitroglou, A., Merrifield, D.L., Carnevali, O., Picchietti, S., Avella, M., Daniels, C., Güroy, D., Davies, S.J., 2011. Microbial manipulations to improve fish health and production - A Mediterranean perspective. Fish Shellfish Immunol. https://doi.org/10.1016/j.fsi.2010.08.009

Dimitroglou, A., Merrifield, D.L., Moate, R., Davies, S.J., Spring, P., Sweetman, J., Bradley, G., 2009. Dietary mannan oligosaccharide supplementation modulates intestinal microbial

ecology and improves gut morphology of rainbow trout, Oncorhynchus mykiss (Walbaum). J. Anim. Sci. 87, 3226–3234. https://doi.org/10.2527/jas.2008-1428

Donald, D.B., Kooyman, A.H., 1977. Food, feeding habits, and growth of goldeye, Hiodon alosoides (Rafinesque), in waters of the Peace–Athabasca Delta. Can. J. Zool. 55, 1038–1047. https://doi.org/10.1139/z77-132

Douben, P.E.T., 2003. PAHs: An Ecotoxicological Perspective, PAHs: An Ecotoxicological Perspective. https://doi.org/10.1002/0470867132

Douglas, G.M., Maffei, V.J., Zaneveld, J., Yurgel, S.N., Brown, J.R., Taylor, C.M., Huttenhower, C., Langille, M.G.I., 2019. PICRUSt2: An improved and extensible approach for metagenome inference. bioRxiv 672295. https://doi.org/10.1101/672295

Edgar, R.C., 2010. Search and clustering orders of magnitude faster than BLAST. Bioinformatics 26, 2460–2461. https://doi.org/10.1093/bioinformatics/btq461

Eichler, S., Christen, R., Höltje, C., Westphal, P., Bötel, J., Brettar, I., Mehling, A., Höfle, M.G., 2006. Composition and Dynamics of Bacterial Communities of a Drinking Water Supply System as Assessed by RNA-and DNA-Based 16S rRNA Gene Fingerprinting. Appl. Environ. Microbiol. 72, 1858–1872. https://doi.org/10.1128/AEM.72.3.1858-1872.2006

Elmqvist, T., Folke, C., Nyström, M., Peterson, G., Bengtsson, J., Walker, B., Norberg, J., 2003. Response diversity, ecosystem change, and resilience. Front. Ecol. Environ. 1, 488–494. https://doi.org/10.1890/1540-9295(2003)001[0488:RDECAR]2.0.CO;2

Environment Canada, 2010. 2010 Pulp and Paper Environmental Effects Monitoring ( EEM ) Technical Guidance Document 481.

Escartín, E., Porte, C., 1999. Hydroxylated PAHs in bile of deep-sea fish. Relationship with xenobiotic metabolizing enzymes. Environ. Sci. Technol. 33, 2710–2714. https://doi.org/10.1021/es9902322

Evariste, L., Barret, M., Mottier, A., Mouchet, F., Gauthier, L., Pinelli, E., 2019. Gut microbiota of aquatic organisms: A key endpoint for ecotoxicological studies. Environ. Pollut. 248,

989–999.

Fadrosh, D.W., Ma, B., Gajer, P., Sengamalay, N., Ott, S., Brotman, R.M., Ravel, J., 2014. An improved dual-indexing approach for multiplexed 16S rRNA gene sequencing on the Illumina MiSeq platform, Microbiome. https://doi.org/10.1186/2049-2618-2-6

Fernandes, A.D., Macklaim, J.M., Linn, T.G., Reid, G., Gloor, G.B., 2013. ANOVA-Like Differential Expression (ALDEx) Analysis for Mixed Population RNA-Seq. PLoS One 8, 67019. https://doi.org/10.1371/journal.pone.0067019

Fernandes, A.D., Reid, J.N., Macklaim, J.M., Mcmurrough, T.A., Edgell, D.R., Gloor, G.B., 2014. Unifying the analysis of high-throughput sequencing datasets: characterizing RNA-seq, 16S rRNA gene sequencing and selective growth experiments by compositional data analysis.

Finucane, M.M., Sharpton, T.J., Laurent, T.J., Pollard, K.S., 2014. A Taxonomic Signature of Obesity in the Microbiome? Getting to the Guts of the Matter. PLoS One 9, 84689. https://doi.org/10.1371/journal.pone.0084689

Fitzpatrick, F.A., Boufadel, M.C., Johnson, R., Lee, K.W., Graan, T.P., Bejarano, A.C., Zhu, Z., Waterman, D., Capone, D.M., Hayter, E., Hamilton, S.K., Dekker, T., Garcia, M.H., Hassan, J.S., 2015. Oil-Particle Interactions and Submergence from Crude Oil Spills in Marine and Freshwater Environments： Review of the Science and Future Science Needs 33. https://doi.org/10.3133/ofr20151076

Forchielli, M.L., Walker, W.A., 2005. The role of gut-associated lymphoid tissues and mucosal defence. Br. J. Nutr. 93, S41. https://doi.org/10.1079/BJN20041356

Friedman, J., Alm, E.J., 2012. Inferring Correlation Networks from Genomic Survey Data. PLoS Comput Biol 8, 1002687. https://doi.org/10.1371/journal.pcbi.1002687

Galley, J.D., Nelson, M.C., Yu, Z., Dowd, S.E., Walter, J., Kumar, P.S., Lyte, M., Bailey, M.T., 2014. Exposure to a social stressor disrupts the community structure of the colonic mucosa-associated microbiota. BMC Microbiol. 14, 189. https://doi.org/10.1186/1471-2180-14-189

Galligan, C.L., Fish, E.N., 2015. Sex differences in the immune response, in: Sex and Gender Differences in Infection and Treatments for Infectious Diseases. Springer International Publishing, pp. 1–29. https://doi.org/10.1007/978-3-319-16438-0_1

Gao, X., Zhang, M., Xue, J., Huang, J., Zhuang, R., Zhou, X., Zhang, H., Fu, Q., Hao, Y., 2018. Body Mass Index Differences in the Gut Microbiota Are Gender Specific. Front. Microbiol. 9. https://doi.org/10.3389/fmicb.2018.01250

Garcia-Moreno, D., Galindo-Villegas, J., de Oliveira, S., Mulero, V., Meseguer, J., 2012. Regulation of immunity and disease resistance by commensal microbes and chromatin modifications during zebrafish development. Proc. Natl. Acad. Sci. 109, E2605–E2614. https://doi.org/10.1073/pnas.1209920109

Gaulke, C.A., Barton, C.L., Proffitt, S., Tanguay, R.L., Sharpton, T.J., 2016. Triclosan exposure is associated with rapid restructuring of the microbiome in adult zebrafish. PLoS One 11, 1–20. https://doi.org/10.1371/journal.pone.0154632

Gelboin, H. V., 1980. Benzo[alpha]pyrene metabolism, activation and carcinogenesis: role and regulation of mixed-function oxidases and related enzymes. Physiol. Rev. https://doi.org/10.1152/physrev.1980.60.4.1107

Ghanbari, M., Kneifel, W., Domig, K.J., 2015. A new view of the fish gut microbiome: Advances from next-generation sequencing. Aquaculture 448, 464–475. https://doi.org/10.1016/j.aquaculture.2015.06.033

Givens, C.E., Ransom, B., Bano, N., Hollibaugh, J.T., 2015. Comparison of the gut microbiomes of 12 bony fish and 3 shark species. Mar. Ecol. Prog. Ser. 518, 209–223. https://doi.org/10.3354/meps11034

Gloor, G.B., Macklaim, J.M., Fernandes, A.D., 2016. Displaying Variation in Large Datasets: Plotting a Visual Summary of Effect Sizes. J. Comput. Graph. Stat. 25, 971–979. https://doi.org/10.1080/10618600.2015.1131161

Gochfeld, M., 2017. Sex Differences in Human and Animal Toxicology: Toxicokinetics.

Toxicol. Pathol. 45, 172–189. https://doi.org/10.1177/0192623316677327

Goldstein, B., Gibson, J., Henderson, R., Hobbie, J., Landrigan, P., Mattison, D., Perera, F., Pfitzer, E., Silbergeld, E., Wogan, G., Thomas, R., Wagener, D., Peter, F., Wakefield, L., 1987. Biological Markers in Environmental. Environ. Health Perspect. 74, 3–9.

Gómez, G.D., Balcázar, J.L., 2008. A review on the interactions between gut microbiota and innate immunity of fish. FEMS Immunol. Med. Microbiol. https://doi.org/10.1111/j.1574-695X.2007.00343.x

Goyal, A., Yeh, A., Bush, B.R., Firek, B.A., Siebold, L.M., Rogers, M.B., Kufen, A.D., Morowitz, M.J., 2018. Safety, Clinical Response, and Microbiome Findings Following Fecal Microbiota Transplant in Children With Inflammatory Bowel Disease. Inflamm. Bowel Dis. 24, 410–421. https://doi.org/10.1093/ibd/izx035

Graspeuntner, S., Loeper, N., Künzel, S., Baines, J.F., Rupp, J., 2018. Selection of validated hypervariable regions is crucial in 16S-based microbiota studies of the female genital tract. Sci. Rep. 8, 1–7. https://doi.org/10.1038/s41598-018-27757-8

Greyson-Gaito, C.J., Bartley, T.J., Cottenie, K., Jarvis, W.M.C., Newman, A.E.M., Stothart, M.R., 2020. Into the wild: Microbiome transplant studies need broader ecological reality. Proc. R. Soc. B Biol. Sci. 287. https://doi.org/10.1098/rspb.2019.2834

Groschwitz, K.R., Hogan, S.P., 2009. Intestinal barrier function: molecular regulation and disease pathogenesis. J. Allergy Clin. Immunol. 124, 3–20; quiz 21–2. https://doi.org/10.1016/j.jaci.2009.05.038

Haiser, H.J., Turnbaugh, P.J., 2013. Developing a metagenomic view of xenobiotic metabolism. Pharmacol. Res. 69, 21–31. https://doi.org/10.1016/j.phrs.2012.07.009

Harvie, E.A., Huttenlocher, A., 2015. Neutrophils in host defense: new insights from zebrafish. J. Leukoc. Biol. 98, 523–537. https://doi.org/10.1189/jlb.4mr1114-524r

Hazen, T.C., Dubinsky, E.A., DeSantis, T.Z., Andersen, G.L., Piceno, Y.M., Singh, N., Jansson, J.K., Probst, A., Borglin, S.E., Fortney, J.L., Stringfellow, W.T., Bill, M., Conrad, M.E.,

Tom, L.M., Chavarria, K.L., Alusi, T.R., Lamendella, R., Joyner, D.C., Spier, C., Baelum, J., Auer, M., Zemla, M.L., Chakraborty, R., Sonnenthal, E.L., D'haeseleer, P., Holman, H.-Y.N., Osman, S., Lu, Z., Van Nostrand, J.D., Deng, Y.Y., Zhou, J., Mason, O.U., 2010. Deep-Sea Oil Plume Enriches Indigenous Oil-Degrading Bacteria. Science. 330, 204–208. https://doi.org/10.1126/science.1195979

He, X., Qi, Z., Hou, H., Qian, L., Gao, J., Zhang, X.X., 2020. Structural and functional alterations of gut microbiome in mice induced by chronic cadmium exposure. Chemosphere 246. https://doi.org/10.1016/j.chemosphere.2019.125747

Hicken, C.E., Linbo, T.L., Baldwin, D.H., Willis, M.L., Myers, M.S., Holland, L., Larsen, M., Stekoll, M.S., Rice, S.D., Collier, T.K., Scholz, N.L., Incardona, J.P., 2011. Sublethal exposure to crude oil during embryonic development alters cardiac morphology and reduces aerobic capacity in adult fish. Proc. Natl. Acad. Sci. U. S. A. 108, 7086–7090. https://doi.org/10.1073/pnas.1019031108

Hiippala, K., Jouhten, H., Ronkainen, A., Hartikainen, A., Kainulainen, V., Jalanka, J., Satokari, R., 2018. The potential of gut commensals in reinforcing intestinal barrier function and alleviating inflammation. Nutrients 10. https://doi.org/10.3390/nu10080988

Ho, Y., Jackson, M., Yang, Y., Mueller, J.G., Pritchard, P.H., 2000. Characterization of fluoranthene-and pyrene-degrading bacteria isolated from PAH-contaminated soils and sediments, Journal of Industrial Microbiology & Biotechnology.

Hoffmann, J.L., Oris, J.T., 2006. Altered gene expression: A mechanism for reproductive toxicity in zebrafish exposed to benzo[a]pyrene. Aquat. Toxicol. 78, 332–340. https://doi.org/10.1016/j.aquatox.2006.04.007

Hol, W.H.G., de Boer, W., Termorshuizen, A.J., Meyer, K.M., Schneider, J.H.M., van Dam, N.M., van Veen, J.A., van der Putten, W.H., 2010. Reduction of rare soil microbes modifies plant-herbivore interactions. Ecol. Lett. 13, 292–301. https://doi.org/10.1111/j.1461-0248.2009.01424.x

Hoseinifar, S.H., Esteban, M.Á., Cuesta, A., Sun, Y., Hossein Hoseinifar, S., Ángeles Esteban, M., Cuesta, A., Sun, Y., 2015. Prebiotics and Fish Immune Response: A Review of Current Knowledge and Future Perspectives. Rev. Fish. Sci. Aquac. 23, 315–328. https://doi.org/10.1080/23308249.2015.1052365

Hunt, D.E., Ward, C.S., 2015. A network-based approach to disturbance transmission through microbial interactions. Front. Microbiol. 6, 1182. https://doi.org/10.3389/fmicb.2015.01182

Ikeda-Ohtsubo, W., Brugman, S., Warden, C.H., Rebel, J.M.J., Folkerts, G., Pieterse, C.M.J., 2018. How Can We Define "Optimal Microbiota?": A Comparative Review of Structure and Functions of Microbiota of Animals, Fish, and Plants in Agriculture. Front. Nutr. https://doi.org/10.3389/fnut.2018.00090

İnceoğlu, Ö., Llirós, M., Crowe, S.A., García-Armisen, T., Morana, C., Darchambeau, F., Borges, A. V, Descy, J.P., Servais, P., 2015. Vertical Distribution of Functional Potential and Active Microbial Communities in Meromictic Lake Kivu. Microb. Ecol. 70, 596–611. https://doi.org/10.1007/s00248-015-0612-9

Inkinen, J., Jayaprakash, B., Santo Domingo, J.W.W., Keinänen-Toivola, M.M.M., Ryu, H., Pitkänen, T., 2016. Diversity of ribosomal 16S DNA- and RNA-based bacterial community in an office building drinking water system. J. Appl. Microbiol. 120, 1723–1738. https://doi.org/10.1111/jam.13144

Irwin, R.J., 1997. Environmental Contaminants Encyclopedia Copper Entry. Environ. Contam. Encycl.

Jacques, R.J.S., Okeke, B.C., Bento, F.M., Peralba, M.C.R., Camargo, F.A.O., 2007. Characterization of a polycyclic aromatic hydrocarbon-degrading microbial consortium from a petrochemical sludge landfarming site. Bioremediat. J. 11, 1–11. https://doi.org/10.1080/10889860601185822

Jašarević, E., Morrison, K.E., Bale, T.L., 2016a. Sex differences in the gut microbiome - Brain axis across the lifespan. Philos. Trans. R. Soc. B Biol. Sci.

https://doi.org/10.1098/rstb.2015.0122

Jašarević, E., Morrison, K.E., Bale, T.L., 2016b. Sex differences in the gut microbiome - Brain axis across the lifespan. Philos. Trans. R. Soc. B Biol. Sci. https://doi.org/10.1098/rstb.2015.0122

Jin, C., Luo, T., Zhu, Z., Pan, Z., Yang, J., Wang, W., Fu, Z., Jin, Y., 2017. Imazalil exposure induces gut microbiota dysbiosis and hepatic metabolism disorder in zebrafish. https://doi.org/10.1016/j.cbpc.2017.08.007

Jones, S.E., Lennon, J.T., Kellogg, W.K., 2010. Dormancy contributes to the maintenance of microbial diversity. PNAS 107, 5881–5886. https://doi.org/10.1073/pnas.0912765107

Jousset, A., Bienhold, C., Chatzinotas, A., Gallien, L., Gobet, A., Kurm, V., Küsel, K., Rillig, M.C., Rivett, D.W., Salles, J.F., Van Der Heijden, M.G.A., Youssef, N.H., Zhang, X., Wei, Z., Hol, G.W.H., 2017. Where less may be more: How the rare biosphere pulls ecosystems strings. ISME J. https://doi.org/10.1038/ismej.2016.174

Juhasz, A.L., Naidu, R., 2000. Bioremediation of high molecular weight polycyclic aromatic hydrocarbons: A review of the microbial degradation of benzo[a]pyrene, International Biodeterioration and Biodegradation. Elsevier. https://doi.org/10.1016/S0964-8305(00)00052-4

Kanehisa, M., Sato, Y., Kawashima, M., Furumichi, M., Tanabe, M., 2015. KEGG as a reference resource for gene and protein annotation. Nucleic Acids Res. 44, 457–462. https://doi.org/10.1093/nar/gkv1070

Kanther, M., Tomkovich, S., Xiaolun, S., Grosser, M.R., Koo, J., Flynn, E.J., Jobin, C., Rawls, J.F., 2014. Commensal microbiota stimulate systemic neutrophil migration through induction of Serum amyloid A. Cell. Microbiol. 16, 1053–1067. https://doi.org/10.1111/cmi.12257

Karami, A., Christianus, A., Ishak, Z., Shamsuddin, Z.H., Masoumian, M., Courtenay, S.C., Hj Shamsuddin, Z., Masoumian, M., Courtenay, S.C., 2012. Use of intestinal Pseudomonas

aeruginosa in fish to detect the environmental pollutant benzo[a]pyrene. J. Hazard. Mater. 215–216, 108–114. https://doi.org/10.1016/j.jhazmat.2012.02.038

Karimi, B., Maron, P.A., Chemidlin-Prevost Boure, N., Bernard, N., Gilbert, D., Ranjard, L., 2017. Microbial diversity and ecological networks as indicators of environmental quality. Environ. Chem. Lett. https://doi.org/10.1007/s10311-017-0614-6

Karimi, B., Meyer, C., Gilbert, D., Bernard, N., 2016. Air pollution below WHO levels decreases by 40 % the links of terrestrial microbial networks. Environ. Chem. Lett. 14, 467–475. https://doi.org/10.1007/s10311-016-0589-8

Kelly, C., Salinas, I., 2017. Under Pressure: Interactions between Commensal Microbiota and the Teleost Immune System. Front. Immunol. 8, 1–9. https://doi.org/10.3389/fimmu.2017.00559

Kelly, C.R., Kahn, S., Kashyap, P., Laine, L., Rubin, D., Atreja, A., Moore, T., Wu, G., 2015. Update on Fecal Microbiota Transplantation 2015: Indications, Methodologies, Mechanisms, and Outlook. Gastroenterology 149, 223–237. https://doi.org/10.1053/j.gastro.2015.05.008

Klindworth, A., Pruesse, E., Schweer, T., Peplies, J., Quast, C., Horn, M., Glöckner, F.O., 2013. Evaluation of general 16S ribosomal RNA gene PCR primers for classical and next-generation sequencing-based diversity studies. Nucleic Acids Res. 41. https://doi.org/10.1093/nar/gks808

Klünemann, M., Schmid, M., Patil, K.R., Klü, M., Schmid, M., Patil, K.R., 2014. Computational tools for modeling xenometabolism of the human gut microbiota, Trends in Biotechnology. https://doi.org/10.1016/j.tibtech.2014.01.005

Knutzen, J., Sortland, B., 1982. Polycyclic aromatic hydrocarbons (PAH) in some algae and invertebrates from moderately polluted parts of the coast of Norway. Water Res. 16, 421–428. https://doi.org/10.1016/0043-1354(82)90166-X

Koontz, J.M., Dancy, B.C.R., Horton, C.L., Stallings, J.D., DiVito, V.T., Lewis, J.A., 2019. The

Role of the Human Microbiome in Chemical Toxicity. Int. J. Toxicol. https://doi.org/10.1177/1091581819849833

Korecka, A., Dona, A., Lahiri, S., Tett, A.J., Al-Asmakh, M., Braniste, V., D'Arienzo, R., Abbaspour, A., Reichardt, N., Fujii-Kuriyama, Y., Rafter, J., Narbad, A., Holmes, E., Nicholson, J., Arulampalam, V., Pettersson, S., 2016. Bidirectional communication between the Aryl hydrocarbon Receptor (AhR) and the microbiome tunes host metabolism. npj Biofilms Microbiomes 2, 16014. https://doi.org/10.1038/npjbiofilms.2016.14

Kurtz, Z.D., Müller, C.L., Miraldi, E.R., Littman, D.R., Blaser, M.J., Bonneau, R.A., 2015. Sparse and Compositionally Robust Inference of Microbial Ecological Networks. PLoS Comput. Biol. 11. https://doi.org/10.1371/journal.pcbi.1004226

Laurie, A.D., Lloyd-Jones, G., 2000. Quantification of phnAc and nahAc in contaminated new zealand soils by competitive PCR. Appl. Environ. Microbiol. 66, 1814–7.

Lederberg, J., McCray, A.T., 2001. `Ome Sweet `Omics--A Genealogical Treasury of Words. Sci. 15, 8.

Lefever, D.E., Xu, J., Chen, Y., Huang, G., Tamas, N., Guo, T.L., 2016. TCDD modulation of gut microbiome correlated with liver and immune toxicity in streptozotocin (STZ)-induced hyperglycemic mice. Toxicol. Appl. Pharmacol. 304, 48–58. https://doi.org/10.1016/j.taap.2016.05.016

Levy, M., Blacher, E., Elinav, E., 2017. Microbiome, metabolites and host immunity. Curr. Opin. Microbiol. https://doi.org/10.1016/j.mib.2016.10.003

Li, T., Long, M., Ji, C., Shen, Z., Gatesoupe, F.-J., Zhang, X., Zhang, Q., Zhang, L., Zhao, Y., Liu, X., Li, A., 2016. Alterations of the gut microbiome of largemouth bronze gudgeon (Coreius guichenoti) suffering from furunculosis. Sci. Rep. 6, 30606. https://doi.org/10.1038/srep30606

Li, X., Yan, Q., Xie, S., Hu, W., Yu, Y., 2013. Gut Microbiota Contributes to the Growth of Fast-Growing Transgenic Common Carp (Cyprinus carpio L.). PLoS One 8, 64577.

https://doi.org/10.1371/journal.pone.0064577

Liang, X., Feswick, A., Simmons, D., Martyniuk, C.J., 2017. Reprint of: Environmental toxicology and omics: A question of sex. https://doi.org/10.1016/j.jprot.2018.03.018

Liu, H., Guo, X., Gooneratne, R., Lai, R., Zeng, C., Zhan, F., Wang, W., 2016. The gut microbiome and degradation enzyme activity of wild freshwater fishes influenced by their trophic levels. Sci. Rep. 6. https://doi.org/10.1038/srep24340

Llewellyn, M.S., Boutin, S., Hoseinifar, S.H., Derome, N., 2014. Teleost microbiomes: the state of the art in their characterization, manipulation and importance in aquaculture and fisheries. Front. Microbiol. 5, 207. https://doi.org/10.3389/fmicb.2014.00207

Lloyd, N.A., Janssen, S.E., Reinfelder, J.R., Barkay, T., 2016. Co-selection of Mercury and Multiple Antibiotic Resistances in Bacteria Exposed to Mercury in the Fundulus heteroclitus Gut Microbiome. Curr. Microbiol. 73, 834–842. https://doi.org/10.1007/s00284-016-1133-6

Loch, T.P., Faisal, M., 2015. Emerging flavobacterial infections in fish: A review. J. Adv. Res. 6, 283–300. https://doi.org/10.1016/j.jare.2014.10.009

Lozano, V.L., Defarge, N., Rocque, L.M., Mesnage, R., Hennequin, D., Cassier, R., de Vendômois, J.S., Panoff, J.M., Séralini, G.E., Amiel, C., 2018. Sex-dependent impact of Roundup on the rat gut microbiome. Toxicol. Reports 5, 96–107. https://doi.org/10.1016/j.toxrep.2017.12.005

Lozupone, C., Knight, R., 2005. UniFrac: a new phylogenetic method for comparing microbial communities. Appl. Environ. Microbiol. 71, 8228–35. https://doi.org/10.1128/AEM.71.12.8228-8235.2005

Lozupone, C.A., Li, M., Campbell, T.B., Flores, S.C., Linderman, D., Gebert, M.J., Knight, R., Fontenot, A.P., Palmer, B.E., 2013. Alterations in the gut microbiota associated with HIV-1 infection. Cell Host Microbe 14, 329–339. https://doi.org/10.1016/j.chom.2013.08.006

Lu, K., Abo, R.P., Schlieper, K.A., Graffam, M.E., Levine, S., Wishnok, J.S., Swenberg, J.A.,

Tannenbaum, S.R., Fox, J.G., 2014. Arsenic exposure perturbs the gut microbiome and its metabolic profile in mice: An integrated metagenomics and metabolomics analysis. Environ. Health Perspect. 122, 284–291. https://doi.org/10.1289/ehp.1307429

Lu, K., Mahbub, R., Fox, J.G., 2015. Xenobiotics: Interaction with the intestinal microflora. ILAR J. 56, 218–227. https://doi.org/10.1093/ilar/ilv018

Lyte, M., 2013. Microbial Endocrinology in the Microbiome-Gut-Brain Axis: How Bacterial Production and Utilization of Neurochemicals Influence Behavior. PLoS Pathog. 9, 9–11. https://doi.org/10.1371/journal.ppat.1003726

Ma, L., Xie, Y., Han, Z., Giesy, J.P., Zhang, X., 2017. Responses of earthworms and microbial communities in their guts to Triclosan. Chemosphere 168, 1194–1202. https://doi.org/10.1016/j.chemosphere.2016.10.079

Ma, M., 2005. Species richness vs evenness: Independent relationship and different responses to edaphic factors. Oikos 111, 192–198. https://doi.org/10.1111/j.0030-1299.2005.13049.x

Macpherson, A.J., Harris, N.L., 2004. Opinion: Interactions between commensal intestinal bacteria and the immune system. Nat. Rev. Immunol. 4, 478–485. https://doi.org/10.1038/nri1373

Malins, D.C., McCain, B.B., Brown, D.W., Varanasi, U., Krahn, M.M., Myers, M.S., Chan, S.L., 1987. Sediment-associated contaminants and liver diseases in bottom-dwelling fish. Hydrobiologia 149, 67–74. https://doi.org/10.1007/BF00048647

Markle, J.G.M.M., Frank, D.N., Mortin-Toth, S., Robertson, C.E., Feazel, L.M., Rolle-Kampczyk, U., Von Bergen, M., Mccoy, K.D., Macpherson, A.J., Danska, J.S., 2013. Sex differences in the gut microbiome drive hormone-dependent regulation of autoimmunity. Science (80-. ). 339, 1084–1088. https://doi.org/10.1126/science.1233521

Martinez Arbizu, P., 2019. pairwiseAdonis: Pairwise multilevel comparison using adonis. R package version 0.3.

Maslowski, K.M., Vieira, A.T., Ng, A., Kranich, J., Sierro, F., Yu, D., Schilter, H.C., Rolph,

M.S., Mackay, F., Artis, D., Xavier, R.J., Teixeira, M.M., Mackay, C.R., 2009. Regulation of inflammatory responses by gut microbiota and chemoattractant receptor GPR43. Nature 461, 1282–1286. https://doi.org/10.1038/nature08530

Mccarthy, J.F., Burrus, L.W., Tolbert, V.R., 2003. Bioaccumulation of Benzo(a)pyrene from Sediment by Fathead Minnows: Effects of Organic Content, Resuspension and Metabolism Environmental Contamination a n d Toxicology. Arch. Environ. Contam. Toxicol 45, 364–370. https://doi.org/10.1007/s00244-003-2148-0

McMurdie, P.J., Holmes, S., 2013. Phyloseq: An R Package for Reproducible Interactive Analysis and Graphics of Microbiome Census Data. PLoS One 8, e61217. https://doi.org/10.1371/journal.pone.0061217

Meinicke, P., 2015. UProC: tools for ultra-fast protein domain classification. Bioinformatics 31, 1382–1388. https://doi.org/10.1093/bioinformatics/btu843

Meinshausen, N., Bühlmann, P., 2006. High-dimensional graphs and variable selection with the Lasso. Ann. Stat. 34, 1436–1462. https://doi.org/10.1214/009053606000000281

Milani, D., Grapentine, L., Burniston, D.A., Graham, M., Marvin, C., 2017. Trends in sediment quality in Hamilton Harbour, Lake Ontario. Aquat. Ecosyst. Heal. Manag. 20, 295–307. https://doi.org/10.1080/14634988.2017.1302780

Miller, K.P., Ramos, K.S., 2001. Impact of cellular metabolism on the biological effects of benzo[a]pyrene and related hydrocarbons. Drug Metab. Rev. 33, 1–35. https://doi.org/10.1081/DMR-100000138

Montalto, M., D ’onofrio, F., Gallo, A., Cazzato, A., Gasbarrini, G., 2009. Intestinal microbiota and its functions. Dig. Liver Dis. Suppl. 3, 30–34. https://doi.org/10.1016/S1594-5804(09)60016-4

Montassier, E., Al-Ghalith, G.A., Ward, T., Corvec, S., Gastinne, T., Potel, G., Moreau, P., de la Cochetiere, M.F., Batard, E., Knights, D., 2016. Pretreatment gut microbiome predicts chemotherapy-related bloodstream infection. Genome Med. 8, 49.

https://doi.org/10.1186/s13073-016-0301-4

Nacci, D.E., Kohan, M., Pelletier, M., George, E., 2002. Effects of benzo[a]pyrene exposure on a fish population resistant to the toxic effects of dioxin-like compounds, Aquatic Toxicology.

Narrowe, A.B., Albuthi-Lantz, M., Smith, E.P., Bower, K.J., Roane, T.M., Vajda, A.M., Miller, C.S., 2015. Perturbation and restoration of the fathead minnow gut microbiome after low-level triclosan exposure. Microbiome 3, 6. https://doi.org/10.1186/s40168-015-0069-6

Navarrete, P., Magne, F., Araneda, C., Fuentes, P., Barros, L., 2012. PCR-TTGE Analysis of 16S rRNA from Rainbow Trout (Oncorhynchus mykiss) Gut Microbiota Reveals Host-Specific Communities of Active Bacteria. PLoS One 7, 31335. https://doi.org/10.1371/journal.pone.0031335

Neff, J.M., Stout, S.A., Gunster, D.G., 2005. Ecological risk assessment of polycyclic aromatic hydrocarbons in sediments: identifying sources and ecological hazard. Integr. Environ. Assess. Manag. 1, 22–33. https://doi.org/10.1897/IEAM_2004a-016.1

Neuman, H., Debelius, J.W., Knight, R., Koren, O., 2015. Microbial endocrinology: the interplay between the microbiota and the endocrine system. FEMS Microbiol. Rev. 39, 509–521. https://doi.org/10.1093/femsre/fuu010

Nichols, J.W., McKim, J.M., Lien, G.J., Hoffman, A.D., Bertelsen, S.L., Elonen, C.M., 1996. A physiologically based toxicokinetic model for dermal absorption of organic chemicals by fish. Fundam. Appl. Toxicol. 31, 229–242. https://doi.org/10.1006/faat.1996.0095

Nierman, W.C., Feldblyum, T. V, Laub, M.T., Paulsen, I.T., Nelson, K.E., Eisen, J., Heidelberg, J.F., Alley, M.R.K., Ohta, N., Maddock, J.R., Potocka, I., Nelson, W.C., Newton, A., Stephens, C., Phadke, N.D., Ely, B., DeBoy, R.T., Dodson, R.J., Durkin, A.S., Gwinn, M.L., Haft, D.H., Kolonay, J.F., Smit, J., Craven, M.B., Khouri, H., Shetty, J., Berry, K., Utterback, T., Tran, K., Wolf, A., Vamathevan, J., Ermolaeva, M., White, O., Salzberg, S.L., Venter, J.C., Shapiro, L., Fraser, C.M., 2001. Complete genome sequence of Caulobacter crescentus. Proc. Natl. Acad. Sci. U. S. A. 98, 4136–4141.

https://doi.org/10.1073/pnas.061029298

Nishimoto, M., Yanagida, G.K., Stein, J.E., Baird, W.M., Varanasi, U., 1992. The metabolism of benzo(a)pyrene by english sole (parophrys vetulus): Comparison between isolated hepatocytes in vitro and liver in vivo. Xenobiotica 22, 949–961. https://doi.org/10.3109/00498259209049901

O'Hara, A.M., Shanahan, F., 2006. The gut flora as a forgotten organ. EMBO Rep. 7, 688–693. https://doi.org/10.1038/sj.embor.7400731

Ohiozebau, E., Tendler, B., Codling, G., Kelly, E., Giesy, J.P., Jones, P.D., 2017. Potential health risks posed by polycyclic aromatic hydrocarbons in muscle tissues of fishes from the Athabasca and Slave Rivers, Canada. Environ. Geochem. Health 39, 139–160. https://doi.org/10.1007/s10653-016-9815-3

Ohiozebau, E., Tendler, B., Hill, A., Codling, G., Kelly, E., Giesy, J.P., Jones, P.D., 2016. Products of biotransformation of polycyclic aromatic hydrocarbons in fishes of the Athabasca/Slave river system, Canada. Environ. Geochem. Health 38, 577–591. https://doi.org/10.1007/s10653-015-9744-6

Oksanen, J., Blanchet, F.G., Friendly, M., Kindt, R., Legendre, P., McGlinn, D., Minchin, P.R., O'Hara, R.B., Simpson, G.L., Solymos, P., Stevens, M.H.H., Szoecs, E., Wagner, H., 2019. vegan: Community Ecology Package.

Olsen, M.A., Aagnes, T.H., Sørmo, W., Mathiesen, S.D., 1996. Chitinolytic bacteria in the minke whale forestomach. Anim. Res. 45, 287. https://doi.org/10.1139/w99-112

Oren, A., 2014. The family Xanthobacteraceae, in: The Prokaryotes: Alphaproteobacteria and Betaproteobacteria. pp. 709–726. https://doi.org/10.1007/978-3-642-30197-1_258

Org, E., Mehrabian, M., Parks, B.W., Shipkova, P., Liu, X., Drake, T.A., Lusis, A.J., 2016. Sex differences and hormonal effects on gut microbiota composition in mice. Gut Microbes 7, 313–322. https://doi.org/10.1080/19490976.2016.1203502

Ortiz-Delgado, J.B., Segner, H., Arellano, J.M., Sarasquete, C., 2007. Histopathological

alterations, EROD activity, CYP1A protein and biliary metabolites in gilthead seabream Sparus aurata exposed to Benzo(a)pyrene. Histol. Histopathol. 22, 417–432. https://doi.org/10.14670/HH-22.417

Osman, M.-A., Neoh, H., Ab Mutalib, N.-S., Chin, S.-F., Jamal, R., 2018. 16S rRNA Gene Sequencing for Deciphering the Colorectal Cancer Gut Microbiome: Current Protocols and Workflows. Front. Microbiol. 9, 767. https://doi.org/10.3389/fmicb.2018.00767

Parks, D.H., Tyson, G.W., Hugenholtz, P., Beiko, R.G., 2014. Genome analysis STAMP: statistical analysis of taxonomic and functional profiles 30, 3123–3124. https://doi.org/10.1093/bioinformatics/btu494

Penders, J., Thijs, C., Vink, C., Stelma, F.F., Snijders, B., Kummeling, I., van den Brandt, P.A., Stobberingh, E.E., 2006. Factors Influencing the Composition of the Intestinal Microbiota in Early Infancy. Pediatrics 118, 511–521. https://doi.org/10.1542/peds.2005-2824

Perez-Muñoz, M.E., Arrieta, M.C., Ramer-Tait, A.E., Walter, J., 2017. A critical assessment of the "sterile womb" and "in utero colonization" hypotheses: Implications for research on the pioneer infant microbiome. Microbiome 5, 1–19. https://doi.org/10.1186/s40168-017-0268-4

Pérez, T., Balcázar, J.L., Ruiz-Zarzuela, I., Halaihel, N., Vendrell, D., De Blas, I., Múzquiz, J.L., Múezquiz, J.L., 2010. Host–microbiota interactions within the fish intestinal ecosystem. Mucosal Immunol. 3, 355–360. https://doi.org/10.1038/mi.2010.12

Phalen, L.J., Köllner, B., Leclair, L.A., Hogan, N.S., Van Den Heuvel, M.R., 2014. The effects of benzo[a]pyrene on leucocyte distribution and antibody response in rainbow trout (Oncorhynchus mykiss). Aquat. Toxicol. 147, 121–128. https://doi.org/10.1016/j.aquatox.2013.12.017

Phelps, D., Brinkman, N.E., Keely, S.P., Anneken, E.M., Catron, T.R., Betancourt, D., Wood, C.E., Espenschied, S.T., Rawls, J.F., Tal, T., 2017. Microbial colonization is required for normal neurobehavioral development in zebrafish. Sci. Rep. 7.

https://doi.org/10.1038/s41598-017-10517-5

Power, M.E., Tilman, D., Estes, J.A., Menge, B.A., Bond, W.J., Mills, L.S., Daily, G., Castilla, J.C., Lubchenco, J., Paine, R.T., 1996. Challenges in the Quest for Keystones. Bioscience 46, 609–620. https://doi.org/10.2307/1312990

Quast, C., Pruesse, E., Yilmaz, P., Gerken, J., Schweer, T., Yarza, P., Peplies, J., Glöckner, F.O., 2013. The SILVA ribosomal RNA gene database project: Improved data processing and web-based tools. Nucleic Acids Res. 41, 590–596. https://doi.org/10.1093/nar/gks1219

R Core Team, 2013. R: A Language and Environment for Statistical Computing.

Rawls, J.F., Samuel, B.S., Gordon, J.I., 2004. From The Cover: Gnotobiotic zebrafish reveal evolutionarily conserved responses to the gut microbiota. Proc. Natl. Acad. Sci. 101, 4596–4601. https://doi.org/10.1073/pnas.0400706101

Revetta, R.P., Matlib, R.S., Santo Domingo, J.W., 2011. 16S rRNA gene sequence analysis of drinking water using RNA and DNA extracts as targets for clone library development. Curr. Microbiol. 63, 50–59. https://doi.org/10.1007/s00284-011-9938-9

Reynaud, S., Deschaux, P., 2006. The effects of polycyclic aromatic hydrocarbons on the immune system of fish: A review, Aquatic Toxicology. Elsevier.

Ribière, C., Peyret, P., Parisot, N., Darcha, C., Déchelotte, P.J., Barnich, N., Peyretaillade, E., Boucher, D., 2016. Oral exposure to environmental pollutant benzo[a]pyrene impacts the intestinal epithelium and induces gut microbial shifts in murine model. Sci. Rep. 6, 1–11. https://doi.org/10.1038/srep31027

Ringø, E., Zhou, Z., Olsen, R.E., Song, S.K., 2012. Use of chitin and krill in aquaculture - the effect on gut microbiota and the immune system: A review. Aquac. Nutr. 18, 117–131. https://doi.org/10.1111/j.1365-2095.2011.00919.x

Ringø, E., Zhou, Z., Vecino, J.L.G.L.G., Wadsworth, S., Romero, J., Krogdahl, Olsen, R.E.E., Dimitroglou, A., Foey, A., Davies, S., Owen, M., Lauzon, H.L.L., Martinsen, L.L.L., De Schryver, P., Bossier, P., Sperstad, S., Merrifield, D.L.L., 2016. Effect of dietary

components on the gut microbiota of aquatic animals. A never-ending story? Aquac. Nutr. 22, 219–282. https://doi.org/10.1111/anu.12346

Roeselers, G., Mittge, E.K., Stephens, W.Z., Parichy, D.M., Cavanaugh, C.M., Guillemin, K., Rawls, J.F., 2011. Evidence for a core gut microbiota in the zebrafish. ISME J. 5, 1595–1608. https://doi.org/10.1038/ismej.2011.38

Rolig, A.S., Parthasarathy, R., Burns, A.R., Bohannan, B.J.M.M., Guillemin, K., 2015. Individual members of the microbiota disproportionately modulate host innate immune responses. Cell Host Microbe 18, 613–620. https://doi.org/10.1016/j.chom.2015.10.009

Salgar-Chaparro, S.J., Machuca, L.L., 2019. Complementary DNA/RNA-Based Profiling: Characterization of Corrosive Microbial Communities and Their Functional Profiles in an Oil Production Facility. Front. Microbiol. 10, 2587. https://doi.org/10.3389/fmicb.2019.02587

Salinas, I., Magadán, S., 2017. Omics in fish mucosal immunity. Dev. Comp. Immunol. 75, 99–108. https://doi.org/10.1016/j.dci.2017.02.010

Sandvik, M., Horsberg, T.E., Skaare, J.U., Ingebrigtsen, K., 1998. Comparison of dietary and waterborne exposure to benzo[a]pyrene: Bioavailability, tissue disposition and CYP1A1 induction in rainbow trout (Oncorhynchus mykiss). Biomarkers 3, 399–410. https://doi.org/10.1080/135475098231048

Scantlebury Manning, T., Gibson, G.R., 2004. Prebiotics. Best Pract. Res. Clin. Gastroenterol. 18, 287–298. https://doi.org/10.1053/ybega.2004.445

Schlenk, D., Celander, M., Gallagher, E.P., George, S., James, M., Kullman, S.W., Van Den Hurk, P., Willett, K., 2008. Biotransformation in fishes. Toxicol. Fishes 153–234. https://doi.org/10.1201/9780203647295

Schnorr, S.L., Candela, M., Rampelli, S., Centanni, M., Consolandi, C., Basaglia, G., Turroni, S., Biagi, E., Peano, C., Severgnini, M., Fiori, J., Gotti, R., De Bellis, G., Luiselli, D., Brigidi, P., Mabulla, A., Marlowe, F., Henry, A.G., Crittenden, A.N., 2014. Gut microbiome of the

Hadza hunter-gatherers. Nat. Commun. 5. https://doi.org/10.1038/ncomms4654

Scott, W.B., Crossman, E.J., 1979. Freshwater fishes of Canada.

Scotti, E., Boué, S., Sasso, G. Lo, Zanetti, F., Belcastro, V., Poussin, C., Sierro, N., Battey, J., Gimalac, A., Ivanov, N. V, Hoeng, J., 2017. Exploring the microbiome in health and disease. Toxicol. Res. Appl. 1, 239784731774188. https://doi.org/10.1177/2397847317741884

Sekirov, I., Russell, S., Antunes, L., 2010. Gut microbiota in health and disease. Physiol. Rev. 90, 859–904. https://doi.org/10.1152/physrev.00045.2009.

Seo, J.S., Keum, Y.S., Li, Q.X., 2009. Bacterial degradation of aromatic compounds, International Journal of Environmental Research and Public Health. https://doi.org/10.3390/ijerph6010278

Sfanos, K.S., Markowski, M.C., Peiffer, L.B., Ernst, S.E., White, J.R., Kenneth, •, Pienta, J., Antonarakis, E.S., Ross, A.E., 2018. Compositional differences in gastrointestinal microbiota in prostate cancer patients treated with androgen axis-targeted therapies. Prostate Cancer Prostatic Dis. 21, 539–548. https://doi.org/10.1038/s41391-018-0061-x

Shannon, P., Markiel, A., Ozier, O., Baliga, N.S., Wang, J.T., Ramage, D., Amin, N., Schwikowski, B., Ideker, T., 2003. Cytoscape: A software Environment for integrated models of biomolecular interaction networks. Genome Res. 13, 2498–2504. https://doi.org/10.1101/gr.1239303

Shimizu, Y., Nakatsuru, Y., Ichinose, M., Takahashi, Y., Kume, H., Mimura, J., Fujii-Kuriyama, Y., Ishikawa, T., 2000. Benzo[a]pyrene carcinogenicity is lost in mice lacking the aryl hydrocarbon receptor. Proc. Natl. Acad. Sci. U. S. A. 97, 779–82. https://doi.org/10.1073/PNAS.97.2.779

Signorell, A., 2019. DescTools: Tools for Descriptive Statistics.

Silbergeld, E.K., 2017. The Microbiome. Toxicol. Pathol. 45, 190–194. https://doi.org/10.1177/0192623316672073

Silva, A.C.F., Hawkins, S.J., Boaventura, D.M., Thompson, R.C., 2008. Predation by small mobile aquatic predators regulates populations of the intertidal limpet Patella vulgata (L.). J. Exp. Mar. Bio. Ecol. 367, 259–265. https://doi.org/10.1016/j.jembe.2008.10.010

Simon, P., 2003. Q-Gene: processing quantitative real-time RT–PCR data. Bioinforma. Appl. NOTE 19, 1439–1440. https://doi.org/10.1093/bioinformatics/btg157

Snyder, S.M., Pulster, E.L., Wetzel, D.L., Murawski, S.A., 2015. PAH Exposure in Gulf of Mexico Demersal Fishes, Post- Deepwater Horizon. Environ. Sci. Technol. 49, 8786–8795. https://doi.org/10.1021/acs.est.5b01870

Sowada, J., Schmalenberger, A., Ebner, I., Luch, A., Tralau, T., 2018. Degradation of benzo[ a ]pyrene by bacterial isolates from human skin 129–139. https://doi.org/10.1111/1574-6941.12276

Sowada, J., Schmalenberger, A., Ebner, I., Luch, A., Tralau, T., 2014. Degradation of benzo[a]pyrene by bacterial isolates from human skin. FEMS Microbiol. Ecol. 88, 129–139. https://doi.org/10.1111/1574-6941.12276

Srogi, K., 2007. Monitoring of environmental exposure to polycyclic aromatic hydrocarbons: A review. Environ. Chem. Lett. https://doi.org/10.1007/s10311-007-0095-0

Stansbury, K.H., Flesher, J.W., Gupta, R.C., 1994. Mechanism of Aralkyl-DNA Adduct Formation from Benzo[ alpyrene in Vivo? Chem. Res. Toxicol 7, 254–259.

Steinmeyer, S., Lee, K., Jayaraman, A., Alaniz, R.C., 2015. Microbiota Metabolite Regulation of Host Immune Homeostasis: A Mechanistic Missing Link. Curr. Allergy Asthma Rep. 15, 24. https://doi.org/10.1007/s11882-015-0524-2

Stephens, Z.W., Burns, A.R., Stagaman, K., Wong, S., Rawls, J.F., Guillemin, K., Bohannan, B.J.M., 2015. The composition of the zebrafish intestinal microbial community varies across development. ISME J. 10, 1–11. https://doi.org/10.1038/ismej.2015.140

Sule, M., Skelly, T., 1985. The life history of the shorthead redhorse, Moxostoma macrolepidotum, in the Kankakee River drainage, Illinois. Illinois Nat. Hist. Surv.

Biological.

Sullam, K.E., Essinger, S.D., Lozupone, C.A., O'Connor, M.P., Rosen, G.L., Knight, R., Kilham, S.S., Russell, J.A., 2012. Environmental and ecological factors that shape the gut bacterial communities of fish: A meta-analysis. Mol. Ecol. 21, 3363–3378. https://doi.org/10.1111/j.1365-294X.2012.05552.x

Sun, X., Chu, L., Mercando, E., Romero, I., Hollander, D., Kostka, J.E., 2019. Dispersant enhances hydrocarbon degradation and alters the structure of metabolically active microbial communities in shallow seawater from the northeastern gulf of mexico. Front. Microbiol. 10, 2387. https://doi.org/10.3389/fmicb.2019.02387

Sun, Y.-Z., Yang, H.-L., Ma, R.-L., Lin, W.-Y., 2010. Probiotic applications of two dominant gut Bacillus strains with antagonistic activity improved the growth performance and immune responses of grouper Epinephelus coioides. https://doi.org/10.1016/j.fsi.2010.07.018

Sun, Y., Yang, H., Ling, Z., Chang, J., Jidan, Y., 2009. Gut microbiota of fast and slow growing grouper. African J. Microbiol. Res. 3, 713–720.

Šyvokiene, J., Mickeniene, L., 2011. Hydrocarbon-degrading bacteria associated with intestinal tract of fish from the baltic sea. J. Environ. Eng. Landsc. Manag. 19, 244–250. https://doi.org/10.3846/16486897.2011.602559

Tacchi, L., Lowrey, L., Musharrafieh, R., Crossey, K., Larragoite, E.T., Salinas, I., 2015. Effects of transportation stress and addition of salt to transport water on the skin mucosal homeostasis of rainbow trout (Oncorhynchus mykiss). Aquac. January 1, 120–127. https://doi.org/10.1016/j.aquaculture.2014.09.027

Tang, Caiming, Tan, J., Fan, R., Zhao, B., Tang, Caixing, Ou, W., Jin, J., Peng, X., 2016. Quasi-targeted analysis of hydroxylation-related metabolites of polycyclic aromatic hydrocarbons in human urine by liquid chromatography–mass spectrometry. J. Chromatogr. A 1461, 59–69. https://doi.org/10.1016/j.chroma.2016.07.051

Tarnecki, A.M., Burgos, F.A., Ray, C.L., Arias, C.R., 2017. Fish intestinal microbiome: diversity and symbiosis unravelled by metagenomics. J. Appl. Microbiol. 123, 2–17. https://doi.org/10.1111/jam.13415

Thaiss, C.A., Zmora, N., Levy, M., Elinav, E., 2016. The microbiome and innate immunity. Nature. https://doi.org/10.1038/nature18847

Thomas, F., Hehemann, J.H., Rebuffet, E., Czjzek, M., Michel, G., 2011. Environmental and gut Bacteroidetes: The food connection. Front. Microbiol. 2. https://doi.org/10.3389/fmicb.2011.00093

Thornton, L.M., Path, E.M., Nystrom, G.S., Venables, B.J., Sellin Jeffries, M.K., 2018. Embryo-larval BDE-47 exposure causes decreased pathogen resistance in adult male fathead minnows (Pimephales promelas). Fish Shellfish Immunol. 80, 80–87. https://doi.org/10.1016/j.fsi.2018.05.059

Torrecillas, S., Makol, A., Caballero, M.J., Montero, D., Dhanasiri, A.K.S., Sweetman, J., Izquierdo, M., 2012. Effects on mortality and stress response in European sea bass, Dicentrarchus labrax (L.), fed mannan oligosaccharides (MOS) after Vibrio anguillarum exposure. J. Fish Dis. 35, 591–602. https://doi.org/10.1111/j.1365-2761.2012.01384.x

Torsvik, V., Sorheim, R., Goksoyr, J., 1996. Total bacterial diversity in soil and sediment communities a review. J. Ind. Microbiol. 17, 170–178.

Turnbaugh, P.J., Ley, R.E., Mahowald, M.A., Magrini, V., Mardis, E.R., Gordon, J.I., 2006. An obesity-associated gut microbiome with increased capacity for energy harvest. Nature 444, 1027–1031. https://doi.org/10.1038/nature05414

Tuvikene, A., 1995. Responses of fish to polycyclic aromatic hydrocarbons (PAHs). Annu. Zool. Fenn. 32, 295–309. https://doi.org/10.2307/23735700

Tylianakis, J.M., Laliberté, E., Nielsen, A., Bascompte, J., 2009. Conservation of species interaction networks. https://doi.org/10.1016/j.biocon.2009.12.004

van de Wiele, T., Gallawa, C.M., Kubachka, K.M., Creed, J.T., Basta, N., Dayton, E.A.,

Whitacre, S., Du Laing, G., Bradham, K., 2010. Arsenic metabolism by human gut microbiota upon in vitro digestion of contaminated soils. Environ. Health Perspect. 118, 1004–1009. https://doi.org/10.1289/ehp.0901794

Van de Wiele, T., Vanhaecke, L., Boeckaert, C., Peru, K., Headley, J., Verstraete, W., Siciliano, S., 2005. Human colon microbiota transform polycyclic aromatic hydrocarbons to estrogenic metabolites. Environ. Health Perspect. 113, 6–10. https://doi.org/10.1289/ehp.7259

Van den Abbeele, P., Verstraete, W., El Aidy, S., Geirnaert, A., Van de Wiele, T., 2013. Prebiotics, faecal transplants and microbial network units to stimulate biodiversity of the human gut microbiome. Microb. Biotechnol. 6, 335–340. https://doi.org/10.1111/1751-7915.12049

Vega-López, A., Martínez-Tabche, L., Galar Martínez, M., 2007. Toxic effects of waterborne polychlorinated biphenyls and sex differences in an endangered goodeid fish (Girardinichthys viviparus). Environ. Int. 33, 540–545. https://doi.org/10.1016/j.envint.2006.09.002

Viñas, M., Sabaté, J., Espuny, M.J., Solanas, A.M., 2005. Bacterial community dynamics and polycyclic aromatic hydrocarbon degradation during bioremediation of heavily creosote-contaminated soil. Appl. Environ. Microbiol. 71, 7008–7018. https://doi.org/10.1128/AEM.71.11.7008-7018.2005

Vinebrooke, R.D., Cottingham, K.L., Norberg, J., Scheffer, M., Dodson, S.I., Maberly, S.C., Sommer, U., 2004. Impacts of multiple stressors on biodiversity and ecosystem functioning: The role of species co-tolerance, in: Oikos. pp. 451–457. https://doi.org/10.1111/j.0030-1299.2004.13255.x

Wang, X., Wang, W.-X., 2006. Bioaccumulation and transfer of benzo(a)pyrene in a simplified marine food chain. Mar. Ecol. Prog. Ser. 312, 101–111. https://doi.org/10.1017/CBO9781107415324.004

Warnecke, F., Hugenholtz, P., 2007. Building on basic metagenomics with complementary technologies. Genome Biol. 8, 231. https://doi.org/10.1186/gb-2007-8-12-231

Wemheuer, F., Taylor, J.A., Daniel, R., Johnston, E., Meinicke, P., Thomas, T., Wemheuer, B., 2018. Tax4Fun2: a R-based tool for the rapid prediction of habitat-specific functional profiles and functional redundancy based on 16S rRNA gene marker gene sequences. bioRxiv 490037. https://doi.org/10.1101/490037

WHO, 2001. Probiotics in food: Health and nutritional properties and guidelines for evaluation, Food and Nutrition Paper. https://doi.org/10.1201/9781420009613.ch16

Wickham, H., 2016. ggplot2: Elegant Graphics for Data Analysis. Springer-Verlag New York.

Williams, C.L., Garcia-Reyero, N., Martyniuk, C.J., Tubbs, C.W., Bisesi, J.H., 2020. Regulation of endocrine systems by the microbiome: Perspectives from comparative animal models. Gen. Comp. Endocrinol. 292, 113437. https://doi.org/10.1016/J.YGCEN.2020.113437

Wong, S., Zac Stephens, W., Burns, A.R., Stagaman, K., David, L.A., Bohannan, B.J.M., Guillemin, K., Rawls, J.F., 2015. Ontogenetic differences in dietary fat influence microbiota assembly in the zebrafish gut. MBio 6, 1–9. https://doi.org/10.1128/mBio.00687-15

Xie, Y., Wang, J., Wu, Y., Ren, C., Song, C., Yang, J., Yu, H., Giesy, J.P., Zhang, X., 2016. Using in situ bacterial communities to monitor contaminants in river sediments. Environ. Pollut. 212, 348–357. https://doi.org/10.1016/j.envpol.2016.01.031

Xie, Y., Zhang, X., Yang, J., Kim, S., Hong, S., Giesy, J.P., Yim, U.H., Shim, J., Yu, H., Khim, J.S., 2018. eDNA-based bioassessment of coastal sediments impacted by an oil spill. https://doi.org/10.1016/j.envpol.2018.02.081

Yan, Q., Li, J., Yu, Y., Wang, J., He, Z., Van Nostrand, J.D., Kempher, M.L., Wu, L., Wang, Y., Liao, L., Li, X., Wu, S., Ni, J., Wang, C., Zhou, J., 2016. Environmental filtering decreases with fish development for the assembly of gut microbiota. Environ. Microbiol. 18, 4739–4754. https://doi.org/10.1111/1462-2920.13365

Yan, Y., Kuramae, E.E., Klinkhamer, P.G.L., van Veena, J.A., 2015. Revisiting the dilution

procedure used to manipulate microbial biodiversity in terrestrial systems. Appl. Environ. Microbiol. 81, 4246–4252. https://doi.org/10.1128/AEM.00958-15

Yang, B., Wang, Y., Qian, P.Y., 2016. Sensitivity and correlation of hypervariable regions in 16S rRNA genes in phylogenetic analysis. BMC Bioinformatics 17. https://doi.org/10.1186/s12859-016-0992-y

Yang, S., Wen, X., Shi, Y., Liebner, S., Jin, H., Perfumo, A., 2016. Hydrocarbon degraders establish at the costs of microbial richness, abundance and keystone taxa after crude oil contamination in permafrost environments. Sci. Rep. 6. https://doi.org/10.1038/srep37473

Yang, Z., Shah, K., Laforest, S., Hollebone, B.P., Situ, J., Crevier, C., Lambert, P., Brown, C.E., Yang, C., 2020. Occurrence and weathering of petroleum hydrocarbons deposited on the shoreline of the North Saskatchewan River from the 2016 Husky oil spill. Environ. Pollut. 258. https://doi.org/10.1016/j.envpol.2019.113769

Ye, J., Coulouris, G., Zaretskaya, I., Cutcutache, I., Rozen, S., Madden, T.L., 2012. Primer-BLAST: A tool to design target-specific primers for polymerase chain reaction. BMC Bioinformatics 13, 134. https://doi.org/10.1186/1471-2105-13-134

Yeoman, C.J., White, B.A., 2014. Gastrointestinal Tract Microbiota and Probiotics in Production Animals. Annu. Rev. Anim. Biosci 2, 469–86. https://doi.org/10.1146/annurev-animal-022513-114149

Yergeau, E., Sanschagrin, S., Beaumier, D., Greer, C.W., 2012. Metagenomic Analysis of the Bioremediation of Diesel-Contaminated Canadian High Arctic Soils. PLoS One 7, 30058. https://doi.org/10.1371/journal.pone.0030058

Ying, S., Zeng, D.-N., Chi, L., Tan, Y., Galzote, C., Cardona, C., Lax, S., Gilbert, J., Quan, Z.-X., 2015. The Influence of Age and Gender on Skin-Associated Microbial Communities in Urban and Rural Human Populations. PLoS One 10, e0141842. https://doi.org/10.1371/journal.pone.0141842

Yoshioka, G., Carpenter, M., 2002. Characteristics of Reported Inland and Coastal Oil Spills.

Yukgehnaish, K., Kumar, P., Sivachandran, P., Marimuthu, K., Arshad, A., Paray, B.A., Arockiaraj, J., 2020. Gut microbiota metagenomics in aquaculture: factors influencing gut microbiome and its physiological role in fish. https://doi.org/10.1111/raq.12416

Yurkovetskiy, L., Burrows, M., Khan, A.A., Graham, L., Volchkov, P., Becker, L., Antonopoulos, D., Umesaki, Y., Chervonsky, A. V., 2013. Gender bias in autoimmunity is influenced by microbiota. Immunity 39, 400–412. https://doi.org/10.1016/j.immuni.2013.08.013

Zappelini, C., Karimi, B., Foulon, J., Lacercat-Didier, L., Maillard, F., Valot, B., Blaudez, D., Cazaux, D., Gilbert, D., Yergeau, E., Greer, C., Chalot, M., 2015. Diversity and complexity of microbial communities from a chlor-alkali tailings dump. Soil Biol. Biochem. 90, 101–110. https://doi.org/10.1016/j.soilbio.2015.08.008

Zeevi, D., Korem, T., Zmora, N., Israeli, D., Rothschild, D., Weinberger, A., Ben-Yacov, O., Lador, D., Avnit-Sagi, T., Lotan-Pompan, M., Suez, J., Mahdi, J.A., Matot, E., Malka, G., Kosower, N., Rein, M., Zilberman-Schapira, G., Dohnalová, L., Pevsner-Fischer, M., Bikovsky, R., Halpern, Z., Elinav, E., Segal, E., 2015. Personalized Nutrition by Prediction of Glycemic Responses. Cell 163, 1079–1094. https://doi.org/10.1016/j.cell.2015.11.001

Zeng, Z., Jin, C., Fu, Z., Jin, Y., 2016. Oral imazalil exposure induces gut microbiota dysbiosis and colonic inflammation in mice. https://doi.org/10.13140/RG.2.1.4802.7123

Zengler, K., Richnow, H.H., Rosselló-Mora, R., Michaelis, W., Widdel, F., 1999. Methane formation from long-chain alkanes by anaerobic microorganisms. Nature 401, 266–269. https://doi.org/10.1038/45777

Zhang, L., Nichols, R.G., Patterson, A.D., 2017. The aryl hydrocarbon receptor as a moderator of host-microbiota communication. Curr. Opin. Toxicol. 2, 30–35. https://doi.org/10.1016/j.cotox.2017.02.001

Zhao, Y., Liu, H., Wang, Q., Li, B., Zhang, H., Pi, Y., 2019. The effects of benzo[a]pyrene on the composition of gut microbiota and the gut health of the juvenile sea cucumber

Apostichopus japonicus Selenka. https://doi.org/10.1016/j.fsi.2019.07.073

Zhao, Y., Zhang, Y., Wang, G., Han, R., Xie, X., 2016. Effects of chlorpyrifos on the gut microbiome and urine metabolome in mouse (Mus musculus). https://doi.org/10.1016/j.chemosphere.2016.03.055

# Appendices

## Appendix A

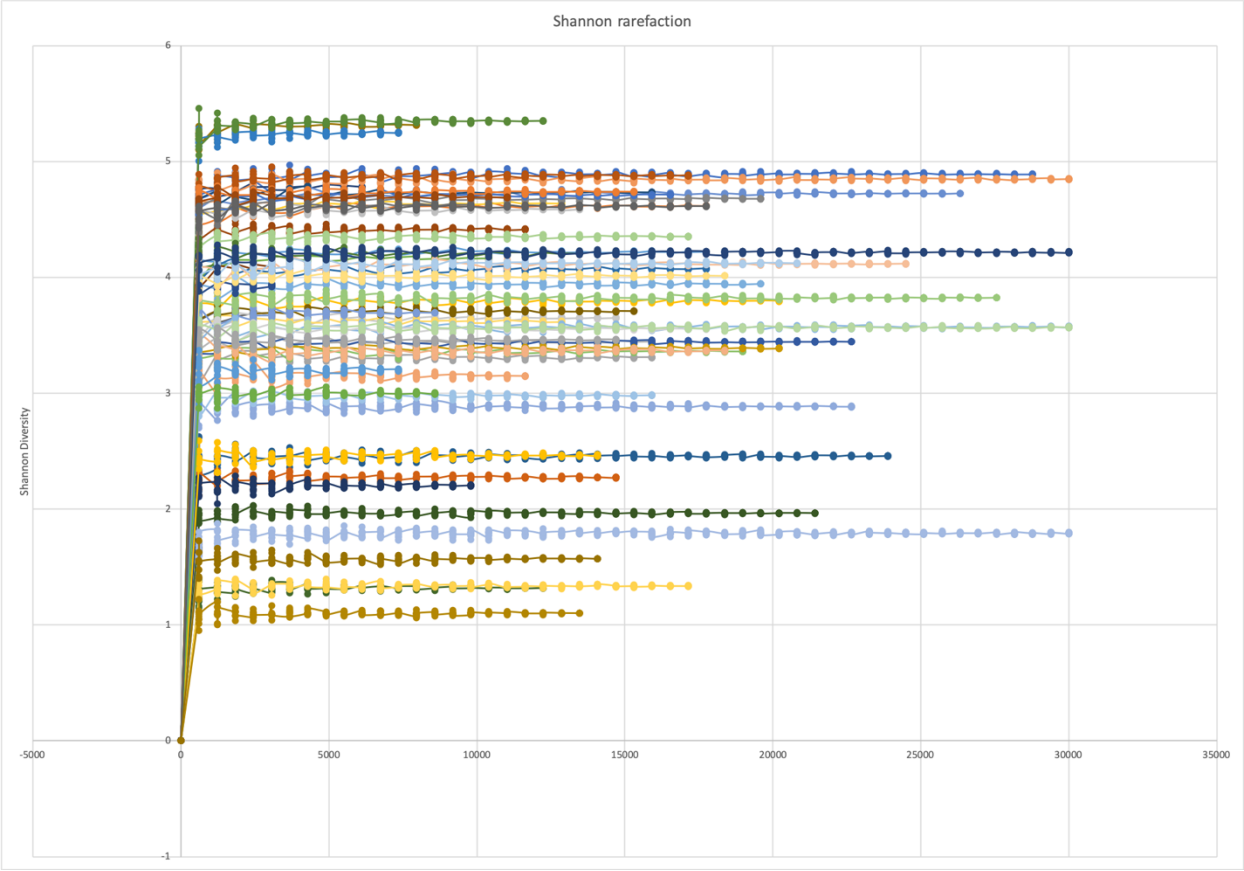


Figure A.1. Rarefaction curve of Shannon diversity for all samples in this study.

Table A.1. Primer sequences and references.

| Gene | Gene name | Purpose | Sequence (5' – 3') | Reference |
|---|---|---|---|---|
| *cyp1a1* | cytochrome p450 1a1 | toxicokinetics | Forward: CCTGCAGGGAGAACTGAG<br>Reverse : TCGACGTACAGTGAGGGA | (Wiseman et al., 2013) |
| *bax* | BCL2 asociated | genotox | AGCCTATACGCGAGGTGA<br>ACCTTAACCGGAATGCTGT | (He et al., 2012) |
| *esr1* | estrogen receptor 1 | estrogenicity | GGCTGAGATTTTCGACATGCTT<br>AAATTCCTCCAGCTTCAGTTTTAGAC | (Garcia-Reyero et al., 2009) |
| *vtg* | vitellogenin | estrogenicity | GCTGCTGCTCCATTTCAAAAG<br>GTGAGAGTGCACCTCAACGC | (Vidal-Dorsch et al., 2013) |
| *ar* | androgen rceptor | estrogenicity | CGCGAGTGTGGCGAGTT<br>TCGCGCTGTCTCCGAAA | (Garcia-Reyero et al., 2009) |
| *ef1* | elongation factor | housekeeping | CCCTCTTGGTCGCTTTGCT<br>ACGCTCTTGATGACACCAACAG | (Lewis and Keller, 2009) |
| *18S* | 18S rRNA | housekeeping | AATGTCTGCCCTATCAACTTTC<br>TGGATGTGGTAGCCGTTTC | (Vidal-Dorsch et al., 2013) |

Table A.2. Metrics indicating input sequences after demultiplexing as well as the number of filtered, denoised, merged, remaining after removal of chimeras, and bacteria only for all samples sequenced in this study.

| sample-id | input | filtered | denoised | merged | non-chimeric | bact only |
|---|---|---|---|---|---|---|
| 4ha1 | 73359 | 70443 | 70266 | 69841 | 68769 | 29247 |
| 4ha2 | 50514 | 48407 | 48275 | 48033 | 46478 | 18076 |
| 4ha4 | 37743 | 36373 | 36295 | 36125 | 35717 | 16158 |
| 4hb1 | 54301 | 52000 | 51784 | 51407 | 50274 | 20791 |
| 4hb2 | 45926 | 44102 | 43806 | 43432 | 41474 | 17983 |
| 4hb4 | 27102 | 25916 | 25708 | 25466 | 24697 | 10860 |
| 4hc1 | 15539 | 14818 | 14666 | 14481 | 14452 | 6322 |
| 4hc2 | 27822 | 26709 | 26550 | 26324 | 26252 | 12182 |
| 4hc4 | 7387 | 7090 | 7045 | 6989 | 6955 | 3004 |
| 4hd1 | 25321 | 23441 | 23233 | 22840 | 22742 | 7997 |
| 4hd2 | 60235 | 57331 | 57170 | 56982 | 56686 | 23939 |
| 4hd4 | 31698 | 30468 | 30374 | 30216 | 30115 | 12835 |
| 4he1 | 65261 | 62371 | 62047 | 61506 | 60706 | 26589 |
| 4he2 | 86258 | 82299 | 81994 | 81485 | 80712 | 34691 |
| 4he4 | 41684 | 39356 | 39212 | 38991 | 38118 | 16334 |
| 4la1 | 35094 | 33510 | 33218 | 32942 | 32287 | 13128 |
| 4la2 | 51276 | 48920 | 48650 | 48360 | 47543 | 20007 |
| 4la4 | 45245 | 43469 | 43305 | 42952 | 40678 | 19109 |
| 4la42 | 58381 | 55923 | 55765 | 55498 | 52952 | 22838 |
| 4lb1 | 34505 | 33358 | 33268 | 33066 | 32706 | 15104 |
| 4lb2 | 43847 | 42458 | 42214 | 41749 | 41336 | 19736 |
| 4lb4 | 51346 | 49269 | 49109 | 48847 | 48256 | 20748 |
| 4lc1 | 18832 | 17646 | 17431 | 17156 | 16806 | 7911 |
| 4lc2 | 27525 | 26328 | 26098 | 25778 | 25428 | 12321 |
| 4lc4 | 50340 | 48450 | 48371 | 48138 | 47746 | 23024 |
| 4ld1 | 45768 | 43535 | 43352 | 42942 | 42632 | 18958 |
| 4ld2 | 37886 | 35833 | 35689 | 35376 | 34793 | 14994 |
| 4ld4 | 31588 | 30283 | 30146 | 29952 | 29537 | 13424 |
| 4le1 | 38568 | 37035 | 36860 | 36603 | 35334 | 16504 |
| 4le2 | 39687 | 38137 | 37928 | 37715 | 36937 | 17571 |

| sample-id | input | filtered | denoised | merged | non-chimeric | bact only |
|---|---|---|---|---|---|---|
| 4ma1 | 15167 | 14644 | 14472 | 14249 | 14110 | 3205 |
| 4ma2 | 2560 | 2462 | 2439 | 2425 | 2425 | 997 |
| 4ma3 | 39080 | 37487 | 37308 | 37022 | 36563 | 15473 |
| 4mb1 | 40276 | 38585 | 38304 | 37922 | 37179 | 16084 |
| 4mb4 | 53389 | 51301 | 51163 | 50820 | 47185 | 21482 |
| 4mc1 | 27773 | 26829 | 26580 | 26184 | 25699 | 11878 |
| 4mc2 | 31347 | 30213 | 30035 | 29780 | 29266 | 13750 |
| 4mc4 | 49492 | 47377 | 47311 | 47118 | 47018 | 17417 |
| 4md1 | 80600 | 77082 | 76814 | 76429 | 74273 | 32387 |
| 4md2 | 63133 | 60306 | 60032 | 59706 | 58726 | 27643 |
| 4md4 | 7831 | 7365 | 7282 | 7163 | 7076 | 3558 |
| 4me1 | 44209 | 42199 | 41920 | 41505 | 39196 | 17458 |
| 4me2 | 28593 | 27394 | 27137 | 26831 | 26342 | 10289 |
| 4me4 | 32009 | 30922 | 30823 | 30687 | 30621 | 13559 |
| 4sa1 | 45127 | 43256 | 43081 | 42838 | 42088 | 18181 |
| 4sa2 | 44966 | 43044 | 42626 | 41071 | 39480 | 13789 |
| 4sa3 | 74346 | 71617 | 71467 | 71212 | 71000 | 35537 |
| 4sa4 | 66587 | 63762 | 63233 | 61780 | 59782 | 24789 |
| 4sa5 | 50084 | 48106 | 47847 | 46762 | 43503 | 18238 |
| 4sb1 | 42820 | 40800 | 40684 | 40518 | 39541 | 18422 |
| 4sb2 | 59031 | 56296 | 56108 | 55737 | 55118 | 21040 |
| 4sb4 | 85241 | 81814 | 81639 | 81286 | 80652 | 35669 |
| 4sc1 | 44399 | 42625 | 42378 | 42010 | 40425 | 16994 |
| 4sc2 | 42086 | 40421 | 40152 | 39823 | 38319 | 15504 |
| 4sc4 | 33055 | 31860 | 31737 | 31498 | 29171 | 15275 |
| 4sd1 | 35673 | 34176 | 34048 | 33829 | 33356 | 14639 |
| 4sd2 | 21220 | 20335 | 20201 | 19992 | 19879 | 7885 |
| 4sd4 | 22895 | 21976 | 21879 | 21648 | 20832 | 8879 |
| 4se1 | 31186 | 29894 | 29641 | 29236 | 28028 | 11527 |
| 4se2 | 47789 | 45815 | 45685 | 45432 | 44307 | 18071 |
| 4se4 | 37519 | 35369 | 35258 | 35105 | 34964 | 14129 |

# Appendix B

Additional Materials and Methods

**Text B.1, Fish husbandry**

Juvenile fathead minnows were obtained from an in-house stock population of the Aquatic Toxicology Research Facility at the University of Saskatchewan. Fish were acclimated at a density of ten juvenile fish per 5-gallon tank containing pretreated facility water, and approximately two-thirds of the water was siphoned and renewed daily. To maintain a temperature of 25 ± 1 °C, tanks were placed in a water bath containing electric heaters. A 16h-light:8h-dark photoperiod was provided. Fish were fed EWOS® Micro Crumble trout chow (Cargill Inc., Wayzata, MN), two times daily on a maintenance food ration (2% of their average wet body mass (bm) per day).

**Text B.2, Quantification of BaP in food**

To quantify BaP in food, stock solutions of BaP and deuterium labelled BaP-d12 were made at 1,000 µg $mL^{-1}$ in acetone. Internal calibration and isotope dilution were used to quantify BaP in samples using an eight-point calibration curve between 0.5 and 500 ng BaP $mL^{-1}$, each containing 100 ng $mL^{-1}$ with BaP-d12. Isotope dilution was used to confirm concentrations of BaP spiked in fish feed used for the dietary exposure. Triplicate samples of feed (control, 1, 10, 100, 1,000 ug $g^{-1}$ nominal concentrations) were weighed (0.05 g) and spiked with BaP-d12 at a target concentration of 100 ng/mL in the final 1 mL extract. Each sample was loaded into an 11-mL accelerated solvent extraction (ASE) cell as follows: filter paper, 8 g Ottawa Sand (Fisher Scientific), filter paper, fish food sample, filter paper, sand to top of cell, filter paper. Pressurized liquid extraction was conducted using a Dionex ASE 200 with a 1:1 dichloromethane: acetone solvent mixture. Two 70% volume extractions were conducted at 100 °C and 1,500 psi for 10 min each. A blank cell (no fish food) was also loaded and extracted to serve as an extraction blank. The resulting ≈15 mL extracts were either blown-down by nitrogen evaporation or diluted and subsampled in order to maintain concentrations within the linear dynamic range of the calibration curve.

Quantification of BaP was done by GC-QE-Orbitrap mass spectrometer system (Q Exactive GC, Thermo Scientific, Mississauga, ON) with a Thermo RSH autosampler and a TRACE 1310 GC with a heated split/splitless injector running in splitless mode. Ionization was by electron impact (EI) ionization at 70 eV. Helium was the carrier gas at a constant flow of 1.0

mL/min. GC separation was achieved on a 60-m DB5ms column (0.1 mm ID, 0.1 µm film thickness) with the following temperature program: 80 °C (5 min hold), ramping at 4 °C/min to 325 °C for a total runtime of 76 min. The instrument was operated at a nominal mass resolution of 120,000 (FWHM) in full scan MS mode (100-425 m/z). Data were acquired and processed in Xcalibur 4.1 (Thermo Scientific, Mississauga, ON).

**Text B.3, Relative quantification of metabolites of BaP in bile**

Bile samples were first weighed, then diluted 1:10 in acetonitrile before analysis. Stock solutions of mono-hydroxylated benzo[a]pyrene (OH-BaP) (Toronto Research Chemicals, North York, Canada) were made in HPLC grade methanol/ACN (Fisher Scientific). A six point OH-BaP calibration curve ranging from 0.3 – 100 µg $L^{-1}$ was used for semi-quantification of the all BaP metabolites. Analysis was conducted using a Vanquish UHPLC and Q-Exactive™ HF Quadrupole-Orbitrap™ mass spectrometer (Thermo-Fisher). LC separation was achieved with an Acclaim Vanquish 2.2µm C18 LC column (150 x 2.1 mm) (Thermo-Fisher) using a gradient elution with water and acetonitrile, both containing 0.1% formic acid at a flow rate of 0.25 mL/min and column temperature of 30 °C. The gradient started and was held at 25% ACN from 0-3 min, ramped from 25% to 100% ACN from 3-15 min, held at 100% ACN from 15-18 min, and re-equilibrated to 25% ACN over 7 min for a total run time of 25 min. Retention times of OH-BaP, OH-BaP-O-glucuronide (BaP-Gluc), and sulfate-BaP (BaP-$SO_4$) were 12.74, 8.39, and 10.82 minutes, respectively.

Samples were ionized by negative mode heated electrospray ionization (HESI) with the following source parameters: sheath gas flow = 35; aux gas flow = 8; sweep gas flow = 1; aux gas heater = 325°C; spray voltage = 2.7 kV; S-lens RF = 55; capillary temperature = 300°C. A Full MS/parallel reaction monitoring (PRM) method was used with the following scan settings: 60,000/30,000 resolution, AGC target = $1x10^6/2x10^5$, max injection time = 100ms/100ms, full MS scan range of 80-500 m/z and PRM isolation window of 2.0 m/z and normalized collision energy = 30. The method monitored the $[M-H]^-$ parent ion m/z 267.080 for OH-BaP and both parent and daughter ions for OH-BaP-O-glucuronide (m/z 443.113 → 267.080) and BaP-$SO_4$ (m/z 347.038 → 267.080).

Concentrations of OH-BaP were quantified directly with the use of analytical standards and external calibration. Semi-quantification of BaP-Gluc and BaP-$SO_4$ was conducted using a relative response factor approach. First, a representative set of bile samples were analyzed

untreated, followed by analysis of samples treated with glucuronidase and arylsulfatase (30/60 U $mL^{-1}$; Sigma Aldrich Roche, Basel, Switzerland) in order to convert all of the BaP-Gluc and BaP-$SO_4$ metabolites present in the untreated samples into OH-BaP. Sample incubations with enzymes were conducted by placing the bile with the enzymes in an incubator for 2 hours at 37°C while shaking at 200 rpm.

These samples provided an instrument response factor for semi-quantification. The response factors for BaP-Gluc and BaP-$SO_4$ were calculated (Equation B.1).

$$Response\ factor = \frac{Peak\ Area\ [OH{-}BaP]_{treated}}{Peak\ Area\ [Gluc/SO4{-}BaP]_{untreated}} \quad \text{(B.1)}$$

Mean response factor for Gluc and $SO_4$ was 21 and 17 respectively, suggesting that for equimolar amounts of OH and Gluc/$SO_4$ BaP, OH-BaP response was 21 and 17 times more sensitive, respectively. Response factors were used to convert peak areas of OH-BaP from the standard curve to Gluc and $SO_4$ BaP peak areas in order to construct external calibration curves for each metabolite. Concentrations of each metabolite measured in the extracted bile samples could then be determined from the peak areas. Final BaP metabolite concentrations were reported as ng $g^{-1}$ bile calculated from the volume of solvent used for extraction and specific bile weight.

Table B.1. Limit of quantification (LOQ) and limit of detection (LOD) of OH-BaP, BaP-Gluc, and BaP-$SO_4$.

| Metabolite | LOQ (ng $ml^{-1}$) | LOD (ng $ml^{-1}$) |
|---|---|---|
| OH-BaP | 0.036 | 0.011 |
| BaP-Gluc | 0.76 | 0.23 |
| BaP-$SO_4$ | 0.61 | 0.19 |

Table B.2. The number of sequenced, filtered, denoised, merged, non-chimeric, and bacteria only reads for each sample.

| sample | sequenced | filtered | denoised | merged | non-chimeric | bacteria only |
|---|---|---|---|---|---|---|
| NTC2D | 593 | 583 | 526 | 429 | 384 | 378 |
| NTCD | 8 | 8 | 2 | 2 | 2 | 2 |
| R11000F2D | 24528 | 24210 | 23414 | 21156 | 16394 | 16388 |
| R11000F2xD | 46308 | 45695 | 45155 | 43248 | 37550 | 36568 |
| R11000F3D | 21345 | 21023 | 20623 | 19381 | 16013 | 16009 |
| R11000F4D | 47 | 36 | 24 | 21 | 21 | 21 |
| R11000F5D | 30502 | 30114 | 29740 | 28581 | 23489 | 23400 |
| R11000F6D | 30042 | 29646 | 29157 | 27573 | 22953 | 22953 |
| R11000F7D | 27175 | 26796 | 26380 | 25064 | 19623 | 19580 |
| R11000F8D | 18001 | 17764 | 17545 | 17008 | 15447 | 15441 |
| R11000F9D | 10587 | 10438 | 10062 | 9189 | 7680 | 7677 |
| R1100F1D | 43898 | 43259 | 42036 | 38420 | 26785 | 26597 |
| R1100F3D | 31053 | 30601 | 29841 | 27756 | 22035 | 21989 |
| R1100F4D | 28685 | 28280 | 27281 | 24189 | 19239 | 19185 |
| R1100F5D | 44317 | 43708 | 42336 | 38300 | 27861 | 27820 |
| R1100F6D | 29577 | 29188 | 28438 | 25964 | 19406 | 19374 |
| R1100F7D | 34935 | 34497 | 33604 | 30873 | 23653 | 23598 |
| R1100F8D | 39662 | 39147 | 38233 | 35030 | 26933 | 26826 |
| R1100F9D | 35455 | 34972 | 33934 | 30656 | 21344 | 21285 |
| R110F10D | 34190 | 33693 | 32889 | 30368 | 25663 | 25609 |
| R110F1D | 21972 | 21697 | 21197 | 19621 | 15677 | 15664 |
| R110F2D | 14952 | 14739 | 14383 | 13384 | 11211 | 11208 |
| R110F3D | 8050 | 7952 | 7802 | 7367 | 6896 | 6866 |
| R110F4D | 42845 | 42260 | 41227 | 38024 | 27518 | 27355 |
| R110F5D | 13815 | 13625 | 13159 | 11694 | 9021 | 9010 |
| R110F6D | 8209 | 8077 | 7936 | 7490 | 6903 | 6895 |
| R110F8D | 33780 | 33259 | 32438 | 29886 | 24788 | 24722 |
| R110F9D | 10 | 8 | 2 | 2 | 2 | 2 |
| R11F10D | 28765 | 28385 | 27741 | 25751 | 21426 | 21388 |
| R11F1D | 29879 | 29489 | 28828 | 27067 | 21454 | 21359 |
| R11F2D | 18 | 16 | 6 | 5 | 5 | 5 |
| R11F3D | 13048 | 12883 | 12802 | 12690 | 12528 | 10974 |

| sample | sequenced | filtered | denoised | merged | non-chimeric | bacteria only |
|---|---|---|---|---|---|---|
| R11F4D | 38155 | 37693 | 37092 | 35137 | 27674 | 27604 |
| R11F5D | 39979 | 39464 | 38901 | 37153 | 31085 | 30999 |
| R11F6D | 18 | 15 | 4 | 4 | 4 | 4 |
| R11F7D | 43702 | 43144 | 42327 | 39722 | 33213 | 33107 |
| R11F8D | 35553 | 35123 | 34584 | 32811 | 28066 | 27971 |
| R11F9D | 18616 | 18358 | 17794 | 16362 | 13725 | 13672 |
| R1CTRLF10D | 13903 | 13659 | 13357 | 12641 | 11313 | 11311 |
| R1CTRLF1D | 33772 | 33184 | 32672 | 31076 | 27971 | 27949 |
| R1CTRLF2D | 16077 | 15860 | 15208 | 13726 | 11426 | 11379 |
| R1CTRLF3D | 37654 | 37198 | 36710 | 35424 | 32097 | 32086 |
| R1CTRLF4D | 26460 | 26084 | 24924 | 21133 | 17539 | 16981 |
| R1CTRLF5D | 30021 | 29557 | 28828 | 26582 | 21724 | 21688 |
| R1CTRLF6D | 10612 | 10363 | 10027 | 8880 | 8102 | 8079 |
| R1CTRLF7D | 29491 | 29066 | 28495 | 26785 | 22104 | 22007 |
| R1CTRLF8D | 1470 | 1433 | 1341 | 1273 | 1230 | 1230 |
| R1CTRLF9D | 19014 | 18642 | 18270 | 16856 | 15491 | 15281 |
| R21000F10D | 26634 | 26276 | 25955 | 24868 | 22882 | 22864 |
| R21000F1D | 37544 | 37055 | 36576 | 34646 | 28700 | 28660 |
| R21000F2D | 31102 | 30705 | 29731 | 26490 | 19163 | 19027 |
| R21000F4D | 35768 | 35319 | 34463 | 31618 | 20538 | 20488 |
| R21000F5D | 26219 | 25906 | 25348 | 23261 | 16013 | 15880 |
| R21000F6D | 8 | 5 | 1 | 0 | 0 | 0 |
| R21000F8D | 43340 | 42826 | 42150 | 39498 | 25869 | 25766 |
| R21000F9D | 33461 | 33005 | 32220 | 29226 | 20045 | 19960 |
| R2100F10D | 14 | 7 | 1 | 0 | 0 | 0 |
| R2100F1D | 189 | 177 | 152 | 142 | 142 | 142 |
| R2100F2D | 33965 | 33529 | 32813 | 30607 | 25113 | 25103 |
| R2100F3D | 31902 | 31011 | 30426 | 28789 | 21133 | 20885 |
| R2100F5D | 33388 | 32950 | 32352 | 30824 | 24409 | 24364 |
| R2100F7D | 35949 | 35413 | 34599 | 32274 | 26667 | 26634 |
| R2100F8D | 36925 | 36414 | 35751 | 34078 | 28240 | 28050 |
| R210F10D | 5298 | 5221 | 5154 | 4970 | 4347 | 4248 |
| R210F12D | 18679 | 18448 | 18307 | 17678 | 13917 | 13806 |
| R210F1D | 34098 | 33618 | 33037 | 31008 | 25465 | 25456 |

| sample | sequenced | filtered | denoised | merged | non-chimeric | bacteria only |
|---|---|---|---|---|---|---|
| R210F3D | 23251 | 22924 | 22486 | 21252 | 18233 | 18229 |
| R210F4D | 32841 | 32421 | 31886 | 29821 | 20698 | 20654 |
| R210F5D | 36028 | 35605 | 35152 | 33732 | 23110 | 22749 |
| R210F6D | 41810 | 41276 | 40330 | 37680 | 31249 | 31179 |
| R210F7D | 37388 | 36922 | 36339 | 34345 | 23449 | 23272 |
| R210F8D | 30929 | 30509 | 29394 | 26532 | 21086 | 20965 |
| R210F9D | 26952 | 26583 | 24992 | 19960 | 13252 | 13134 |
| R21F10D | 34123 | 33676 | 32785 | 29814 | 20214 | 20065 |
| R21F1D | 33629 | 33229 | 32624 | 30757 | 19448 | 19191 |
| R21F2D | 24195 | 23893 | 23439 | 21877 | 18393 | 18373 |
| R21F3D | 16267 | 14868 | 14641 | 13464 | 11733 | 10273 |
| R21F5D | 27110 | 26698 | 25733 | 22621 | 16307 | 16057 |
| R21F6D | 28127 | 27793 | 27344 | 25662 | 17195 | 17058 |
| R21F7D | 28397 | 28021 | 27659 | 26393 | 22659 | 22636 |
| R21F8D | 34782 | 34341 | 33180 | 30067 | 23286 | 23266 |
| R21F9D | 30093 | 29753 | 29532 | 28952 | 20128 | 16178 |
| R2CTRLF10D | 40173 | 39635 | 38774 | 35994 | 27074 | 26539 |
| R2CTRLF1D | 31 | 5 | 1 | 0 | 0 | 0 |
| R2CTRLF2D | 35690 | 35274 | 34447 | 31624 | 24248 | 24098 |
| R2CTRLF3D | 96 | 88 | 74 | 70 | 68 | 68 |
| R2CTRLF4D | 30654 | 30272 | 29914 | 28893 | 25424 | 25416 |
| R2CTRLF5D | 37700 | 37251 | 36776 | 35102 | 28721 | 28687 |
| R2CTRLF7D | 33363 | 32945 | 32245 | 29951 | 24715 | 24626 |
| R2CTRLF8D | 37737 | 37252 | 36184 | 33047 | 22901 | 22785 |
| R2CTRLF9D | 32345 | 31846 | 30092 | 23719 | 15740 | 13311 |
| R31000F10D | 5134 | 5030 | 4881 | 4546 | 4057 | 4056 |
| R31000F1D | 29779 | 29262 | 28954 | 28137 | 26197 | 26159 |
| R31000F2D | 88 | 41 | 1 | 0 | 0 | 0 |
| R31000F3D | 23779 | 23445 | 23001 | 21863 | 19548 | 19448 |
| R31000F4D | 36202 | 35616 | 34772 | 32009 | 25881 | 25407 |
| R31000F5D | 1363 | 1334 | 1283 | 1191 | 1184 | 1182 |
| R31000F6D | 31470 | 31059 | 30870 | 30342 | 26761 | 26441 |
| R31000F7D | 28007 | 27605 | 26989 | 25430 | 21549 | 21526 |
| R31000F8D | 17612 | 17253 | 17056 | 16621 | 15768 | 15731 |

| sample | sequenced | filtered | denoised | merged | non-chimeric | bacteria only |
|---|---|---|---|---|---|---|
| R31000F9D | 34138 | 33575 | 33183 | 32269 | 28318 | 28306 |
| R3100F1D | 36683 | 36137 | 35740 | 34692 | 31262 | 31208 |
| R3100F2D | 29681 | 29098 | 28894 | 28181 | 27662 | 16746 |
| R3100F3D | 34886 | 34371 | 33819 | 32023 | 26378 | 26352 |
| R3100F4D | 1135 | 594 | 497 | 459 | 459 | 202 |
| R3100F5D | 2087 | 2033 | 1929 | 1768 | 1705 | 1692 |
| R3100F6D | 26512 | 25568 | 25457 | 25258 | 25184 | 20550 |
| R3100F7D | 18421 | 16971 | 16812 | 16410 | 16073 | 12218 |
| R3100F8D | 20364 | 19953 | 19370 | 17981 | 14989 | 14982 |
| R3100F9D | 26781 | 26420 | 26280 | 25966 | 24224 | 24197 |
| R310F10D | 44 | 25 | 5 | 5 | 5 | 5 |
| R310F1D | 28751 | 28387 | 27580 | 25150 | 19952 | 19905 |
| R310F2D | 12459 | 12176 | 11993 | 11711 | 11080 | 11080 |
| R310F3D | 36440 | 35946 | 34868 | 31865 | 25590 | 25339 |
| R310F4D | 33567 | 33043 | 32372 | 30241 | 23391 | 23354 |
| R310F5D | 24745 | 24427 | 24098 | 23016 | 20549 | 20482 |
| R310F6D | 6650 | 6536 | 6384 | 6174 | 5773 | 5770 |
| R310F7D | 37 | 36 | 23 | 21 | 21 | 21 |
| R310F8D | 104 | 84 | 39 | 35 | 35 | 27 |
| R310F9D | 30553 | 30155 | 29592 | 27760 | 25368 | 25268 |
| R31F10D | 32904 | 32422 | 31552 | 28801 | 20181 | 20157 |
| R31F1D | 29987 | 29436 | 28802 | 26672 | 21926 | 21916 |
| R31F2D | 20212 | 19879 | 19598 | 18900 | 17216 | 17214 |
| R31F3D | 25492 | 25122 | 24348 | 21880 | 15622 | 15570 |
| R31F4D | 41450 | 40898 | 39855 | 36432 | 26684 | 26538 |
| R31F5D | 35381 | 34957 | 34208 | 31252 | 23189 | 23118 |
| R31F6D | 4938 | 4804 | 4694 | 4478 | 4231 | 4225 |
| R31F7D | 34032 | 33550 | 32629 | 29466 | 22426 | 22352 |
| R31F8D | 6110 | 6008 | 5901 | 5676 | 5233 | 5233 |
| R31F9D | 32479 | 31898 | 30841 | 27627 | 20337 | 20306 |
| R3ContF10D | 23776 | 23424 | 22929 | 21408 | 17630 | 17598 |
| R3ContF1D | 22425 | 22122 | 21545 | 20059 | 16922 | 16914 |
| R3ContF2D | 34475 | 33940 | 33036 | 30195 | 23544 | 23341 |
| R3ContF3D | 31928 | 31542 | 30659 | 27440 | 21189 | 21138 |

| sample | sequenced | filtered | denoised | merged | non-chimeric | bacteria only |
|---|---|---|---|---|---|---|
| R3ContF4D | 40813 | 40245 | 39134 | 35765 | 27974 | 27922 |
| R3ContF5D | 52 | 32 | 4 | 4 | 4 | 4 |
| R3ContF6D | 36224 | 35702 | 34681 | 31672 | 24333 | 24165 |
| R3ContF7D | 28595 | 28170 | 27358 | 25048 | 20325 | 20306 |
| R3ContF8D | 32153 | 31698 | 30675 | 27429 | 20396 | 20328 |
| R3ContF9D | 34758 | 34213 | 33167 | 29857 | 22128 | 22115 |
| R1100F5xD | 27855 | 27437 | 26923 | 25381 | 21244 | 21148 |
| R11F7xD | 69315 | 68451 | 67156 | 62550 | 46406 | 46075 |
| R21000F2xD | 47439 | 46427 | 45531 | 42317 | 29519 | 29367 |
| R2100F8xD | 3 | 3 | 2 | 0 | 0 | 0 |
| R2CTRLF4xD | 28104 | 27731 | 26670 | 23549 | 15624 | 15501 |
| R31F10xD | 39858 | 39337 | 38236 | 35397 | 27388 | 27222 |

Table B.3. Concentrations of benzo[*a*]pyrene (BaP) in food and metabolites of BaP in bile. Reported as mean ± standard errors (S.E.).

| **Nominal Exposure** | **Food** | **OH-BaP** | **BaP-Gluc** | **BaP-$SO_4$** | **Bile Sum** |
|---|---|---|---|---|---|
| µg $g^{-1}$ | µg $g^{-1}$ | ng $g^{-1}$ | ng $g^{-1}$ | ng $g^{-1}$ | ng $g^{-1}$ |
| 0 | 0.06 ± 0.02 | 0 ± 0 | 0 ± 0 | 165 ± 45.4 | 165 ± 45.4 |
| 1 | 0.98 ± 0.04 | 0 ± 0 | 1.2 ± 1.2 | 52.4 ± 18.8 | 53.7 ± 19.6 |
| 10 | 8.03 ± 1.61 | 0 ± 0 | 10.8 ± 2.6 | 1426 ± 264 | 1437 ± 266 |
| 100 | 104 ± 3.08 | 6.6 ± 2.9 | 113 ± 28.0 | 9532 ± 2458 | 9651 ± 2468 |
| 1,000 | 1170 ± 32.1 | 46.9 ± 13.6 | 260 ± 76.3 | 50763 ± 9408 | 51071 ± 9403 |

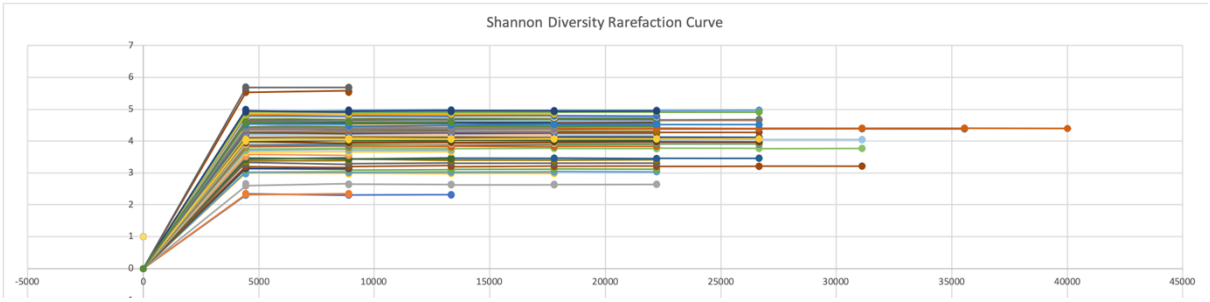

Figure B.1. Rarefaction curve of Shannon Diversity values across sequencing depths.

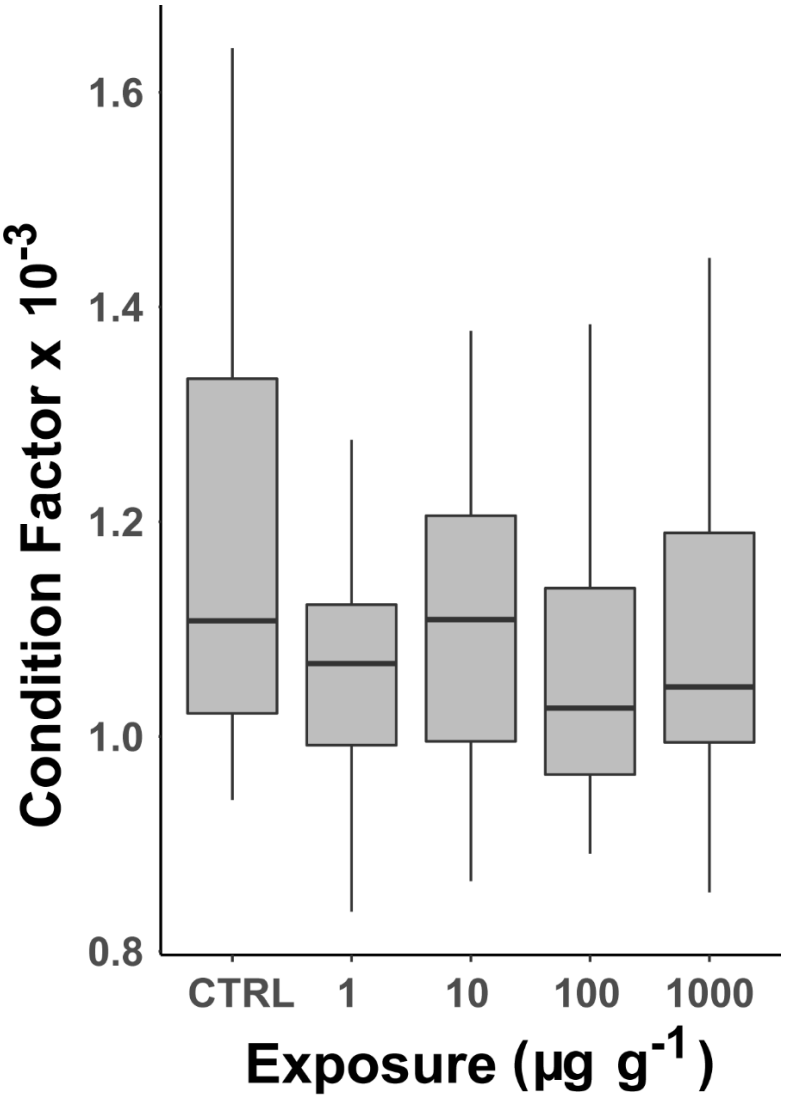


Figure B.2. Condition factor of fish exposed to BaP within each exposure group. Exposure did not significantly affect the condition factors of these fish.

A

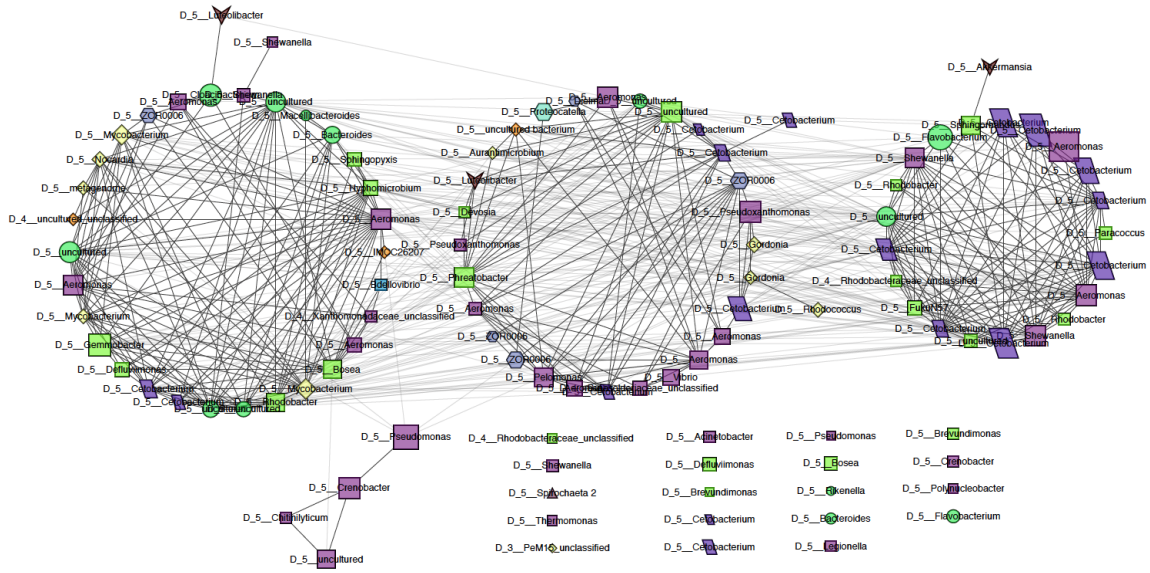
D_5__Limnohabitans
D_5__Shewanella
D_5__Akkermansia
D_5__Aeromonas
D_5__uncultured
D_5__ZOR0006
D_5__Mycobacterium
D_5__Nocardia
D_5__Bacteroides
D_5__Sphingopyxis
D_5__Hyphomicrobium
D_5__Aeromonas
D_5__Pseudoxanthomonas
D_5__Gordonia
D_5__Rhodococcus
D_5__Fluviicola
D_5__Haliangium
D_5__Gemmobacter
D_5__Diffluimonas
D_5__Bosea
D_5__Rhodobacter
D_5__Pseudomonas
D_5__Crenobacter
D_5__Cellulyticum
D_5__uncultured
D_4__Rhodobacteraceae_unclassified
D_5__Shewanella
D_5__Spirochaeta 2
D_5__Thermomonas
D_3__PeM15_unclassified
D_5__Acinetobacter
D_5__Diffluimonas
D_5__Brevundimonas
D_5__Cetobacterium
D_5__Cetobacterium
D_5__Pseudomonas
D_5__Bosea
D_5__Elkenella
D_5__Bacteroides
D_5__Escherichia
D_5__Brevundimonas
D_5__Crenobacter
D_5__Polynucleobacter
D_5__Flavobacterium

B

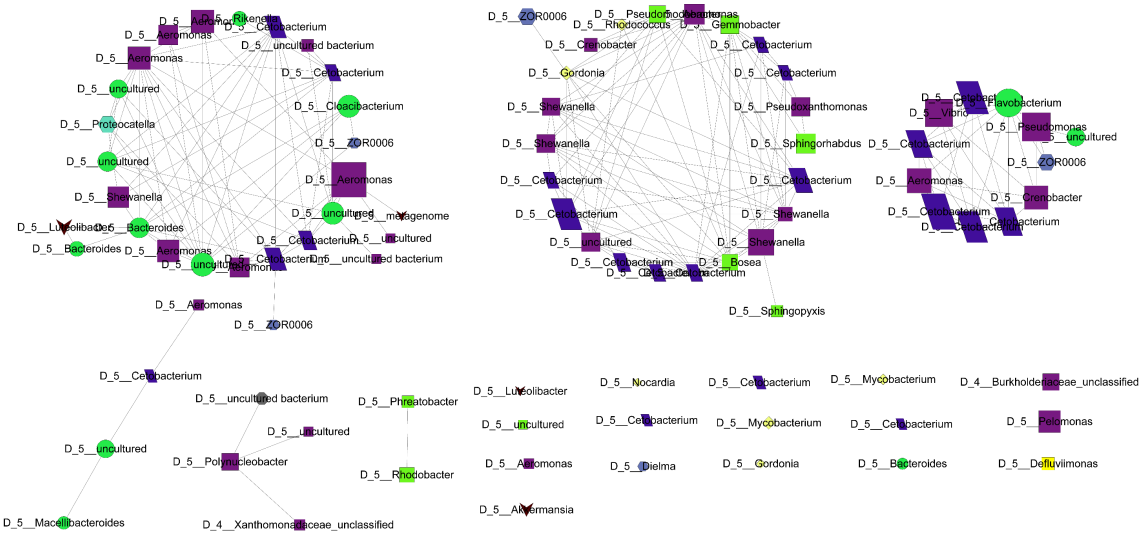
D_5__Aeromonas
D_5__uncultured bacterium
D_5__Cetobacterium
D_5__uncultured
D_5__Cloacibacterium
D_5__Proteocatella
D_5__ZOR0006
D_5__Shewanella
D_5__metagenome
D_5__Lucifera
D_5__Bacteroides
D_5__Pseudomonas
D_5__Gemmobacter
D_5__Gordonia
D_5__Pseudoxanthomonas
D_5__Sphingorhabdus
D_5__Catobacterium
D_5__Bosea
D_5__Sphingopyxis
D_5__Flavobacterium
D_5__Vibrio
D_5__Crenobacter
D_5__Catobacterium
D_5__Phreatobacter
D_5__Polynucleobacter
D_5__Rhodobacter
D_5__Nocardia
D_5__Mycobacterium
D_4__Burkholderiaceae_unclassified
D_5__Pelomonas
D_5__Dielma
D_5__Defluvimonas
D_5__Akkermansia
D_5__Macellibacteroides
D_4__Xanthomonadaceae_unclassified

C

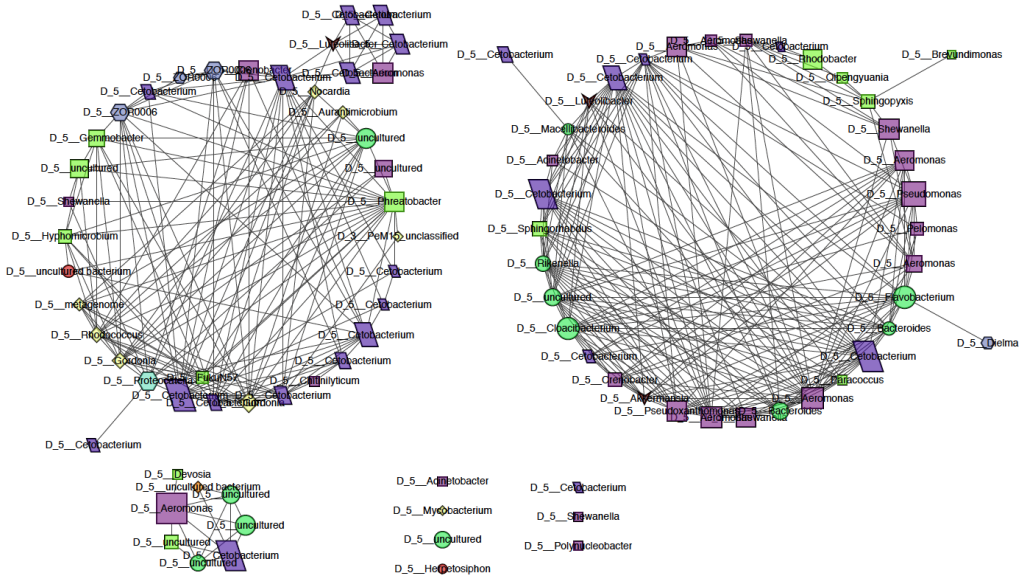
D_5__Cetobacterium
D_5__uncultured
D_5__ZOR0006
D_5__Germmobacter
D_5__Phreatobacter
D_5__Nocardia
D_5__Aurantimicrobium
D_5__HyphoMicrobium
D_5__uncultured bacterium
D_5__metagenome
D_5__Rhodococcus
D_5__Gordonia
D_5__Flavobacterium
D_5__Shewanella
D_5__Aeromonas
D_5__Pseudomonas
D_5__Sphingopyxis
D_5__Brevundimonas
D_5__Rikenella
D_5__Acinetobacter
D_5__Macellibacteroides
D_5__Bacteroides
D_5__Dielma
D_5__Defluvimonas
D_5__Desvosia
D_5__Mycobacterium
D_5__Polynucleobacter
D_5__Herbaspirillum

D

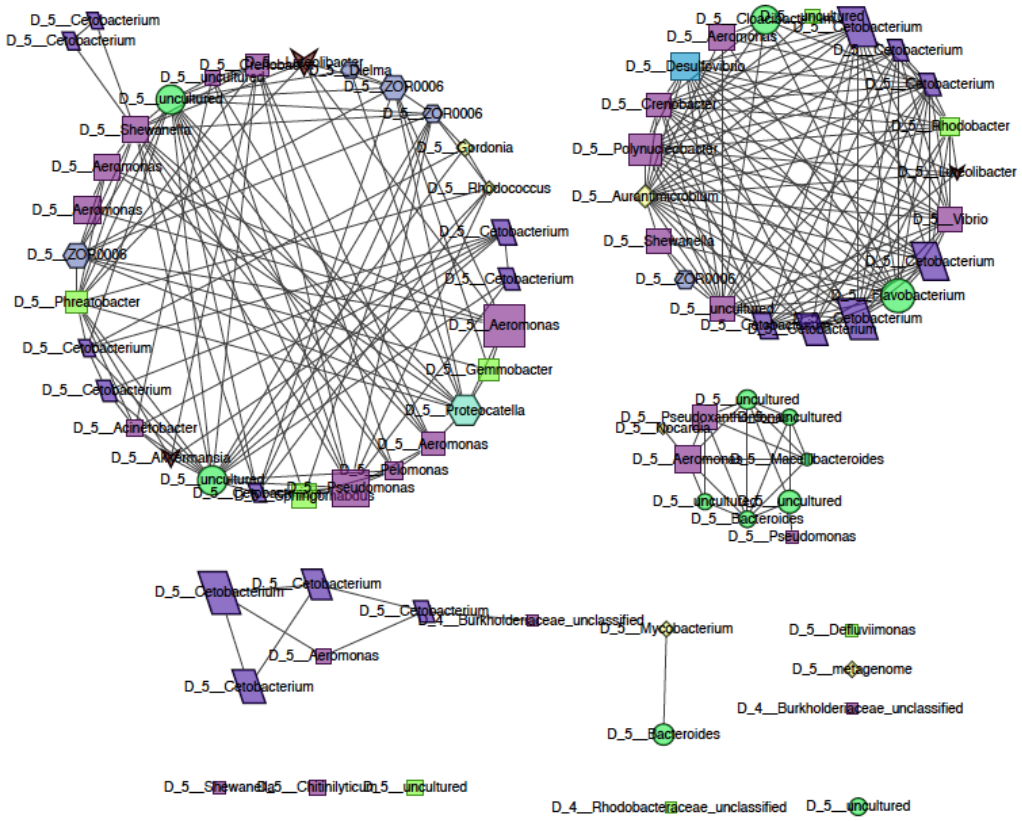
D_5__Cetobacterium
D_5__Cetobacterium
D_5__Shewanella
D_5__Aeromonas
D_5__Aeromonas
D_5__ZOR0006
D_5__Phreatobacter
D_5__Cetobacterium
D_5__Cetobacterium
D_5__Acinetobacter
D_5__Arthrobacter
D_5__uncultured
D_5__Pelomonas
D_5__Pseudomonas
D_5__ZOR0006
D_5__Gordonia
D_5__Rhodococcus
D_5__Cetobacterium
D_5__Cetobacterium
D_5__Aeromonas
D_5__Gemmobacter
D_5__Proteocatella
D_5__Aeromonas
D_5__Aeromonas
D_5__Desulfovibrio
D_5__Cetobacterium
D_5__Rhodobacter
D_5__Vibrio
D_5__Cetobacterium
D_5__Flavobacterium
D_5__Cetobacterium
D_5__ZOR0006
D_5__Shewanella
D_5__Aeromonas
D_5__Mycobacteroides
D_5__uncultured
D_5__Bacteroides
D_5__Pseudomonas
D_5__Cetobacterium
D_5__Cetobacterium
D_5__Aeromonas
D_5__Cetobacterium
D_5__Cetobacterium
D_5__Mycobacterium
D_5__Defluviimonas
D_5__metagenome
D_4__Burkholderiaceae_unclassified
D_5__Bacteroides
D_5__Shewanella
D_5__uncultured
D_4__Rhodobacteraceae_unclassified
D_5__uncultured

E

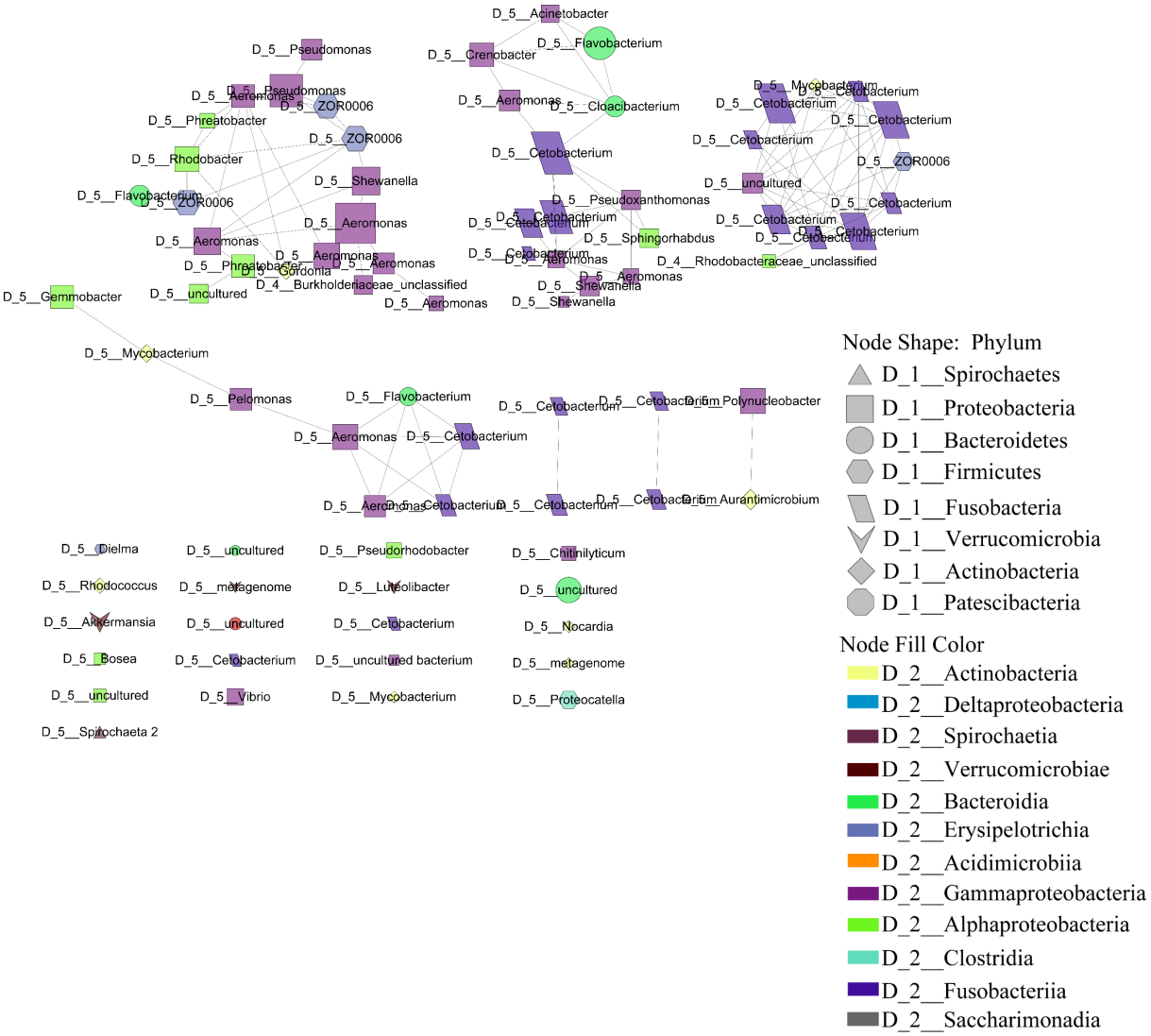


Figure B.3. Association networks generated through SparCC assembled at the level of genera for fathead minnows exposed to (A) Control, (B) 1, (C) 10, (D) 100, and (E) 1000 µg $g^{-1}$ BaP.

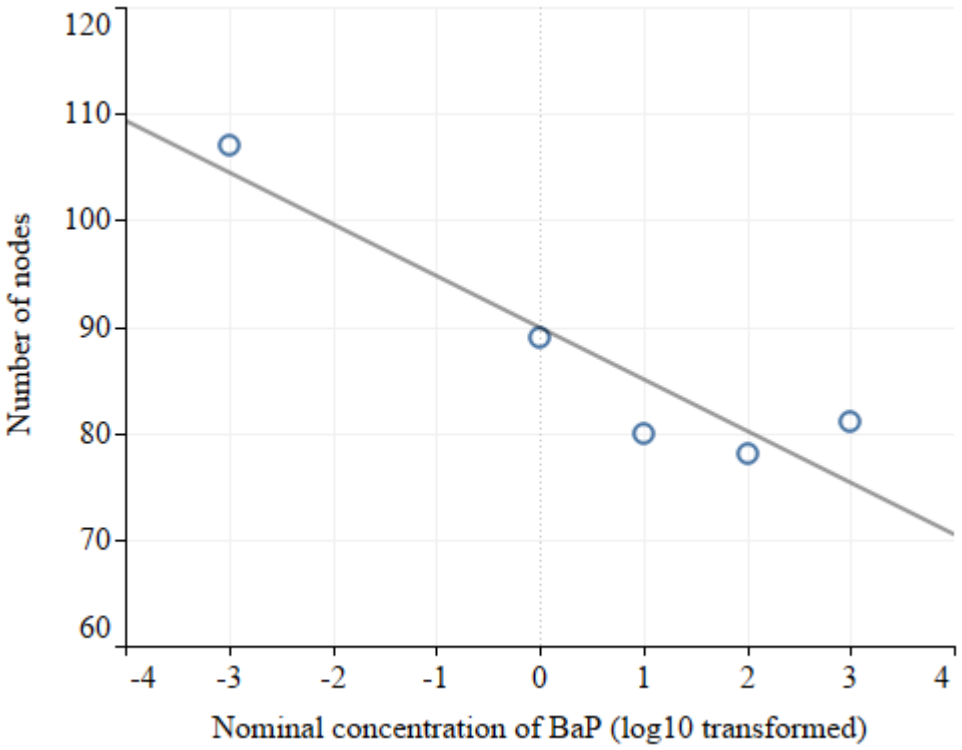


Figure B.4. Number of nodes generated through SparCC relative to $\log_{10}$-transformed nominal concentrations of BaP ($p < 0.05$, $R^2 = 0.88$).

## Appendix C

Table C.1. The number of counts of sequenced, filtered, denoised, merged, non-chimeric, and bacteria only reads for each sample.

| sample-id | input | filtered | denoised | merged | non-chimeric | bact only |
|---|---|---|---|---|---|---|
| R11000F1C | 41391 | 40661 | 40018 | 38155 | 32565 | 32539 |
| R11000F2C | 44524 | 43970 | 43792 | 43363 | 40261 | 39744 |
| R11000F3C | 49160 | 48119 | 47383 | 45381 | 36812 | 36812 |
| R11000F4C | 34808 | 34108 | 33681 | 32416 | 27072 | 27057 |
| R11000F5C | 53894 | 53128 | 52715 | 50719 | 40097 | 39118 |
| R11000F6C | 7 | 6 | 4 | 3 | 3 | 3 |
| R11000F7C | 61653 | 60684 | 60077 | 58006 | 49835 | 49703 |
| R11000F9C | 47633 | 46812 | 46030 | 43728 | 34523 | 34504 |
| R1100F10C | 61568 | 60537 | 59646 | 56383 | 41408 | 40360 |
| R1100F1C | 54401 | 53459 | 52329 | 48760 | 37757 | 37725 |
| R1100F2C | 5 | 5 | 3 | 0 | 0 | #N/A |
| R1100F3C | 50236 | 49364 | 48500 | 45809 | 35609 | 35483 |
| R1100F4C | 40079 | 39424 | 38632 | 36128 | 29070 | 29042 |
| R1100F5C | 45038 | 44115 | 43619 | 41551 | 34398 | 34358 |
| R1100F6C | 56392 | 55524 | 54897 | 52087 | 37808 | 37801 |
| R1100F7C | 46141 | 45461 | 44828 | 42785 | 34480 | 34471 |
| R1100F8C | 36281 | 35554 | 34956 | 32813 | 25350 | 25258 |
| R1100F9C | 3 | 1 | 1 | 1 | 1 | #N/A |
| R110F10C | 57091 | 56185 | 55494 | 53461 | 45056 | 45048 |
| R110F1C | 18010 | 17759 | 17494 | 16601 | 14365 | 14345 |
| R110F2C | 55878 | 55043 | 54341 | 52187 | 42803 | 42781 |
| R110F3C | 33241 | 32608 | 32166 | 30928 | 28649 | 28438 |
| R110F4C | 41132 | 40410 | 39860 | 38065 | 30891 | 30874 |
| R110F5C | 50829 | 50012 | 49164 | 46087 | 35532 | 35428 |
| R110F6C | 58978 | 58126 | 57509 | 55458 | 45249 | 45130 |
| R110F8C | 15 | 13 | 3 | 0 | 0 | #N/A |
| R11F10C | 14 | 14 | 9 | 9 | 4 | 4 |
| R11F1C | 40030 | 39470 | 38883 | 36711 | 31641 | 31615 |
| R11F2C | 16079 | 15295 | 14996 | 14627 | 14146 | 12475 |
| R11F3C | 43 | 43 | 26 | 26 | 26 | 26 |
| R11F4C | 55141 | 54207 | 53467 | 51071 | 43399 | 43244 |
| R11F5C | 16916 | 16586 | 16251 | 15150 | 12060 | 11919 |
| R11F6C | 41771 | 41011 | 40684 | 39463 | 34465 | 34394 |
| R11F7C | 55930 | 55043 | 54097 | 51417 | 40942 | 40873 |

| sample-id | input | filtered | denoised | merged | non-chimeric | bact only |
|---|---|---|---|---|---|---|
| R11F7xC | 65 | 40 | 32 | 31 | 31 | 31 |
| R11F8C | 39823 | 39318 | 38884 | 37399 | 33388 | 33384 |
| R11F9C | 11 | 11 | 6 | 0 | 0 | #N/A |
| R1CTRLF10C | 59382 | 58454 | 57659 | 54854 | 44361 | 44304 |
| R1CTRLF1C | 51253 | 50377 | 49887 | 47677 | 39181 | 39158 |
| R1CTRLF2C | 50171 | 49394 | 48319 | 45196 | 33658 | 33614 |
| R1CTRLF3C | 43047 | 42464 | 41891 | 40344 | 31932 | 31904 |
| R1CTRLF4C | 47658 | 46875 | 46217 | 43965 | 34418 | 34394 |
| R1CTRLF5C | 12 | 12 | 4 | 4 | 4 | 4 |
| R1CTRLF6C | 15899 | 15674 | 15336 | 14468 | 11601 | 11601 |
| R1CTRLF7C | 12655 | 12251 | 11884 | 11072 | 9732 | 9696 |
| R1CTRLF8C | 58582 | 57368 | 56726 | 54342 | 46943 | 46943 |
| R1CTRLF9C | 41067 | 40460 | 40153 | 39134 | 36947 | 36853 |
| R21000F10C | 36394 | 35914 | 35248 | 33387 | 30871 | 29983 |
| R21000F1C | 31 | 30 | 15 | 13 | 13 | 13 |
| R21000F2C | 18683 | 18365 | 17886 | 16345 | 13265 | 13237 |
| R21000F2xC | 32705 | 32248 | 31619 | 29892 | 24443 | 24443 |
| R21000F4C | 55913 | 55152 | 54201 | 50599 | 36175 | 36008 |
| R21000F4xC | 34659 | 34146 | 33290 | 30790 | 23901 | 23837 |
| R21000F5C | 30559 | 30105 | 29647 | 28017 | 23855 | 23838 |
| R21000F6C | 34411 | 33719 | 33094 | 30965 | 25158 | 25085 |
| R21000F9C | 37068 | 36550 | 36049 | 34131 | 25583 | 25577 |
| R2100F1C | 18539 | 17887 | 17312 | 15656 | 11293 | 3698 |
| R2100F2C | 20890 | 20587 | 20214 | 18762 | 12812 | #N/A |
| R2100F3C | 26803 | 26406 | 25896 | 24036 | 17040 | 17036 |
| R2100F3xC | 30099 | 29674 | 29193 | 27662 | 20053 | 20000 |
| R2100F4C | 28870 | 28426 | 27894 | 26125 | 18873 | 18864 |
| R2100F5C | 40995 | 40261 | 39375 | 36747 | 27268 | 27134 |
| R2100F7C | 26568 | 26176 | 25530 | 23659 | 17333 | 17292 |
| R2100F8C | 8982 | 8822 | 8565 | 7912 | 6680 | 6680 |
| R210F10C | 21335 | 21041 | 20761 | 19952 | 17171 | 15994 |
| R210F10xC | 38850 | 38105 | 37349 | 35067 | 27238 | 27065 |
| R210F2C | 29395 | 29016 | 28593 | 27141 | 21727 | 21720 |
| R210F3C | 40 | 38 | 27 | 26 | 26 | 26 |
| R210F4C | 27564 | 27082 | 26749 | 25593 | 19652 | 19498 |
| R210F5C | 30894 | 30479 | 30203 | 29379 | 25407 | 25404 |
| R210F6C | 33152 | 32709 | 32146 | 30285 | 22589 | 22540 |
| R210F7C | 40075 | 39461 | 38829 | 36684 | 29471 | 29424 |
| R210F8C | 30279 | 29839 | 28896 | 26131 | 21146 | 21034 |

| sample-id | input | filtered | denoised | merged | non-chimeric | bact only |
|---|---|---|---|---|---|---|
| R210F9C | 36430 | 35878 | 34566 | 30780 | 24685 | 24433 |
| R21F10C | 30 | 28 | 13 | 11 | 11 | #N/A |
| R21F1C | 38820 | 38242 | 37619 | 35514 | 27145 | 27139 |
| R21F2C | 25789 | 25438 | 24919 | 23171 | 17997 | 17993 |
| R21F3C | 23113 | 22822 | 22589 | 21936 | 21090 | 20622 |
| R21F5C | 39583 | 38994 | 38064 | 35348 | 29381 | 29372 |
| R21F6C | 34915 | 34327 | 33619 | 31263 | 22793 | 22733 |
| R21F7C | 32474 | 31897 | 31371 | 30024 | 25559 | 25503 |
| R21F8C | 34159 | 33595 | 32697 | 29768 | 22723 | 22424 |
| R21F9C | 36042 | 35458 | 34819 | 32692 | 27081 | 27069 |
| R2CTRLF10C | 34791 | 34218 | 33522 | 31242 | 26591 | 26351 |
| R2CTRLF1C | 39431 | 38939 | 38703 | 37961 | 35014 | 34839 |
| R2CTRLF2C | 33942 | 33319 | 32589 | 30211 | 25004 | 24990 |
| R2CTRLF3C | 27448 | 26994 | 26546 | 25182 | 19046 | 19030 |
| R2CTRLF3xC | 31210 | 30791 | 30333 | 29020 | 20922 | 20916 |
| R2CTRLF4C | 43137 | 42466 | 41805 | 39471 | 31555 | 31471 |
| R2CTRLF4xC | 31473 | 30940 | 29927 | 26850 | 21340 | 21279 |
| R2CTRLF5C | 42068 | 41519 | 40814 | 38490 | 30695 | 30655 |
| R2CTRLF7C | 31967 | 31582 | 31359 | 30997 | 27427 | 27162 |
| R2CTRLF8C | 30215 | 29760 | 28842 | 26466 | 21119 | 21102 |
| R2CTRLF9C | 34457 | 33953 | 32929 | 29713 | 24340 | 24070 |
| R31000F10C | 26306 | 25977 | 25258 | 23668 | 17306 | 17294 |
| R31000F1C | 8249 | 8140 | 7948 | 7537 | 6719 | 6707 |
| R31000F2C | 34925 | 34523 | 33675 | 30642 | 24525 | 23439 |
| R31000F3C | 36637 | 36206 | 35494 | 33445 | 26726 | 26423 |
| R31000F3xC | 13039 | 12858 | 12593 | 11896 | 9361 | 8966 |
| R31000F4C | 44859 | 44311 | 43566 | 41105 | 30841 | 30794 |
| R31000F4xC | 42566 | 42021 | 41371 | 40057 | 35889 | 34964 |
| R31000F6C | 40860 | 40354 | 40042 | 39090 | 31464 | 30926 |
| R31000F7C | 36548 | 36072 | 35412 | 33470 | 24630 | 24517 |
| R31000F8C | 19926 | 19683 | 19200 | 17823 | 14559 | 14255 |
| R31000F9C | 12049 | 11826 | 11596 | 11079 | 8387 | 8240 |
| R3100F1C | 25920 | 25589 | 24996 | 23473 | 18943 | 18931 |
| R3100F2C | 48581 | 47948 | 47340 | 45056 | 42431 | 40731 |
| R3100F4C | 12608 | 12407 | 12250 | 11880 | 11722 | 11309 |
| R3100F5C | 27813 | 27494 | 26881 | 25370 | 19849 | 19694 |
| R3100F6C | 19972 | 19675 | 19393 | 18848 | 18627 | 18575 |
| R3100F7C | 45992 | 45242 | 44540 | 42714 | 38492 | 38113 |
| R3100F8C | 13542 | 13363 | 12946 | 11621 | 8622 | 8576 |

| sample-id | input | filtered | denoised | merged | non-chimeric | bact only |
|---|---|---|---|---|---|---|
| R3100F9C | 29413 | 29048 | 28802 | 28232 | 24831 | 24784 |
| R310F1C | 47951 | 47330 | 46148 | 42512 | 30453 | 30424 |
| R310F2C | 29819 | 29460 | 28787 | 26296 | 17800 | #N/A |
| R310F3C | 45244 | 44675 | 43695 | 40633 | 29411 | 29406 |
| R310F4C | 39842 | 39348 | 38639 | 36007 | 25145 | 25108 |
| R310F5C | 265 | 260 | 249 | 244 | 244 | 244 |
| R310F6C | 12866 | 12705 | 12193 | 10919 | 7816 | 7808 |
| R310F7C | 40334 | 39869 | 39240 | 36578 | 25497 | 25414 |
| R310F8C | 44285 | 43770 | 43368 | 41973 | 37471 | 36956 |
| R310F9C | 35287 | 34839 | 34101 | 31433 | 22655 | 22649 |
| R31F10C | 59346 | 58502 | 57188 | 51853 | 30988 | 30776 |
| R31F10xC | 1370919 | 1353110 | 1344492 | 1285214 | 904422 | 898579 |
| R31F1C | 34672 | 34215 | 33241 | 29863 | 19799 | 19694 |
| R31F2C | 7 | 7 | 1 | 0 | 0 | #N/A |
| R31F3C | 39553 | 38996 | 38153 | 34830 | 22807 | 22766 |
| R31F4C | 34656 | 34169 | 33381 | 30482 | 19372 | 19324 |
| R31F5C | 11 | 11 | 4 | 4 | 4 | 4 |
| R31F6C | 12471 | 12315 | 11859 | 10399 | 7454 | 7439 |
| R31F7C | 14 | 14 | 6 | 3 | 3 | 3 |
| R31F8C | 5 | 5 | 1 | 0 | 0 | #N/A |
| R31F9C | 10944 | 10810 | 10398 | 9139 | 6288 | 6282 |
| R3CTRLF10C | 39469 | 39014 | 38215 | 35391 | 25109 | 25016 |
| R3CTRLF1C | 31954 | 31586 | 30702 | 27870 | 18735 | 18726 |
| R3CTRLF2C | 9 | 9 | 3 | 2 | 2 | 2 |
| R3CTRLF3C | 33344 | 32868 | 31920 | 28533 | 19179 | 19006 |
| R3CTRLF4C | 12 | 12 | 4 | 2 | 2 | 2 |
| R3CTRLF5C | 36667 | 36181 | 35240 | 32203 | 24879 | 22707 |
| R3CTRLF6C | 39882 | 39396 | 38400 | 35026 | 26088 | 25950 |
| R3CTRLF7C | 40002 | 39435 | 38283 | 34250 | 23283 | 23224 |
| R3CTRLF8C | 33680 | 33311 | 32432 | 29354 | 20577 | 20560 |
| R3CTRLF9C | 44403 | 43843 | 42560 | 37778 | 24163 | 22309 |
| NTC2D | 593 | 583 | 526 | 429 | 384 | 378 |
| NTCD | 8 | 8 | 2 | 2 | 2 | 2 |

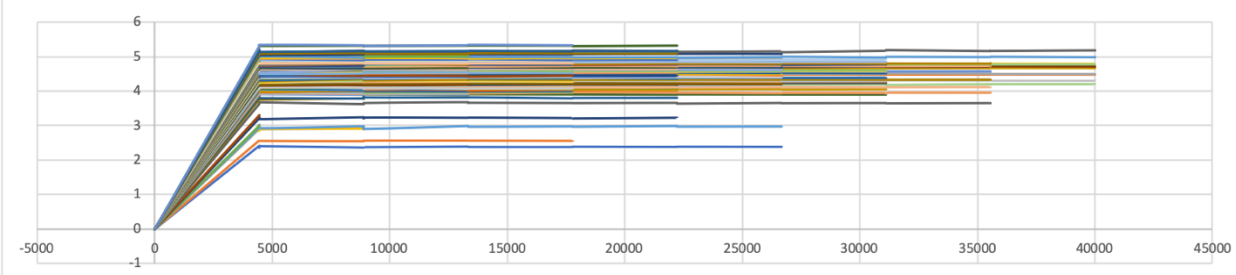


Figure C.1. Rarefaction curve of Shannon Diversity values across sequencing depths.

Table C.2. Concentration of food and BaP metabolites along with respective standard errors for the different exposure groups.

| Exposure | Food (µg $g^{-1}$) | OH-BaP (ng $g^{-1}$) | BaP-Gluc (ng $g^{-1}$) | BaP-SO4 (ng $g^{-1}$) |
|---|---|---|---|---|
| **CTRL** | 0.06 ± 0.02 | 0 | 0 | 178.12 ± 51.28 |
| **1** | 0.98 ± 0.04 | 0 | 1.44 ± 1.44 | 46.67 ± 17.87 |
| **10** | 8.03 ± 1.61 | 0 | 9.63 ± 2.88 | 1385.3 ± 307.71 |
| **100** | 104.61 ± 3.08 | 7.67 ± 3.32 | 157.07 ± 46.88 | 8084.58 ± 2281.28 |
| **1000** | 1166.45 ± 32.07 | 48.98 ± 16.66 | 280.35 ± 92.64 | 41003.53 ± 9556.2 |

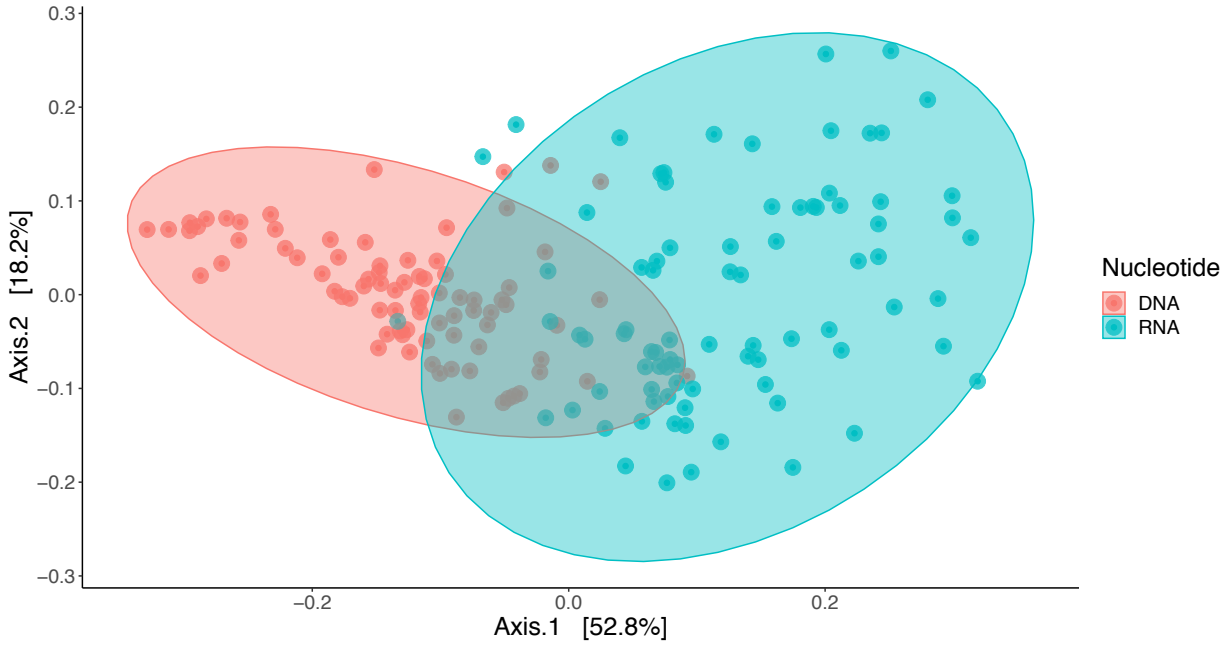


Figure C.2. PCoA of log-transformed Bray-Curtis dissimilarities of DNA- and RNA-based 16S rRNA metagenetics, shown in red and blue, respectively.

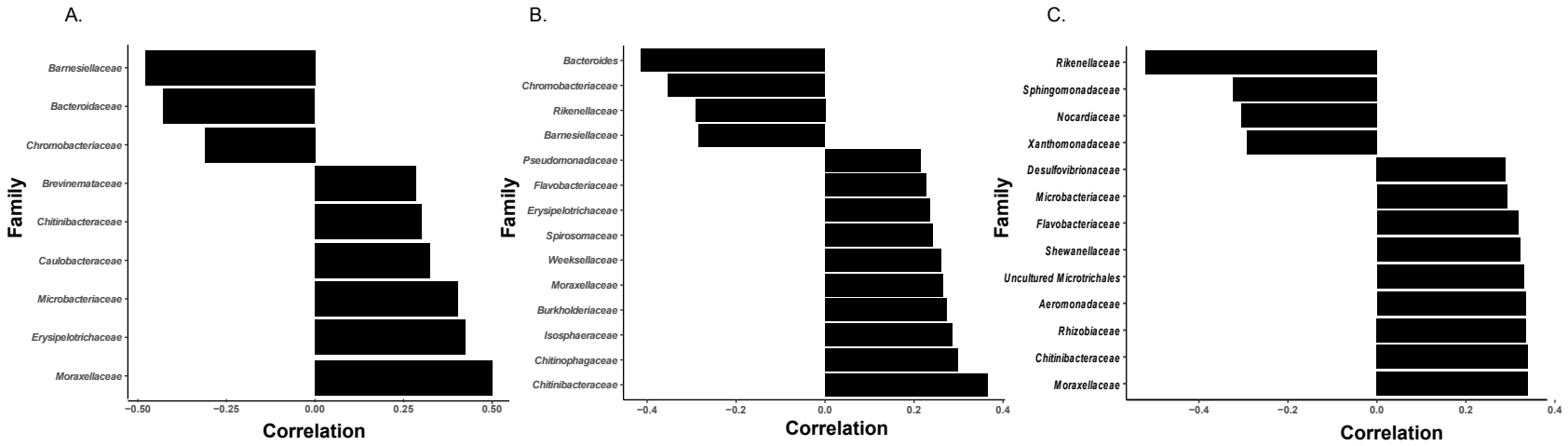


Figure C.3. (A). Genomic (from Chapter 3), (B). Active and (C). DNA-normalized families from the microbiome that are significantly correlated with log-transformed BaP-$SO_4$, along with the correlation values.

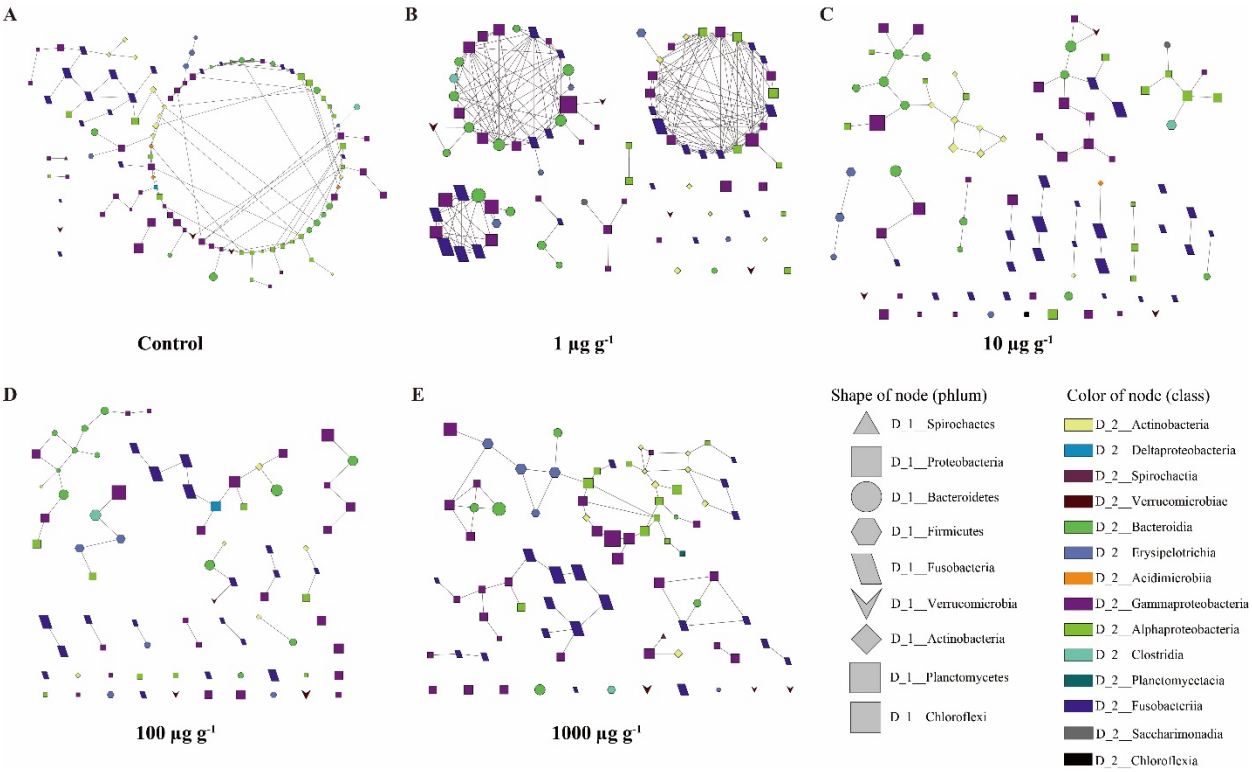


Figure C.4. Neighborhood selection networks of the genomic gut microbiome, as determined with SPIEC-EASI, from exposure to (A). Control, (B). 1, (C). 10, (D). 100, (E). 1000 µg $g^{-1}$ BaP. Shape of node: bacterial phylum; color of node: bacterial class; Size of node: abundance of ASV.

Table C.3. Number of nodes and edges from the neighborhood selection networks, as determined with SPIEC-EASI, of the genomic gut microbiome, as discovered by DNA metabarcoding.

| Treatment | Number of nodes | Number of nodes (non-alone) | Number of edges | cluster-edges |
|---|---|---|---|---|
| Control | 107 | 104 | 131 | 111 |
| 1 μg $g^{-1}$ | 89 | 73 | 240 | 197 |
| 10 μg $g^{-1}$ | 90 | 71 | 60 | 57 |
| 100 μg $g^{-1}$ | 78 | 56 | 44 | 42 |
| 1,000 μg $g^{-1}$ | 81 | 70 | 75 | 69 |

## Appendix D

Table D.1. Sampling locations with corresponding latitudes and longitudes as well as indication of whether the sites were up or downstream from the oil spill. Mossy River Delta was a far-field reference site.

| Site Name | Latitude | Longitude | Up/Down |
|---|---|---|---|
| Highway 17 | 53.59836 | -109.99125 | Up |
| Highway 3 | 53.523602 | -109.62017 | Up |
| Point of Entry | 53.41288 | -109.51712 | Down |
| Highway 21 | 53.39806 | -109.29679 | Down |
| Paynton Ferry | 53.02572 | -108.84361 | Down |
| Mossy River Delta | 54.01482 | -102.6329 | Far-field |

Table D.2. Number of input, filtered, denoised, merged, non-chimeric, and bacteria-only reads for each sample.

| sample-id | input | filtered | denoised | merged | non-chimeric | bact only |
|---|---|---|---|---|---|---|
| CH018 | 27327 | 27044 | 26817 | 26397 | 22825 | 22825 |
| CH019 | 5253 | 5197 | 5131 | 5008 | 4955 | 4939 |
| CH024x | 23017 | 22768 | 22647 | 22327 | 18613 | 18613 |
| CH025 | 22691 | 22429 | 22309 | 22206 | 18631 | 18621 |
| CTRL1 | 3663 | 3608 | 3585 | 3561 | 3542 | 3542 |
| CTRL2 | 88 | 87 | 62 | 56 | 56 | 56 |
| CTRL4 | 71 | 70 | 19 | 10 | 10 | 10 |
| CTRL5 | 94 | 93 | 75 | 68 | 68 | 68 |
| CTRL6 | 422 | 416 | 384 | 380 | 365 | 365 |
| dCH019 | 1850 | 1792 | 1745 | 1525 | 1525 | 831 |
| dH03001 | 857 | 848 | 846 | 844 | 844 | 726 |
| dH03005 | 11150 | 11039 | 11023 | 10976 | 10967 | 10667 |
| DH03010 | 25995 | 25776 | 25733 | 25643 | 25643 | 25430 |
| dH03012 | 675 | 668 | 665 | 665 | 665 | 658 |
| dH03013 | 342 | 339 | 337 | 337 | 337 | 337 |
| dH03023 | 2712 | 2683 | 2681 | 2638 | 2638 | 1952 |
| dH03024 | 48935 | 48479 | 48403 | 48303 | 47759 | 46911 |
| dH17005 | 1 | 1 | 1 | 1 | 1 | 1 |

| sample-id | input | filtered | denoised | merged | non-chimeric | bact only |
|---|---|---|---|---|---|---|
| dH17008 | 9217 | 9122 | 9114 | 9111 | 9110 | 8342 |
| dH17013 | 1715 | 1695 | 1694 | 1690 | 1684 | 1341 |
| dH17019 | 423 | 419 | 402 | 394 | 394 | 254 |
| dMRD021 | 8093 | 8002 | 7935 | 7913 | 7820 | 5799 |
| dPF007 | 522 | 510 | 490 | 490 | 490 | 484 |
| dPOE001 | 613 | 609 | 595 | 589 | 589 | 522 |
| H03001 | 3805 | 3767 | 3740 | 3641 | 3630 | 3105 |
| H03002 | 46189 | 45599 | 45558 | 45358 | 44693 | 42981 |
| H03003 | 48102 | 47633 | 47568 | 47386 | 46768 | 46732 |
| H03004 | 20802 | 20590 | 20481 | 20431 | 20344 | 20327 |
| H03004x | 8321 | 8231 | 8202 | 8159 | 8121 | 8028 |
| H03005 | 29444 | 29160 | 29011 | 28735 | 28457 | 27874 |
| H03006 | 13104 | 12966 | 12773 | 12356 | 12332 | 11402 |
| H030077 | 7709 | 7633 | 7584 | 7576 | 6801 | 6757 |
| H03008 | 53 | 53 | 38 | 38 | 38 | 36 |
| H03008xx | 16000 | 15814 | 15805 | 15796 | 15796 | 15543 |
| H03009 | 17977 | 17788 | 17784 | 17714 | 17626 | 17095 |
| H03010XX | 18170 | 17995 | 17945 | 17879 | 17876 | 17872 |
| H03011xx | 35466 | 35011 | 34993 | 34989 | 34984 | 33377 |
| H03012x | 3610 | 3563 | 3559 | 3549 | 3549 | 3525 |
| H03013 | 2 | 2 | 1 | 0 | 0 | #N/A |
| H03014 | 8219 | 8142 | 8045 | 7888 | 6694 | 6694 |
| H03015x | 7726 | 7617 | 7615 | 7600 | 7423 | 7221 |
| H03016x | 23562 | 23284 | 22404 | 20986 | 20503 | 18770 |
| H03018 | 21244 | 20973 | 19796 | 18528 | 18286 | 13297 |
| H03018x | 18882 | 18681 | 16251 | 12745 | 11729 | 10311 |
| H03019 | 26863 | 26544 | 25976 | 24941 | 24677 | 23473 |
| H03020 | 54960 | 54372 | 54012 | 53047 | 50155 | 50072 |
| H03021 | 11152 | 11036 | 10758 | 10333 | 10201 | 9579 |
| H03023xx | 28367 | 28052 | 27716 | 27197 | 27083 | 26818 |
| H03024 | 28303 | 27992 | 27848 | 27614 | 27473 | 26690 |
| H03025 | 94743 | 93750 | 92557 | 88196 | 65515 | 65279 |
| H03026 | 14201 | 14030 | 13965 | 13880 | 13872 | 13865 |
| H17004 | 11759 | 11614 | 11528 | 11403 | 11319 | 10261 |
| H17005x | 5888 | 5831 | 5806 | 5703 | 5614 | 5024 |
| H17006 | 32069 | 31704 | 31324 | 30809 | 30759 | 30076 |
| H17007 | 967 | 961 | 957 | 957 | 957 | 957 |
| H17008x | 16246 | 16077 | 15986 | 15733 | 15461 | 14348 |
| H17013x | 69073 | 68318 | 68176 | 67669 | 67189 | 66177 |

| sample-id | input | filtered | denoised | merged | non-chimeric | bact only |
|---|---|---|---|---|---|---|
| H17014x | 35158 | 34750 | 34694 | 34608 | 34585 | 34585 |
| H17015 | 10423 | 10332 | 10282 | 10201 | 9717 | 9717 |
| H17016 | 3654 | 3586 | 3552 | 3541 | 3541 | 3469 |
| H17017x | 33967 | 33583 | 33398 | 33272 | 31584 | 31581 |
| H17018 | 20080 | 19876 | 19789 | 19623 | 19168 | 19166 |
| H17019xx | 21126 | 20906 | 20611 | 19972 | 19777 | 15067 |
| H17020 | 2915 | 2896 | 2875 | 2874 | 2822 | 2795 |
| H21012 | 38365 | 37901 | 37883 | 37853 | 33422 | 33422 |
| H210121 | 25196 | 24962 | 24139 | 22395 | 22145 | 19714 |
| H21013x | 24569 | 24270 | 23810 | 23177 | 22785 | 22130 |
| H21014xx | 18053 | 17846 | 17828 | 17739 | 17203 | 17057 |
| H21015 | 29656 | 29331 | 27702 | 24723 | 24115 | 20419 |
| H21016 | 20812 | 20513 | 20482 | 20392 | 18636 | 18151 |
| H21017 | 37963 | 37392 | 37157 | 36462 | 31653 | 31462 |
| H21018 | 8056 | 7989 | 7911 | 7723 | 7675 | 6981 |
| H21020 | 53948 | 53325 | 52660 | 51237 | 49607 | 24091 |
| H21021 | 18911 | 18696 | 17721 | 16251 | 16123 | 13378 |
| H21022xx | 42793 | 42292 | 39957 | 36436 | 35643 | 32568 |
| H21023x | 5885 | 5832 | 5825 | 5822 | 5443 | 4976 |
| H21024 | 92881 | 92051 | 91861 | 91329 | 89283 | 89132 |
| H21025x | 2651 | 2626 | 2618 | 2617 | 2614 | 2283 |
| M03017 | 12858 | 12731 | 12469 | 11946 | 11846 | 10470 |
| MRD003 | 49507 | 48971 | 48526 | 47733 | 32840 | 32840 |
| MRD004 | 27769 | 27411 | 27263 | 27122 | 23254 | 23064 |
| MRD006 | 26547 | 26268 | 26161 | 26039 | 24277 | 24270 |
| MRD008 | 24148 | 23880 | 23773 | 23225 | 19715 | 19715 |
| MRD010 | 20163 | 19943 | 19914 | 19886 | 19793 | 19793 |
| MRD012.1 | 11528 | 11392 | 11341 | 11290 | 10972 | 10972 |
| MRD013 | 38083 | 37622 | 37609 | 37550 | 35437 | 35262 |
| MRD014 | 66123 | 65396 | 65302 | 65230 | 64870 | 64870 |
| MRD015 | 18626 | 18426 | 18290 | 18140 | 18076 | 18029 |
| MRD018 | 12369 | 12257 | 12199 | 12103 | 11896 | 10606 |
| MRD018x | 58860 | 58273 | 58213 | 58099 | 57767 | 57734 |
| MRD019 | 7144 | 7080 | 7061 | 7056 | 7056 | 7056 |
| MRD021 | 12606 | 12436 | 12309 | 12202 | 12195 | 12009 |
| MRD023 | 3214 | 3181 | 3153 | 3120 | 3120 | 3120 |
| MRD025 | 38014 | 37604 | 37238 | 36389 | 28844 | 28844 |
| PF001 | 21802 | 21570 | 21065 | 20205 | 19249 | 18997 |
| PF003 | 11459 | 11298 | 11250 | 11206 | 11170 | 11140 |

| sample-id | input | filtered | denoised | merged | non-chimeric | bact only |
|---|---|---|---|---|---|---|
| PF004 | 4787 | 4616 | 4566 | 4536 | 4525 | 4265 |
| PF005x | 13148 | 13020 | 12942 | 12876 | 12592 | 12546 |
| PF006 | 14480 | 14344 | 14320 | 14271 | 14130 | 13513 |
| PF007 | 1031 | 1019 | 1018 | 1017 | 1003 | 950 |
| PF008 | 12350 | 12246 | 12074 | 11855 | 11368 | 11237 |
| PF009 | 5203 | 5155 | 5146 | 5136 | 5136 | 5136 |
| PF011 | 21090 | 20879 | 20826 | 20706 | 20605 | 20566 |
| PF012x | 48956 | 48360 | 48202 | 47940 | 47621 | 46505 |
| PF013 | 23619 | 23328 | 23192 | 22758 | 20493 | 20491 |
| PF014 | 12402 | 12289 | 12194 | 12009 | 11941 | 11924 |
| PF015 | 16776 | 16595 | 16502 | 16423 | 16224 | 16178 |
| PF016 | 26773 | 26497 | 25363 | 21754 | 19751 | 12957 |
| POE001x | 11555 | 11437 | 11388 | 11342 | 11298 | 10676 |
| POE002x | 18036 | 17854 | 17786 | 17698 | 17605 | 17553 |
| POE003 | 1302 | 1294 | 1290 | 1286 | 1286 | 1242 |
| POE004 | 19206 | 18993 | 18381 | 17800 | 17099 | 16756 |
| POE005xx | 42027 | 41636 | 41514 | 41167 | 40641 | 39221 |
| POE006x | 793 | 346 | 318 | 308 | 304 | 301 |
| POE009 | 3 | 3 | 1 | 0 | 0 | #N/A |
| POE009xx | 201149 | 199098 | 192064 | 173822 | 149865 | 144425 |
| POE011 | 60830 | 60141 | 59746 | 58710 | 54060 | 54060 |
| POE012 | 8497 | 8404 | 8300 | 8122 | 8082 | 7775 |
| POE013 | 4 | 4 | 1 | 0 | 0 | #N/A |
| POE014x | 63415 | 62679 | 62565 | 62353 | 60331 | 60275 |
| POE015xx | 11364 | 11236 | 11111 | 10987 | 10741 | 10741 |
| POE016 | 10373 | 10278 | 10142 | 9239 | 5825 | 5825 |
| POE021 | 76125 | 75342 | 74023 | 71511 | 69397 | 68557 |
| POE022 | 11696 | 11557 | 10761 | 9810 | 9081 | 8955 |
| POE023x | 27998 | 27665 | 27549 | 27320 | 24084 | 24078 |
| POE029 | 24756 | 24471 | 24040 | 23674 | 23417 | 22889 |

Table D.3. Shared bacterial genera from the gut microbiomes of shorthead redhorse, walleye, northern pike, and goldeye.

| **Shared genera** |
|---|
| D_0__Bacteria;D_1__Actinobacteria;D_2__Actinobacteria;D_3__Corynebacteriales;D_4__Corynebacteriaceae;D_5__Corynebacterium |
| D_0__Bacteria;D_1__Actinobacteria;D_2__Actinobacteria;D_3__Micrococcales;D_4__Micrococcaceae;D_5__Renibacterium |
| D_0__Bacteria;D_1__Actinobacteria;D_2__Actinobacteria;D_3__Propionibacteriales;D_4__Propionibacteriaceae;D_5__Cutibacterium |
| D_0__Bacteria;D_1__Cyanobacteria;D_2__Oxyphotobacteria;D_3__Synechococcales;D_4__Cyanobiaceae;D_5__Cyanobium |
| D_0__Bacteria;D_1__Firmicutes;D_2__Bacilli;D_3__Bacillales;D_4__Bacillaceae;D_5__Caldalkalibacillus |
| D_0__Bacteria;D_1__Firmicutes;D_2__Bacilli;D_3__Bacillales;D_4__Bacillaceae;D_5__Geobacillus |
| D_0__Bacteria;D_1__Firmicutes;D_2__Bacilli;D_3__Lactobacillales;D_4__Carnobacteriaceae;D_5__Carnobacterium |
| D_0__Bacteria;D_1__Firmicutes;D_2__Bacilli;D_3__Lactobacillales;D_4__Streptococcaceae;D_5__Lactococcus |
| D_0__Bacteria;D_1__Firmicutes;D_2__Clostridia;D_3__Clostridiales;D_4__Clostridiaceae;D_5__unclassified |
| D_0__Bacteria;D_1__Firmicutes;D_2__Clostridia;D_3__Clostridiales;D_4__Lachnospiraceae;D_5__Epulopiscium |
| D_0__Bacteria;D_1__Firmicutes;D_2__Clostridia;D_3__Clostridiales;D_4__Peptostreptococcaceae;D_5__Paraclostridium |
| D_0__Bacteria;D_1__Firmicutes;D_2__Clostridia;D_3__Clostridiales;D_4__Peptostreptococcaceae;D_5__Romboutsia |
| D_0__Bacteria;D_1__Fusobacteria;D_2__Fusobacteriia;D_3__Fusobacteriales;D_4__Fusobacteriaceae;D_5__Cetobacterium |
| D_0__Bacteria;D_1__Proteobacteria;D_2__Deltaproteobacteria;D_3__Desulfovibrionales;D_4__Desulfovibrionaceae;D_5__Desulfovibrio |
| D_0__Bacteria;D_1__Proteobacteria;D_2__Gammaproteobacteria;D_3__Aeromonadales;D_4__Aeromonadaceae;D_5__Aeromonas |
| D_0__Bacteria;D_1__Proteobacteria;D_2__Gammaproteobacteria;D_3__Enterobacteriales;D_4__Enterobacteriaceae;D_5__Citrobacter |
| D_0__Bacteria;D_1__Proteobacteria;D_2__Gammaproteobacteria;D_3__Enterobacteriales;D_4__Enterobacteriaceae;D_5__Escherichia-Shigella |
| D_0__Bacteria;D_1__Proteobacteria;D_2__Gammaproteobacteria;D_3__Enterobacteriales;D_4__Enterobacteriaceae;D_5__Hafnia-Obesumbacterium |
| D_0__Bacteria;D_1__Proteobacteria;D_2__Gammaproteobacteria;D_3__Enterobacteriales;D_4__Enterobacteriaceae;D_5__Plesiomonas |
| D_0__Bacteria;D_1__Proteobacteria;D_2__Gammaproteobacteria;D_3__Enterobacteriales;D_4__Enterobacteriaceae;D_5__Serratia |
| D_0__Bacteria;D_1__Proteobacteria;D_2__Gammaproteobacteria;D_3__Pseudomonadales;D_4__Pseudomonadaceae;D_5__Pseudomonas |
| D_0__Bacteria;D_1__Tenericutes;D_2__Mollicutes;D_3__Mycoplasmatales;D_4__Mycoplasmataceae;D_5__Candidatus |
| D_0__Bacteria;D_1__Tenericutes;D_2__Mollicutes;D_3__Mycoplasmatales;D_4__Mycoplasmataceae;D_5__Mycoplasma |

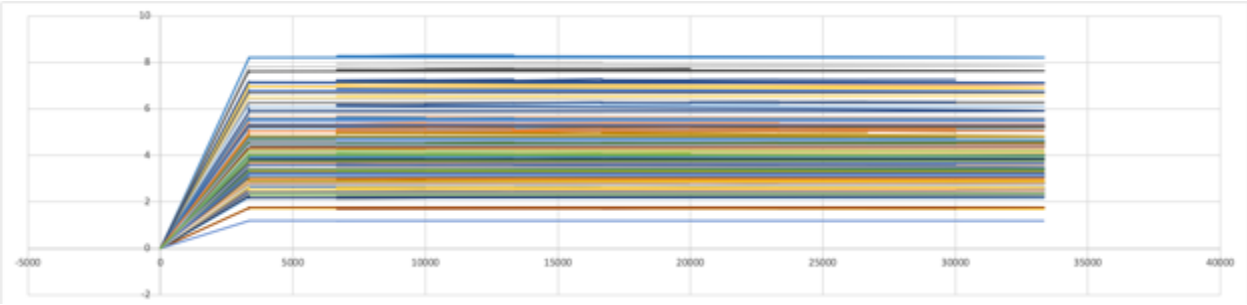


Figure D.1. Rarefaction curve for estimated Shannon diversity of each sample.

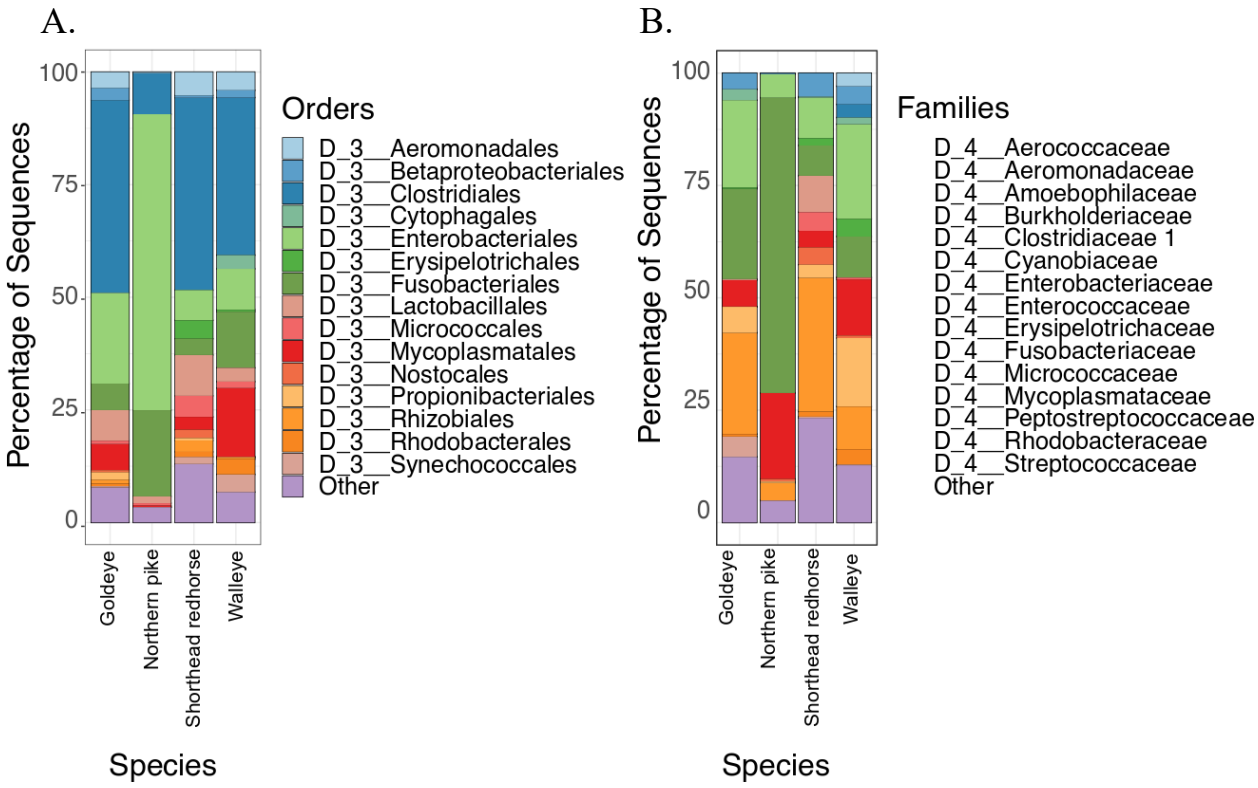


Figure D.2. Fifteen most abundant (A). orders and (B). families found in the guts of goldeye, northern pike, shorthead redhorse, and walleye.

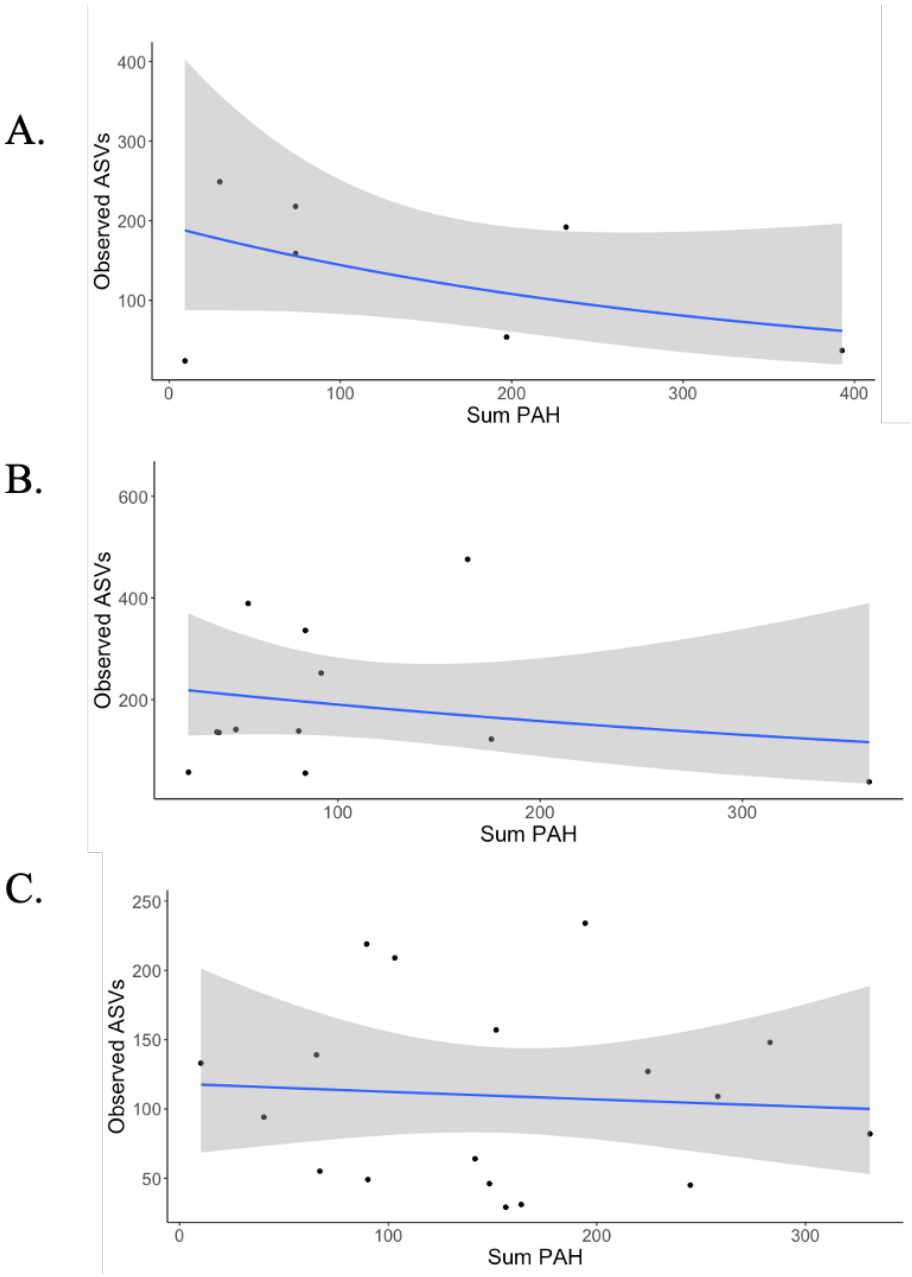


Figure D.3. Number of observed ASVs relative to sum PAH concentration (ng/g) along with 95% confidence intervals, shaded in grey, for (A). goldeye, (B). shorthead redhorse, and (C). walleye.

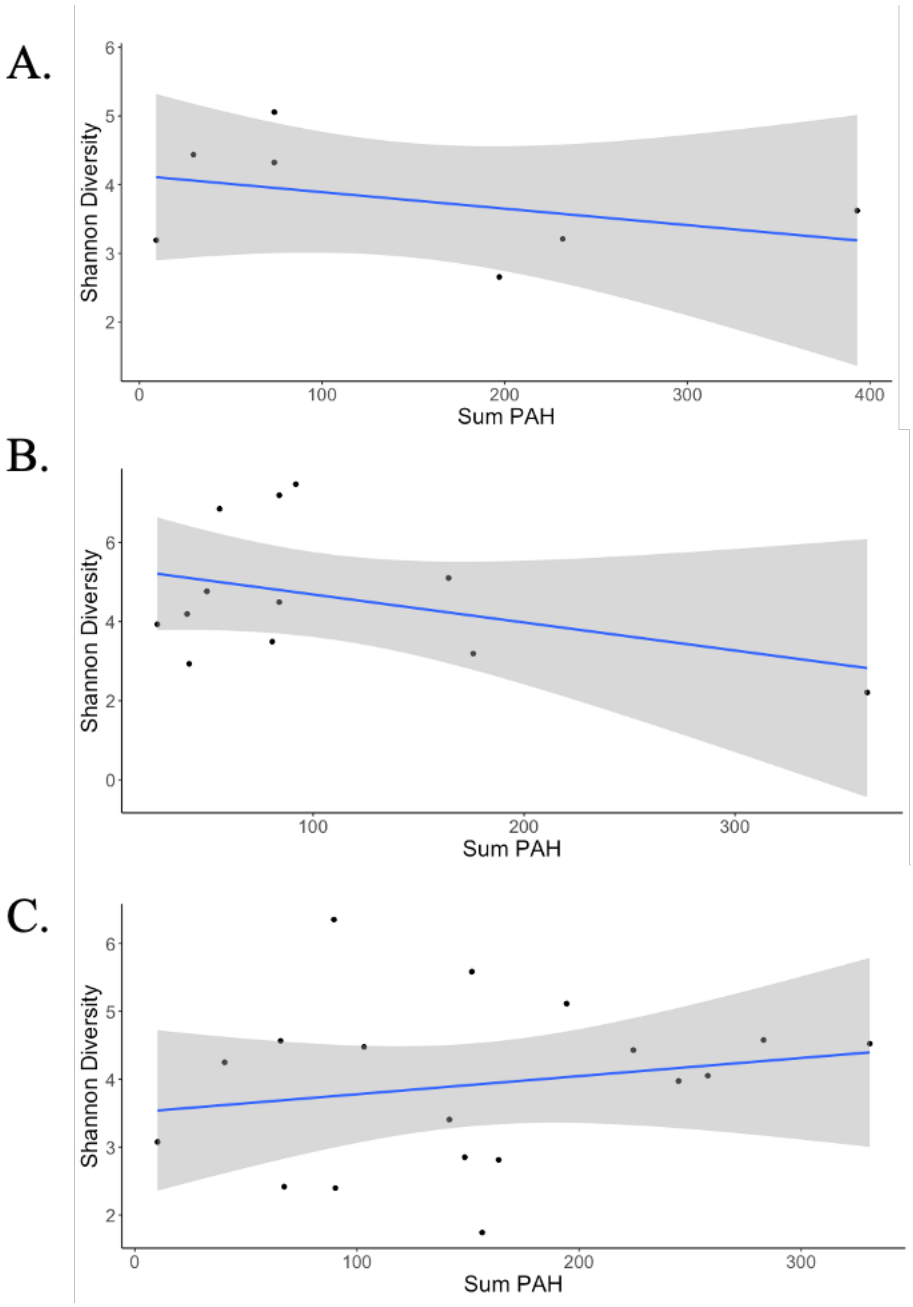


Figure D.4. Shannon diversity index relative to sum PAH concentration (ng/g), along with 95% confidence intervals, shaded in grey, for (A). goldeye, (B). shorthead redhorse, and (C). walleye.